

Deep Characterisation and
Functional Analysis of
CD4⁺HLA-DR⁺PD-1⁺ T Cells in
Chronic Lymphocytic Leukaemia



Peter Henley

Supervisors:

Dr. Stephen Man | Prof. Chris Fegan

*A thesis submitted in candidature for the degree of
Doctor of Philosophy*

December 2021

Acknowledgements

I would firstly like to thank Cancer Research Wales, who funded this project and have been supportive and understanding throughout, particularly with regard to the Covid-19 pandemic.

Second, but no less vital to this project, I would like to thank my supervisors Dr Steve Man and Prof Chris Fegan. Their guidance, support and insight have been second to none and I am truly grateful for everything they have done for me over the last four or so years. I could not have asked for a better supervisory team.

I would also like to show my appreciation to those who have contributed to the work in this thesis. Cath Naseriyan, Ann Kift-Morgan, Amanda Redfern and Claudia Consoli from Central Biotechnology Services for providing invaluable knowledge and assistance with experiments, as well a good chat when it was needed! Sumukh Deshpande and Rob Andrews for their help with the microarray data and Dr Beth Walsby for training me and integrating me into the lab back in 2017.

It is often said that it is not where you work, but who you work with that matters and I was lucky to spend my PhD working alongside some great people. My fellow PhD students Alys, Helene, Isabel, Tom and Stefan, whose friendship made coming into the office a pleasure. My “work mum” Trish, with whom countless cups of tea were shared. Julia, who sometimes seemed like the only person keeping the department afloat. Jo, Rhi, all the other members of the Baird group – the list goes on!

I must also acknowledge my friend group from day 1, the YYMCA. Beth, Ed, Jack Owen, Roanne and I have lived through the entire PhD experience together, from the 'Sound & Light Tube' to lockdown drinks in the park, becoming great friends along the way. The whole journey has been so much the better for their company.

Finally, thanks to all my other friends, my family and of course my parents. Everyone I know has been supportive and interested and helped to remind me that the research we do is both fascinating and meaningful.

Abstract

Chronic Lymphocytic Leukaemia (CLL) is the most common adult leukaemia in the Western world and is characterised by an accumulation of mature B cells in the circulation which can lead to hypogammaglobulinaemia and leaves patients highly susceptible to infections. There is currently no known cause for CLL, but there are considerable differences in its incidence: CLL is around twice as common in men as women, is rarely observed in Asian populations and has increasing prevalence with age, with a median age at diagnosis of 72 years.

Despite being a cancer of B cells, CLL patients also show marked differences in the T cell compartment of the immune system. As well as changes in numbers and in the distribution of subsets, T cells in CLL often demonstrate widespread dysfunction including an impaired ability to form immune synapses. Whether the development of CLL leads to this T cell dysfunction, or whether T cell dysfunction precedes and permits the development of CLL, remains unclear.

In this study, T cells from over 200 untreated, Stage A CLL patients were analysed in order to validate and build on previous work from our laboratory. That work identified CD4⁺:CD8⁺ T cell ratio and the frequency of CD4⁺HLA-DR⁺PD-1⁺ T cells as potential prognostic factors in CLL. Here, flow cytometry, gene expression analysis and functional assays were used to validate the prognostic potential of these two T cell parameters and to explore the nature and function of the CD4⁺HLA-DR⁺PD-1⁺ T cell population.

Using a larger cohort of CLL patients, this study confirmed that both CD4⁺:CD8⁺ T cell ratio and the frequency of CD4⁺HLA-DR⁺PD-1⁺ T cells can be used to stratify patients, both in terms of progression-free survival and time to first treatment, with a similar prognostic power to other currently used CLL cell markers.

Phenotyping of CD4⁺HLA-DR⁺PD-1⁺ T cells revealed this population to be highly heterogeneous, although there was a significant enrichment for markers of proliferation and cytotoxicity. Gene expression analysis conducted on CLL T cells revealed a strong association with exhaustion signalling, as well as changes to metabolic processes, while TOX was found to be the most significantly enriched gene in CD4⁺HLA-DR⁺PD-1⁺ T cells. However, no evidence of CLL T cell exhaustion was observed in cytokine production experiments and T cells expressing TOX appeared to have a greater proliferative response to stimulation *in vitro*.

Overall, this study provides evidence that T cell parameters could represent valuable new prognostic markers in CLL. Although the exact role of CD4⁺HLA-DR⁺PD-1⁺ T cells remains unclear, it is evident that this population is abnormal. Further investigation into this T cell population could provide useful information about how this subset impacts CLL disease and inform future treatment strategies.

Contents

Acknowledgements	i
Abstract.....	iii
Contents.....	v
Figures	xi
Tables.....	xiv
1 Introduction	1
1.1 Chronic Lymphocytic Leukaemia	1
1.1.1 Epidemiology	1
1.1.2 Pathology and Aetiology	2
1.1.3 Diagnosis and Staging	3
1.1.4 Prognosis.....	4
1.1.5 Treatment	6
1.2 T Cell Immunology	12
1.2.1 T Cell Development.....	12
1.2.1.1 Double Negative Thymocytes and β -Selection	13
1.2.1.2 Double Positive Thymocytes and Positive Selection	14
1.2.1.3 Single Positive Thymocytes and Negative Selection	15

1.2.2	Major Types of T Cell.....	19
1.2.2.1	CD4 ⁺ Conventional T Cells	19
1.2.2.2	CD8 ⁺ Conventional T Cells	23
1.2.2.3	Non-Conventional T Cells.....	26
1.2.3	Recognition of Antigen and T Cell Activation.....	30
1.2.4	T Cell Memory.....	32
1.3	T Cells in CLL.....	36
1.3.1	Composition of the T Cell Compartment in CLL.....	36
1.3.2	T Cell Differentiation and Ageing	39
1.3.3	T Cell Exhaustion	41
1.4	Aims of This Study.....	43
2	Materials and Methods.....	45
2.1	Basic Consumables.....	45
2.1.1	Media and Buffers.....	45
2.2	Blood Samples.....	45
2.2.1	Blood Donors	45
2.2.2	PBMC Isolation from Whole Blood	46
2.2.3	PBMC Counting and Viability Assessment	47
2.3	Absolute T Cell Counting.....	47
2.4	Flow Cytometric Analysis of T Cells.....	49

2.4.1	Equipment and Software	49
2.4.2	Surface Staining	49
2.4.3	Intracellular Staining	49
2.4.4	Flow Cytometer Fluorescence Compensation	50
2.4.5	Flow Cytometry Controls	51
2.4.6	Flow Cytometry Data Analysis and Statistics	52
2.5	Flow Cytometry Antibody Panels.....	53
2.6	Microarray Analysis of T Cell Subset Genetic Signatures.....	56
2.6.1	T Cell Enrichment	56
2.6.2	Fluorescence-Activated Cell Sorting of CD4 ⁺ T Cell Populations	57
2.6.3	RNA extraction from CD4 ⁺ T Cell Populations.....	59
2.6.4	Quality Assessment and Microarray Analysis of RNA	60
2.6.5	Microarray Data Processing.....	60
2.7	Flow Cytometric Validation of Microarray Results	62
2.8	qPCR Validation of Microarray Results	63
2.8.1	Selection of Genes for qPCR Analysis.....	63
2.8.2	Primer Design.....	66
2.8.3	Reverse Transcription and RNA Concentration.....	69
2.8.4	qPCR Plate Preparation	71
2.8.5	qPCR Setup and Running.....	72

2.9	Cytokine Production Assays	73
2.9.1	T Cell Stimulation	73
2.9.2	Flow Cytometric Analysis of Cytokine Production	73
2.10	T Cell Proliferation Assays	74
2.10.1	T Cell Stimulation	74
2.10.2	Flow Cytometric Analysis of Proliferation	75
3	Characterisation of CD4 ⁺ HLA-DR ⁺ PD-1 ⁺ T Cells in CLL.....	77
3.1	Populations of CD4 ⁺ HLA-DR ⁺ PD-1 ⁺ T Cells	80
3.1.1	CD4 ⁺ HLA-DR ⁺ PD-1 ⁺ T Cell Frequency	80
3.1.2	CD4 ⁺ HLA-DR ⁺ PD-1 ⁺ T Cell Counts	87
3.2	Phenotyping of CD4 ⁺ HLA-DR ⁺ PD-1 ⁺ T Cells	90
3.2.1	Initial Characterisation	90
3.2.2	Phenotypic Overview	94
3.3	Longitudinal Analysis of CD4 ⁺ HLA-DR ⁺ PD-1 ⁺ T Cells.....	103
3.3.1	Longitudinal Changes in Untreated CLL Patients	104
3.3.2	Longitudinal Changes in Ibrutinib-Treated Patients.....	108
3.4	Effect of T Cell Parameters on CLL Patient Outcomes	113
3.4.1	Progression-Free Survival.....	113
3.4.2	Time to First Treatment	116
3.5	Discussion	118

4	Gene Expression Analysis of CD4 ⁺ T Cells in CLL	128
4.1	Experimental Scheme for DNA Microarray Experiments.....	130
4.2	Gene Expression Analysis.....	133
4.3	Ingenuity Pathway Analysis	140
4.3.1	Diseases and Functions	145
4.3.1.1	CD4 ⁺ HLA-DR ⁻ PD-1 ⁻ vs. CD4 ⁺ HLA-DR ⁺ PD-1 ⁺ T Cells	145
4.3.1.2	CLL vs. Healthy Donor T Cells	148
4.3.2	Canonical Pathways	151
4.3.2.1	CD4 ⁺ HLA-DR ⁻ PD-1 ⁻ vs. CD4 ⁺ HLA-DR ⁺ PD-1 ⁺ T Cells	151
4.3.2.2	CLL vs. Healthy Donor T Cells	154
4.3.3	Upstream Regulators	157
4.3.3.1	CD4 ⁺ HLA-DR ⁻ PD-1 ⁻ vs. CD4 ⁺ HLA-DR ⁺ PD-1 ⁺ T Cells	157
4.3.3.2	CLL vs. Healthy Donor T Cells	158
4.4	Gene Expression Validation	161
4.4.1	qPCR Validation of Gene Expression	161
4.4.2	Flow Cytometry Validation of Gene Expression.....	165
4.5	Discussion	168
5	Investigating Exhaustion and the Role of TOX in CD4 ⁺ T Cells in CLL.....	179
5.1	Cytokine Production	181
5.1.1	Cytokine Production in Total CD4 ⁺ T Cells.....	184

5.1.2	Cytokine Production in CD4 ⁺ T Cell Subsets	187
5.1.3	Effect of TOX Expression on Cytokine Production in CD4 ⁺ T Cells...	192
5.2	T Cell Proliferation	198
5.2.1	Proliferation of Total CD4 ⁺ T Cells	200
5.2.2	Proliferation of CD4 ⁺ T Cell Subsets	203
5.2.3	Effect of TOX Expression on Proliferation of CD4 ⁺ T Cells.....	207
5.3	Discussion	212
6	General Discussion.....	218
7	Bibliography	230
8	Appendices	267
	267

Figures

Figure 1.1: CLL Incidence by Age.....	1
Figure 1.2: Schematic of T Cell Development in the Thymus	18
Figure 1.3: The Primary T Cell Types.....	29
Figure 2.1: Example Flow Cytometry Plot Obtained with Trucount Tubes.....	48
Figure 2.2: Example Flow Cytometry Histogram of CD38 Expression.....	51
Figure 2.3: Process for T Cell Enrichment From Whole Blood.	56
Figure 2.4: Representative Gating Strategy for FACS.....	58
Figure 3.1: Representative Gating Strategy for Phenotyping of T Cells.....	79
Figure 3.2: CD4+HLA-DR+PD-1+ T cells are enriched in CLL patients and in CLL ^{IR} patients compared to CLL ^{NR} patients.....	82
Figure 3.3: Increased CD4+HLA-DR+PD-1+ Cell Frequencies Cannot be Explained by Changes in T Cell Proportions or Subset Distributions	85
Figure 3.4: CD4 ⁺ HLA-DR ⁺ PD-1 ⁺ T Cells Do Not Correlate with T Cell Proportions or CD4:CD8 Ratio.....	86
Figure 3.5: CLL Patients Have Higher Absolute Counts of T Cells and CD4 ⁺ HLA-DR ⁺ PD- 1 ⁺ T Cells.....	89
Figure 3.6: CD4 ⁺ HLA-DR ⁺ PD-1 ⁺ Cells Show Greater Proliferation and Cytotoxicity than Total CD4 ⁺ T Cells in both CLL Patients and Healthy Donors	93
Figure 3.7: Overview of CD4 ⁺ T Cell Phenotypic Marker Expression	97
Figure 3.8: Characterisation of CD4 ⁺ HLA-DR ⁺ PD-1 ⁺ T Cell Sub-Populations	98

Figure 3.9: Characterisation of CD4 ⁺ HLA-DR ⁺ PD-1 ⁺ T Cell Differentiation Markers..	99
Figure 3.10: Untreated CLL Patients Show Variable Stability in T Cell Parameters	107
Figure 3.11: Impact of Ibrutinib Treatment on T Cell Parameters	112
Figure 3.12: Progression-Free Survival is Significantly Different in CLL Patients Stratified by T Cell Parameters	115
Figure 3.13: Time to First Treatment is Significantly Different in CLL Patients Stratified by T Cell Parameters	117
Figure 4.1: Schematic Diagram of the Analysed Comparisons Between Microarray Samples.....	132
Figure 4.2: PCA Plot Showing Distinct Clustering of Microarray Samples.....	135
Figure 4.3: Gene Expression Patterns are Different Between T Cell Subsets and Between CLL Patients and Healthy Donors.....	138
Figure 4.4: T Cells from CLL Patients Have a Distinctive Gene Expression Signature	139
Figure 4.5: Numbers of Significantly Differentially Expressed Genes between Different Comparison Groups.....	141
Figure 4.6: Top Diseases and Functions in CD4 ⁺ HLA-DR ⁻ PD-1 ⁻ and CD4 ⁺ HLA-DR ⁺ PD-1 ⁺ T Cells.....	147
Figure 4.7: Top Diseases and Functions in CLL and Healthy Donor T Cells	150
Figure 4.8: Top Canonical Pathways Activated in CD4 ⁺ HLA-DR ⁻ PD-1 ⁻ and CD4 ⁺ HLA-DR ⁺ PD-1 ⁺ T Cells	153
Figure 4.9: Top Canonical Pathways in CLL and Healthy Donor T Cells.....	156
Figure 4.10: Top Upstream Regulators	160

Figure 4.11: qPCR Validation of SLAMF6 and PELI1 Expression.....	164
Figure 4.12: CD4 ⁺ HLA-DR ⁺ PD-1 ⁺ T Cells Express Higher Levels Granzyme A and TOX	167
Figure 5.1: CD4 ⁺ T Cells Have Similar Cytokine Production Capabilities in CLL and Healthy Donors.....	186
Figure 5.2: CD4 ⁺ HLA-DR ⁺ PD-1 ⁺ T Cells Are Not More Exhausted Than Other T Cell Subsets.....	191
Figure 5.3: TOX Expression is More Common in CLL T Cells But is Not Affected by Stimulation.....	196
Figure 5.4: TOX Expression Does Not Affect Cytokine Production in CLL	197
Figure 5.5: Representative CFSE Dilution Plot	198
Figure 5.6: CD4 ⁺ T Cells from Healthy Donors Respond Better to Stimulation Than Those from CLL Patients	202
Figure 5.7: CD4 ⁺ HLA-DR ⁺ PD-1 ⁺ T Cells Are the Most Proliferative and Respond Best to Physiological Stimulation	206
Figure 5.8: TOX ⁺ T Cells Have a Better Proliferation Response to Physiological Stimulation Than TOX ⁻ T Cells in CLL.....	210
Figure 5.9: TOX ⁺ T Cells Respond Better to Physiological Stimulation Than TOX ⁻ T Cells in Healthy Donors	211
Figure 8.1: Gene Expression Patterns of Key Genes of Interest Match Phenotypic Observations.....	267

Tables

Table 1: Phenotyping Panel 1	53
Table 2: Phenotyping Panel 2	53
Table 3: Phenotyping Panel 3	54
Table 4: Longitudinal Monitoring Panel.....	54
Table 5: T Cell Cytokine Production Panel	55
Table 6: T Cell Proliferation Panel.....	55
Table 7: Granzyme A Validation Panel.....	62
Table 8: Selected Genes for qPCR Validation of Microarray Results	65
Table 9: Primer Pairs for Selected Genes.....	68
Table 10: Components of Reverse Transcription Mix for cDNA Production.....	69
Table 11: Components of qPCR Mix	71
Table 12: Run Method for qPCR Experiments	72
Table 13: Characteristics of CLL Patients and Healthy Donors Used in DNA Microarray Experiments.....	132
Table 14: Genes Upregulated Solely in Healthy Donor CD4 ⁺ HLA-DR ⁺ PD-1 ⁺ T Cells	269
Table 15: Most Highly Enriched Gene Sets in CLL-Derived CD4 ⁺ HLA-DR ⁺ PD-1 ⁺ T Cells	270
Table 16: Most Highly Enriched Gene Sets in Healthy Donor-Derived CD4 ⁺ HLA-DR ⁺ PD-1 ⁺ T Cells.....	270

1 Introduction

1.1 Chronic Lymphocytic Leukaemia

1.1.1 *Epidemiology*

Chronic Lymphocytic Leukaemia (CLL) is the most common form of adult leukaemia in the Western world, accounting for over 40% of leukaemia cases in over 65s (1). Studies have shown significant gender and racial biases in CLL prevalence, with a male:female ratio of around 2:1 and the disease being 20-30 times more common in Caucasian and Black populations compared to Asian ones, although the reasons for these discrepancies remain undefined (1,2). The median age of diagnosis is 72 years old, and there is increasing prevalence with age (see *Figure 1.1*) (2,3). Overall, the incidence rate of CLL is around 7.2 per 100,000, with around 4700 new cases expected in the UK per year (3).

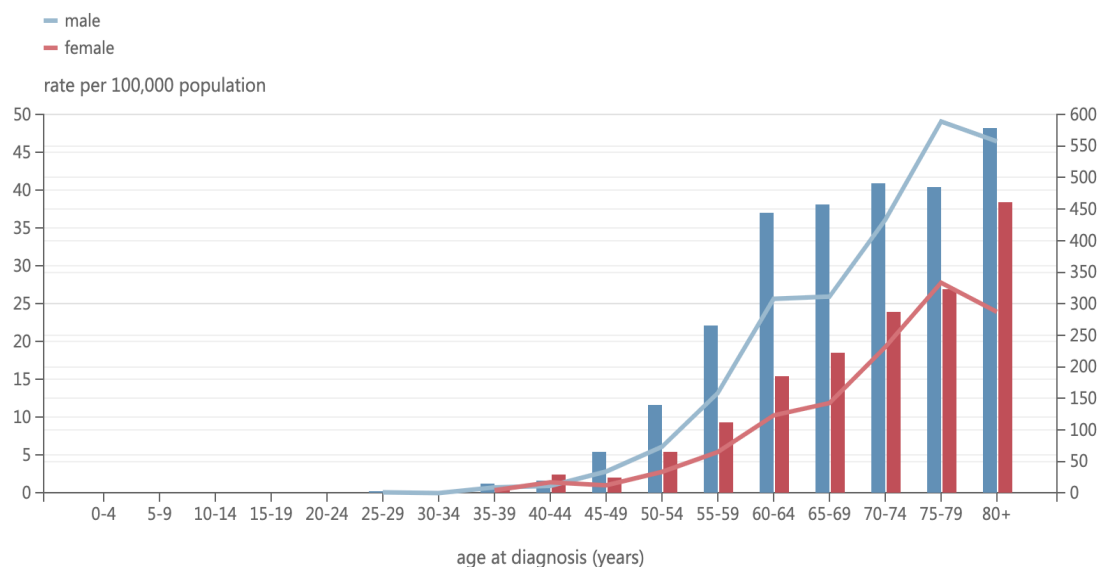


Figure 1.1: CLL Incidence by Age

The estimated incidence rate of CLL per 100,000 people in the UK, stratified by age group. Adapted from Haematological Malignancy Research Network (www.hmrn.org/statistics/incidence)

1.1.2 Pathology and Aetiology

CLL disease is characterised by an accumulation of circulating malignant CD5⁺CD19⁺ B cells, which often express markers of activation (4,5). The monoclonal nature of these B cells can lead to hypogammaglobulinaemia, with many patients presenting with reduced serum immunoglobulin levels and therefore impaired immunity, which worsens with advancing disease stage (6–8). This immunodeficiency can be severe and CLL patients are highly susceptible to infections, particularly in the respiratory and urinary tracts, from bacteria including *E. coli* and fungi such *Candida albicans* (5,6,9). Furthermore, viral reactivation is commonly seen, particularly in the cases of *Herpes Simplex Virus*, *Epstein-Barr Virus* and *Cytomegalovirus* (CMV) (6,10). Infections are therefore very common and account for a large proportion of mortality in CLL patients, with reports suggesting varying *Figures* of between 25-80% of deaths being caused by infection (6,9).

There remains no known cause for CLL, or its associated pre-leukaemic condition monoclonal B lymphocytosis (MBL), however there does appear to be an inheritable genetic component to this disease (11). Although genome-wide association studies have identified some minor risk polymorphisms, no major candidate has yet been found (12). Despite this, around 15% of CLL patients report a family member with either CLL or a related lymphoproliferative disease and a family history of these disorders confers a greatly enhanced risk (12–14).

Several potential drivers for CLL have been postulated over the years. One such hypothesis was infection with CMV, with several groups finding expanded T cell populations showing CMV specificity in CLL and correlating this with worse outcomes

(10,15,16). However, not all CLL patients are seropositive for CMV (17) and in 2016 Parry *et al.* showed that there was no difference between CMV⁺ and CMV⁻ patients in terms of overall survival and time to first treatment (18). There has also been no link demonstrated between CMV seropositivity and prognostic T cell factors (19). Other suggested factors such as diet and exposure to ionising radiation have also been shown to have little to no link with CLL pathogenesis (20,21).

1.1.3 Diagnosis and Staging

CLL patients at diagnosis have a very heterogeneous presentation and fall into one of two main groups: those with indolent or progressive disease. Indolent disease is marked by a stable phenotype with few, if any, symptoms and does not require immediate treatment. Conversely, other patients have an aggressive form of CLL that requires treatment and is associated with considerably worse prognosis (2,6,22). Although symptoms may be experienced, these are often mild and not specific to CLL – these most commonly include tiredness, night sweats and weight loss (2). Instead, a large proportion of patients are asymptomatic and are serendipitously diagnosed during routine blood tests (1,23). Diagnosis is based on several factors, chiefly a lymphocyte count of $>5 \times 10^9/l$ and confirmation of the clonality of the leukaemia cells by flow cytometry. The immunophenotype of the leukaemic cells is also taken into account, including expression of CD5 and CD23 and low levels of CD20 (2,23–25).

At diagnosis, CLL patients are classified into groups using one of two predominant clinical staging systems: the older Rai system (26) is most commonly used in the United States of America, while in Europe the Binet system (27) is

preferred. The Binet system makes use of features that form part of routine clinical examination and blood testing of patients, allowing for relatively straightforward classification of patients into one of three stages. These features are thrombocytopenia (platelet count $<100 \times 10^9/l$), anaemia (haemoglobin $<10g/dl$) and CLL cell infiltration to specified key lymphoid tissues: liver, spleen and axillary, inguinal and cervical lymph nodes (either uni- or bilaterally). Stage A patients are determined by having fewer than three of the above tissues infiltrated by CLL cells, with no thrombocytopenia or anaemia and have a median survival of more than 10 years. Stage B patients also have no thrombocytopenia or anaemia, but have three or more lymphoid infiltrations, with a median survival of over 8 years. Stage C patients are classified as those with either thrombocytopenia, anaemia or both, regardless of lymphoid tissue infiltration and have a median survival of around 6.5 years (24,25,27).

1.1.4 Prognosis

As well as clinical staging, there are a large number of markers that can be assessed to give prognostic information, with varying degrees of accuracy and usefulness. These include, but are not limited to, expression levels of CD38 or ZAP70, mutations in NOTCH1, SF3B1 or MYD88 and chromosomal deletions at 11q (24). However, the three key prognostic markers defined by the International Workshop on CLL are Immunoglobulin Heavy Chain Variable Region (IGHV) mutation status, β_2 -microglobulin levels in the blood and genetic aberrations affecting the TP53 gene (25).

IGHV mutation status has been a known prognostic marker in CLL for around twenty years and remains an effective method of stratification (28,29). The IGHV forms part of the B cell receptor (BCR) and the genes encoding this region undergo somatic hypermutation during an immune response to produce high affinity BCRs (30). In CLL, up to half of patients present with a leukaemic clone that has undergone somatic hypermutation, such that their IGHV genes have <98% homology to the germ line (IGHV mutated). Those patients whose leukaemia cells show greater than 98% homology to germ line IGHV genes are termed IGHV unmutated (24). Studies have demonstrated that IGHV mutated patients have significantly better prognosis, with around three times longer overall survival than IGHV unmutated patients (28,29,31). This is probably due to increased genetic instability in leukaemic cells from IGHV unmutated patients, increasing the risk of other detrimental mutations occurring (24).

B₂-microglobulin is one of the four component chains of the Major Histocompatibility Complex class 1 (MHCI) molecule, present on all nucleated cells, and can be found in its soluble form in serum, urine and other fluids (32,33). When measured in serum, the levels of β₂-microglobulin have been shown to correlate with increasing disease stage in CLL. There is also a significant link between serum β₂-microglobulin and both the response to chemoimmunotherapy and survival following treatment (34,35).

The gene TP53, found on the p arm of chromosome 17, encodes the extensively studied protein p53, dubbed 'the Guardian of the Genome' (36). This protein is one of the key regulators of the cell's response to stress, particularly DNA

damage, functioning to protect the cell from malignant transformation (37). This is achieved by several mechanisms, including p53-induced changes to transcription of proteins involved in the cell cycle and the induction of apoptosis by activation of caspases via the BCL2 protein family (38,39). In CLL, 17p deletions and/or mutations in the TP53 gene are observed in 5-8% of patients at diagnosis, but in a much greater proportion of patients with progressive or treatment-refractory disease (38,40,41). Patients harbouring p53 function loss have been shown to have significantly worse prognosis and reduced responsiveness to therapies, in particular chemoimmunotherapy (41–43). As a result, patients carrying a 17p deletion or p53 mutation are considered high risk and are recommended for novel therapies (24,44).

1.1.5 Treatment

At diagnosis, patients will be assigned a clinical stage and may be assessed for some or all of the prognostic markers in *Section 1.1.4*. Depending on the outcomes of these assessments, decisions on whether to treat, and which therapy is most appropriate, can be made.

Those patients who are classified as Stage A, along with asymptomatic Stage B patients, are recommended to be assigned to a ‘watch and wait’ strategy. This involves no treatment, with patients instead monitored with regular clinic visits every 3-12 months (25). A number of studies have shown that immediate therapeutic intervention for early stage CLL has no long-term survival benefit for patients (45–47), while reducing patient quality of life due to the side effects of frontline chemoimmunotherapy. Therefore, although it may seem unusual when compared to

many other cancers, not treating early stage CLL patients has become routine clinical practice, although this strategy may change with the advent of lower toxicity targeted therapies.

Treatment for CLL is indicated for symptomatic Stage B patients and Stage C patients at diagnosis, as well as for patients following a 'watch and wait' strategy who go on to progress to 'active disease' (25). 'Active disease' is defined as progressive and/or symptomatic disease, and can be constituted by a number of criteria as stipulated by the International Workshop on CLL (25). These are as follows:

- 1) Development or worsening of anaemia/thrombocytopaenia.
- 2) Massive or progressive splenomegaly.
- 3) Massive or progressive lymphadenopathy.
- 4) Lymphocyte doubling time <6 months (or lymphocytosis increase of >50% in 2 months).
- 5) Autoimmune complications.
- 6) Lymphocyte infiltration outside of lymphoid organs.
- 7) Significant symptoms:
 - i) Weight loss >10% in 6 months
 - ii) Fatigue preventing work/activity
 - iii) Persistent fever without infection
 - iv) Persistent night sweats with infection.

When 'active disease' is observed, the standard frontline treatment for CLL without p53 mutation is combination chemoimmunotherapy, comprising the purine

analogue Fludarabine, the DNA cross-linking agent Cyclophosphamide and the anti-CD20 monoclonal antibody Rituximab (together termed FCR) (24). This combination has been in use for over ten years, following reports of improved patient outcomes compared to the previous standard therapy of just Fludarabine and Cyclophosphamide (48). Subsequent studies have confirmed that FCR can induce durable remissions and provides significant improvements in patient survival (49), showing particular efficacy in patients in the more favourable IGHV mutated subgroup (35), as well as qualified success for relapsed/refractory patients (34). The drawbacks of FCR centre around toxicities, with patients being treated with this combination highly susceptible to opportunistic infections, thanks in part to prolonged neutropaenia (48). A further complication arises in IGHV unmutated patients and/or patients with p53 deletions, who both have significantly reduced responses to and beneficial outcomes from FCR (35,44).

In elderly patients who may be less able to tolerate the associated toxicities of FCR, but are otherwise healthy, a combination of the alkylating agent Bendamustine and Rituximab (BR) is recommended. This is due to BR both being more tolerable than FCR and causing fewer severe infections in patients (50). For elderly patients who suffer from comorbidities, the recommended treatment is a combination of the alkylating agent Chlorambucil with either Rituximab or an alternative anti-CD20 monoclonal antibody, such as Obinutuzumab or Ofatumumab – these combinations are more tolerable than other chemoimmunotherapies and have shown clinically significant improvements to outcomes in these patients (51,52).

For those patients who have p53 deletions, or fail to respond to or relapse from chemoimmunotherapy, there are several alternative treatment options. These are often referred to as targeted therapies due to their specificities, and include Idelalisib, Venetoclax and Ibrutinib.

Idelalisib is an orally-given selective inhibitor of PI3K δ , one of the four isoforms of the enzyme phosphoinositide-3-kinase (PI3K). Expression of the delta isoform of PI3K is mainly restricted to haematologic cells, where this enzyme is known to play a key role in B cell function (53). Of particular relevance to CLL, PI3K δ is found downstream of the BCR, where it acts as a signal transducer by activating AKT and mTOR signalling leading to pleiotropic effects (54,55). Since BCR signalling is vital for CLL cell survival, there was therefore a strong rationale for targeting PI3K δ (56). It has shown that Idelalisib can effectively inhibit downstream BCR signalling in CLL and inhibit CLL cell survival and proliferation (53). Subsequent studies have sought to combine Idelalisib with the anti-CD20 monoclonal antibody Rituximab to increase efficacy and have proven that Idelalisib gives a significant improvement to patient outcomes.

Venetoclax is an orally-available, highly-selective inhibitor of the key anti-apoptotic protein Bcl-2. The BCL2 protein family is a large group comprising both pro-survival and pro-apoptotic proteins that together set the threshold for apoptosis in the cell – the balance of these proteins determines activation of the mitochondrial apoptosis pathway (57). The level of expression of Bcl-2 has been seen to correlate with patient outcomes in CLL, with Bcl-2 appearing to be important in CLL cell survival (58,59). Initial studies using Venetoclax were conducted in the relapsed/refractory

CLL setting, and showed promising responses even in patients with high risk prognostic markers including p53 deletion, along with acceptable toxicities (60–62). Although these early data are promising, a caveat is the emergence of Venetoclax resistance in patients after several years of therapy, via mutations in Bcl-2 that render Venetoclax ineffective (63,64). Such resistance could potentially be avoided by the addition of other therapeutic agents in a combination regimen, and a number of recent follow-up studies have begun to address this (65). Addition of both Rituximab and Obinutuzumab to Venetoclax have demonstrated significant clinical benefit (66,67), while trials of Venetoclax plus Ibrutinib are ongoing and showing remarkable success (68,69). In all of these cases, the time-limited nature of the Venetoclax treatment may help to reduce the induction of resistance.

Ibrutinib is an orally-delivered selective inhibitor of Bruton's Tyrosine Kinase (BTK), approved in the UK for treatment of relapsed/refractory and p53 mutated CLL in 2017. BTK is a signal transducing enzyme downstream of the BCR, meaning that Ibrutinib has a similar mechanism of action to that of Idelalisib (70,71). Several studies have provided promising results, with Ibrutinib able to induce long-term responses with significant patient benefit (72–74), including for patients with p53 deletions (75). Of particular interest is the relatively mild toxicity associated with Ibrutinib treatment compared to chemoimmunotherapy, making Ibrutinib an attractive first-line therapy for older and less fit patients (76). A potential drawback of Ibrutinib therapy is that it is usually prescribed for life, increasing the opportunity for resistance mutations to arise, a phenomenon that has already been observed (77,78). In patients where resistance develops, subsequent outcomes have been

shown to be poor (79). Therefore, as with Venetoclax, combinations of Ibrutinib with other agents may be the best option to avoid resistance.

Idelalisib, Venetoclax and Ibrutinib represent the three most investigated and widely-used targeted therapies for CLL, however there are several other treatments at varying stages of trials and research that may hold promise as future weapons in the therapeutic arsenal (80).

Acalabrutinib is a second-generation inhibitor of BTK that has shown increased specificity and reduced off-target effects compared to Ibrutinib, while maintaining clinical efficacy (81,82).

The enzyme SYK forms part of the BCR signal transduction pathway and JAK performs a similar role downstream of the IL-4 receptor, which is engaged by CLL cells in lymph nodes. Therefore, these pathways have been targeted in CLL with Cerdulatinib, a dual inhibitor of both SYK and JAK, with promising *in vitro* results both alone and in combination with Venetoclax (83).

There has also been interest in inhibitors of Exportin 1, a nuclear protein which regulates translocation of proteins including pro-apoptotic proteins out of the nucleus. Studies have demonstrated efficacy for these inhibitors in pre-clinical and also Ibrutinib-resistant models, potentially opening a new therapeutic angle (84,85).

1.2 T Cell Immunology

The immune system is comprised of two main arms, the innate and the adaptive immune systems, which perform complementary roles in protecting the host from pathogenic infections and cancer. Both systems are able to discriminate between self and non-self targets in order to prevent autoimmune responses that could harm the host. The innate immune system consists of a number of evolutionarily conserved defence mechanisms, including proteins and a variety of cell types which recognise and rapidly respond to commonly expressed targets on pathogens. In contrast, the cells of the adaptive immune system can respond in a specific manner to individual infections or non-self antigens, with the repertoire of recognised antigens unique to each person (86,87).

The adaptive immune system comprises two primary cell types: B cells and T cells. These specialist lymphocytes are named after their development locations – B cells develop in the bone marrow while T cell development occurs in the thymus. B cells are responsible for humoral immunity, producing antibodies that recognise non-self antigens with very high affinity. T cells are the central protagonists of cell-mediated immune responses, playing vital roles both in killing infected or cancerous cells and in supporting the activity of other immune cells (86,87).

1.2.1 T Cell Development

T cell development is a tightly controlled process (summarised in *Figure 1.2*) that takes place in the thymus. This is a specialised primary lymphoid organ that

nurtures and directs the development of T cell precursors, which are known as thymocytes while resident in the thymus (88,89). The purpose of the thymus is twofold: to produce a repertoire of T cells with a wide range of specificities and to restrict autoreactivity to prevent potentially harmful T cells from reaching the periphery (88). Key to these functions are the structure and cellular composition of the thymus itself. The thymus is composed of two lobular lobes, containing two distinct regions of stroma: the outer cortex and the inner medulla. Both of these stromal areas are formed from an organised network of cells, including thymic epithelial cells (TECs) and fibroblasts, that together provide the requisite cytokines, chemokines and other signals that direct and control thymocyte maturation and migration (89–92).

1.2.1.1 Double Negative Thymocytes and β -Selection

The process of T cell development begins with immature haematopoietic precursors, which travel in the peripheral blood from the bone marrow to the thymus, entering at the cortico-medullary junction where they undergo a period of expansion before migrating through the thymic cortex. These cells do not express either CD4 or CD8 and are therefore termed double negative (DN), and can be subdivided into four developmental stages (DN1-4) (93,94). By the DN3 stage, Recombination-Activating (RAG) genes have been upregulated, allowing VDJ recombination to take place. During this process, the variable (V), diversity (D) and joining (J) gene segments of the T cell receptor (TCR) β , γ and δ chains genes are randomly rearranged by recombinase enzymes to give a final exon that can be

expressed (95). Successful rearrangement of the TCR γ and TCR δ chains commits the thymocyte to becoming a $\gamma\delta$ T cell, the process of which will not be covered in further detail here. In contrast, productive rearrangement of the TCR β chain will lead to this being expressed at the cell surface, in a complex with an invariant pre-T α chain and CD3, termed the pre-TCR. If the pre-TCR is functional, signalling through it will promote maturation of the thymocyte to the DN4 stage as well as proliferation. This signalling also triggers allelic exclusion, which prevents further rearrangement of the TCR β chain by switching off RAG genes. In cases where the pre-TCR is non-functional, the thymocyte will undergo apoptosis. This process of verifying successful rearrangement of the TCR β chain is known as β -selection (93,94).

1.2.1.2 Double Positive Thymocytes and Positive Selection

Continued signalling through the pre-TCR in DN4 thymocytes induces expression of both CD4 and CD8, to give double positive (DP) thymocytes. In these DP cells, there is a re-expression of RAG genes to facilitate rearrangement of the TCR α chain gene, via the same mechanisms used previously. The newly generated TCR α chain can displace the pre-T α from the pre-TCR to form a mature TCR complex (90,96). Since each thymocyte will express a unique TCR, the pool of thymocytes will contain a wide range of specificities. Therefore, TCRs on DP thymocytes must be assessed for major histocompatibility complex (MHC) restriction by cortical TECs, which express a diverse range of rare peptides to be presented by MHC molecules (90,91). This process, termed positive selection, aims to produce a pool of potentially

competent T cells by blocking the development of both harmful and non-functional thymocytes.

The outcome of the interaction between the nascent TCR and TEC-bound MHC depends on the affinity of the binding, with three possible results. Thymocytes with a high TCR:MHC binding affinity are induced undergo apoptosis, due to their potentially detrimental autoreactivity. In thymocytes whose TCR fails to bind to MHC, further rounds of TCR α gene rearrangement, controlled by RAG genes, can take place, with the new TCR α chain replacing the previous one. This process can be repeated for as long as the thymocyte survives, usually only a few days (97). Those thymocytes whose TCR can bind MHC complexes with low to moderate affinity receive the requisite signals for survival and maturation into single positive (SP) cells, expressing either CD4 or CD8 alone. Which lineage each cell follows also depends on the TCR:MHC interaction – binding to MHCI promotes SP8 differentiation, while binding to MHCII leads to SP4 differentiation (90,96,98).

1.2.1.3 Single Positive Thymocytes and Negative Selection

Following differentiation into SP cells, thymocytes migrate from the thymic cortex to the medulla. Having undergone the process of positive selection, there remains a broad range of TCR specificities, some of which may recognise self-peptides and cause autoimmunity. In order to prevent this, thymocytes are screened for reactivity to self-peptides in the process of negative selection (96,98).

Within the thymic medulla reside a large number of medullary TECs, which are the main protagonists of thymocyte negative selection. These cells display

the unique property of being able to express, and present on MHC molecules, a diverse range of tissue-restricted antigens – self-peptides whose expression is otherwise confined solely to individual peripheral tissues. This characteristic promiscuous gene expression is the result of epigenetic mechanisms under the control of the autoimmune regulator (Aire) gene (99–101). Studies have demonstrated that the Aire gene is pivotal in developing self-tolerance in the T cell pool, with loss of Aire function being fatal in mice and causing the autoimmune disease APECED (Autoimmune PolyEndocrinopathy Candidiasis Ectodermal Dystrophy) in humans (101,102). Medullary TECs have also been shown to be able to transfer self-peptide:MHC complexes to medulla-resident dendritic cells, allowing these cells to also screen for autoreactive thymocytes (103).

Similarly to positive selection (see *Section 1.2.1.2*), the outcome of the negative selection process depends on the affinity of the interaction between the TCR and self-peptide:MHC complexes in the medulla. High affinity TCRs represent the potential for harmful autoimmunity and thymocytes carrying such receptors are induced to undergo apoptosis. For thymocytes whose TCR can only bind with low affinity, this interaction promotes their survival and maturation (96,98). Mature thymocytes upregulate sphingosine 1-phosphate receptor 1, which permits these cells to emigrate from the thymus into the peripheral blood by following the sphingosine 1-phosphate (S1P) gradient created by the high concentration of S1P in the blood (104). Thymocytes which express a TCR of moderate affinity for self-peptide:MHC upregulate the transcription factor FoxP3, directing these cells to

become natural regulatory T cells (nT_{Reg}), which promote immune tolerance in the periphery (105).

1.2.2 Major Types of T Cell

Following their emigration from the thymus as fully developed naïve cells, T cells travel in the blood and can home to a variety of tissue and lymphoid system locations. The functions, as well as the locations, of mature T cells in the body are in part determined by the subtype of each T cell, as well as other factors including cytokines and the impact of molecules such as vitamin D (106). Broadly, T cells can be categorised as conventional (comprising the classical $\alpha\beta$ T cells described throughout *Section 1.2.1*) and non-conventional (consisting of a number of subtypes) (86). Both categories, and the subpopulations they contain, will be discussed in this section.

1.2.2.1 CD4⁺ Conventional T Cells

CD4⁺ T cells are the key orchestrators of the adaptive immune response, supporting and regulating the functions of other immune cells. CD4⁺ T cells are activated by recognition of cognate antigens presented by MHCII on APC, in the presence of co-stimulatory molecules and their functional significance extends across pathogenic infections, autoimmune diseases, allergies and cancer (107).

The CD4⁺ pool represents a highly diverse array of different subsets, which have complementary and sometimes overlapping effector functions. A varying number of subsets can be defined, with new and increasingly specific subpopulations regularly described in the literature. However, the extent to which these subsets differ and the boundaries between the various populations are frequently not clear, often due to differences in the depth of phenotypic and functional analysis carried

out. Nevertheless, there are several widely accepted subsets that have been the subject of much research and will be discussed here: T_H1 , T_H2 , T_H17 , T_{FH} and T_{Reg} (86,108).

T_H1 cells play a vital role in the immune response to intracellular pathogens, including bacteria and viruses. The transcription factor T-bet is the master regulator of the T_H1 phenotype, with upregulation of this protein induced by activation of naïve T cells in the presence of IL-12, which is secreted by macrophages and dendritic cells as part of the innate immune response to infection (109). T-bet induction, and therefore T_H1 polarisation, is also aided by IFN γ , which is produced by a subset of NK cells in lymph nodes (108,110,111). T_H1 cells are characterised by their production of IFN γ , which can then promote other T cells to become T_H1 polarised in a positive feedback loop, with other cytokines produced including IL-2 (108,111). IFN γ functions to activate macrophages and increase their ability to kill pathogens, as well as increasing MHC expression in target cells (112), while IL-2 stimulates T cell proliferation and plays a role in the induction of memory T cells (113). CXCR3 expression is also characteristic of T_H1 cells, with this chemokine receptor playing a vital role in allowing entry to inflamed tissues (108,114).

T_H2 cells are key players in host defence against extracellular parasites and are also involved in allergies (111,115). Development of a T_H2 phenotype is directed by the transcription factor GATA-3 (116,117), expression of which is induced when naïve T cells are activated in the presence of IL-4, with IL-2 also playing a critical role (118–120). T_H2 cells can be characterised by their expression of CCR4 and CRTH2 (121,122). This latter molecule is a receptor for prostaglandin D2, which is produced

by both mast cells and T_H2 cells themselves (123). Activation of this receptor mediates chemotaxis and prevents apoptosis, as well as inducing expression of the characteristic T_H2 cytokines (124). These cytokines include IL-4, IL-5 and IL-13, with IL-4 production aiding the generation of further T_H2 cells in a positive feedback loop (116). The functional role of IL-4 is to mediate B cell antibody class switching to IgE, promoting basophil and mast cell activation (107,125). IL-5 is the key regulator of eosinophil recruitment to the site of immune challenge (126), while IL-13 is the primary cytokine responsible for helminth expulsion from the gut, and can also induce IgE class switching (127).

T_H17 cells have a critical function in the host immune response to extracellular bacteria and fungi, but have also been found to play a role in autoimmunity (128). The master regulator of the T_H17 phenotype is the transcription factor ROR γ t (129), induction of which occurs upon activation of naïve T cells alongside signalling from a number of cytokines, including TGF β , IL-6 and IL-21 (129–131). A role for IL-23 in T_H17 development has also been shown, although this effect is seen only after initial differentiation has occurred (108,132). T_H17 cells are so named due to their characteristic production of IL-17, with the IL-17a and IL-17f forms most prominent (133). The functions of IL-17 are highly pro-inflammatory and include recruitment of neutrophils and other immune cells via upregulation of chemokines, increasing cytokine production by macrophages and T cells and promoting the barrier function of epithelia (107,133). T_H17 cells can also produce IL-21, which can stimulate further T_H17 cell differentiation as well as increasing NK cell cytotoxicity and promoting plasma cell differentiation (131,134). Other characteristic

markers of T_H17 cells include expression of the chemokine receptors CCR6 and CCR4, which control tissue homing, and the IL-23 receptor, signalling through which promotes proliferation and cytokine production (135,136).

T follicular helper (T_{FH}) cells are a specialist subset with a crucial function in regulating B cell activities, which includes roles in the formation of germinal centres, antibody class switching and affinity maturation and the development of B cell memory (137–139). The T_{FH} phenotype is driven by expression of the transcription factor BCL6 (140), but the exact factors that determine differentiation of naïve T cells into T_{FH} have not been fully elucidated (108). Similar to T_H17 cells, the cytokines IL-6 and IL-21 have been shown to be important for T_{FH} development, but with no role for TGFβ – there is some debate as to whether T_{FH} cells develop as an independent lineage or from other helper T cell subsets (137,141,142). The definitive marker for T_{FH} is CXCR5, a chemokine receptor which permits homing to B cell follicles, while there is also characteristic expression of ICOS and PD-1 (143–145). Functionally, T_{FH} cells produce IL-4 and IL-21 and provide survival and proliferative signals such as CD40L for germinal centre B cells, as well as being able to induce apoptosis in B cells via FasL (146–148).

T_{Reg} cells are the major antagonists of adaptive immunity, acting to prevent autoimmune reactions and suppress immune responses to avoid damage to the host (149). The master regulator of the T_{Reg} phenotype is the transcription factor FoxP3 (150), which can be induced intra- or extra-thymically. In the thymus, thymocytes expressing a moderate affinity TCR during negative selection are induced to express FoxP3 and are termed nT_{Reg} cells (105). In the periphery, activation of naïve T cells in

the presence of TGF β and IL-2 has been shown to induce FoxP3 expression and a regulatory phenotype – these cells are termed induced T_{Reg} (iT_{Reg}) cells (151–153). As well as constitutive FoxP3 expression, T_{Reg} cells can be characterised by the combination of high CD25 and low CD127 (154). The functional activity of T_{Reg} cells is underpinned by several mechanisms, including expression of a number of immunosuppressive cytokines such as TGF β (which can help to promote further T_{Reg} cell differentiation), IL-10 and IL-35 (155–157). The characteristic high expression of CD25, which is a high affinity receptor for IL-2, allows T_{Reg} cells to deplete IL-2 and therefore reduce other effector T cell proliferation (158). Also, T_{Reg} may be able to directly lyse effector cells using granzymes and perforin (159).

1.2.2.2 CD8⁺ Conventional T Cells

Where CD4⁺ T cells are the orchestrators of adaptive immune responses, controlling and directing the differentiation and function of other immune cells, CD8⁺ T cells play a more direct effector role in these responses, through their ability to directly kill pathogens and cancerous cells (160).

Following emigration from the thymus, naïve CD8⁺ T cells circulate between the peripheral blood and lymph nodes, where they can be primed by recognition of their cognate antigen displayed by antigen-presenting cells (APCs) (160). APCs present antigenic peptides on MHC I and express co-stimulatory molecules such as CD28 and CD40, which combined lead to activation of CD8⁺ T cells (161). Following their activation CD8⁺ T cells can differentiate into cytotoxic T lymphocytes (CTLs). This process is directed by signalling from a number of cytokines, in particular IL-2, as well

IL-12, IL-21 and IL-27. IL-2 signalling leads to the upregulation of the transcription factor BLIMP-1, which acts a master regulator of CTL differentiation (162,163).

CTLs are the major protagonists of adaptive immune system cytotoxicity. Several proteins are utilised to carry out this cytotoxic function, with granzyme B and perforin of particular importance. Perforin molecules insert directly into the target cell membrane and assemble polymeric structures that form pores – these function both to induce osmotic lysis of the target cell and to provide a route of entry for granzymes (164,165). Granzymes are a family of serine proteases with non-redundant complementary mechanisms of action that function to induce cell death. Granzyme B is the most potent molecule and acts by cleaving and activating the pro-apoptotic protein BID, leading to further downstream apoptotic signalling (166). Granzyme A acts to disrupt mitochondrial metabolic activity, leading to reactive oxygen species production and triggering DNA damage and apoptosis (167). The non-redundant mechanisms of granzymes increase the effectiveness of cell killing, allowing resistance mechanisms, such as upregulation of anti-apoptotic proteins, to be overcome (165).

CTLs harbour huge quantities of their main effector molecules perforin and granzyme B in cytoplasmic granules – over 1×10^7 molecules per cell of each protein have been observed recently (168). These granules are maintained ready for rapid release upon TCR recognition of the CTL target antigen presented on MHCI (169). Such recognition triggers downstream signalling that causes cytoskeletal rearrangement, allowing trafficking of the cytotoxic granules to the immune synapse for directed release towards the target cell (170). Each CTL stores sufficient granules

to kill multiple target cells and can also secrete granzymes and perforin directly, without trafficking into granules, in cases of serial killing (171).

Secretion of perforin and granzymes is not the only method by which CTLs can kill target cells. A feature of CTLs is expression of Fas ligand, which is stored intracellularly and transported to the cell surface following release of perforin and granzyme B (172). Fas ligand can then bind to its receptor Fas, which is widely expressed across most cell types (173). Engagement of Fas ligand with Fas triggers activation of caspases and leads to apoptotic cell death (174,175). This Fas-Fas ligand interaction can also be used by CD4⁺ cells to trigger apoptosis in some circumstances (176).

As well as their direct cytotoxic effects, CD8⁺ T cells can contribute to the control of immune responses by cytokine release. Although to a lesser extent than their CD4⁺ counterparts, CD8⁺ cells can secrete IL-2, prompting a positive feedback loop to promote differentiation of CTLs (177). Furthermore, CD8⁺ cells can produce IFN γ and TNF α , promoting T_H1 cell differentiation and enhancing the local immune response (178,179).

CD8⁺ T cells can also have an immune antagonistic, regulatory function. During immune responses, CD8⁺ cells can upregulate production of the immunosuppressive cytokine IL-10, becoming the major source of IL-10 in local inflamed tissue (180,181). These IL-10 secreting cells demonstrate greater cytotoxicity and cytokine production than IL-10⁻ cells, meaning that they combine effector and regulatory functions (160).

1.2.2.3 Non-Conventional T Cells

Outside of conventional CD4⁺ and CD8⁺ T cells, there are a number of other types of T cell that form small, but important, minorities of the overall pool. These cells often function as a bridge between the innate and adaptive immune responses, displaying characteristics usually associated with only one system. The number of defined non-conventional T cell types, and the distinctions between them, changes frequently as deeper analysis and ever more powerful cell sorting techniques are developed, but three of the most well-characterised will be discussed here (182).

Natural killer T (NKT) cells are a distinct population of T cells, comprising around 0.1% of peripheral blood T cells in humans, which develop in the thymus but diverge from the conventional development pathway (183). These NKT cells express a very limited range of TCRs – invariant NKT cells express an invariant TCR α chain complexed with a constrained repertoire of TCR β chains, while Type II NKT cells have one of a small number of certain TCR α chains (184). As a result, NKT cells recognise and bind glycolipids presented by the MHC-like molecule CD1d on cortical DP thymocytes for their positive selection, as opposed to conventional thymocytes binding to MHC (184). Restriction to recognition of glycolipid antigens, such as bacterial cell wall components, via their presentation by CD1d is the key distinguishing feature of NKT cells (185). Functionally, following activation after recognition of an antigen NKT cells can kill target cells and can rapidly produce large amounts of cytokines. The specific cytokine profile of each cell depends on both the subset (NKT subsets analogous to T_{H1}, T_{H2}, T_{H17}, T_{Reg} and T_{FH} cells have been described) and the location/surrounding cells (183,186). The conserved TCR

specificity combined with the range of effector functions means NKT cells a form of 'hybrid' between the innate and adaptive immune responses (183).

Another 'hybrid' non-conventional T cell population is mucosal-associated invariant T (MAIT) cells, which share a number of similarities with NKT cells and can comprise up to 10% of blood T cells (182). MAIT cells also undergo the early stages of development in thymus, but are positively selected by productive binding to the MHC-like molecule MR1, which is expressed on DP thymocytes (187). Like NKT cells, MAIT cells express a conserved, invariant TCR α chain in complex with a TCR β chain from a small repertoire, which bestows on them their characteristic MR1 restriction and recognition of B vitamin metabolites (188). Such antigens are mainly associated with bacteria, and MAIT cells are highly enriched in the gut where they are likely to play a role in preventing opportunistic infections from the microbiome. MAIT cells are functionally similar to NKT cells, able to act as direct cytotoxic killer cells as well as producing cytokines to support the wider immune response and cross-talk with both innate and adaptive immune cells (182,189).

The subject of much recent interest, $\gamma\delta$ T cells combine some of the innate-adaptive 'hybrid' features of NKT and MAIT cells with more conventional T cell characteristics to form a heterogeneous and complex population (190). $\gamma\delta$ T cells comprise 0.5-10% of peripheral blood lymphocytes but are often found resident in tissues such as the skin and the lung (182,191). As mentioned in *Section 1.2.1.1* $\gamma\delta$ T cells develop in the thymus from early T cell progenitors, when VDJ recombination produces functional TCR γ and TCR δ chains – however, the final TCR is not MHC-restricted, meaning these cells can potentially respond to non-peptide antigens.

Although the recombination process has the potential to give rise to a hugely diverse repertoire of TCRs, some populations of $\gamma\delta$ T cells, such as those in the epidermis, are highly oligoclonal, perhaps recognising specific conserved pathogenic antigens (190). This reduced repertoire of antigen recognition means that $\gamma\delta$ T cells can respond more rapidly than conventional T cells to immune challenge and as such form a bridge between innate and adaptive immune responses. As well producing inflammatory cytokines (including IL-17) and carrying out cytotoxic functions, $\gamma\delta$ T cells can also act as APCs, migrating from their resident tissue to lymph nodes to enhance the conventional adaptive immune response (190,191).

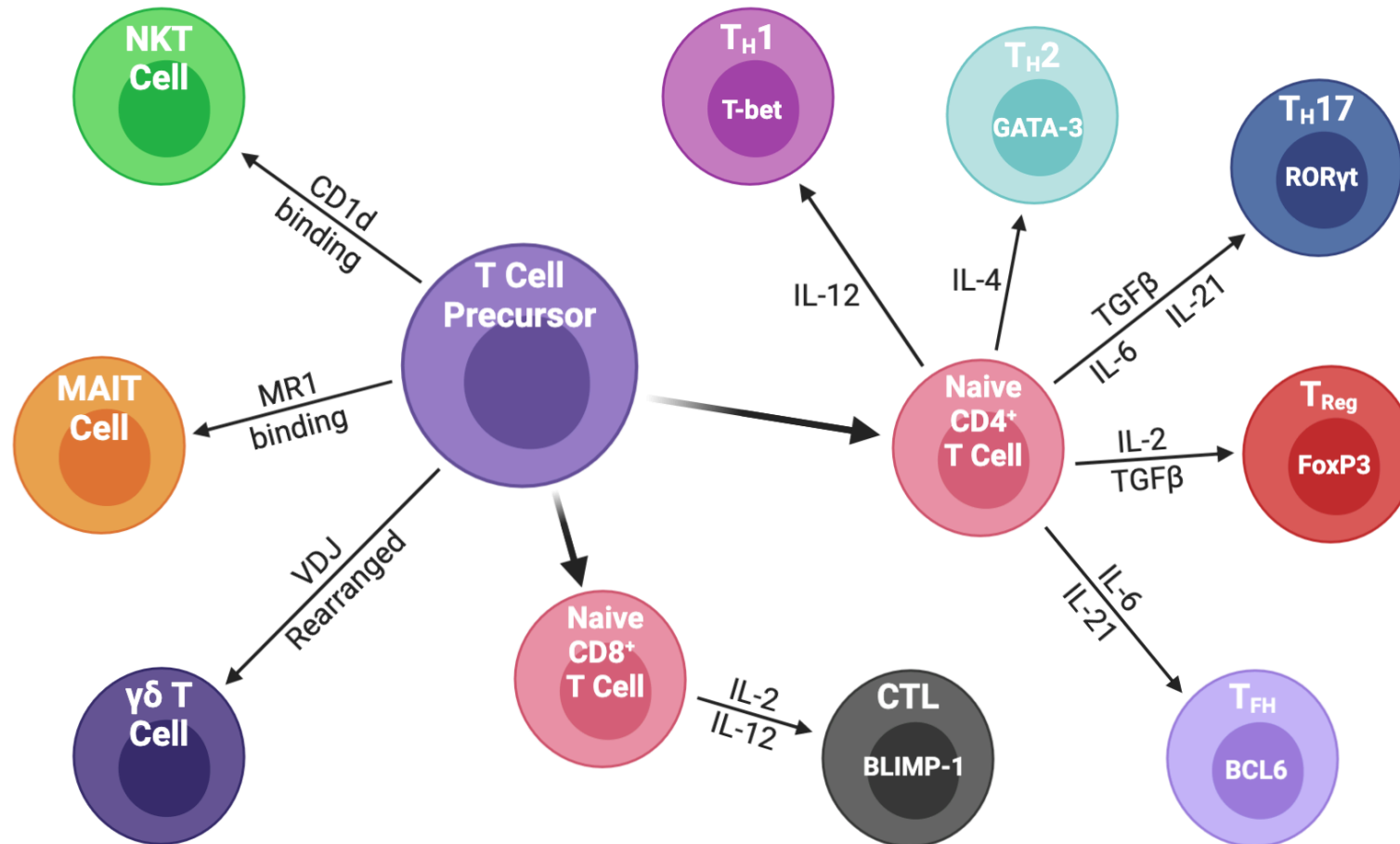


Figure 1.3: The Primary T Cell Types

T cell precursors from the bone marrow to the thymus, where they develop and mature into conventional naïve T cells or non-conventional T cells. Conventional naïve CD4⁺ T cells can differentiate into five major subtypes upon activation, dependent on the simultaneous cytokine signals received, with each differentiation programme control by a master transcription factor. Conventional naïve CD8⁺ T cells can differentiate into cytotoxic T lymphocytes (CTL) following appropriate cytokine signalling, under the control of the transcription factor BLIMP-1.

1.2.3 Recognition of Antigen and T Cell Activation

As mentioned previously, conventional T cells require recognition of their cognate antigen, presented by MHC molecules, for their activation. Non-conventional T cells also recognise antigens through their TCR, with these antigens presented by MHC-like molecules utilising alternative antigen processing mechanisms that will not be covered here. The specificity of the TCR ensures that only the appropriate T cells can receive full activation signalling, both at sites of infection or cancer and in secondary lymphoid organs (192).

The cell presenting peptide:MHC complexes to T cells is known as an antigen-presenting cell (APC). Most cells within the body can act as targets for CD8⁺ T cells, since they express MHCI and so present peptides from intracellular pathogens or mutant proteins – TCR recognition of these complexes will lead to direct cell killing by activated CTLs (160). However, for the priming of CD8⁺ T cells and the activation of CD4⁺ T cells, so called professional APCs are required. The main professional APCs are dendritic cells (DCs), but the role is also shared by B cells, macrophages and some monocytes (193–196). DCs are defined by their capacity to take up and process antigens and present these to T cells, and are specialised for this function by their expression of both MHCI and MHCII, as well as co-stimulatory molecules including CD28 and CD40 (193,197). B cells also constitutively express MHCI and MHCII, but only upregulate expression of co-stimulatory molecules after activation (194). Macrophages and monocytes can express MHCI and MHCII, as well as co-stimulatory molecules, and can survey tissues for antigens while circulating between blood, tissues and lymph nodes (195,196).

The presentation of antigen on MHCI, for CD8⁺ T cells, relies on the processing of endogenous proteins in cancerous or infected cells. Proteins in the cytosol, either host cell-derived or virally encoded, are degraded by the proteasome into short peptide fragments (198). During an immune response, IFN γ signalling leads to the formation of the immunoproteasome, which bears different cleavage specificities and so generates an alternative peptide repertoire for presentation (199). The newly generated peptides are transported into the endoplasmic reticulum and processed by aminopeptidase enzymes to reduce them to 8-11 amino acid fragments. These fragments are loaded onto MHCI molecules by the multimeric peptide-loading complex, which also controls the formation of the MHCI complex itself (192). In cases of a high affinity binding of the peptide fragment to MHCI, the peptide:MHC complex will be transported to the cell surface via the Golgi apparatus. Where peptide:MHC complexes are sub-optimal, they may be returned to the peptide-loading complex for further modification (192,200).

Whereas MHCI can be found on almost all cells, MHCII is expressed by professional APC and certain epithelial cells (201). MHCII molecules usually present exogenous proteins, which must be captured from the extracellular milieu via endocytic mechanisms, such as phagocytosis or clathrin-mediated endocytosis. Endogenous proteins can also be presented following degradation, with autophagy believed to be a key pathway in the formation of peptides (202). For endocytosed proteins, fusion of the endosome with lysosomes allows proteases to begin to degrade the protein. MHCII molecules are formed in the endoplasmic reticulum,

similar to their MHCI counterparts, but are bound by an invariant pseudopeptide to block the peptide binding groove. This complex is then transported, via the cell surface, to a specialised endosome known as the MHC Class II compartment (MIIC) (203), wherein cathepsin proteases lyse the invariant pseudopeptide, which is replaced by the peptide CLIP in the MHCII peptide binding groove. The partially degraded extracellular proteins in the endolysosome, or endogenous peptide fragments, can enter the MIIC where they can be further processed into fragments 10-30 amino acids long (192). Catalysed by the protein HLA-DM, peptide fragments with sufficient binding affinity can be exchanged for CLIP and bind to the MHCII complex, which is then transported to the cell surface for presentation (204).

1.2.4 T Cell Memory

During an immune response to either infection or cancer, naïve T cells that have not 'seen' their cognate antigen before are activated. This activation process leads to large expansion of the activated cells and the differentiation of naïve cells into one of two broad categories: short-lived effector cells (SLECs) or memory precursor effector cells (MPECs) (205,206). SLECs comprise the majority of the differentiated population (90-95%) and carry out their effector functions before undergoing apoptosis following resolution of the immune response. MPECs form the smaller proportion of the population, and can also carry out effector functions, but are destined to avoid apoptotic death and instead develop into long-lived memory cells that can rapidly respond to future stimulation with the same antigen (207–209).

Despite their different fates, both SLECs and MPECs demonstrate similar levels of effector functionality, such as cytotoxicity, during the immune response (205,210).

There are two primary subsets of memory T cells formed from the MPEC pool: central memory (T_{CM}) and effector memory (T_{EM}) cells. T_{CM} are mainly constrained to secondary lymphoid organs while T_{EM} cells are usually found circulating between the blood and tissues (211–213). In order to home to, and be retained in, lymph nodes, T_{CM} constitutively express the homing receptors CCR7 and CD62L. In contrast, T_{EM} do not express CCR7, instead being able to express a range of chemokine receptors required for homing to different tissues, such CXCR4 and CCR5 (111,214). Both T_{CM} and T_{EM} express the CD45RO isoform, distinguishing them from naïve T cells which instead express the CD45RA isoform.

The roles of the two subsets are complementary and this is reflected in their expression of key proteins and cytokines. T_{EM} act as sentinels, providing a rapid effector response at local sites upon reinfection. This response includes cytotoxic function via perforin and granzyme release from $CD8^+$ T_{EM} and secretion of cytokines including IFN γ and IL-4 from $CD4^+$ T_{EM} . In contrast, T_{CM} secrete IL-2 and retain a high proliferative capacity, meaning they can rapidly expand and differentiate into effector cells following a repeat antigen challenge. In this manner, T_{EM} cells provide immediate responses to local challenge but lack the capacity for expansion, while T_{CM} can respond to systemic challenge and give rise to a second wave of effector cells to support T_{EM} responses (214–216). The proportions of each subset differs between $CD4^+$ and $CD8^+$, with a majority of $CD4^+$ cells found to be T_{CM} , while T_{EM} comprise most of the $CD8^+$ T cell population (213,214).

A third subset of memory T cells has been described, which represents cells that are terminally differentiated. These cells are termed T_{EMRA} due to their characteristic re-expression of CD45RA in place of CD45RO, and lack expression of the homing receptors CCR7 and CD62L and the co-stimulatory molecules CD27 and CD28 (111,217). These T_{EMRA} cells have a reduced proliferative capacity and bear hallmarks of replicative senescence, including expression of CD57, as well as being susceptible to apoptosis (217–219). However, T_{EMRA} cells demonstrate potent effector functions, including cytotoxicity and secretion of pro-inflammatory cytokines such as $IFN\gamma$ (217,219,220). Interestingly, this replicative senescence phenotype may not be permanent, with several studies showing that proliferative potential could be at least partially restored in T_{EMRA} cells (221–223).

Until recently, the paradigm of memory T cell differentiation followed a linear pattern through the three subsets outlined above: $T_{CM} \rightarrow T_{EM} \rightarrow T_{EMRA}$. However, the existence of another memory subset has been demonstrated, which sits below T_{CM} as the least differentiated population (224). These cells have been termed T memory stem cells (T_{SCM}) due to their stem cell-like properties, particularly self-renewal and the capability to differentiate into all of the various memory and effector T cell subsets (224,225). In terms of surface markers, T_{SCM} resemble naïve T cells in their expression of CD45RA and CCR7, along with CD62L, CD28 and CD27, although they do also express molecules not associated with naïve cells, including Fas (224). However, functionally T_{SCM} are more similar to T_{CM} and T_{EM} than naïve cells, displaying high proliferative capacity and potent antitumour activities (224,226). The

balance between the T_{SCM} phenotype and development into more differentiated subsets is controlled by the transcription factors T-bet and EOMES, the activities of which can be regulated by asymmetric cell division (227,228). Overall, T_{SCM} appear to be a crucial T cell subset that can maintain the pool of more differentiated memory T cells. This is of particular importance in the context of chronic infections and cancer, where generation of terminally-differentiated and exhausted T cells leads to the requirement for replenishment of the pool of less-differentiated effector cells (225).

Recent studies have reported a new family of memory T cells, termed tissue resident memory cells (T_{RM}), which follow a separate differentiation pathway from the conventional paradigm above (229). The role of these T_{RM} cells is to enhance local protection from immune challenge, particularly at mucosal sites, similar to T_{EM} cells. Despite similarities in their function, T_{RM} and T_{EM} have been demonstrated to have different transcriptional signatures (230). T_{RM} cells have been shown to develop from the same naïve T cells as conventional memory cells, but are generated when these naïve cells migrate through epithelia into tissues and receive signals such as IL-15 and TGF β (230,231). However, the phenotype of T_{RM} cells appears to be heterogeneous, with different patterns of marker expression found in different tissue contexts – it is likely that differences in local signalling lead to the development of the heterogeneity observed (229,232).

1.3 T Cells in CLL

CLL is a cancer of B cells, however it is not only in this compartment where stark differences are observable in CLL patients – the other key protagonists of the adaptive immune system, T cells, are also affected. At a basic level, changes to the numbers of T cells, and the distribution of memory subsets, are seen. Furthermore, although they are not malignant, the T cells in CLL patients display a range of abnormalities and functional differences when compared with those from healthy counterparts.

When investigating CLL, it is important not to consider only the leukaemic cells in isolation. Although currently not well elucidated, the cross-talk and interactions between CLL cells and abnormal T cells are vital to understanding the pathophysiology of CLL. However, there remain a number of unanswered questions about the nature and role of T cells in CLL, most pertinently whether they drive disease development or are bystanders reacting to the malignant environment around them.

1.3.1 Composition of the T Cell Compartment in CLL

The fact that CLL patients display abnormalities in the T cell compartment alongside their leukaemic B cells has been known for over 40 years. Initial studies, although rather crude, were able to determine that CLL patients had greater numbers of T cells than healthy controls, with a particular increase in the number of CD8⁺ T cells (233,234). Further work in this area observed that in many CLL patients,

the ratio of CD4⁺:CD8⁺ T cells was changed in comparison to healthy controls, in whom the ratio is approximately 2:1. There appeared to be preferential expansion of the CD8⁺ compartment leading to a decreased, and sometimes inverted, CD4⁺:CD8⁺ ratio, wherein CD8⁺ T cells outnumbered their CD4⁺ counterparts (235–237). Although such changes in ratio could alternatively be explained by a loss of CD4⁺ cells, increasing the relative proportion of CD8⁺ cells, as seen in HIV infection (238), this was found not to be the case, with both subsets having increased numbers in CLL (233).

The presence or absence of an inverted ratio has been shown to have clinical relevance and may be an important marker of patient prognosis. Initial work observed an association between inverted ratios and advancing disease stage (236), as well as the key CLL feature hypogammaglobulinaemia (234). More recently, a number of studies have investigated patient outcomes in relation to CD4⁺:CD8⁺ ratio. An inverted ratio was demonstrated to be an independent factor associated with both shorter time to first treatment (TTFT) and overall survival in CLL patients, irrespective of other prognostic factors (19,239). The inverse was also observed, with a ratio of greater than 1, considered normal, was a factor associated with stable, non-progressive CLL (22).

As well as changes in the numbers of T cells and the CD4⁺:CD8⁺ ratio, CLL patients often present with differences in the various subsets of T cells, particularly within the CD4⁺ compartment.

The most commonly investigated of these subsets has been T_{Reg} cells, owing to their important role in many cancers. A number of studies have been able to demonstrate significant increases in the frequency of T_{Reg} cells in CLL patients compared to healthy controls (240–242), as well as associating these increases with advancing disease stage (243). The effect appears to be enhanced within the lymph nodes, wherein a significantly greater proportion of T_{Reg} can be found compared to the peripheral blood (244). However, whether there is an active role in CLL pathogenesis for these T_{Reg} remains unclear. Despite their increased frequency, T_{Reg} still constitute only a small proportion of the overall T cell population and there appears to be significant heterogeneity within the T_{Reg} population itself (241). The heterogeneity may extend to T_{Reg} function, with some studies demonstrating T_{Reg} lose their immunosuppressive abilities in CLL patients (242) while others suggest that the CD4⁺ T cell population as a whole is driven towards a regulatory function in CLL (240). The contrary nature of the observations of T_{Reg} in CLL make a definitive role for this subset difficult to elucidate.

Although not well studied, several other functional T cell subsets have been reported to show differences in CLL. T_H17 cells, which secrete the pro-inflammatory cytokine IL-17, have been observed to be significantly increased in CLL compared to healthy donors (242). These cells may confer a protective effect for CLL patients, with T_H17 lower frequencies associated with poor prognostic markers (245). As may be expected in a B cell malignancy T_{FH} cells, which provide support to B cells in germinal centres, have been observed at increased frequencies in CLL patients (246,247), with a significantly greater proportion found in the lymph nodes compared to peripheral

blood (244). However, unlike T_H17 cells, no associations were found between T_{FH} frequency and either disease stage or IGHV mutation status (246). Unusually, CD4⁺ T cells expressing the cytotoxic molecules granzyme B and perforin can be detected at significantly increased frequencies in CLL (248). These cells are typically rare in healthy controls, except in conditions of chronic viral infection, and were found to be phenotypically similar to mature CD8⁺ CTLs and mainly from a T_H2 background.

With few studies having been conducted to date, it is difficult to draw strong conclusions regarding the roles potentially played by the various expanded T cell subsets in CLL. Taken together though, the changes in subsets are indicative of the wider abnormality of the T cell population in CLL patients.

1.3.2 T Cell Differentiation and Ageing

As well as expansions of various functional types of T cell, CLL patients also present with distinctive changes in the distribution of T cells along differentiation and memory pathways. A number of studies have consistently observed a decrease in the proportion of naïve T cells in CLL, with a concomitant increase in the frequency of more highly differentiated cells (249–252). As well as being observable in CLL patients as a whole, the magnitude of the shift towards greater differentiation appears to be correlated with disease prognosis – those patients with high risk ZAP70 expression (249) or unmutated IGHV genes (252) showed greater relative reductions in naïve T cells and increases in effector memory cells.

The biasing of the T cell compartment towards more differentiated cells is not constrained solely to CLL, in fact it is a characteristic hallmark of the ageing process

(253). A large scale study in Sweden observed that the number of naïve T cells decreased throughout adult life, particularly in the elderly (>60 years old) – interestingly this phenomenon was markedly more pronounced in males (254). With CLL being a disease mainly of the elderly and showing significant gender bias, as well as increased T cell differentiation, there could be an argument that ageing, rather than disease, can explain the changes observed in CLL. However, CLL patients consistently show greater T cell memory subset skewing than age-matched controls, while a significant proportion of CLL patients would not be considered elderly. Therefore, it appears that though ageing may be important, it cannot fully explain the differences in the distribution of T cell memory subsets in CLL.

Changes to the T cell compartment caused by ageing are also unable to fully account for the high prevalence of inverted CD4⁺:CD8⁺ ratios in CLL patients. Although the number of healthy individuals presenting with an inverted ratio doubles when comparing 60-94 year olds to 20-59 year olds, it still only comprises 16% of the elderly population (254). By contrast, the proportion of CLL patients with an inverted ratio is much higher and can be up to 40% (19,255,256). In both healthy individuals and CLL patients, discovery of a definitive cause of the large CD8⁺ T cell expansion that leads to ratio inversion remains elusive. Previously, infection by CMV was postulated as a driver of ratio inversion, with studies in both healthy older people (257) and CLL patients (10,15) showing links between CMV infection and expansions of CD8⁺ T cells. However, a number of more recent studies have demonstrated expanded CD8⁺ T cell populations in CMV-seronegative CLL patients (19,258,259),

while CMV status has been shown to no effect on disease outcome, unlike the inverted ratio (18).

1.3.3 T Cell Exhaustion

Exhaustion of T cells during immune responses has become a widely acknowledged and studied area in recent years. Often associated with chronic viral infections, and more recently in many cancers, T cell exhaustion is a state of acquired dysfunction. Characteristically, exhausted T cells display impaired effector functions and can be defined by their unique protein transcription profiles (260), both in part caused and sustained by the expression of a number of inhibitory receptors (261). The most highly studied of these receptors in the context of exhaustion is PD-1, which has been observed at high levels on T cells in chronic viral infections (261), solid cancers (262) and blood cancers (263). Such a wide ranging expression pattern has driven interest in PD-1 as a therapeutic target, with the aim of blocking PD-1 and thus reducing immune suppression via this inhibitory receptor (264,265). Several anti-PD-1 therapies, including the most well-known Pembrolizumab (266), are now approved in Europe for a number of different cancers, such as melanoma and Hodgkin lymphoma.

With the widespread nature of T cell dysfunction in CLL patients, interest in whether the exhaustion of T cells plays a role in CLL has grown significantly. Similarly to other haematological cancers, a number of recent studies have demonstrated increased frequencies of T cells expressing PD-1 in CLL (258,267,268). However, this does not appear to confer dysfunction across all CLL T cells, with those cells

responsible for responses against CMV observed to be fully functional (269). Furthermore, T cells in CLL that express PD-1 do not share the phenotypic profile of classical exhausted cells from chronic viral infections, in fact showing normal or increased production of key cytokines despite other functional defects (258). In addition, a clinical trial of the anti-PD-1 antibody Pembrolizumab observed no response in any of the CLL patients treated (270).

It may be the case that PD-1⁺ T cells in CLL are in fact not exhausted at all – there is evidence that activated T cells can express PD-1 while retaining normal, non-exhausted gene signatures and functional capabilities (271), and high frequencies of T cell activation have been observed in CLL (272). Further studies have suggested that PD-1 expression is more closely linked to both T cell differentiation and activation as opposed to exhaustion (273).

1.4 Aims of This Study

Previous work from our group has identified several T cell biomarkers that may be useful in CLL: chiefly, the CD4⁺:CD8⁺ ratio and the frequency of CD4⁺HLA-DR⁺PD-1⁺ T cells (19,256). While other studies have also observed the link between inverted CD4⁺:CD8⁺ ratios and poor prognosis in CLL (234,236), the association with the CD4⁺HLA-DR⁺PD-1⁺ T cell phenotype is novel. The frequency of cells with this phenotype was demonstrated to be the strongest variable associated with PFS in a multivariate analysis of 74 CLL patients (256). However, CD4⁺HLA-DR⁺PD-1⁺ T cells have never been previously described in CLL or other diseases, and as such little is known about this subset. It is not clear whether the CD4⁺HLA-DR⁺PD-1⁺ phenotype represents T cells that are exhausted or activated and whether these cells play an active role in disease progression or are simply bystanders.

Therefore, this study aims to confirm and build upon the previous work using a larger cohort of untreated CLL patients. As well as confirming the relationship between the frequency of CD4⁺HLA-DR⁺PD-1⁺ T cells and disease prognosis, this study will attempt to determine the role and function of these T cells through phenotypic, gene expression and functional analyses.

The aims of this study are as follows:

- 1.** To confirm previous observations of increased frequencies of CD4⁺HLA-DR⁺PD-1⁺ T cells in CLL patients compared to healthy controls using a larger cohort of over 200

CLL patients. Then, using collated data from over 20 years of patient records, to assess the impact of both CD4⁺:CD8⁺ ratio and CD4⁺HLA-DR⁺PD-1⁺ T cell frequency on patient outcomes, including progression-free survival and time to first treatment. The longitudinal stability of these two parameters, including following treatment, will also be investigated.

2. To investigate the nature of the CD4⁺HLA-DR⁺PD-1⁺ T cell subset. This will initially be conducted using flow cytometric analysis of phenotypic markers, including markers of activation, cytotoxicity and proliferation. Subsequently, microarray analysis will be used to explore gene expression signatures in CD4⁺HLA-DR⁺PD-1⁺ T cells from CLL patients and healthy donors, as well as control populations expressing only one or neither of these markers.

3. To analyse the functions of CD4⁺HLA-DR⁺PD-1⁺ T cells and the manner in which they might influence disease progression in CLL. Using well-established flow cytometry-based techniques, the ability of CD4⁺HLA-DR⁺PD-1⁺ and control T cell subsets to produce key cytokines, to degranulate and to proliferate, in response to stimulation, will be assessed.

2 Materials and Methods

2.1 Basic Consumables

2.1.1 *Media and Buffers*

FACS Buffer

1% w/v Foetal Calf Serum in Phosphate Buffered Saline (both *Gibco*).

Cell Fixation/Permeabilisation Solution

Prepared according to the manufacturer's instructions: 1 part concentrate to 3 parts diluent. (Foxp3/Transcription Factor Staining Buffer Set (*Invitrogen*))

Permeabilisation Buffer

1X solution prepared from 10X stock by diluting 1:10 with distilled water. (Foxp3/Transcription Factor Staining Buffer Set (*Invitrogen*))

FACS Lysing Solution

1X solution prepared by diluting 10X FACS Lysing solution (*BD Biosciences*) 1:10 with distilled water.

2.2 Blood Samples

2.2.1 *Blood Donors*

Following appropriate ethical approval (South East Wales Research Ethics Committee 13/WA/0346), anonymised blood samples were obtained from CLL patients attending haematology clinics at University Hospital Wales or Llandough

Hospital, with their informed consent. Controls were obtained from either age-matched non-CLL patients at these haematology clinics or from age-matched healthy volunteers, with their informed consent. Samples were collected from 210 individual patients (139 male and 71 female) with a median age of 72.5 years (range: 42.7 – 93.1) and from 17 healthy donors (8 male and 9 female) with a median age of 73.7 years (range: 59 – 88).

2.2.2 PBMC Isolation from Whole Blood

Isolation of PBMC was performed using the well-established density gradient centrifugation method within 24 hours of sample collection. Whole blood was gently layered onto an equal volume of Histopaque-1077 (*Sigma*) and immediately centrifuged at 726 RCF (Relative Centrifugal Force) with no brake for 20 minutes. This separates the blood into its component parts, with PBMCs forming a monolayer between the Histopaque and the serum. The PBMC monolayer was collected using a Pasteur pipette and transferred to a 15ml falcon tube before addition of PBS for washing – this involved the sample being centrifuged at 261 RCF for 5 minutes and the supernatant being removed to leave just the cell pellet. Red blood cells have poor structural integrity, so pellets were vigorously resuspended using 1ml of water to mechanically lyse the red blood cells while leaving PBMCs intact. PBS was added immediately to the samples to prevent osmotic lysis of PBMCs and samples were centrifuged at 261 RCF for 5 minutes. Following removal of the supernatant, the pellet was resuspended in 1-3ml of PBS (based on pellet size) ready to for counting.

2.2.3 PBMC Counting and Viability Assessment

Counts of cells were obtained using a Vi-Cell cell counter (*Beckman Coulter*), which uses trypan blue dye to distinguish live and dead cells. 50µl of suspended cell sample was diluted 1:10 with 450µl of PBS in a sample cup and placed into the appropriate slot in the Vi-Cell machine. For each of the samples an ID, the dilution factor and the cell type (to set expected cell size parameters) was entered into the Vi-Cell software. Samples were analysed individually, with the software counting the number of viable cells in each of 25 images obtained by the machine. Viable cells were detected based on cell size, cell shape and staining with trypan blue (which is excluded from live cells). Following image acquisition, the software automatically calculated the number of viable cells per ml of sample using the number of viable cells detected and the volume of analysed sample.

2.3 Absolute T Cell Counting

Absolute counts of T cells and T cell subpopulations in whole blood samples were determined using Trucount Tubes (BD), according to the manufacturer's instructions. These Trucount Tubes contain a known number of fluorescent beads that can be detected by a flow cytometer alongside the cells of interest – the ratio of beads to cells is used to calculate absolute cell counts.

One Trucount Tube was used per sample and was labelled accordingly, following verification that the lyophilised pellet of fluorescent beads was present and intact below the retainer in each tube. 20µl of the appropriate surface antibody mix

diluted in FACS buffer (see *Section 2.4, Table 2.5*) was added directly to each Trucount Tube just above the retainer. Then, 50µl of whole blood was added to each tube, again just above the retainer. Each tube was gently vortex mixed and then incubated at room temperature in the dark for 15 minutes. 1X FACS Lysing solution was prepared and 450µl of this 1X solution was added to each Trucount Tube. Following a gentle vortex mix, tubes were incubated at room temperature in the dark for 15 minutes, then immediately analysed using a LSRFortessa (*BD Biosciences*).

In order to calculate absolute counts of T cells and T cell subpopulations, both the number of bead events and the number of cell events collected by the flow cytometer must be known. The population of fluorescent beads is clearly defined when samples are analysed by flow cytometry (see *Figure 2.1*). T Cells could be defined by their expression of CD3 and other subpopulations, such as CD8⁺ or CD4⁺HLA-DR⁺PD-1⁺ cells could be gated within the T cell population. To calculate an absolute count for a population (A), the number of cell events collected (X) was divided by the number of bead events collected (Y) then multiplied by the bead concentration (number of beads per Trucount tube (N) divided by the volume (V)). This gives the overall equation $A = (X/Y) \times (N/V)$.

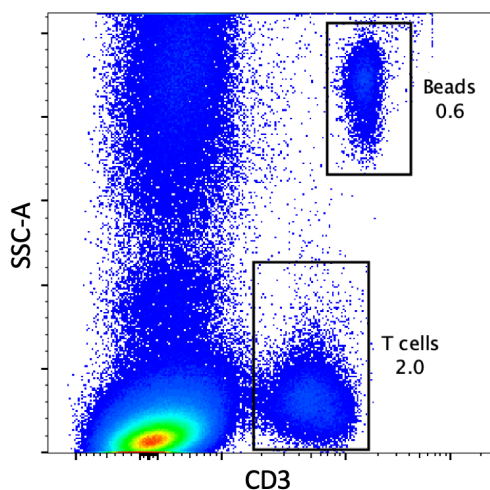


Figure 2.1: Example Flow Cytometry Plot Obtained with Trucount Tubes

Whole blood from CLL samples was stained with fluorescent antibodies in Trucount tubes and analysed by flow cytometry. Fluorescent beads and T cells were gated based on side scatter and CD3 expression and T cell subpopulations were gated based on marker expression.

2.4 Flow Cytometric Analysis of T Cells

2.4.1 Equipment and Software

Flow cytometry experiments were conducted on either a FACSCanto II or an LSRFortessa, using FACSDiva software (all *BD Biosciences*). Analysis of flow cytometry data was carried out using FlowJo software (v10, *FlowJo LLC*), SPICE software (Simplified Presentation of Incredibly Complex Evaluations) (274) and R (275).

2.4.2 Surface Staining

PBMCs were collected and counted as in *Sections 2.2.2* and *2.2.3*. Between $1-2 \times 10^6$ PBMCs were transferred to a 5ml FACS tube and 200 μ l of PBS was added – samples were washed by centrifugation as before. 100 μ l of the appropriate surface antibody mix diluted in FACS buffer (see *Section 2.5*) was added directly to the cells and samples were incubated at 4°C in the dark for 30 minutes. 200 μ l of PBS was added to the samples and they were washed by centrifugation as before. Following this samples were either resuspended in PBS to be analysed immediately or fixed in 1% Paraformaldehyde (PFA) if analysis could not be carried out immediately.

2.4.3 Intracellular Staining

PBMCs were stained as above (*Section 2.4.2*) with surface antibodies and washed by centrifugation with PBS. Cell fixation/permeabilisation solution was prepared and samples were resuspended in 200 μ l of this solution for 1 hour at 4°C in the dark. Samples were centrifuged at 261 RCF for 5 minutes and the supernatant

removed, before the cell pellets were washed with permeabilisation buffer by centrifugation. 100µl of the appropriate intracellular antibody mix diluted in permeabilisation buffer (see *Section 2.5*) was added directly to the cells and samples were incubated for 30 minutes at room temperature in the dark. Samples were washed by centrifugation, once with permeabilisation buffer and once with PBS, then either resuspended in PBS to be analysed immediately or fixed in 1% PFA if analysis could not be carried out immediately.

2.4.4 Flow Cytometer Fluorescence Compensation

Emission spectra from different fluorochromes can overlap, leading to false positive events being detected by the flow cytometer. In order to prevent this, compensation must be applied to negate fluorescence spillover. In these experiments, compensation matrices were determined automatically by the BD FACSDiva software following analysis of specific compensation samples.

These samples were prepared using Anti-Mouse Ig, κ/Negative Control Compensation Particles Set (*BD*). One drop of both positive and negative compensation beads was added to FACS tubes containing 100µl of FACS buffer, one FACS tube for each antibody used in the appropriate panel. Each antibody was added to a separate tube at half the concentration used on the cell samples and incubated at 4°C in the dark for 20-30 minutes. 200µl of PBS was added and tubes were washed by centrifugation as before. The beads pellet was resuspended in 200µl of PBS ready to run.

Within the compensation section of the FACSDiva software, each tube of single-stained beads was analysed on the flow cytometer and beads were gated using forward and side scatter profiles. Using histogram plots, acquisition voltages for each fluorochrome were adjusted where necessary in order that the positive and negative peaks could be visualised within the software's inbuilt parameter limits. Both peaks were then gated around as tightly as possible, using bi-exponential plots if needed. Following analysis of every tube, the FACSDiva software calculated the compensation matrix required and this was applied to all samples. Acquisition voltages were noted and used for future experiments.

2.4.5 Flow Cytometry Controls

Flow cytometry experiments require negative controls to determine which populations are genuinely expressing a given marker. In these experiments, both unstained samples (cells that have not had any antibodies added to them) and fluorescence minus one (FMO) controls were used. FMOs involve staining samples with all of antibodies except the one being controlled for using the same method as described above. In this way, during analysis gating can be more accurately performed on the negative populations, while also accounting for spillover from

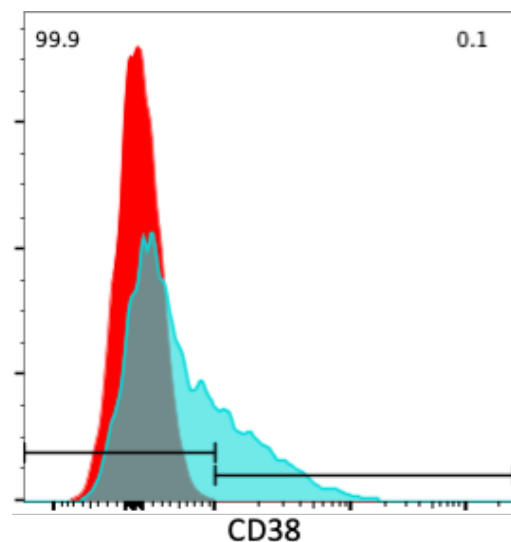


Figure 2.2: Example Flow Cytometry Histogram of CD38 Expression. Blue histogram represents CD4⁺ T cells from a CLL patient; red histogram represents CD38 FMO control.

other fluorescent channels, which becomes a greater problem as the number of fluorochromes used increases. FMOs were used for markers which do not have obviously distinct positive and negative populations, instead only showing a fluorescence shift, such as CD38 (see *Figure 2.2*). For these markers, gates were set at the end of the histogram tail of the FMO control, which guarantees that cells in the positive gate express the marker but may exclude some cells with very low expression.

2.4.6 Flow Cytometry Data Analysis and Statistics

Phenotypic data was collated and managed in Excel, while most graphing and statistical analysis was conducted using Prism 8 software (*GraphPad*). The D'Agostino and Pearson Normality Test was applied to datasets to determine whether they displayed Gaussian distributions. When all variables were Gaussian, Student's T-Test was used to compare two variables and ANOVA was used to compare three or more variables. For data that did not have a Gaussian distribution, non-parametric tests were used – Mann-Whitney Test for two variable comparisons and the Kruskal-Wallis Test with Dunn's Multiple Comparisons for three or more variables.

Patient outcome data was also analysed in Prism 8. Kaplan-Meier curves were plotted for progression-free survival and time to first treatment to compare stratified patient groups.

2.5 Flow Cytometry Antibody Panels

The following tables detail the antibody panels used for flow cytometry experiments, including T cell cytokine production and proliferation assays.

Target	Fluorochrome	Supplier	Category Number	Clone
CD3	A700	Biologend	344822	SK7
CD4	V500	BD	560768	RPA-T4
CD8	PE Dazzle	Biologend	300930	HIT8a
HLA-DR	PE	Biologend	361606	Tu36
PD-1	APC	Biologend	329908	EH12.2H7
CD57	FITC	Biologend	322306	HCD57
TIGIT	PE-Cy7	Biologend	372714	A15153G
Ki67	PerCP-Cy5.5	Biologend	350520	Ki-67
Granzyme B	Pacific Blue	Biologend	515408	GB11

Table 1: Phenotyping Panel 1

Target	Fluorochrome	Supplier	Category Number	Clone
CD3	A700	Biologend	344822	SK7
CD4	V500	BD	560768	RPA-T4
CD8	PE Dazzle	Biologend	300930	HIT8a
HLA-DR	PE	Biologend	361606	Tu36
PD-1	APC	Biologend	329908	EH12.2H7
CD57	FITC	Biologend	322306	HCD57
TIGIT	PE-Cy7	Biologend	372714	A15153G
CD38	APC-Cy7	Biologend	303534	HIT2
Ki67	PerCP-Cy5.5	Biologend	350520	Ki-67
Granzyme B	Pacific Blue	Biologend	515408	GB11

Table 2: Phenotyping Panel 2

<u>Target</u>	<u>Fluorochrome</u>	<u>Supplier</u>	<u>Category Number</u>	<u>Clone</u>
CD3	A700	Biologend	344822	SK7
CD4	V500	BD	560768	RPA-T4
CD8	PE Dazzle	Biologend	300930	HIT8a
HLA-DR	PE	Biologend	361606	Tu36
PD-1	APC	Biologend	329908	EH12.2H7
CD57	FITC	Biologend	322306	HCD57
CD28	PE-Cy7	Biologend	309925	CD28.2
CD38	APC-Cy7	Biologend	303534	HIT2
CD27	PerCP-Cy5.5	Biologend	356407	M-T271
Granzyme B	Pacific Blue	Biologend	515408	GB11

Table 3: Phenotyping Panel 3

<u>Target</u>	<u>Fluorochrome</u>	<u>Supplier</u>	<u>Category Number</u>	<u>Clone</u>
CD3	A700	Biologend	344822	SK7
CD4	V500	BD	560768	RPA-T4
CD8	PE Dazzle	Biologend	300930	HIT8a
HLA-DR	PE	Biologend	361606	Tu36
PD-1	APC	Biologend	329908	EH12.2H7

Table 4: Longitudinal Monitoring Panel

Target	Fluorochrome	Supplier	Category Number	Clone
CD3	A700	Biologend	344822	SK7
CD4	V500	BD	560768	RPA-T4
IFN γ	PE	Biologend	506506	B27
HLA-DR	PE Dazzle	Biologend	307653	L243
PD-1	Pacific Blue	Biologend	329915	EH12.2H7
CD107a	FITC	Biologend	328605	H4A3
IL-2	PE-Cy7	Biologend	500325	MQ1-17H12
ef780 Viability Dye	APC-Cy7	Thermo Scientific	65-0865-14	N/a
TNF α	PerCP-Cy5.5	Biologend	502925	Mab11
TOX	APC	Miltenyi	130-118-335	REA473

Table 5: T Cell Cytokine Production Panel

Target	Fluorochrome	Supplier	Category Number	Clone
CD3	A700	Biologend	344822	SK7
CD4	V500	BD	560768	RPA-T4
HLA-DR	PE Dazzle	Biologend	307653	L243
PD-1	Pacific Blue	Biologend	329915	EH12.2H7
CFSE	FITC	Biologend	423801	N/a
ef780 Viability Dye	APC-Cy7	Thermo Scientific	65-0865-14	N/a
TOX	APC	Miltenyi	130-118-335	REA473

Table 6: T Cell Proliferation Panel

2.6 Microarray Analysis of T Cell Subset Genetic Signatures

2.6.1 T Cell Enrichment

Enriched T cells were prepared from whole blood samples using the RosetteSep Human T Cell Enrichment Cocktail (*StemCell Technologies*) following the manufacturer's protocol.

Whole blood samples were transferred to 15ml falcon tubes, which were used to estimate the volume of blood. The volume of RosetteSep Human T Cell Enrichment Cocktail required was calculated (50 μ l of cocktail per 1ml of whole blood) and this was added directly to the samples and mixed thoroughly. Samples were incubated at room temperature for 20 minutes and then diluted in a 1:1 ratio with PBS containing 2% FCS. The samples were layered onto a volume of Histopaque-1077 equal to the

original volume of whole blood and were then centrifuged at 261 RCF with no brake for 20 minutes. Following centrifugation, the enriched T cells collected as a monolayer on top of the Histopaque and could be transferred to a 15ml falcon tube

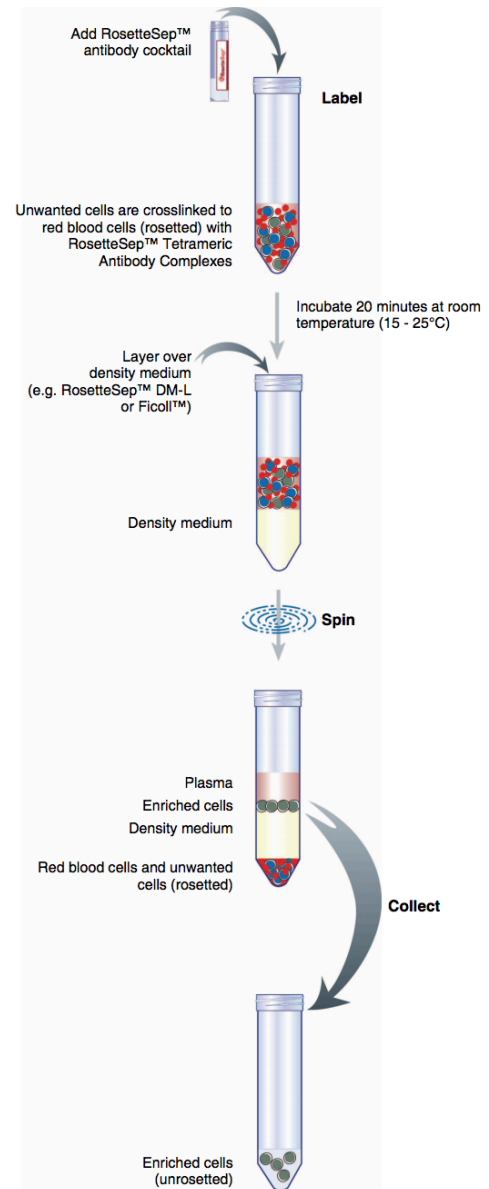


Figure 2.3: Process for T Cell Enrichment From Whole Blood.
From *StemCell Technologies*

using a Pasteur pipette. The cells were washed with PBS and resuspended in 1ml PBS before counting on the Vi-Cell cell counter.

2.6.2 Fluorescence-Activated Cell Sorting of CD4⁺ T Cell Populations

Fluorescence-Activated Cell Sorting (FACS) was carried out by Dr Catherine Naseriyan or Dr Ann Kift-Morgan (*Central Biotechnology Services, Cardiff University*), using a FACSAria™ III cell sorter (*BD Biosciences*). Similar to other flow cytometers, this instrument can detect a large number of fluorescent parameters which allows for detection of specific cell populations – however, specified populations can be directed into individual collection vessels to give highly enriched cell populations. For these experiments, fluorescence compensation was achieved as in *Section 2.4.4* and FMO controls were used for PD-1 and HLA-DR expression.

Enriched T cells were prepared as in *Section 2.6.1* and up to 10×10^6 cells were stained for surface markers (see *Section 2.4.2*), with 200 μ l of diluted antibody mix was used. Following washing, cells were used immediately and not fixed.

Figure 2.4 shows a representative gating strategy for FACS. Lymphocytes were gated based on their forward and side scatter profile and single cells selected using forward scatter area vs. forward scatter height plots. T cells were selected by gating CD3⁺ events on a histogram and these cells were further segregated into CD4⁺ and CD8⁺ using a scatter plot. Within the CD4⁺ compartment, a scatter plot of PD-1 vs. HLA-DR was used to determine the populations to be collected by the sorter: HLA-DR⁻PD-1⁻, HLA-DR⁻PD-1⁺ and HLA-DR⁺PD-1⁺. At least 5×10^4 cells were collected from each population directly into 5ml FACS tubes containing 500 μ l of PBS.

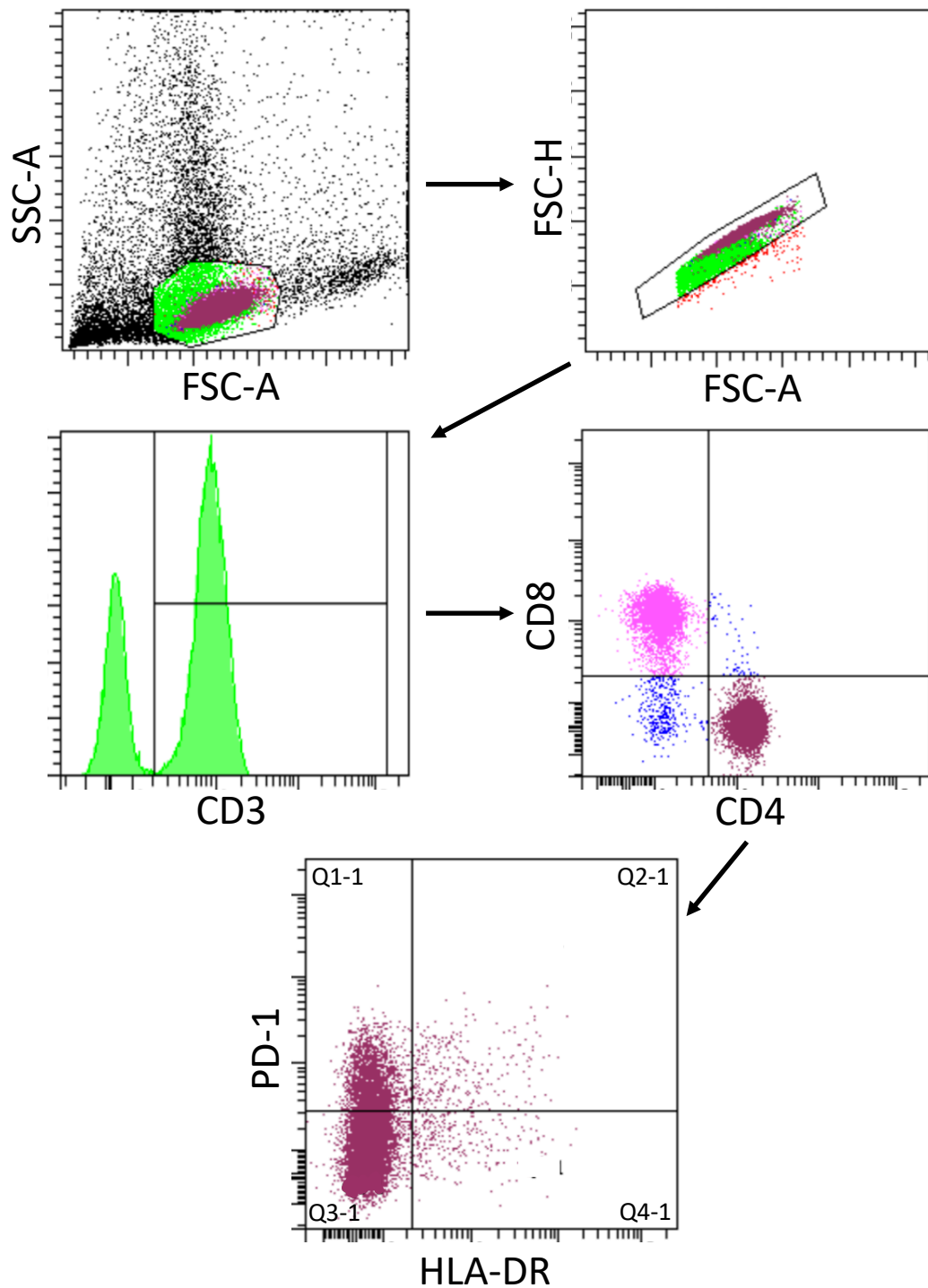


Figure 2.4: Representative Gating Strategy for FACS

Lymphocytes were gated based on forward scatter and side scatter characteristics and single cells were then selected using forward scatter area and forward scatter height parameters. T cells were gated as CD3⁺ cells on a histogram and were then separated based on CD4 and CD8 expression. Within the CD4⁺ population HLA-DR⁺PD-1⁻ (Q2-1), HLA-DR⁻PD-1⁺ (Q3-1), HLA-DR⁺PD-1⁺ (Q1-1) and HLA-DR⁻PD-1⁻ (Q4-1) cells were collected. These cells were distinguished using fluorescence minus one controls. FACS was carried out on a BD FACSAria™ III cell sorter.

2.6.3 RNA extraction from CD4⁺ T Cell Populations

Following FACS, RNA extraction was carried out using either the RNeasy Micro Kit or RNeasy Mini Kit (*Qiagen*) according to the manufacturer's protocol.

Cells were centrifuged at 261 RCF for 5 minutes to pellet them and the supernatant was removed. Lysis buffer was added to each tube and samples were homogenised using a vortex mixer before 70% ethanol was added and mixed by pipetting. Samples were then transferred to specialised columns containing nucleic acid-binding membranes and centrifuged at 21,000 RCF for 15 seconds, with the flow-through discarded. Columns were then washed by addition of the washing buffer RW1 and centrifuged at 21,000 RCF for 15 seconds. Following removal of the flow-through, a DNase 1 solution was prepared using 1 part DNase 1 to 7 parts buffer RDD and 80µl of this solution was added directly to each column membrane. Samples were incubated at room temperature for 15 minutes, then buffer RW1 was added and columns centrifuged at 21,000 RCF for 15 seconds. The flow-through was discarded and the samples were washed by addition of buffer RPE and centrifuged at 21,000 RCF for 15 seconds. Following disposal of the flow-through, 70% ethanol was added to the columns and samples were centrifuged at 21,000 RCF for 2 minutes. Columns were transferred into new collection tubes and centrifuged at 13,000rpm for 5 minutes with the lid open to dry the membranes. Columns were transferred into 1.5ml collection tubes and 14µl of RNase-free water was added directly to each membrane. Samples were centrifuged at 21,000 RCF for 1 minute to elute RNA.

2.6.4 Quality Assessment and Microarray Analysis of RNA

Analysis of extracted RNA samples by microarrays was conducted by Dr Amanda Redfern (*Central Biotechnology Services, Cardiff University*).

Extracted RNA samples were assessed on an Agilent 2100 Bioanalyzer, which uses electrophoresis to separate RNA fragments based on their size in microchannels on pre-made chips. The bands can then be analysed by measurement of fluorescence to provide quantitation and purity analysis, including an RNA Integrity Number (RIN) which gives an objective quantified assessment of RNA quality. For these experiments, the Agilent RNA 6000 Pico Kit was used, to ensure the small amounts of RNA could be analysed successfully.

All RNA samples obtained from FACS sorted cells were quality checked on the Agilent 2100 Bioanalyzer. The RNA yield was variable between patients and dependent on the number of cells in each sorted population. To ensure that there was sufficient RNA of good quality for microarray analysis, cut-offs of 500pg/ μ l and a RIN of >8 were used.

For microarray analysis of samples above the cut-offs, the GeneChip™ Human Gene 2.0 ST Array (*Applied Biosystems*) was used.

2.6.5 Microarray Data Processing

DNA microarray data processing was conducted by Dr Sumukh Deshpande (*Central Biotechnology Services, Cardiff University*), using R version 4.0.3.

Data from the GeneChip™ Human Gene 2.0 ST Arrays were stored in CEL files, which were imported into R using the Bioconductor package Oligo (276). The data

were normalised using the Robust Multi-array Average method, developed by Irizarry *et al.* (277). Differential expression analysis was performed for pairwise comparisons, between T cell subsets and for CLL patients vs. healthy donors (see *Figure 4.1*), using the limma package for Bioconductor (278). For each gene within the data, linear models were generated and an estimated global variance was calculated using empirical Bayes methods (279). Finally, moderated *t*-statistics were calculated for each gene and the resultant *p*-values were adjusted, to control the false discovery rate, by the Benjamini-Hochberg method (280).

In order to permit simplified downstream analysis, the data were annotated with gene names and gene symbols – this was achieved using the Affymetrix hugene20 annotation data package within Bioconductor (281).

2.7 Flow Cytometric Validation of Microarray Results

Microarray data give a valuable insight into the gene expression profile of cells, but these data must be recapitulated by other methods in order to prove their validity.

Flow cytometry can be used to investigate, at the protein level, the expression of genes of interest. Candidate genes were shortlisted based on having a statistically significant difference in expression between CD4⁺HLA-DR⁻PD-1⁻ cells and CD4⁺HLA-DR⁺PD-1⁺ cells, then ranked by log fold change between these two populations. Granzyme A was selected due to its high log fold change of 4.20 and the commercial availability of flow cytometry antibodies. The antibody panel in *Table 7* was used to investigate Granzyme A expression and cells were surface and intracellularly stained as in *Sections 2.4.2 & 2.4.3*.

Target	Fluorochrome	Supplier	Category Number	Clone
CD3	A700	Biolegend	344822	SK7
CD4	V500	BD	560768	RPA-T4
CD8	PE Dazzle	Biolegend	300930	HIT8a
HLA-DR	PE	Biolegend	361606	Tu36
PD-1	APC	Biolegend	329908	EH12.2H7
Granzyme A	PE-Cy7	Biolegend	507221	CB9
Ki67	PerCP-Cy5.5	Biolegend	350520	Ki-67
Granzyme B	Pacific Blue	Biolegend	515408	GB11

Table 7: Granzyme A Validation Panel

2.8 qPCR Validation of Microarray Results

2.8.1 Selection of Genes for qPCR Analysis

Due to the small quantities of RNA available from each sample following usage in the microarrays and the requirements of the reverse transcription step of qPCR, RNA samples from all three cell populations were pooled for each of CLL patients and healthy donors. These two pooled RNA samples provided sufficient quantities of RNA for analysis of genes that had shown differential expression between CLL patients and healthy donors in the microarray experiments.

Candidate genes for validation of the microarray results were chosen based on several factors. Of foremost importance was a significant and consistent difference in expression between CLL patient and healthy donor cells across all three T cell populations, of sufficient magnitude to be measurable by qPCR. A log fold change cut-off of >2 was used, with significance taken as an adjusted p value of <0.05 , and only genes that met these criteria in CD4⁺HLA-DR⁻PD-1⁻, CD4⁺HLA-DR⁻PD-1⁺ and CD4⁺HLA-DR⁺PD-1⁺ T cells were considered further. From this shortlist, genes were selected that bore functional relevance to the key pathways and processes identified by analysis of the microarray experiments. The final panel of genes selected is shown in *Table 8* below.

Further to the genes of interest, a housekeeping gene was analysed in order to normalise the qPCR data. The ubiquitously-expressed enzyme Glyceraldehyde 3-phosphate dehydrogenase (GAPDH) was chosen due to its consistent level of

expression across all of the samples analysed in the microarray experiments (mean expression 3.52, standard deviation 0.31).

Gene Name	Gene Symbol	Average Expression	HLA-DR ⁻ PD-1 ⁻		HLA-DR ⁻ PD-1 ⁺		HLA-DR ⁺ PD-1 ⁺	
			logFC	Adj P Value	logFC	Adj P Value	logFC	Adj P Value
Sorting nexin 9	SNX9	4.10	2.39	2.44E-06	2.82	3.56E-07	2.63	4.09E-07
Chromodomain Helicase DNA Binding Protein 1	CHD1	4.96	2.33	1.05E-07	2.21	1.95E-07	2.46	2.89E-08
Pellino E3 Ubiquitin Protein Ligase 1	PELI1	5.57	2.58	4.40E-07	2.46	8.67E-07	2.40	5.80E-07
GTPase, IMAP Family Member 4	GIMAP4	4.59	- 2.73	1.81E-06	- 2.93	8.49E-07	- 2.97	3.42E-07
Oxoglutarate Dehydrogenase	OGDH	5.19	- 2.25	6.38E-07	- 2.15	1.17E-06	- 2.27	3.46E-07
SLAM Family Member 6	SLAMF6	4.77	- 2.52	4.86E-09	- 2.27	1.96E-08	- 2.21	1.73E-08

Table 8: Selected Genes for qPCR Validation of Microarray Results

2.8.2 Primer Design

Design of appropriate forward and reverse primers to the gene of interest is vital to successful qPCR experiments. Here, design was facilitated by use of Primer-BLAST (282), a tool that provides a list of suggested primer sequences based on user-defined parameters.

Firstly, the NCBI mRNA Reference Sequence identification for the gene of interest was entered. The PCR amplicon size was stipulated to be in the range 80-200 base pairs and the primer melting temperature (the temperature at which half of the DNA duplex is dissociated) was set to the range 57-63°C, with a maximum difference in melting temperature of 3°C between the primers in a pair. The 'Exon junction span' option was specified as "Primer must span an exon-exon junction" and the organism was defined as human. All other options were kept at the defaults set by the programme.

Following running of the Primer-BLAST tool, a list of potential primer pairs was generated. In order to select the most appropriate pair of primers, a number of optimum criteria were applied where possible, as follows: primer length of 16-24 base pairs, a GC nucleotide content between 40-60% and the presence of a 'GC clamp' (where the primer ends with either a G or C base). Further criteria that were included where possible were the avoidance of di-nucleotide repeats, the avoidance of runs of a single nucleotide and low self-complementarity scores.

Once the best primer pair had been selected, the sequence was entered into the BLASTn tool (283). This mapping programme attempts to match the input DNA sequence with sequences within the genome of the user-defined species, here

human. The purpose of this step was to confirm that the selected primers did not recognise any genomic DNA sequences outside of the gene of interest, and thus avoiding off-target amplification and inaccurate qPCR results.

With confirmation that optimal, specific primer sequences had been selected, these were used to order custom-made primers (Eurofins Genomics). A list of the primers ordered can be seen in *Table 9*.

Gene Symbol	Sequence (5' → 3')	Template Strand	Length (bp)	T _M (°C)
SNX9	CTGGGCCTGAGCGTCGAG	Plus	18	62.5
	ATACATAACCCGAGCCTTGGTG	Minus	22	60.2
CHD1	GACTCTTGCTTACCCCGAGAC	Plus	21	60.1
	GACTCTCCTTTGATTCACCGGC	Minus	22	61.3
PELI1	CCGTGGTCAACTTCCCCTC	Plus	19	60.0
	TTATTTCCGGACAATTGCTGGTG	Minus	23	59.8
GIMAP4	GGAGTTCAAGCGACAATGGC	Plus	20	59.8
	CCTTCCAGGCCCATAACTGG	Minus	20	60.1
OGDH	ATCCACAGACAAACTTGGGTTC	Plus	22	58.8
	CCCCAATATGCTGGCAGTAGG	Minus	21	60.6
SLAMF6	AGGGCAAAAACATTGACTGCC	Plus	21	59.9
	CTACATTCCCTGGGCCAAAGC	Minus	21	61.3
GAPDH	GTCTCCTCTGACTTCAACAGCG	Plus	22	62.1
	ACCACCCTGTTGCTGTAGCCAA	Minus	22	62.1

Table 9: Primer Pairs for Selected Genes

2.8.3 Reverse Transcription and RNA Concentration

Component	Volume for 1 Reaction
10x Reverse Transcription Buffer	2.0 μ l
25x dNTP Mix	0.8 μ l
10x Random Primers	2.0 μ l
Multiscribe Reverse Transcriptase	1.0 μ l
Nuclease-free H ₂ O	4.2 μ l
Diluted RNA	10.0 μ l
Total	20.0 μl

Table 10: Components of Reverse Transcription Mix for cDNA Production

Final qPCR validation of candidate genes was conducted using the pooled RNA samples from CLL patients and healthy donors used in the microarray experiments described in *Section 2.8.1*. Optimisation and troubleshooting experiments were carried out using a CD4⁺ T cell clone (284), chosen due to its highly activated state.

In order to generate samples for analysis by qPCR, reverse transcription (RT) reactions were required. These reactions convert RNA into DNA molecules with a complementary sequence (cDNA), which is then used downstream. RT reactions were carried out using the High-Capacity cDNA Reverse Transcription kit and a SimpliAmp Thermal Cycler (both *Applied Biosystems*).

The concentration of RNA in each sample was measured using a NanoDrop 1000 (*Thermo Scientific*) spectrophotometer. For each reaction, 1 μ g of RNA was added to a PCR tube and the volume made up to 10 μ l. Then, using the volumes in *Table 10* multiplied by the number of reactions to be carried out, a master mix of RT reaction components was made and 10 μ l of this mix was added to each diluted RNA

sample. An extra control tube was included, containing all of the components in *Table 10* except the Multiscribe Reverse Transcriptase, to allow verification that no genomic DNA contamination of the RNA samples had occurred. Following brief centrifugation to remove any air bubbles, tubes were transferred to the SimpliAmp Thermal Cycler. The thermal cycler was programmed to use the following conditions: 25°C for 10 minutes, 37°C for 120 minutes, 85°C for 5 minutes then 4°C indefinitely. cDNA samples could then be used immediately or stored at -20°C.

In some cases RNA samples were of low concentration, such that more than 10µl would be needed for the RT reaction. Therefore, in order to obtain sufficiently concentrated RNA the samples required further processing, for which the GeneJET RNA Cleanup and Concentration Micro kit (*Thermo Scientific*) was used.

For this kit, RNA samples were diluted with nuclease-free water and Binding Buffer and 70% ethanol was added to precipitate the RNA. Using similar technology to the RNA extraction kits in *Section 2.6.3*, samples were added to specialised columns containing nucleic acid-binding membranes and centrifuged at 13,000rpm for 30 seconds to bind the RNA to the membranes. Following discarding of the flow-through, membranes were washed using Wash Buffer 1 and centrifuged again, before two further washes with Wash Buffer 2, centrifuging each time. Following a final centrifuging at 13,000rpm for 1 minute to remove residual buffers, RNA was eluted in 6-10µl of nuclease-free water, ready for use in RT reactions.

2.8.4 qPCR Plate Preparation

Component	Volume for 1 Reaction
PowerUp SYBR Green Master Mix	10.0 μ l
Forward Primer	0.5 μ l
Reverse Primer	0.5 μ l
Nuclease-Free H ₂ O	4.0 μ l
Diluted cDNA	5.0 μ l
Total	20.0 μl

Table 11: Components of qPCR Mix

Following RT reactions, synthesised cDNA was analysed using a NanoDrop 1000 to assess concentration and purity. Samples were then diluted 1:5 in nuclease-free H₂O ready for use.

qPCR reaction mixes were made up for each gene of interest, using the appropriate primer pair, following the ratios in *Table 11*. Each mix was prepared in either duplicate or triplicate depending on the experiment. 20 μ l of qPCR reaction mix per well was added to a 96-well MicroAmp plate (*Applied Biosystems*). For each gene of interest a control well was included, to which was added the same qPCR reaction mix minus the cDNA, to check for contamination.

Once prepared, the MicroAmp plate was sealed with MicroAmp Optical Adhesive Film (*Applied Biosystems*) and centrifuged at 1200 rpm for 1 minute to remove air bubbles. The plate was then ready for analysis.

2.8.5 qPCR Setup and Running

All qPCR experiments were conducted using a ViiA7 Real-Time PCR System and QuantStudio Real-Time PCR software (*Applied Biosystems*).

First the sealed MicroAmp plate was placed into the ViiA7 System plate holder ready for analysis, before experimental parameters were defined in the QuantStudio software. This initially involved selecting the correct instrument, plate and reagent types as well as selecting the 'Fast' run setting. Next, all target genes and individual samples were defined and mapped to their location on the MicroAmp plate. Finally, the run method outlined in *Table 12* was input, ensuring that a melt curve analysis was included after the completion of the amplification cycles.

Step	Temperature	Time	Number of Cycles
1	50°C	120 s	1
2	95°C	120 s	1
3	95°C	1 s	40
4	60°C	30 s	

Table 12: Run Method for qPCR Experiments

2.9 Cytokine Production Assays

2.9.1 T Cell Stimulation

T cells from CLL patients and healthy donors were enriched and counted as in *Section 2.6.1*, from whole blood samples. The enriched T cells were then resuspended in sufficient medium to give a concentration of 8×10^5 cells/ml. T cells were then divided into 3 wells of a 48-well plate, one for each stimulation condition to be used (PMA/Ionomycin, CD3/CD28 and no stimulation).

To each well was added Brefeldin A, at a concentration of $1 \mu\text{l/ml}$ of medium, to prevent secretion of produced cytokines from T cells. Also added to every well was CD107a-FITC antibody, at a concentration of $2 \mu\text{l/ml}$ of medium. For the wells receiving PMA/Ionomycin stimulation, Cell Activation Cocktail (*Biolegend*) was added at a concentration of $1 \mu\text{l}/1 \times 10^6$ cells. For those wells receiving CD3/CD28 stimulation, Dynabeads Human T-Activator beads were added to give a 1:1 ratio of beads to T cells, as per manufacturer's instructions. For cells receiving no stimulation, DMSO was added at a concentration of $2 \mu\text{l/ml}$ of medium.

Following addition of these reagents, the T cells were cultured at 37°C for 6 hours. This duration was used due to the limits of practicality imposed by restricted laboratory access during the Covid-19 pandemic.

2.9.2 Flow Cytometric Analysis of Cytokine Production

Following the stimulation, T cells were harvested and transferred to 5ml FACS tubes, with the well being washed out with $500 \mu\text{l}$ of medium to maximise recovery.

T cells were washed by centrifugation as described in *Section 2.2.2*, followed by a further wash in 200µl of PBS. 100µl of the appropriate surface antibody mix diluted in FACS buffer (see *Section 2.5*) was added directly to the cells and samples were incubated at 4°C in the dark for 30 minutes. 200µl of PBS was added to the samples and they were washed by centrifugation as before.

Following staining with surface antibodies, cell fixation/permeabilisation solution was prepared and T cells were resuspended in 200µl of this solution overnight at 4°C in the dark. Cells were centrifuged at 1200rpm for 5 minutes and the supernatant removed, before the cell pellets were washed with permeabilisation buffer by centrifugation. 100µl of the appropriate intracellular antibody mix diluted in permeabilisation buffer (see *Section 2.5*) was added to the cells and samples were incubated for 30 minutes at room temperature in the dark. Samples were washed by centrifugation, once with permeabilisation buffer and once with PBS, then resuspended in PBS to be analysed.

Flow cytometric analysis was conducted using an LSRFortessa, with FACSDiva software (all *BD Biosciences*). Analysis of flow cytometry data was carried out using FlowJo software (v10, *FlowJo LLC*).

2.10 T Cell Proliferation Assays

2.10.1 T Cell Stimulation

T cells from CLL patients and healthy donors were enriched and counted as in *Section 2.6.1*, from whole blood samples. T cells were then resuspended in PBS

containing 5 μ M CFSE (CFSE Cell Division Tracker Kit, *Biolegend*) and incubated at 37°C for 20 minutes. After this time, the CFSE was quenched by the addition of medium containing 10% FCS and the T cells were washed by centrifugation. Following this, T cells were resuspended in medium and incubated at 37°C for 10 minutes. The cells were then washed by centrifugation and resuspended in sufficient medium to give a concentration of 8x10⁵ cells/ml. T cells were then divided into 3 wells of a 48-well plate, one for each stimulation condition to be used (PMA/Ionomycin, CD3/CD28 and no stimulation).

For the wells receiving PMA/Ionomycin stimulation, Cell Activation Cocktail (Biolegend) was added at a concentration of 1 μ l/1x10⁶ cells. For those wells receiving CD3/CD28 stimulation, Dynabeads Human T-Activator beads were added to give a 1:1 ratio of beads to T cells, as per manufacturer's instructions. For cells receiving no stimulation, DMSO was added at a concentration of 2 μ l/ml of medium. Following addition of these reagents, the T cells were cultured at 37°C for 4 days. This duration was used to maximise experimental data collection within the limits imposed by restricted laboratory access and limited patient clinics caused by the Covid-19 pandemic.

2.10.2 Flow Cytometric Analysis of Proliferation

Following the stimulation, T cells were harvested and transferred to 5ml FACS tubes, with the well being washed out with 500 μ l of medium to maximise recovery. T cells were washed by centrifugation as described in *Section 2.2.2*, followed by a further wash in 200 μ l of PBS. 100 μ l of the appropriate surface antibody mix diluted

in FACS buffer (see *Section 2.5*) was added directly to the cells and samples were incubated at 4°C in the dark for 30 minutes. 200µl of PBS was added to the samples and they were washed by centrifugation as before.

Following staining with surface antibodies, cell fixation/permeabilisation solution was prepared and T cells were resuspended in 200µl of this solution at 4°C in the dark for 1 hour. Cells were centrifuged at 1200rpm for 5 minutes and the supernatant removed, before the cell pellets were washed with permeabilisation buffer by centrifugation. 100µl of the appropriate intracellular antibody mix diluted in permeabilisation buffer (see *Section 2.5*) was added to the cells and samples were incubated for 30 minutes at room temperature in the dark. Samples were washed by centrifugation, once with permeabilisation buffer and once with PBS, then resuspended in PBS to be analysed.

Flow cytometric analysis was conducted using an LSRFortessa, with FACSDiva software (all *BD Biosciences*). Analysis of flow cytometry data was carried out using FlowJo software (v10, *FlowJo LLC*).

3 Characterisation of CD4⁺HLA-DR⁺PD-1⁺ T Cells in CLL

CLL is inherently a disease of B cells, but there has long been noted a widespread dysfunction of T cells that occurs concurrently. The lack of an effective T cell response against leukaemic cells is almost certainly a major contributor to CLL pathogenesis and therefore is of great interest for research.

In healthy individuals, there are on average around twice as many CD4⁺ T cells as CD8⁺ T cells, but previous work on CLL has uncovered that a subset of patients develops an inversion of this normal CD4:CD8 T cell ratio. In these patients CD8⁺ cells outnumber CD4⁺ cells and this is caused by a preferential expansion of CD8⁺ T cells compared to their CD4⁺ counterparts. Since these inverted ratio (CLL^{IR}) patients showed significantly poorer prognosis (19), stratification of patients by their ratio is a useful method of exploring CLL phenotypes in further detail.

In addition to a number of tumour-associated prognostic markers that are well-characterised, such as 17p deletion, a recent study has shown that a CD4⁺ subset of T cells expressing both HLA-DR and PD-1 is an indicator of patient prognosis (285). These cells express both a classical activation marker in HLA-DR and a classical marker of exhaustion in PD-1, although there is some controversy in the use of PD-1 exclusively as an exhaustion marker for human T cells, with a body of evidence that it is also expressed following T cell activation (271). Due to the unusual nature of their cell surface marker expression, and their prognostic value, investigating the nature

and function of these CD4⁺HLA-DR⁺PD-1⁺ cells may be of significant value to understanding how T cells impact on CLL pathogenesis.

This chapter aims to explore the phenotype of CD4⁺HLA-DR⁺PD-1⁺ T cells using polychromatic flow cytometry. PBMC from 176 untreated CLL patients and 13 healthy donors were prepared from peripheral blood samples and analysed using several flow cytometry panels. The use of untreated patient samples was key, as they permit the investigation of patient prognosis and remove the possible interference of previous or ongoing therapy on the T cell population.

Patients were investigated as whole cohorts and also stratified based on their CD4:CD8 T cell ratio, as in Nunes *et al.* (19), using a ratio of 1.0 as the cut-off point above which patients were termed normal.

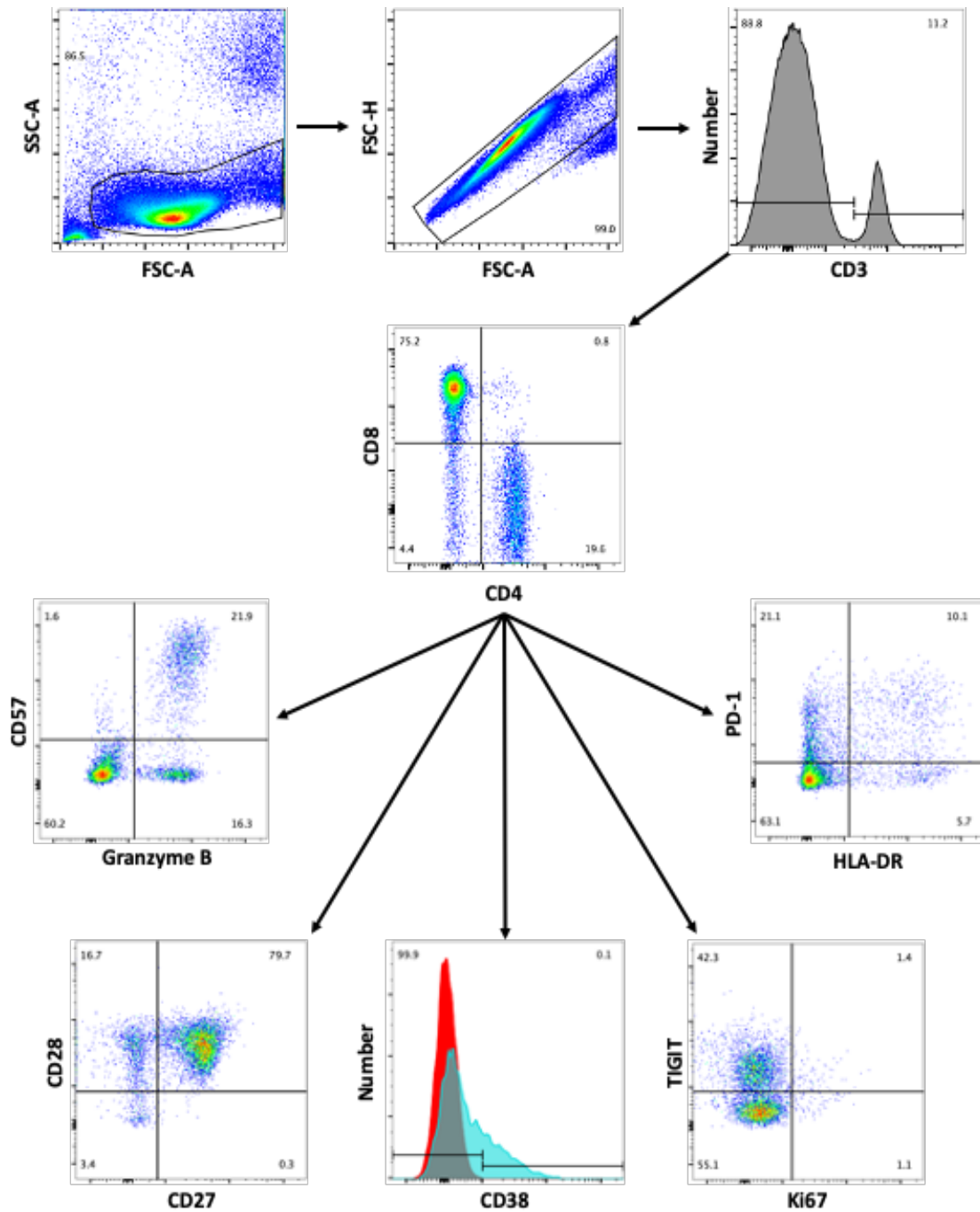


Figure 3.1: Representative Gating Strategy for Phenotyping of T Cells.

Lymphocytes were gated based on forward scatter and side scatter characteristics and single cells were then selected using forward scatter area and forward scatter height parameters. T cells were gated as CD3⁺ cells on a histogram and were then separated based on CD4 and CD8 expression. Phenotypic markers were gated as shown, both in the CD4⁺ subset and within the CD4⁺HLA-DR⁺PD-1⁺ population. Fluorescence minus one controls were used to distinguish positive expression where appropriate and HLA-DR expression on CD3⁻ CLL cells was used a positive control. Events were collected on a BD Fortessa and were analysed using Flowjo v10 software.

3.1 Populations of CD4⁺HLA-DR⁺PD-1⁺ T Cells

3.1.1 CD4⁺HLA-DR⁺PD-1⁺ T Cell Frequency

Before phenotypic analysis of CD4⁺HLA-DR⁺PD-1⁺ T cells was undertaken, it was important to determine the frequency of these cells in this cohort of CLL patients, as previous work has shown elevated levels of CD4⁺HLA-DR⁺PD-1⁺ cells in CLL (285). The gating strategy demonstrated in *Figure 3.1* was used in the analysis of flow cytometry data to investigate cell frequencies.

As shown in *Figure 3.2A*, within the CD4⁺ T cell compartment there was a significantly increased proportion of cells in the CD4⁺HLA-DR⁺PD-1⁺ subset in CLL patients compared to healthy controls ($p < 0.001$). In healthy donors, CD4⁺HLA-DR⁺PD-1⁺ cells accounted for a median proportion of 1.1% with a maximum of just 5.9%. In contrast, the range of CD4⁺HLA-DR⁺PD-1⁺ cell percentages was much greater in CLL patients, with the median being 3.0% and a maximum frequency of 31.9%. This demonstrates the heterogeneity of CLL patients and illustrates why a large cohort of patients is needed to show the full range of phenotypes.

It has been shown previously that an inversion of the CD4:CD8 T cell ratio correlates with poorer clinical prognosis (19), so CLL patients were stratified based on this ratio. *Figure 3.2B* shows the proportions of CD4⁺HLA-DR⁺PD-1⁺ T cells within the CD4⁺ compartment in normal ratio CLL^{NR} (n=125) and inverted ratio CLL^{IR} (n=71) patients and healthy donors (n=17). CLL^{IR} patients had significantly higher percentages of CD4⁺HLA-DR⁺PD-1⁺ cells than CLL^{NR} patients, with a median of 4.3%

compared to 2.5%. Both CLL^{IR} and CLL^{NR} patients had significantly higher proportions of CD4⁺HLA-DR⁺PD-1⁺ cells than healthy donors (median 1.1%).

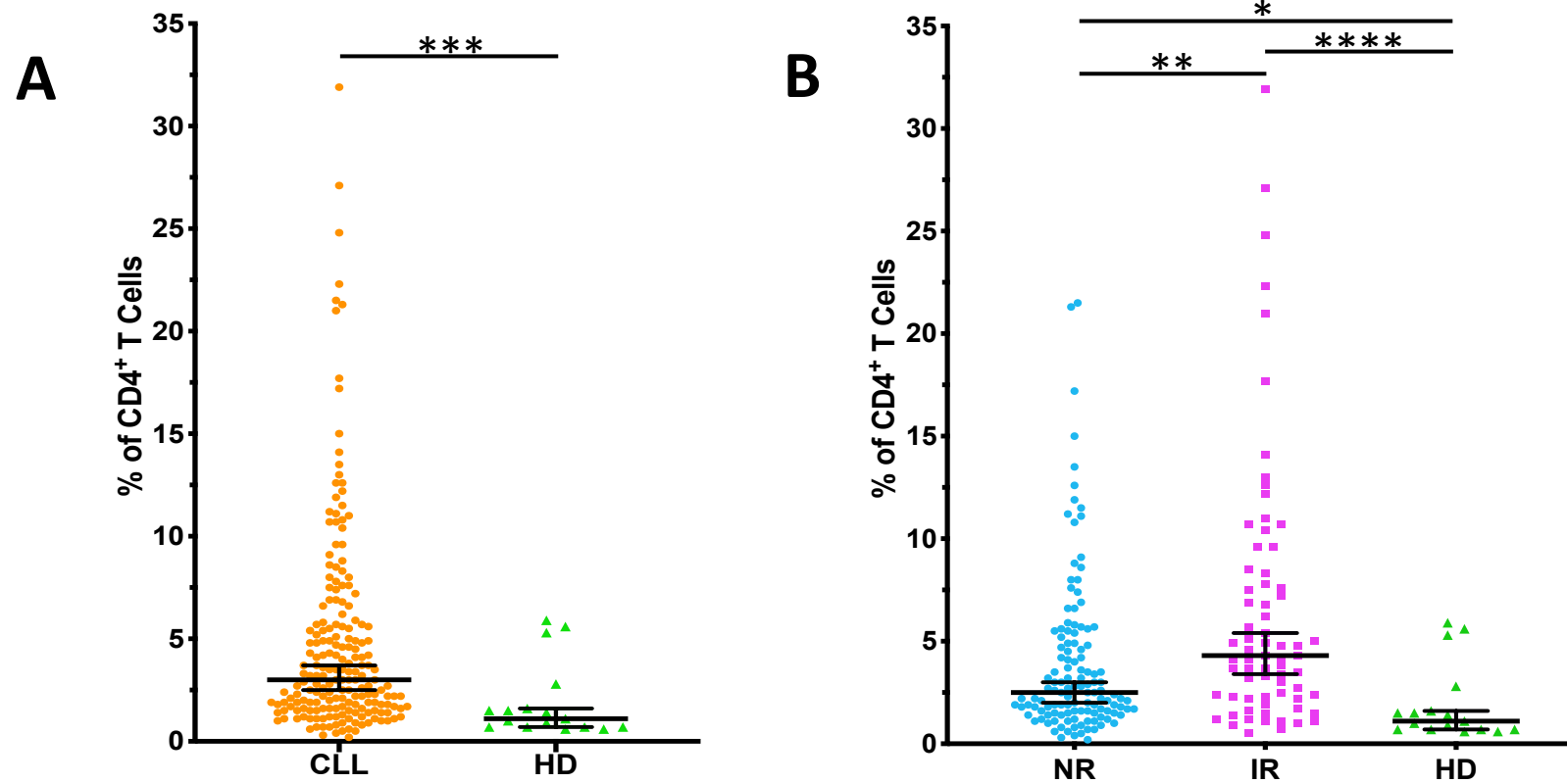


Figure 3.2: CD4⁺HLA-DR⁺PD-1⁺ T cells are enriched in CLL patients and in CLL^{IR} patients compared to CLL^{NR} patients.

PBMC were analysed by flow cytometry. Samples were collected from 196 CLL patients and 17 healthy donors. Bars represent median \pm 95% CI.

A) CD4⁺HLA-DR⁺PD-1⁺ T cells formed a significantly higher proportion of CD4⁺ T cells in CLL patients than in healthy donors. Significance determined by Mann-Whitney test ***= $p < 0.001$

B) CLL patients were stratified based on CD4:CD8 ratio. CLL^{IR} patients (n=71) had a significantly higher proportion of CD4⁺HLA-DR⁺PD-1⁺ T cells in the CD4⁺ compartment compared to CLL^{NR} patients (n=125) – in both CLL^{NR} and CLL^{IR} patients CD4⁺HLA-DR⁺PD-1⁺ T cells were a larger proportion of CD4⁺ cells than in healthy donors. Significance determined by Kruskal-Wallis test with Dunn's multiple comparisons *= $p < 0.05$ **= $p < 0.01$ ****= $p < 0.0001$

To investigate whether the enrichment of CD4⁺HLA-DR⁺PD-1⁺ T cells in CLL patients is related to other T cell factors, the proportions of T cells in the total PBMC and the CD4 vs. CD8 composition of the T cell compartment were analysed.

Figure 3.3A shows that, as would be expected, the proportions of T cells (CD3⁺) in CLL (median 8.0%) are significantly lower than in healthy donors (median 49.6%) – this is due to the large expansion of CLL cells, rather than a reduction in T cell numbers. When patients are stratified by CD4:CD8 ratio (*Figure 3.3B*) no significant difference is observed, with the median CD3⁺ percentage in CLL^{NR} (7.7%) very similar to that in CLL^{IR} patients (8.8%). Therefore, the increased frequencies of CD4⁺HLA-DR⁺PD-1⁺ T cells in CLL^{IR} patients compared to CLL^{NR} patients is not due to a difference in the proportions of T cells between the two groups. This is supported by *Figure 3.4A*, which shows no correlation between the proportion of CD4⁺HLA-DR⁺PD-1⁺ T cells and the percentage of T cells in the total PBMC in CLL patients.

Figure 3.3B demonstrates that CLL^{IR} patients have significantly lower frequencies of CD4⁺ T cells than CLL^{NR} patients, which is what would be expected since patients with an inverted ratio by definition have a greater proportion of CD8⁺ cells than CD4⁺ cells. Since CLL^{IR} patients also have greater proportions of CD4⁺HLA-DR⁺PD-1⁺ T cells than CLL^{NR} patients (*Figure 3.2B*), it could be suggested that CD4⁺ percentage is a key factor in determining the enrichment of CD4⁺HLA-DR⁺PD-1⁺ cells. However, no significant difference was observed for CD4⁺ percentage between CLL^{NR} CLL patients and healthy donors – this almost certainly reflects the fact that the large majority of healthy donors have a normal ratio. But

since CD4⁺HLA-DR⁺PD-1⁺ T cells are enriched in CLL^{NR} patients compared to healthy donors, this suggests that the level of CD4⁺ cells is not the determining factor responsible for the frequencies of CD4⁺HLA-DR⁺PD-1⁺ cells observed.

To explore this further, CD4:CD8 T cell ratio was compared to the frequency of CD4⁺HLA-DR⁺PD-1⁺ cells, shown in *Figure 3.4B*. This *Figure* demonstrates that the proportion of CD4⁺HLA-DR⁺PD-1⁺ cells in CLL patients does not directly correlate with CD4:CD8 ratio ($R^2 = 0.06$), despite the significant differences observed in the proportions of CD4⁺HLA-DR⁺PD-1⁺ cells between the CLL^{NR} and CLL^{IR} groups (*Figure 3.2B*). However, the heterogeneity of CLL patients and the much greater range of “normal” ratios compared to inverted ratios make a direct correlation analysis problematic.

These results demonstrate that CD4⁺HLA-DR⁺PD-1⁺ T cells are significantly enriched in CLL patients, in particular in those with an inverted CD4:CD8 ratio. Other patient-intrinsic T cell factors, including T cell percentage and CD4⁺ T cell percentage do not show strong correlations with the proportions of CD4⁺HLA-DR⁺PD-1⁺ cells and so cannot explain the observed frequency increases.

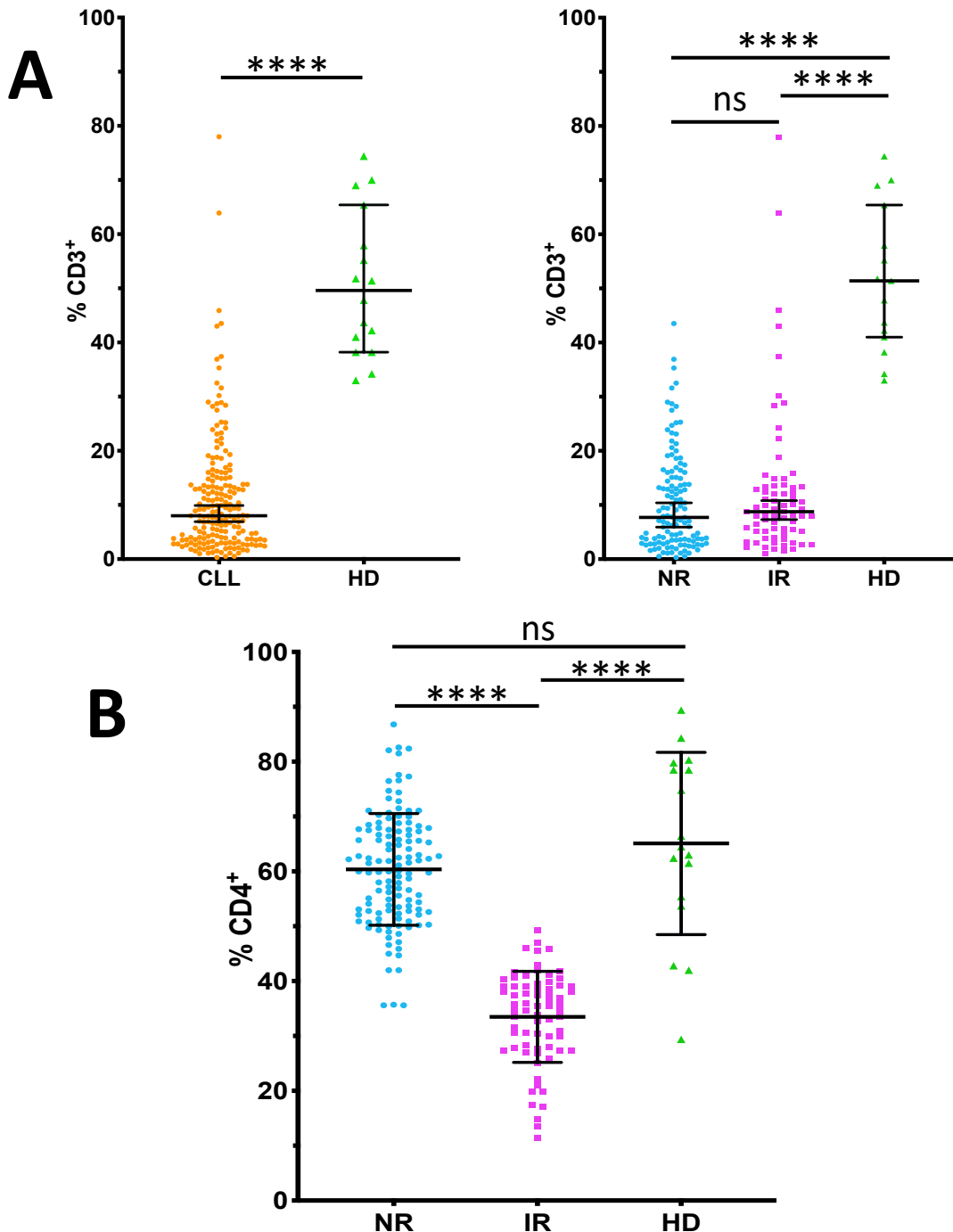


Figure 3.3: Increased CD4⁺HLA-DR⁺PD-1⁺ Cell Frequencies Cannot be Explained by Changes in T Cell Proportions or Subset Distributions

PBMC were analysed by flow cytometry. Bars represent median \pm 95% CI.

A) The percentage of PBMC comprised by T cells (CD3⁺) was not significantly different between CLL^{NR} and CLL^{IR} patients, but was significantly higher in healthy donors (HD) compared to both CLL^{NR} and CLL^{IR} patients. Significance determined by Mann Whitney test or Kruskal-Wallis test with Dunn's multiple comparisons ****= $p < 0.0001$.

B) The proportion of CD4⁺ T cells showed no significant difference between healthy donors (HD) and CLL^{NR} patients, however CLL^{IR} patients had significantly lower CD4⁺ percentages compared to both CLL^{NR} patients and healthy donors. Significance determined by one-way ANOVA ****= $p < 0.0001$

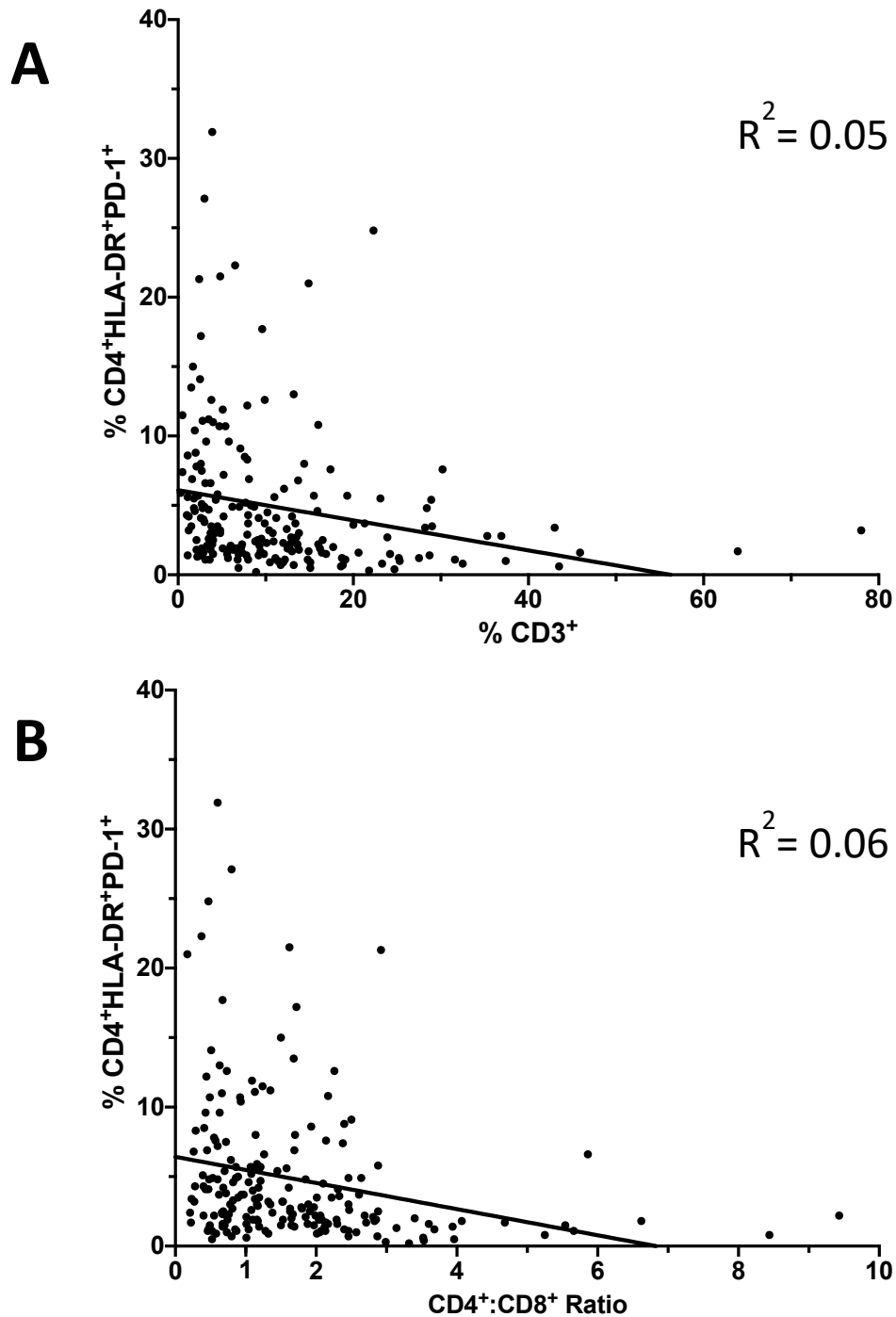


Figure 3.4: CD4⁺HLA-DR⁺PD-1⁺ T Cells Do Not Correlate with T Cell Proportions or CD4:CD8 Ratio

PBMC from 197 CLL patients were analysed by multi-parametric flow cytometry.

A) The proportion of total PBMC comprised by T cells (CD3⁺) was plotted against the proportion of CD4⁺HLA-DR⁺PD-1⁺ T cells in the CD4⁺ compartment. *Correlation was assessed by simple linear regression.*

B) The CD4:CD8 T cell ratio was plotted against the proportion of CD4⁺HLA-DR⁺PD-1⁺ T cells in the CD4⁺ compartment for each CLL patient sample analysed. *Correlation was assessed by simple linear regression.*

3.1.2 CD4⁺HLA-DR⁺PD-1⁺ T Cell Counts

Following on from the above experiments investigating the frequency of T cell populations in CLL patients and healthy donors, the absolute numbers of T cell populations in these two groups were investigated. Frequencies of T cell populations in the blood can vary due to relative changes in the numbers of cells in other subsets, therefore it is important to verify any findings for a given population using the absolute cell counts, which will be unaffected by changes in other cells.

Although CLL patients have a significantly lower proportion of T cells within the PBMC population (*Figure 3.3A*), the absolute number of T cells is actually significantly greater in CLL patients (median 181 cells/ μ L) than in healthy controls (median 105 cells/ μ L), as seen in *Figure 3.5A*. The discrepancy between T cell numbers and proportions in CLL is explained by the massive expansion of CLL cells, which can comprise up to 99% of the PBMC.

CD4⁺HLA-DR⁺PD-1⁺ T cells were found to occur at significantly higher frequencies in CLL compared to healthy donors. This observation could be explained either by an increase in the number of CD4⁺HLA-DR⁺PD-1⁺ T cells specifically, or by a decrease in the numbers of other CD4⁺ subsets. The former is seen in *Figure 3.5B*, in which the median count of CD4⁺HLA-DR⁺PD-1⁺ T cells in 46 CLL patients (8.5 cells/ μ L) was significantly greater than in the 6 healthy control samples (3.5 cells/ μ L). A decrease in the CD8⁺ T cell count would increase the frequency of all CD4⁺ subsets, however in these samples the absolute count of CD8⁺ T cells was also greater in CLL than healthy donors, illustrating that the increased numbers of CD4⁺HLA-DR⁺PD-1⁺ cells is responsible for the high frequencies of these cells. Following stratification of

CLL patients into CLL^{NR} and CLL^{IR} groups, the pattern of absolute counts was similar to that observed in the frequencies of CD4⁺HLA-DR⁺PD-1⁺ cells seen in *Figure 3.2B*. The median count of CD4⁺HLA-DR⁺PD-1⁺ cells in CLL^{IR} patients (9.0 cells/ μ L) was significantly greater than that in healthy controls (3.5 cells/ μ L) with a trend for higher counts in CLL^{IR} compared to CLL^{NR} (median 7.0 cells/ μ L) patients, although this did not reach statistical significance.

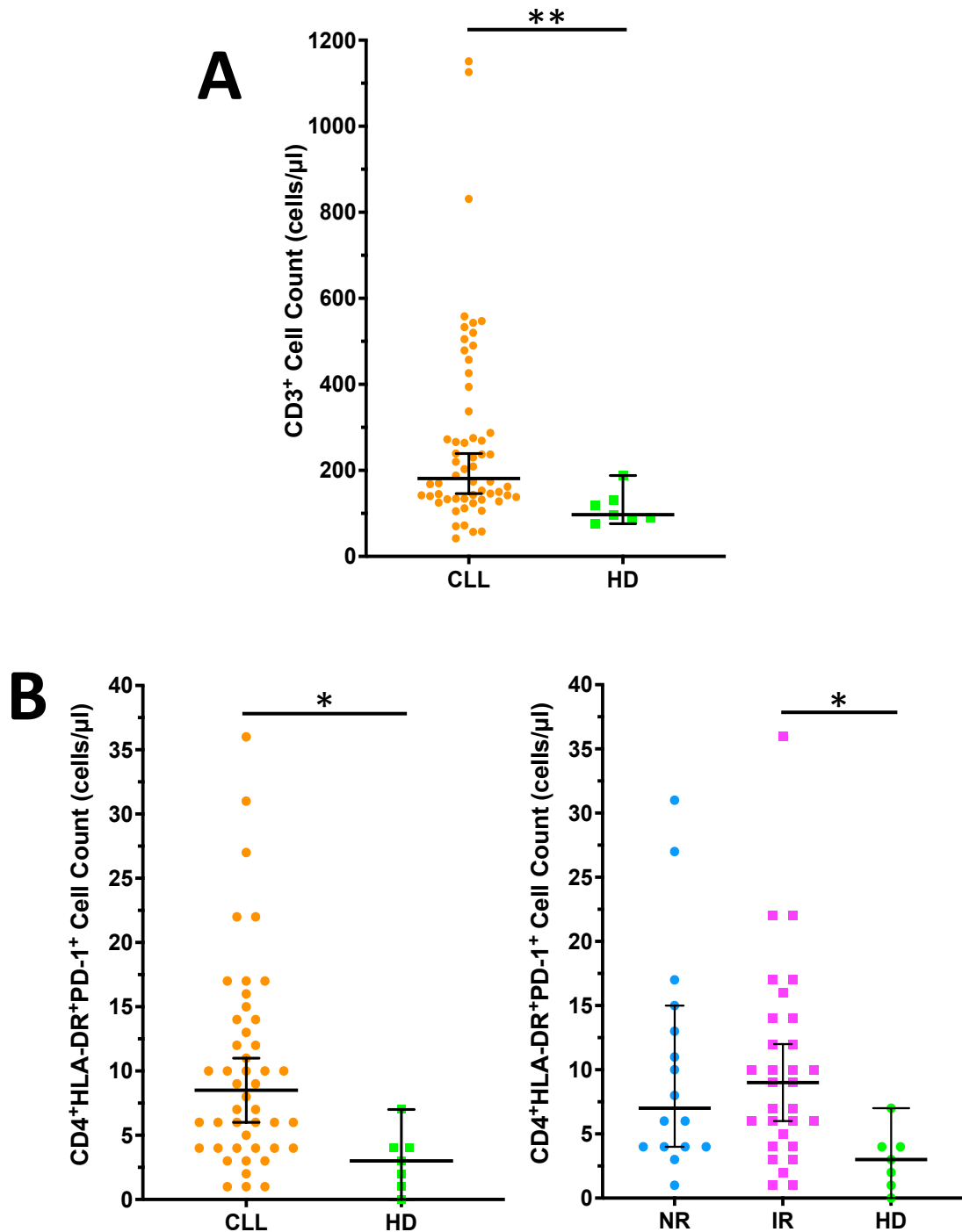


Figure 3.5: CLL Patients Have Higher Absolute Counts of T Cells and CD4⁺HLA-DR⁺PD-1⁺ T Cells

Cells were counted using Trucount Tubes. Bars represent median \pm 95% CI.

A) The absolute count of T cells (CD3⁺) was significantly greater in CLL patients (n=58) than healthy donors (n=6). Significance determined by Mann Whitney test ** = p<0.01.

B) Absolute counts of CD4⁺HLA-DR⁺PD-1⁺ T cells was significantly greater in CLL patients (n=46) than healthy donors (n=6), with CLL^{IR} patients having higher counts than CLL^{NR} patients. Significance determined by Mann Whitney test or Kruskal-Wallis test with Dunn's multiple comparisons * = p<0.05

3.2 Phenotyping of CD4⁺HLA-DR⁺PD-1⁺ T Cells

CD4⁺HLA-DR⁺PD-1⁺ cells express a classical marker of activation (HLA-DR) and a classical marker of exhaustion (PD-1), although PD-1 has been suggested to also act as an acute activation marker in healthy individuals (271,286). Since the vast majority of T cells in healthy donors are resting and not activated, cells co-expressing HLA-DR and PD-1 would be expected to be rarely observed, as was seen in *Figure 3.2*. Therefore, having confirmed previous findings that the frequencies of CD4⁺HLA-DR⁺PD-1⁺ T cells are significantly greater in CLL patients than in healthy donors, the next step was to investigate these cells in greater depth, with a wide-ranging phenotypic analysis conducted to attempt to determine the nature of these cells.

3.2.1 Initial Characterisation

The enrichment of CD4⁺HLA-DR⁺PD-1⁺ cells in CLL patients, combined with the expansion of the T cell compartment that is characteristic in CLL, suggest that the CD4⁺HLA-DR⁺PD-1⁺ T cell subset may be an actively proliferating population of cells. To investigate this, expression of Ki67 was assessed by flow cytometry. Ki67 is a nuclear protein involved in the cell cycle which cannot be detected in quiescent cells, only those transitioning through the cell cycle, and is therefore an extremely useful marker of active cellular proliferation (287).

Figure 3.6B demonstrates that the proportion of CD4⁺HLA-DR⁺PD-1⁺ T cells that express Ki67, and are therefore actively proliferating, is significantly greater than the proportion observed in the total CD4⁺ compartment in both CLL patients and in

healthy donors. Interestingly, although the median proportion of Ki67⁺ cells in the CD4⁺ compartment was similar in CLL (2.3%) and healthy controls (1.9%), within the CD4⁺HLA-DR⁺PD-1⁺ population the Ki67⁺ fraction was more than 2-fold larger in healthy donors (30.0%) than CLL (12.2%).

These observations concur with the hypothesis that the expansion of the CD4⁺HLA-DR⁺PD-1⁺ population in CLL is driven at least in part by actively proliferating cells. However, it is noteworthy that despite the proportion of proliferating CD4⁺HLA-DR⁺PD-1⁺ cells being greater than their CD4⁺ counterparts, the median percentage of cells expressing Ki67 was only 12.2%, so a large majority of this subset are either not proliferative or divided at an earlier timepoint.

Cytotoxicity via mechanisms involving molecules such as perforin and various granzymes is most commonly associated with CD8⁺ T cells, in their role as the “killer” cells of the adaptive immune system (288). However, CD4⁺ T cells can also be cytotoxic (289–291). Such CD4⁺ cells are rare in healthy individuals but are detectable in viral infections, such as influenza, and autoimmune diseases including colitis (289). Similar to these conditions, CLL also displays an atypical immune profile, so CD4⁺HLA-DR⁺PD-1⁺ T cells were investigated to assess whether they were cytotoxic. Expression of Granzyme B, a serine protease usually found in and released via lytic granules in cytotoxic cells and frequently used as a marker for cytotoxicity, was assessed by flow cytometry.

The proportions of cells expressing Granzyme B in the total CD4⁺ T cell compartment and the CD4⁺HLA-DR⁺PD-1⁺ T cell subset of both CLL patients and

healthy controls are shown in *Figure 3.6B*. CD4⁺HLA-DR⁺PD-1⁺ T cells demonstrated a significant enrichment of Granzyme B-expressing cells (median = 19.0%) compared to total CD4⁺ cells (5.0%) in CLL. However, although a similar trend was observed in healthy donors this did not reach statistical significance, probably due to the wide range of the proportion of Granzyme B⁺ cells in the CD4⁺HLA-DR⁺PD-1⁺ population (0.4 - 54.0%). It is worth noting however that, mirroring the pattern observed with Ki67 expression, the large majority of CD4⁺HLA-DR⁺PD-1⁺ cells did not express Granzyme B in CLL. It was interesting to note that the minority of CD4⁺HLA-DR⁺PD-1⁺ cells that expressed Ki67 were not the same minority that expressed Granzyme B, with little correlation between the expression of the two markers.

These initial experiments with two functional markers demonstrate that the CD4⁺HLA-DR⁺PD-1⁺ T cell population is enriched for cells that are proliferating and are potentially cytotoxic when compared to the total CD4⁺ compartment. This showed promise with regard to the hypothesis that CD4⁺HLA-DR⁺PD-1⁺ T cells would have an unusual phenotype. However, neither the proliferating nor cytotoxic cells constituted a majority of this subset, suggesting the presence of heterogeneous sub-populations requiring further elucidation.

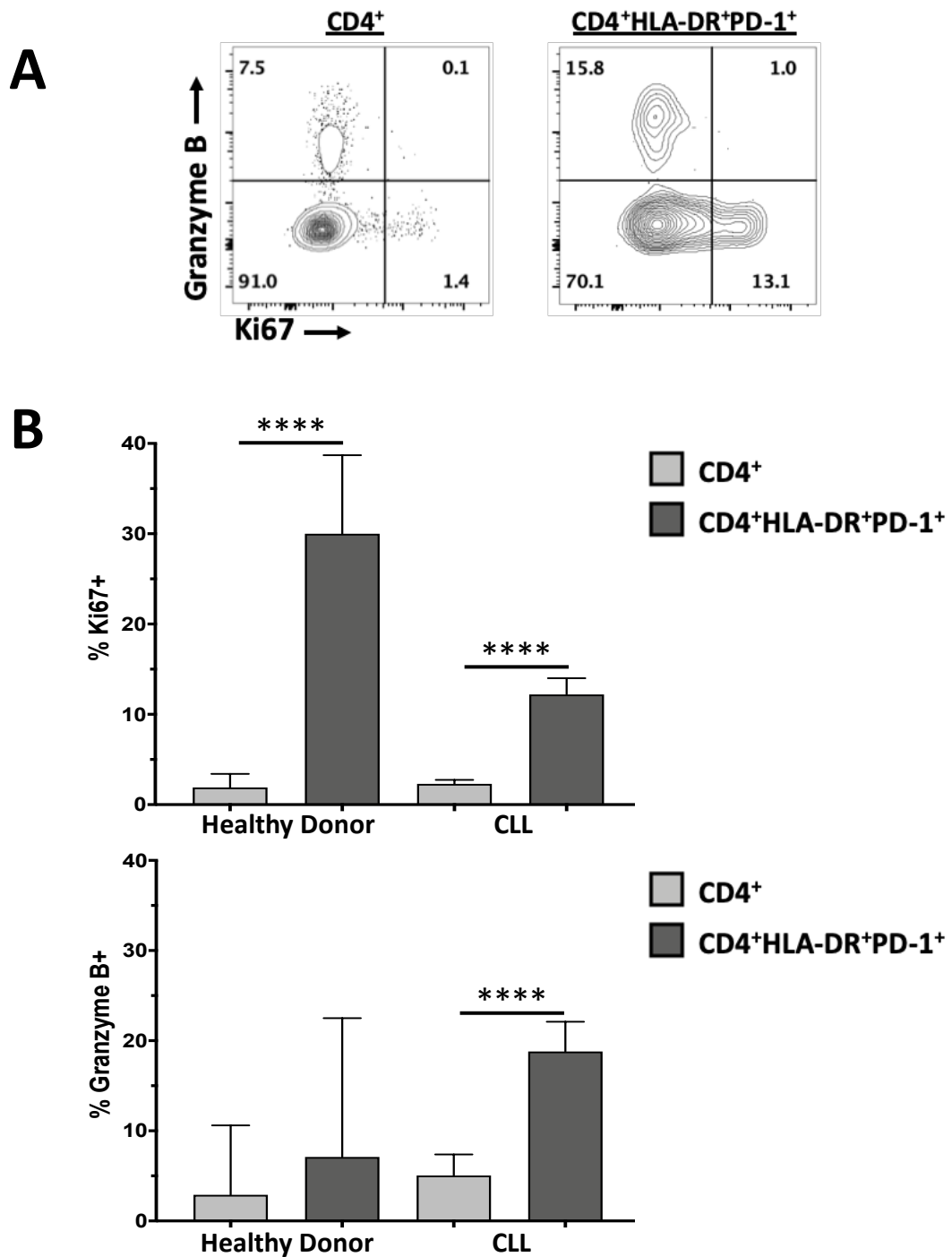


Figure 3.6: CD4⁺HLA-DR⁺PD-1⁺ Cells Show Greater Proliferation and Cytotoxicity than Total CD4⁺ T Cells in both CLL Patients and Healthy Donors

Using multi-parametric flow cytometry, expression of Ki67, a marker of proliferation, and Granzyme B, a marker of cytotoxicity, was assessed in CD4⁺HLA-DR⁺PD-1⁺ T cells and in the total CD4⁺ compartment from 183 CLL samples and 15 age-matched healthy donors.

A) Representative flow cytometry plots showing expression of Ki67 and Granzyme B in CLL. **B)** CD4⁺HLA-DR⁺PD-1⁺ T cells showed a significantly increased proportion of Ki67-expressing cells compared to the total CD4⁺ population in both CLL and healthy donors. The proportion of cells expressing Granzyme B was significantly higher in CD4⁺HLA-DR⁺PD-1⁺ cells in CLL, but not in healthy donors. Bars represent mean \pm standard deviation. Significance was determined by Kruskal-Wallis test with Dunn's multiple comparisons ****= $p < 0.0001$

3.2.2 Phenotypic Overview

Following on from the initial phenotyping experiments, a larger panel of markers was devised to give a deeper characterisation of CD4⁺HLA-DR⁺PD-1⁺ T cells. As well as the cytotoxicity marker Granzyme B and the proliferation marker Ki67, a further five antigens were analysed: CD38, CD57, TIGIT, CD27 and CD28.

CD38 is a cell surface glycoprotein which functions enzymatically to generate and hydrolyse cyclic ADP-ribose, as well as having roles in calcium regulation – expression of CD38 is commonly used a marker of cellular activation, particularly in the context of viral infections (292).

CD57 is a carbohydrate antigen attached to cell surface proteins, in particular adhesion molecules, following the activity of the B3GAT1 enzyme – CD57 is detectable in terminally-differentiated immune cells and as such is a marker of cellular senescence (293).

TIGIT (T cell immunoreceptor with ImmunoGlobulin and ITIM domains) is one of a family of inhibitory receptors expressed by immune cells, which also includes PD-1, that act to decrease effector functions and promote tolerance and can also be used as markers of exhaustion (294). It was assessed here since these inhibitory receptors are often co-expressed and as such TIGIT may be expected to be expressed by CD4⁺HLA-DR⁺PD-1⁺ cells if their PD-1 expression was indeed indicative of exhaustion.

CD27 is a member of the Tumour Necrosis Factor receptor superfamily, with a role in the activation of immune cells. Expression of CD27 is usually restricted to

naïve and central memory T cells and is lost following terminal differentiation and is therefore a useful marker of “early” T cells (295).

CD28 is a vital co-stimulatory receptor on T cells that binds its ligands CD80 and CD86 to provide the co-signal required for full T cell activation following ligation of the T cell receptor with a cognate antigen – failure of the CD28 signal during activation leads to the generation of an anergic T cell. Like CD27, expression of CD28 is usually downregulated in more differentiated T cells (296). Together, a CD27⁻CD28⁻ phenotype is associated with replicative senescence, whereby cells can no longer proliferate but may still carry out effector functions (297).

Figure 3.7 depicts a heatmap summarising the overall frequency of expression of 5 of the aforementioned phenotypic markers, which comprised Phenotyping Panel 2 (see *Section 2.5*), in an initial cohort of 67 CLL patients and 7 healthy donor samples. The heatmap shows the proportion of cells expressing each marker, without considering co-expression patterns.

Each of the markers showed the highest frequency of expression for both CLL and healthy controls in CD4⁺HLA-DR⁺PD-1⁺ T cells, with the exception of Granzyme B which was most frequently expressed in CD4⁺HLA-DR⁻PD-1⁺ cells. For this cohort, the proportion of Granzyme B⁺ cells in each population was greater in healthy donors, in contrast to that observed in *Figure 3.6B*. TIGIT was the most highly expressed marker with very high frequencies of TIGIT⁺ cells in the CD4⁺HLA-DR⁺PD-1⁺ population. Similar to *Figure 3.6A*, Ki67 showed very little expression in either CD4⁺HLA-DR⁻PD-1⁻ or CD4⁺HLA-DR⁻PD-1⁺ cells, with a notable increase in the CD4⁺HLA-DR⁺PD-1⁺

population. The high expression of CD38, alongside the enrichment for Ki-67⁺ cells, suggests that CD4⁺HLA-DR⁺PD-1⁺ T cells are an activated, proliferating subset.

The data shown in *Figure 3.7* gives an indication of the frequency of expression of individual phenotypic markers, but it is desirable to be able to investigate their patterns of co-expression. *Figures 3.8 and 3.9* make use of a software package known as SPICE (Simplified Presentation of Incredibly Complex Evaluations) to visualise and analyse the same dataset in a manner permitting interrogation of subpopulations within the CD4⁺HLA-DR⁻PD-1⁻, CD4⁺HLA-DR⁻PD-1⁺ and CD4⁺HLA-DR⁺PD-1⁺ T cell subsets. In order to generate the data for input into SPICE, a Boolean gating strategy was utilised. First, histograms were used to determine positive and negative populations for each individual marker in turn, using FMO controls where appropriate. Following this, the Boolean Gating feature of FlowJo was used – this determines every possible combination of the chosen markers (this is equal to 2^n , where n =number of markers) and calculates the percentage of the population that expresses each combination based on the positive and negative thresholds specified. The SPICE software allows for direct entry of the Boolean gating output and therefore these data can be visualised simply and analysed statistically without the need for complex data manipulation.

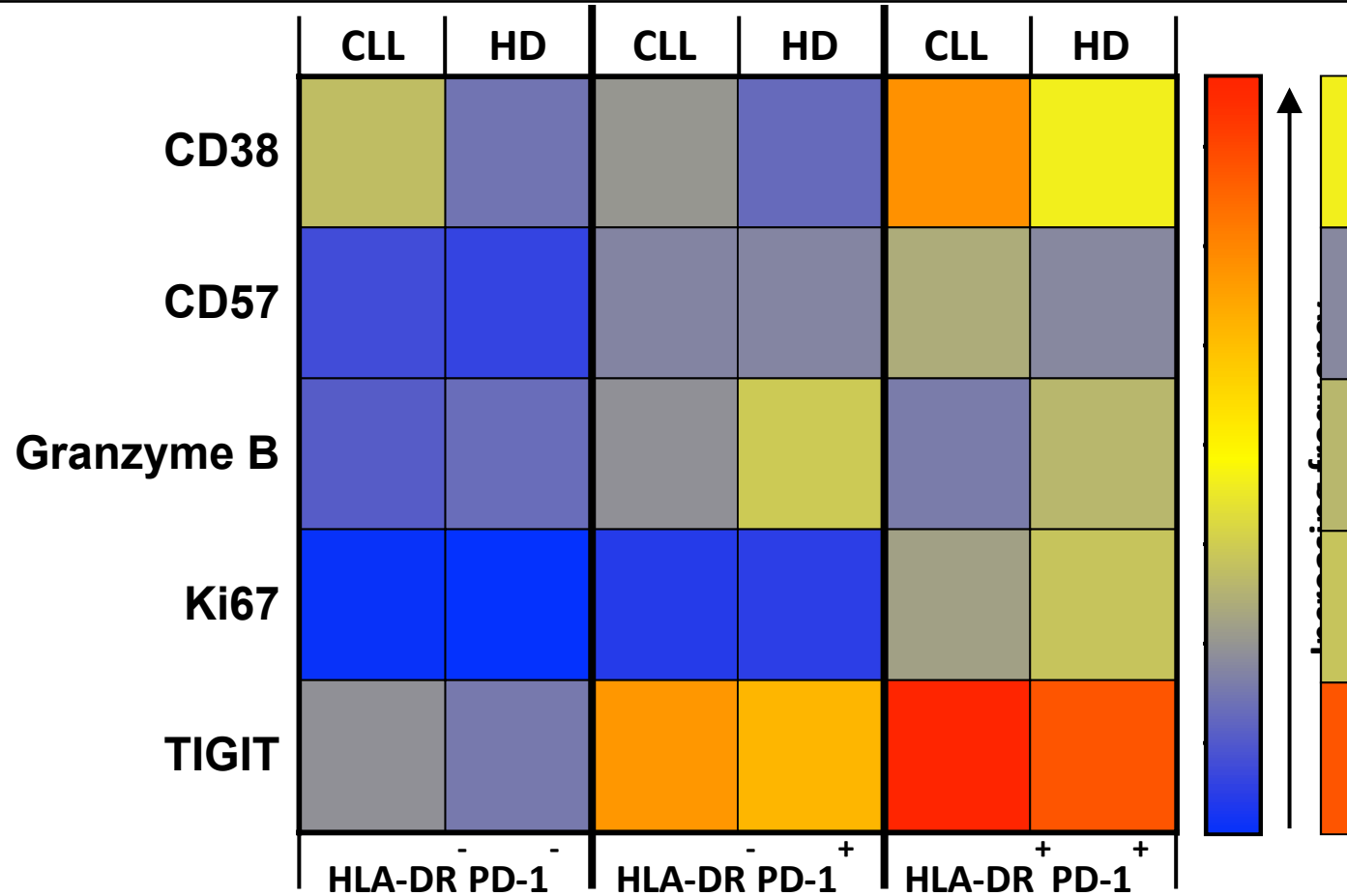


Figure 3.7: Overview of CD4⁺ T Cell Phenotypic Marker Expression

Expression of five phenotypic markers was assessed by flow cytometry on CD4⁺HLA-DR⁻PD-1⁻, CD4⁺HLA-DR⁺PD-1⁻ and CD4⁺HLA-DR⁺PD-1⁺ T cells from 67 CLL patient samples and 7 healthy donor samples. The heatmap shows the proportion of each population that expressed each marker. All of the markers except Granzyme B, showed the greatest expression in CD4⁺HLA-DR⁺PD-1⁺ cells in both CLL and healthy donor samples, with a particularly high percentage of TIGIT⁺ cells. Frequencies range from 0% (dark blue) to 80% (red). Heatmap was generated using GraphPad Prism software.

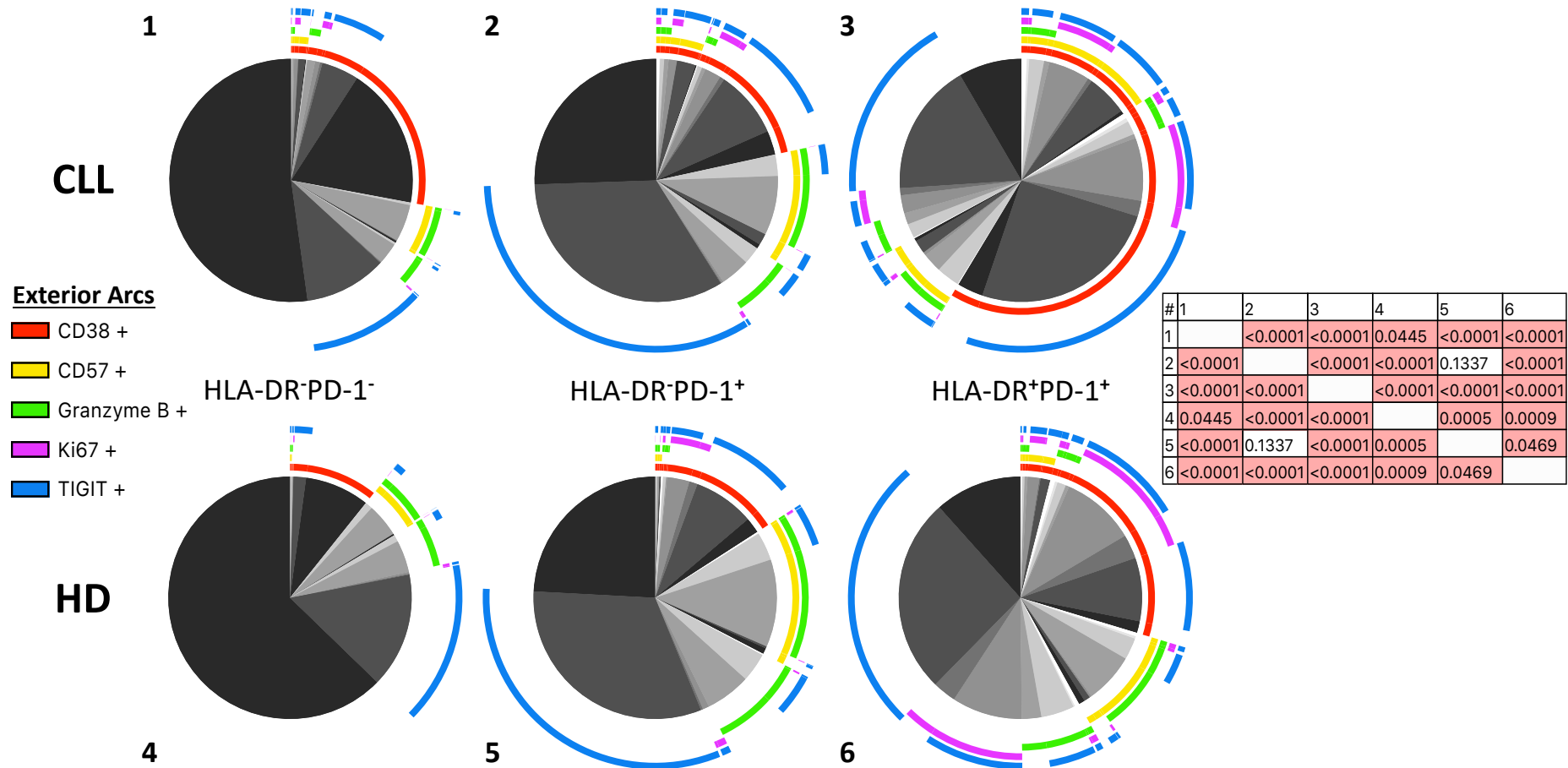


Figure 3.8: Characterisation of CD4⁺HLA-DR⁺PD-1⁺ T Cell Sub-Populations

Expression of five phenotypic markers was assessed by flow cytometry on CD4⁺ T cells from 67 CLL patient samples and 7 healthy donor samples. The patterns of expression of these markers were significantly different between CD4⁺HLA-DR⁺PD-1⁺ cells and both CD4⁺HLA-DR⁻PD-1⁻ and CD4⁺HLA-DR⁻PD-1⁺ cells, which were used as a comparison. There was also a significant difference between cells from CLL patients and healthy donors in the CD4⁺HLA-DR⁺PD-1⁺ population, but not for both CD4⁺HLA-DR⁻PD-1⁻ and CD4⁺HLA-DR⁻PD-1⁺ cells. Pie charts were created and analysed using SPICE software. The presence or absence of each exterior arc outside of a pie segment denotes the presence or absence of that marker in the population represented by that segment. Statistical significance was determined using a permutation test, with p values for each combination presented in the table.

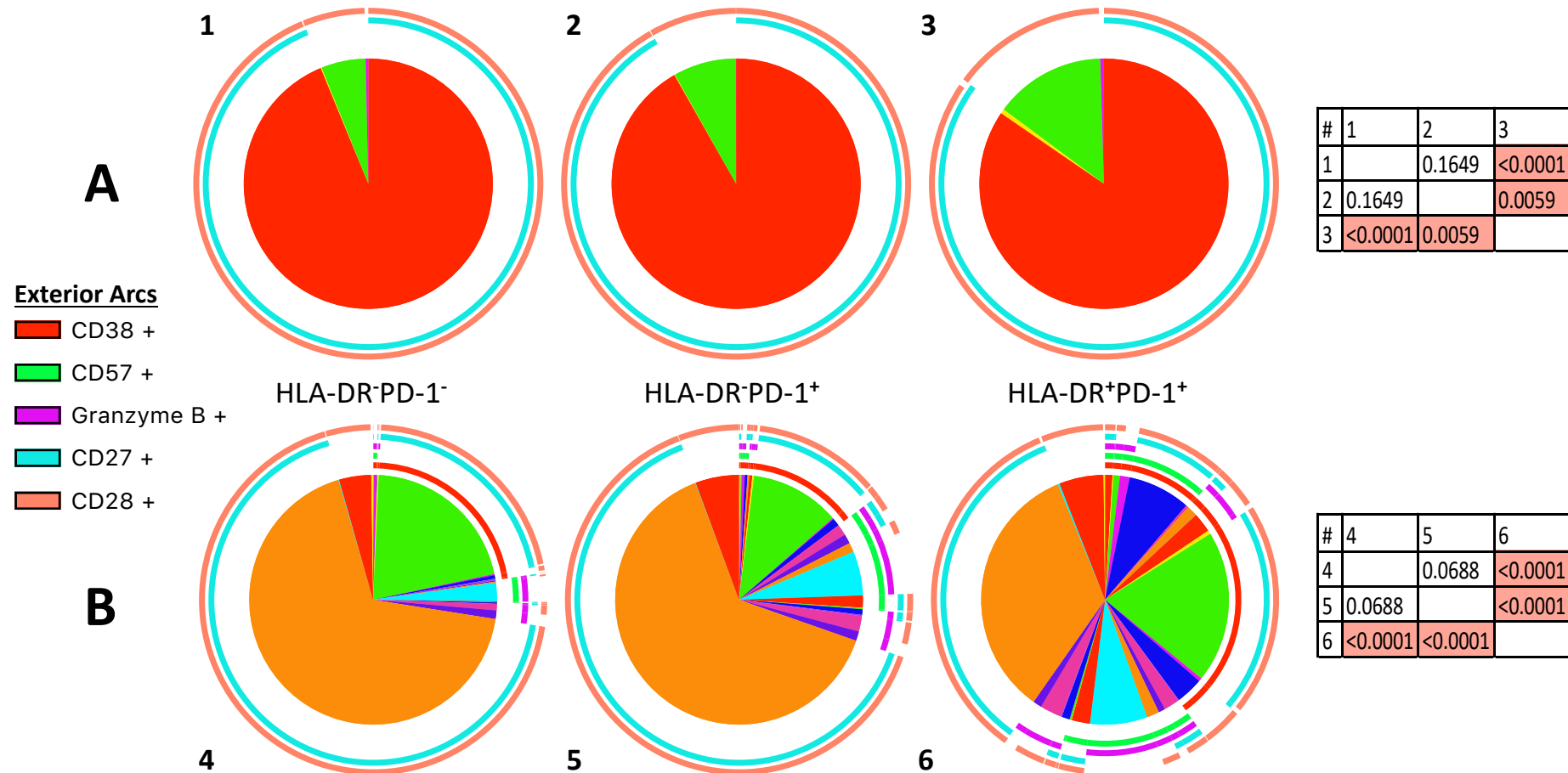


Figure 3.9: Characterisation of CD4⁺HLA-DR⁺PD-1⁺ T Cell Differentiation Markers

Expression of five phenotypic markers was assessed by flow cytometry on CD4⁺ T cells from 19 CLL patients. **A)** CD4⁺HLA-DR⁺PD-1⁺ cells had significantly lower proportions of cells co-expressing CD27 and CD28 compared to CD4⁺HLA-DR⁻PD-1⁻ and CD4⁺HLA-DR⁻PD-1⁺ cells. **B)** When combined with three other phenotypic markers, there was a significant difference in the patterns of expression and co-expression between CD4⁺HLA-DR⁺PD-1⁺ T cells and CD4⁺HLA-DR⁻PD-1⁻ and CD4⁺HLA-DR⁻PD-1⁺ cells. Pie charts were created and analysed using SPICE software. The presence or absence of each exterior arc outside of a pie segment denotes the presence or absence of that marker in the population represented by that segment. Statistical significance was determined using a permutation test, with *p* values for each combination presented in the table. Statistical significance was determined using permutation tests, with *p* values for each combination presented in the tables.

Figure 3.8 demonstrates that the activation marker CD38 shows greatest expression in CD4⁺HLA-DR⁺PD-1⁺ cells in CLL and healthy donors. This concurs with expectation since HLA-DR is also a marker of activation, however CD4⁺HLA-DR⁻PD-1⁻ cells also showed substantial CD38 expression. Interestingly, the proportion of CD38-expressing cells was also seen to be increased in CD4⁺HLA-DR⁻PD-1⁻ compared to CD4⁺HLA-DR⁻PD-1⁺ cells. In all of the subsets, CLL patients showed higher frequencies of CD38⁺ cells compared to their healthy counterparts.

CD57-expressing cells were observed at their lowest frequency in CD4⁺HLA-DR⁻PD-1⁻ T cells in CLL and healthy donors. Both the CD4⁺HLA-DR⁻PD-1⁺ and CD4⁺HLA-DR⁺PD-1⁺ subsets had similar proportions of CD57⁺ cells, with only a minimal difference between CLL and healthy donors. However, the patterns of co-expressed markers was different between CLL and healthy donor T cells, particularly in the CD4⁺HLA-DR⁺PD-1⁺ subset where a much greater proportion of CD57⁺ cells co-expressed CD38 in CLL.

In concurrence with the results in *Figure 3.6*, Granzyme B expression was observed at a higher frequency in CD4⁺HLA-DR⁺PD-1⁺ cells, compared to CD4⁺HLA-DR⁻PD-1⁻ cells in CLL. However, there appeared to be a correlation with PD-1 expression, with the both the CD4⁺HLA-DR⁻PD-1⁺ and CD4⁺HLA-DR⁺PD-1⁺ populations showing frequencies of Granzyme B⁺ cells that were much greater than for CD4⁺HLA-DR⁻PD-1⁻ cells. Similar to *Figure 3.7*, the proportions of cells expressing Granzyme B were higher in healthy donors than CLL, with a slightly increased frequency in the CD4⁺HLA-DR⁻PD-1⁺ subset compared to the CD4⁺HLA-DR⁺PD-1⁺ subset.

A different pattern of expression was observed for Ki67, which correlated with HLA-DR expression. In both the CD4⁺HLA-DR⁻PD-1⁻ and CD4⁺HLA-DR⁻PD-1⁺ populations very few Ki67⁺ cells could be detected, with CD4⁺HLA-DR⁺PD-1⁺ showing the highest expression in both CLL and healthy donor T cells. There were similar proportions of Ki67-expressing cells when comparing each subset between CLL and healthy donors, which contrasts with *Figure 3.6* where the frequency of CD4⁺HLA-DR⁺PD-1⁺ cells expressing Ki67 was significantly greater in healthy donors.

Inhibitory receptors are known to often be co-expressed on T cells and *Figure 3.8* shows this for TIGIT and PD-1, where there was a large increase in the frequency of TIGIT⁺ cells in the CD4⁺HLA-DR⁻PD-1⁺ compared to the CD4⁺HLA-DR⁻PD-1⁻ population, both in CLL and healthy donors. Interestingly, the proportion of TIGIT-expressing cells was further increased in the CD4⁺HLA-DR⁺PD-1⁺ population, more noticeably in CLL. T cells from CLL patients showed similar frequencies of TIGIT⁺ cells to those from healthy donors in the CD4⁺HLA-DR⁻PD-1⁻ and CD4⁺HLA-DR⁻PD-1⁺ subsets, but the proportion was greater in CD4⁺HLA-DR⁺PD-1⁺ cells from CLL.

Since both CD27 and CD28 are associated with “early” T cells, a CD27⁻CD28⁻ phenotype is indicative of replicative senescence (297,298). *Figure 3.9A* demonstrates that the CD4⁺HLA-DR⁺PD-1⁺ population has a lower proportion of CD27⁺CD28⁺ cells than either the CD4⁺HLA-DR⁻PD-1⁻ or the CD4⁺HLA-DR⁻PD-1⁺ populations. This is mainly caused by a reduced frequency of CD27-expressing CD4⁺HLA-DR⁺PD-1⁺ cells, since all three populations show very high expression of CD28. To some extent this follows the results shown in *Figure 3.8 and 3.9B* in which CD57 shows its highest frequency of expression in CD4⁺HLA-DR⁺PD-1⁺ cells – higher

CD57 and lower CD27 expression suggests a shift towards terminal differentiation (299). However, the very low frequency of CD27⁻CD28⁻ cells in the CD4⁺HLA-DR⁺PD-1⁺ subset suggests that there are very few, if any, senescent cells in this population. When combined with the results for Ki67 expression, it appears that the CD4⁺HLA-DR⁺PD-1⁺ T cell population contains a subset of actively proliferating cells and that those cells that are not proliferating are not senescent *i.e.* still have the capacity to proliferate.

As well as differences in the expression of individual markers, the overall pattern of expression and co-expression of CD38, CD57, Granzyme B, Ki67, TIGIT, CD27 and CD28 is strikingly more complex in CD4⁺HLA-DR⁺PD-1⁺ cells when compared to CD4⁺HLA-DR⁻PD-1⁺ and CD4⁺HLA-DR⁻PD-1⁻ cells. This suggests that there is a greater deal of heterogeneity within the CD4⁺HLA-DR⁺PD-1⁺ population. Interestingly, this same observation is made in both CLL patients and healthy donors (*Figure 3.8*), which would perhaps suggest that this cell population is similar between the two groups. There is however, a statistically significant difference between the patterns of marker expression and co-expression in CD4⁺HLA-DR⁺PD-1⁺ cells in CLL patients and healthy donors. Therefore, it would appear that it is not simply the enrichment of the CD4⁺HLA-DR⁺PD-1⁺ T cell population in CLL patients that may be important, but also the phenotype and functional nature of the cells within this population.

3.3 Longitudinal Analysis of CD4⁺HLA-DR⁺PD-1⁺ T Cells

As well as determining the phenotypic profile of CD4⁺HLA-DR⁺PD-1⁺ T cells in CLL, an important element of this study was to assess the cell frequencies and patient parameters investigated in *Section 3.1* over time. This includes the study of both the dynamics of stable disease in untreated, indolent patients and, where clinical data is available, the impacts of therapy on T cell populations.

Longitudinal studies of T cells are uncommon in untreated CLL patients due to several key difficulties associated with the disease. Firstly, the highly heterogenous nature of CLL means that many samples are needed to be able to draw accurate conclusions, especially as each sample is only a 'snapshot' of a specific time point. However, the 'watch and wait' strategy employed by clinicians with CLL patients who have indolent disease means that many patients only visit clinics at infrequent intervals, often 6 or 12 months apart, meaning that obtaining enough serial samples over the course of a single project can prove problematic. Furthermore, around half of patients with indolent disease will progress during their disease course – it remains difficult to predict if and when this progression will occur, even with some known prognostic markers available (22,29,300,301). Therefore, a substantial proportion of patients being followed longitudinally are likely to progress and require treatment during the study period. However, this does provide an opportunity to investigate whether T cell parameters can be used prognostically with regard to CLL disease progression. There remains a large amount unknown both in terms of the immediate impact of treatment on T cells and on the kinetics of T cell recovery. Therefore,

patients who currently have stable disease but have previously been treated should be considered with caution when investigating T cell parameters.

In this study, these difficulties have been overcome by combining data collected over a period of up to almost 10 years from several related projects. Although each project focused on different aspects of CLL, measurement of variables including the frequency of T cells and the CD4:CD8 ratio were common to each one and as such those data can be added to the data collected in this study to give long-term follow-up that is not usually possible over the course of a single project. Additionally, access to clinical information, kindly provided by Prof. Chris Fegan, allows for the stratification of untreated patients to ensure the consistency of the data.

3.3.1 Longitudinal Changes in Untreated CLL Patients

Figure 3.10 shows the stability of T cell parameters for untreated patients. For each patient, the earliest time point at which data was available for each measured parameter was taken as the baseline for that parameter and the absolute change from that baseline was plotted for each subsequent time point. The number of time points available for any given patient depends both on the data collected from each of their samples and the number of samples analysed over the period in question. As described above, the number of samples for a given patient is affected by factors including disease progression requiring treatment.

The changes in the frequency of T cells in untreated patients as a proportion of total lymphocytes is shown in *Figure 3.10A*. These data suggest that the

percentage of T cells can stay very stable, with some patients showing a remarkable lack of change even almost 10 years after their first measurement. However, there are also a great number of patients who display the opposite dynamics, with large changes in T cell frequency within just a few months. In the most extreme cases, this is seen to be a loss of over 20% T cells within around 1 year, which is likely to be sign of disease progression associated with a large increase in the number of CLL cells. Over the course of the whole study, the large majority of patient samples show a decrease in the frequency of T cells compared to baseline measurements, which is perhaps to be expected. Since there is an expansion in the numbers of T cells in CLL, the key determinant of T cell percentage is the number of CLL cells – as these leukaemic cells accumulate over time, as reflected in the increasing total lymphocyte count, the proportion of T cells should naturally decrease in turn. However, as with any heterogenous disease, there are patients who do not fit this pattern and show increased T cell frequencies at some time points. The explanation for this is likely to be twofold: firstly, fluctuations in the number of CLL cells are common and since a given sample represents a single ‘snapshot’ it may not reflect the overall pattern of change in that patient; secondly, co-morbidities including common infections can cause temporary expansions in the number of T cells which, although unrelated to their CLL, will be seen as an increased percentage of T cells in the patient (302).

Figure 3.10B shows the absolute changes in CD4:CD8 ratio observed in untreated CLL patients. As was the case for the frequency of T cells shown in *Figure 3.10A*, there was a subset of patients who had very stable CD4:CD8 ratio values, with very little change over periods of up to 6 years. In the shorter term, the

vast majority of patients showed stable ratios, with only minimal changes within 1 year of their first sample. There was a small number of patients whose CD4:CD8 ratio changed by a larger amount in the first year, but longer-term patients with significant changes in ratio became the majority. Most of these less-stable patients displayed a decrease in CD4:CD8 ratio after 5-6 years, suggesting that either an increase in CD8⁺ cells or a decrease in CD4⁺ cells had occurred. Since an inversion of the CD4:CD8 ratio caused by expansions of the CD8⁺ compartment is associated with disease progression and poor prognosis (19), it is likely that these data reflect patients whose disease is progressing.

The absolute changes in the frequency of CD4⁺HLA-DR⁺PD-1⁺ T cells is displayed in *Figure 3.10C*. It is important to note that, due to the availability of data, this graph only covers a period of around 1.5 years rather than the longer time shown in *Figures 3.10A* and *3.10B*. However, this helps to demonstrate the more dynamic nature of CD4⁺HLA-DR⁺PD-1⁺ T cell frequency when compared to the frequency of T cells or in particular the CD4:CD8 ratio. Although a number of patients did show stable percentages of CD4⁺HLA-DR⁺PD-1⁺ cells, the vast majority of patients had significant differences, even in periods as short as 2-3 months. In almost all cases, the proportion of the CD4⁺ compartment comprised of CD4⁺HLA-DR⁺PD-1⁺ cells increased compared to baseline during the measured period. The trend towards a decrease in the CD4:CD8 ratio show in *Figure 3.10B* and the increased frequency of CD4⁺HLA-DR⁺PD-1⁺ T cells in patients with an inverted ratio (*Figure 3.2*) may help to explain the pattern of change in CD4⁺HLA-DR⁺PD-1⁺ T cells.

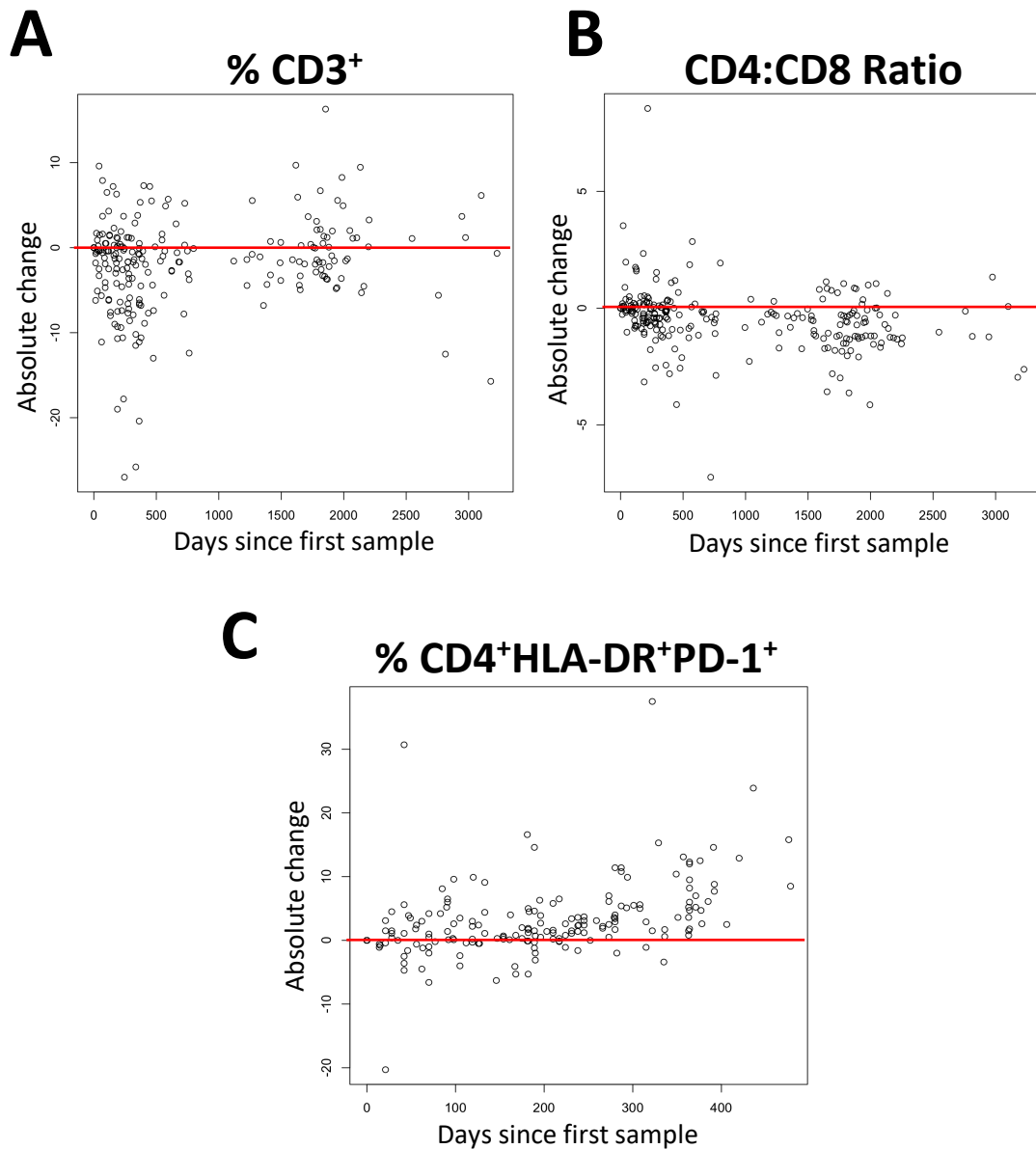


Figure 3.10: Untreated CLL Patients Show Variable Stability in T Cell Parameters

Blood samples from untreated CLL patients were assessed for several T cell parameters by flow cytometry. Where available, data was plotted for a period of up to almost 10 years. All data analysed using R.

A) Absolute change in percentage of CD3⁺ lymphocytes, representing 406 samples.

B) Absolute change in CD4:CD8 T cell ratio, representing 427 samples.

C) Absolute change in the percentage of CD4⁺HLA-DR⁺PD-1⁺ T cells, representing 360 samples.

3.3.2 Longitudinal Changes in Ibrutinib-Treated Patients

Bruton's Tyrosine Kinase (BTK) is a key enzyme in the signalling cascade downstream of the B Cell Receptor (BCR) and as such plays an important role in CLL, since the leukaemic B cells rely on constitutive BCR signalling to survive and proliferate. Ibrutinib is an inhibitor of BTK which has shown great promise as a CLL therapy. Although only occasionally used as a frontline treatment, Ibrutinib has been indicated in the UK for use in relapsed/refractory CLL and in CLL patients presenting with high risk genetic abnormalities, such as 17p chromosomal deletions. Unlike with some other therapies, once prescribed Ibrutinib must be taken for life. Therefore, understanding the direct and indirect effects of this drug is important for CLL patients who may be taking Ibrutinib for many years.

Treatment with Ibrutinib can have dramatic effects, with mass lymph node emigration and CLL cell lysis commonly observed (303). However, not much is known about the effect of Ibrutinib treatment on T cells (reviewed here (304)). The few recent studies have provided conflicting results, regarding both the numbers of T cells and the distribution of T cell subsets post-Ibrutinib, but a common finding has been decreased expression of PD-1 on T cells. Overall, the lack of consensus in this area means the impact of Ibrutinib on T cells warrants further investigation.

In this study, the access to serial CLL samples over a period of time facilitates the investigation of Ibrutinib therapy on T cell parameters. Where possible, samples were assessed while patients were untreated and then at a minimum of one timepoint subsequent to Ibrutinib treatment beginning. The results of this are shown in *Figure 3.11*. If the first sample taken following the initiation of Ibrutinib therapy

was less than 1 month after treatment began it was labelled 1 in *Figure 3.11*, if it was more than 1 month post-initiation it was labelled 2. The longest follow-up for any of the depicted patients was 10 months post-treatment initiation.

Figure 3.11A shows the frequency of T cells as measured in 13 CLL patients pre- and post-treatment with Ibrutinib. These results suggest that, in most patients, the frequency of T cells was very stable after the start of Ibrutinib therapy. For the 4 patients for whom short-term (less than 1 month) follow-up was available, 3 of them showed a decrease in the percentage of T cells in total lymphocytes – this would be expected in patients who respond well to therapy, since the emigration of large numbers of CLL cells from the lymph nodes would ‘dilute’ the T cells in the blood. However, longer follow-up showed mainly minor changes in the proportion of CD3⁺ cells in the majority of patients. One exception to this was a patient with a very large increase in the frequency of T cells around 9 months after treatment initiation. At this timepoint this patient had a decreased total lymphocyte count, approaching normal healthy range (data not shown), suggesting that Ibrutinib therapy had been highly effective in killing CLL cells – however such a large change in T cell frequency could also reflect a concomitant infection with no relation to CLL (305) and therefore further follow-up will be needed to make an informed conclusion. Across all 14 patients, there were no major decreases in T cell frequency following Ibrutinib initiation or subsequently, which suggests that no patients had worsening disease. Overall, T cell frequency does not appear to be affected by treatment with Ibrutinib, although the low numbers of patients for whom the appropriate data was available mean more investigation will be required.

Shown in *Figure 3.11B* is the impact of Ibrutinib treatment on CD4:CD8 T cell ratio in 14 CLL patients. The results demonstrate that the ratio is quite stable in patients following their initiation of therapy and subsequently. This seems to be particularly true for patients with an inverted ratio – all 3 CLL^{IR} patients that were assessed showed very little change in ratio over a period of up to 9 months. For those with a normal ratio, 2 patients had significant ratio decreases following Ibrutinib treatment, with one of these showing an inversion of their ratio at the time of their second follow-up sample. Among the other CLL^{NR} patients there was a trend of slowly decreasing ratio over time, however whether this is due to an increase in CD8⁺ T cell numbers or a loss of CD4⁺ T cells is unclear. Since an inverted ratio is a marker of poor prognosis, it will be of great interest to continue to follow patients whose ratios have changed from normal to inverted – it may be that these patients are experiencing a side effect of Ibrutinib treatment or that their disease is progressing in spite of their therapy.

Perhaps of greatest interest to this study was the question of whether treatment with Ibrutinib has any effect on the CD4⁺HLA-DR⁺PD-1⁺ T cell subset. In untreated CLL patients (*Figure 3.10C*) it was observed that the percentage of CD4⁺HLA-DR⁺PD-1⁺ cells in the CD4⁺ compartment was dynamic and similar results were obtained in the Ibrutinib-treated patients, with some showing considerable variability between samples (*Figure 3.11C*). Although there were only a small number of patients with available data (n=12), it did appear that the frequency of CD4⁺HLA-DR⁺PD-1⁺ T cells was fairly stable once the patients were on treatment, except in one case in which the patient (treated sample 5, 21.1%) was known to have an incident

of pneumonia that may have affected their results. Overall however, there appeared to be no consistent pattern to the results with some patients showing increasing CD4⁺HLA-DR⁺PD-1⁺ cell frequencies and others decreasing frequencies following Ibrutinib initiation. It may be that changes in the percentage of CD4⁺HLA-DR⁺PD-1⁺ cells followed by relative stability over a longer period reflect the impact of Ibrutinib on the CLL cells, with patients requiring a stabilisation period following the start of their treatment.

Overall, these results show a minimal impact of Ibrutinib treatment on the T cell compartment, with no consistent pattern of Ibrutinib-induced changes to any of the parameters studied. However, these data do not rule out a longer-term effect of Ibrutinib therapy, since this investigation only collected data over a 10 month follow-up period.

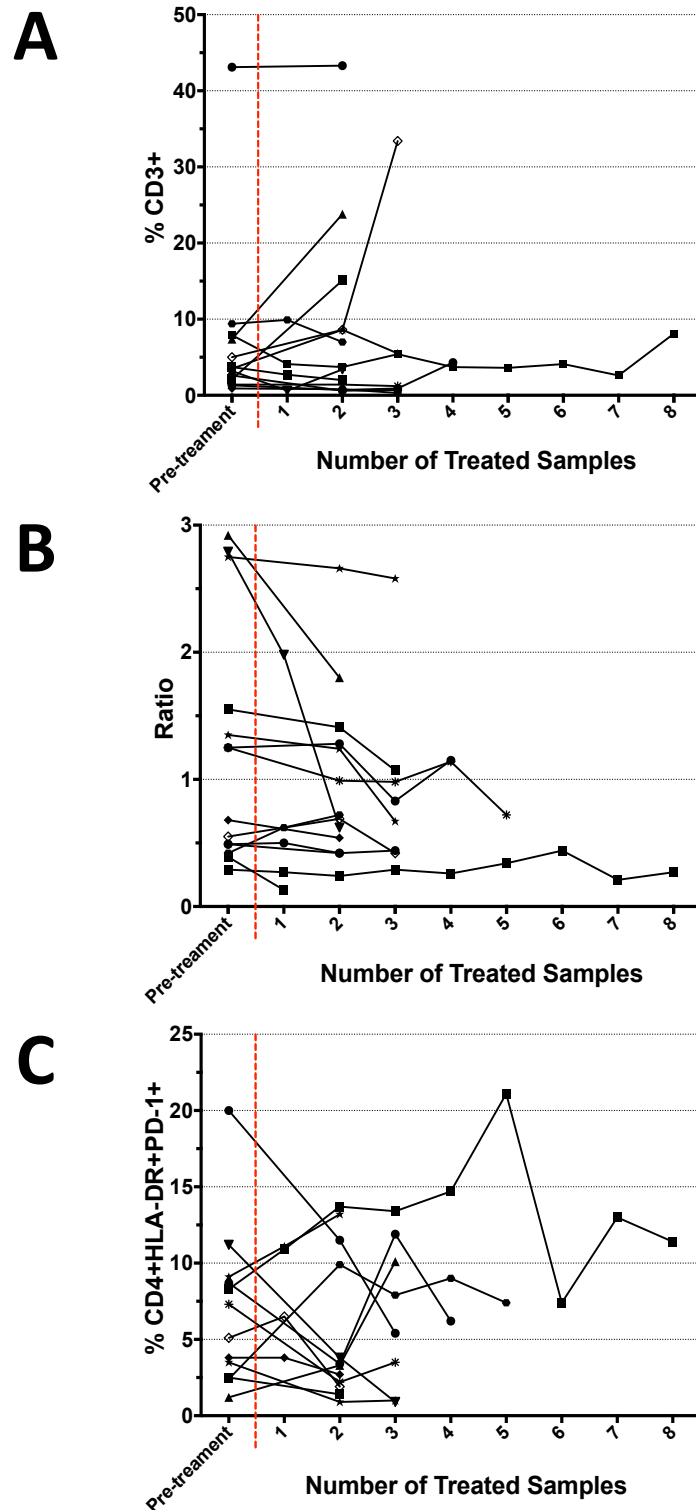


Figure 3.11: Impact of Ibrutinib Treatment on T Cell Parameters

Blood samples from CLL patients were analysed by flow cytometry prior to therapy initiation and then at least once after beginning treatment with Ibrutinib. The first treated sample analysed was only labelled 1 if it was assessed less than 1 month after treatment began, otherwise it was designated as 2 on the above graphs. **A)** The effect of Ibrutinib treatment on the frequency of T cells as a proportion of total lymphocytes in 13 patients. **B)** The impact of Ibrutinib treatment on CD4:CD8 ratio in 14 patients. **C)** The effect of Ibrutinib treatment on the frequency of CD4⁺HLA-DR⁺PD-1⁺ T cells in the CD4⁺ compartment in 12 patients.

3.4 Effect of T Cell Parameters on CLL Patient Outcomes

The data presented in *Figure 3.10* demonstrate that T cell parameters in CLL, including CD4⁺:CD8⁺ ratio and the frequency of CD4⁺HLA-DR⁺PD-1⁺ cells, can be dynamic and variable over time, with the changes in some cases likely to reflect disease progression. However, it would be of great value to be able to predict patients who were at higher risk of progressing before any such changes in their T cells, particularly with the infrequent clinic visits of many patients making longitudinal T cell monitoring challenging. Therefore, using the clinical information obtained from Prof. Chris Fegan, this study investigated whether T cell parameters could act as predictive biomarkers for CLL progression.

3.4.1 Progression-Free Survival

Kaplan-Meier survival curves depicting Progression-Free Survival (PFS) for a cohort of 209 CLL patients from the South Wales area are shown in *Figure 3.12*. For these graphs, PFS was measured from the date of diagnosis, with any progression events determined and recorded by clinicians.

Figure 3.12A shows PFS when CLL patients are stratified based on their CD4:CD8 T cell ratio, with 80 CLL^{IR} patients and 129 CLL^{NR} patients. The curves were significantly different for the two groups ($p=0.0009$), with a hazard ratio of 2.56. Over the 20 year period, 51.6% of CLL^{IR} patients progressed compared to 43.1% of CLL^{NR} patients. Within this time frame, the median PFS was not reached for CLL^{NR} patients while for CLL^{IR} patients this was 7.8 years. Interestingly, there were no progressions within the CLL^{IR} group after around 8 years from diagnosis – this perhaps suggests

the presence of two subgroups within this patient population: those with long-term stable disease and those who will progress, with the latter group mainly seeing progression early in their disease course.

Previous work has suggested that CD4⁺HLA-DR⁺PD-1⁺ T cell frequency may be useful as a predictive biomarker for CLL progression (256), so this study aimed to confirm this in a larger cohort of patients. In *Figure 3.12B* are shown PFS data for 209 CLL patients stratified based on the median frequency of CD4⁺HLA-DR⁺PD-1⁺ T cells, which was 3.0% – there were 102 patients in the low (<3.0%) group and 107 patients in the high (>3.0%) group. Over the course of the study period, the two groups diverged significantly ($p=0.0045$), with 57.1% of the high group progressing compared to just 29.0% of the low group, giving a hazard ratio of 2.15. The median PFS for the high group was 17.9 years but was not reached for the low group with the timeframe of this study.

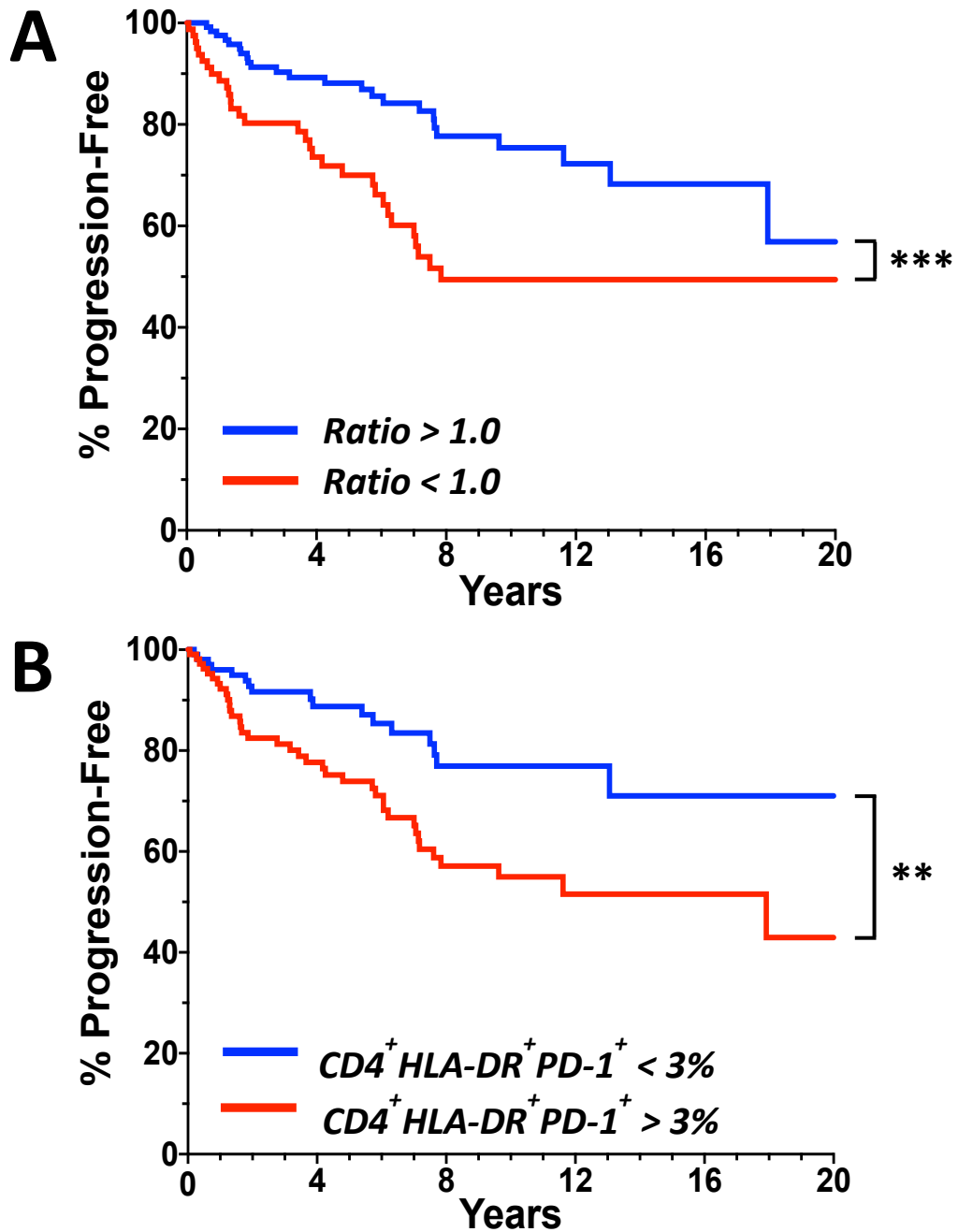


Figure 3.12: Progression-Free Survival is Significantly Different in CLL Patients Stratified by T Cell Parameters

T cell parameters in blood samples from 209 CLL patients were analysed by flow cytometry and the results used to stratify the patients. Progression-free survival was measured from diagnosis. *Kaplan-Meier curves were plotted and analysed using GraphPad Prism. Hazard ratios were calculated using the logrank method.*

***= $p < 0.01$, ***= $p < 0.001$.*

A) CLL^{IR} patients had a significantly shorter progression-free survival than CLL^{NR} patients. *Hazard ratio 2.39, confidence interval 1.47-4.45*

B) CLL patients with a CD4⁺HLA-DR⁺PD-1⁺ T cell frequency greater than the median value (3.0%) had a significantly reduced progression-free survival compared to those with a frequency below the median. *Hazard ratio 2.24, confidence interval 1.32-3.79*

3.4.2 Time to First Treatment

Figure 3.13 depicts Kaplan-Meier survival curves for the same cohort of 209 CLL patients comparing Time to First Treatment (TTFT). Not all patients who progress receive therapy immediately, due to differences in the severity of their disease, so TTFT provides a measure of only those patients who have progressed to a severe phenotype and so is more stringent than PFS. The TTFT statistic was measured from the date of diagnosis to the date of treatment initiation as recorded by clinicians.

In *Figure 3.13A*, the Kaplan-Meier curve for TTFT is displayed for patients stratified into CLL^{NR} (n=129) and CLL^{IR} (n=80). There was a significant difference between the two groups (p=0.0002), giving a hazard ratio of 2.84, and 52.3% of CLL^{IR} patients were treated during the study period compared to 43.9% of patients in the CLL^{NR} group. For the CLL^{IR} group the median TTFT was 7.6 years, however the median was not reached within the timeframe for CLL^{NR} patients. Similar to the pattern seen in *Figure 3.12A*, there were no patients treated for the first time in the CLL^{IR} group after around 8 years from diagnosis, again suggesting a subgrouping of these patients with long-term stable disease.

The TTFT for patients divided into groups based on their frequency of CD4⁺HLA-DR⁺PD-1⁺ T cells is shown in *Figure 3.13B*. As in *Figure 3.12B*, the median frequency (3.0%) was used a cut-off to stratify patients into high and low groups. The TTFT for the two groups was significantly different (p=0.0023), with a hazard ratio of 2.26. Over the 20 year period, 58.8% of the high group required treatment compared to just 29.4% of the low group. Therefore, the low group did not reach the median TTFT during this study, while the median TTFT for the high group was 12.1 years.

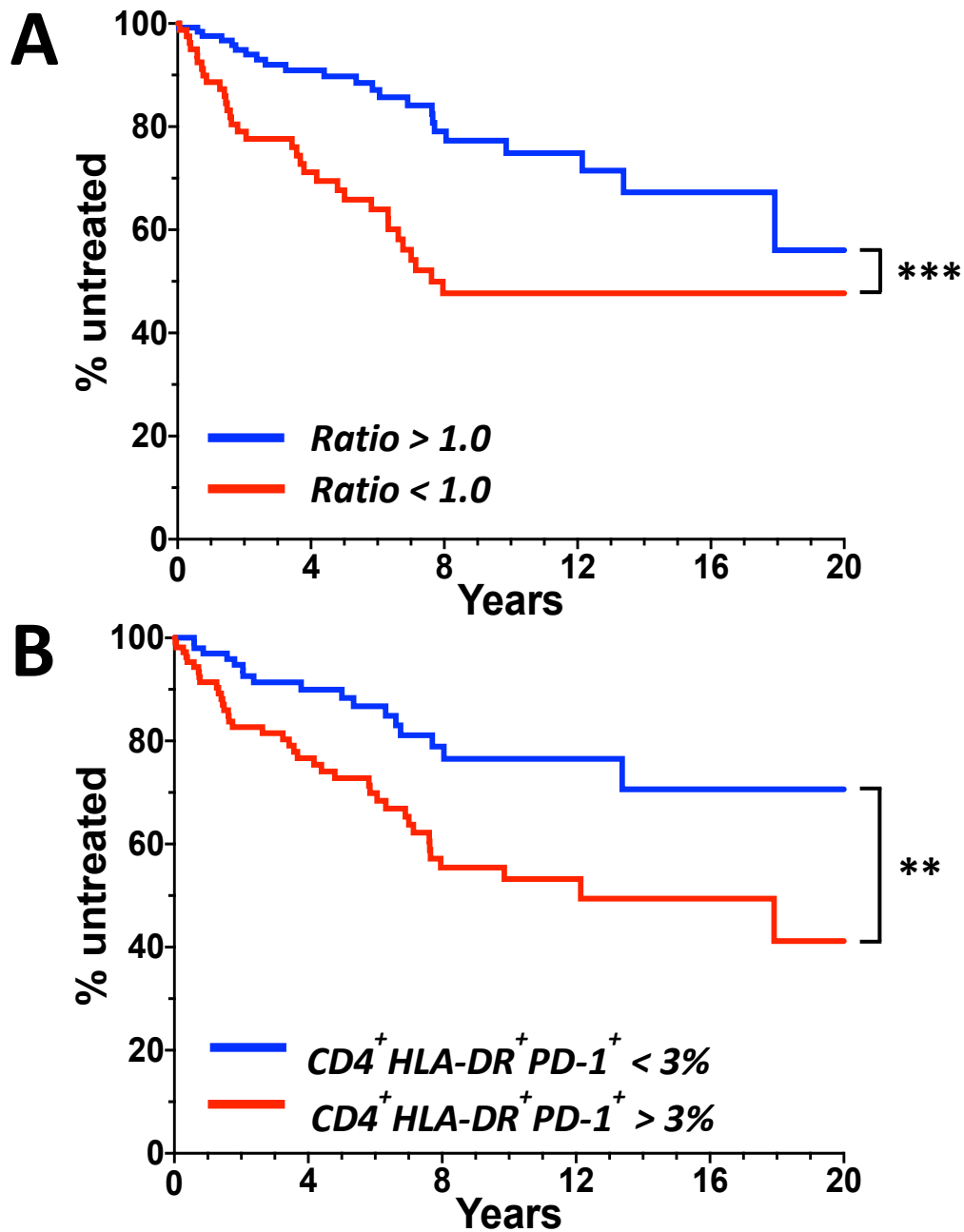


Figure 3.13: Time to First Treatment is Significantly Different in CLL Patients Stratified by T Cell Parameters

T cell parameters in blood samples from 209 CLL patients were analysed by flow cytometry and the results used to stratify the patients. Time to first treatment was measured from diagnosis. *Kaplan-Meier curves were plotted and analysed using GraphPad Prism. Hazard ratios were calculated using the logrank method.*

***= $p < 0.01$, ***= $p < 0.001$.*

A) CLL^{IR} patients had a significantly shorter time to first treatment than CLL^{NR} patients. *Hazard ratio 2.64, confidence interval 1.53-4.57*

B) CLL patients with a CD4⁺HLA-DR⁺PD-1⁺ T cell frequency greater than the median value (3.0%) had a significantly reduced time to first treatment compared to those with a frequency below the median. *Hazard ratio 2.36, confidence interval 1.40-3.98*

3.5 Discussion

This chapter aimed to define phenotypically the nature of CD4⁺HLA-DR⁺PD-1⁺ T cells, which have previously been shown to not be T_{Reg} or T_{FH} cells (256). As well as defining a detailed phenotype for these CD4⁺HLA-DR⁺PD-1⁺ cells, this chapter has also investigated the dynamics of CD4⁺HLA-DR⁺PD-1⁺ T cell frequency alongside several other T cell parameters in a longitudinal study, which based on available literature has not been attempted on this scale in CLL before. Furthermore, where samples have been available the impact of Ibrutinib treatment on CD4⁺HLA-DR⁺PD-1⁺ cells, as well as other T cell parameters, has been investigated. Finally, this chapter has sought to verify previous data showing that there was significant prognostic value in the frequency of CD4⁺HLA-DR⁺PD-1⁺ T cells (256) by examining patient outcomes in a large cohort of early stage CLL patients.

This study has mainly focused on further investigation of CD4⁺HLA-DR⁺PD-1⁺ T cells, which were previously identified as the most important prognostic subset of the CD4⁺ T cell population in a multivariate analysis (285). In a new, larger cohort of CLL patients, it was shown that there were elevated frequencies of these CD4⁺HLA-DR⁺PD-1⁺ T cells compared to age-matched healthy controls, which is in line with previous results. Further, it was found that the proportions of CD4⁺HLA-DR⁺PD-1⁺ T cells were significantly greater in CLL patients with an inverted CD4:CD8 ratio (CLL^{IR}) compared to those with a normal ratio >1.0 (CLL^{NR}). However, even CLL^{NR} patients had higher frequencies of CD4⁺HLA-DR⁺PD-1⁺ cells than healthy donors, suggesting that CD4:CD8 T cell ratio is not the only determining factor of

CD4⁺HLA-DR⁺PD-1⁺ T cell percentage. This was supported by the lack of correlation between CD4⁺HLA-DR⁺PD-1⁺ T cell proportions and CD4:CD8 ratio in CLL patients.

CLL patients are known to have increased numbers of T cells and more proliferating T cells than healthy donors (268). With the increased frequencies of CD4⁺HLA-DR⁺PD-1⁺ cells in CLL patients observed in this study, it was hypothesised that CD4⁺HLA-DR⁺PD-1⁺ cells may be an actively proliferating population. Compared to the whole CD4⁺ compartment, there were significantly more Ki67-expressing CD4⁺HLA-DR⁺PD-1⁺ cells, suggesting that the increased proportion of these cells is driven in part by their proliferation. However, the majority of CD4⁺HLA-DR⁺PD-1⁺ cells did not express Ki67 and were therefore not actively proliferating – molecular analysis of telomeres would allow investigation of the replicative history of these cells to determine whether they had previously proliferated. Previous studies have associated expanded CD4⁺ T cells in CLL with cytomegalovirus (CMV) specificity (10), however the frequency of CD4⁺HLA-DR⁺PD-1⁺ cells has been shown to have no correlation with CMV serostatus (285). Nevertheless, it would be of interest to investigate whether CD4⁺HLA-DR⁺PD-1⁺ cells show recognition of an alternative virus that could similarly account for their expansion in CLL.

There was a significant increase in the frequency of Granzyme B-expressing cells in the CD4⁺HLA-DR⁺PD-1⁺ population compared to the total CD4⁺ compartment. Cytotoxicity is a property usually associated with CD8⁺ T cells, but there have been several previous reports of cytotoxic CD4⁺ T cells in CLL (16,248,306). With a number of patients in this study demonstrating over 50% Granzyme B⁺ cells in the

CD4⁺HLA-DR⁺PD-1⁺ subset, it is possible that these cells can account for the previously reported enrichments of cytotoxic CD4⁺ cells. It would usually be expected that cytotoxic CD4⁺ T cells would kill tumour cells if they were tumour specific (289), so the enrichment of Granzyme B-expressing cells in CLL seems paradoxical. However, there are numerous reports of T cell dysfunction in CLL, particularly centred around impairment of the formation of immune synapses (258,307–309). Since the interaction mediated by the immune synapse is essential to cytotoxic function (310,311), it may be the case that the development of CLL drives a cytotoxicity phenotype that is ultimately unable to control tumour cells due to defective immune synapse engagement.

The expression on CD4⁺HLA-DR⁺PD-1⁺ cells of a classical activation marker (HLA-DR) along with PD-1, which can be a marker of activation or exhaustion (260,271,312), made it unclear whether the CD4⁺HLA-DR⁺PD-1⁺ population represented activated or exhausted T cells. Therefore, analysis of other markers associated with activation (CD38) and exhaustion (TIGIT) was conducted to attempt to resolve this, along with several other phenotypic markers chosen to give a broader profile of the nature of CD4⁺HLA-DR⁺PD-1⁺ T cells.

The most frequently expressed of the markers studied, in both CLL and healthy donors, was the immunomodulatory receptor T Cell Immunoglobulin and Immunoreceptor Tyrosine-Based Inhibitory Motif Domain (TIGIT). As a member of the PD-1 family of inhibitory receptors TIGIT, along with other similar receptors such as Lag-3, is often co-expressed with PD-1 (294). Studies have demonstrated a role for

TIGIT in both chronic viral infections (313) and in several haematological cancers (314–316), mainly related to its role in T cell exhaustion. However in CLL, Catakovic *et al.* have suggested a tumour-supportive role for TIGIT⁺CD4⁺ T cells (317). Their other finding that TIGIT expression in CD4⁺ cells is greater in CLL than in healthy donors was found to be true in the new cohort in this chapter, and mirrors the pattern also seen in the CD4⁺HLA-DR⁺PD-1⁺ population. Taken together with several other studies that show a role for CD4⁺ cells in promoting CLL (318,319), the data here suggest it would be valuable to determine whether CD4⁺HLA-DR⁺PD-1⁺ cells can also support CLL cell survival.

The expression of the activation marker CD38 on T cells has been previously linked to CLL prognosis (320). In this cohort, CD38 expression was most frequent in CD4⁺HLA-DR⁺PD-1⁺ T cells followed closely by CD4⁺HLA-DR⁻PD-1⁻ cells, with the lowest frequency in CD4⁺HLA-DR⁻PD-1⁺ cells. This perhaps reflects the inhibitory nature of PD-1 (321), whereby activation has been attenuated leading to downregulation of both HLA-DR and CD38. Interestingly, although there have been no published demonstrations of the involvement of a CD4⁺HLA-DR⁺PD-1⁺ phenotype in other disease settings, Eller *et al.* have reported a role for CD4⁺HLA-DR⁺PD-1⁺CD38⁺ T cells in HIV (322). Increased levels of these highly activated cells correlated with viral load and the loss of CD4⁺ T cells characteristic of disease progression in HIV. When considered with previous findings in CLL that CD4⁺HLA-DR⁺PD-1⁺ cells reflect a poorer prognosis, it could be hypothesised that the significant proportion of these cells which express CD38 is responsible for, or associated with, the effects observed on patient outcomes. Previous work did not find CD38-expressing CD4⁺ T cells to have

prognostic value in CLL (285), however co-expression of HLA-DR, PD-1 and CD38 was not investigated in that study.

There are several reports of expansions of terminally differentiated senescent T cells both in CLL (19,323) and in association with advancing age (257,324–326) – however, the focus in almost all cases has been on CD8⁺ T cells. Nunes *et al.* did report an increased frequency of these cells within the CD4⁺ compartment in CLL (19), and this has subsequently been observed again (285), particularly in CLL^{IR} patients. In contrast to the CD4⁺ T cells in these previous studies, CD4⁺HLA-DR⁺PD-1⁺ T cells appeared to show no signs of a senescence phenotype in the current study. The frequency of CD27⁻CD28⁻ cells in this population was very low, with CD57 co-expressed in only a fraction of these. Due to antibody panel constraints, Ki67 expression could not be investigated alongside CD27 and CD28, but it would be expected that no Ki67 expression would be detectable in the CD27⁻CD28⁻ cells (299). Overall, it can be hypothesised that a CD4⁺ compartment with considerable senescence, concurrent with an actively proliferating CD4⁺HLA-DR⁺PD-1⁺ subset, may account for the enrichment of CD4⁺HLA-DR⁺PD-1⁺ cells in CLL observed here and previously (285).

Studies have suggested that PD-1 expression on CD4⁺ T cells in CLL may have prognostic value (327), while previous work has demonstrated promising results that suggest CD4⁺HLA-DR⁺PD-1⁺ T cell frequency and CD4:CD8 ratio could be used as a markers to stratify patients at high risk of disease progression (19,256,285). This study has made use of a considerably larger CLL patient cohort to extend and confirm

these findings. Using long-term outcome data from over 200 patients, it was observed that both CD4:CD8 ratio and the frequency of CD4⁺HLA-DR⁺PD-1⁺ T cells were able to significantly stratify patients into different risk groups. CLL^{IR} patient and those with a CD4⁺HLA-DR⁺PD-1⁺ T cell frequency greater than the cohort median were more than twice as likely to progress, demonstrating a similar level of stratification as that originally observed for IGHV mutation status and CD38 expression (28,29). Moving beyond the previous work, this study also examined the time from diagnosis to first treatment (TTFT) in these patients, seeing a similar level of stratification between high risk and low risk phenotypes. In general, TTFT takes into account more serious progressions, as patients who progress but do not have severe disease may not be treated immediately. However, the decision of when to commence treatment is subjective and will vary between different hospitals and clinicians.

Although CD4:CD8 ratio and the frequency of CD4⁺HLA-DR⁺PD-1⁺ cells appear to have prognostic value, it is important to remember that any given sample is only a “snapshot” of the patient phenotype at that moment. Therefore, it is important to understand whether these specific prognostic phenotypes (high frequency of CD4⁺HLA-DR⁺PD-1⁺ cells and inverted ratio) are temporary, occurring alongside disease progression, or permanent having arisen early in the disease course. In the case of a set, permanent phenotype, this would increase the value of analysing a sample taken at diagnosis, allowing the earliest possible prediction of patient prognosis. In order to explore this, serial samples have been collected over a period

of up to 10 years in order to follow patient progress and investigate the dynamics of CLL patient T cells, on a scale that has hitherto not been reported. A potential limitation of this study occurs due to the fact that the data have been collected by six different people, with variations in the antibody panels and flow cytometers used. However, most of the T cell parameters investigated here, such as CD4:CD8 ratio, represent large populations of cells, so the impact of this variation should be limited compared to cells that make up only a small fraction of the T cell compartment, such as regulatory T cells.

The great heterogeneity of CLL is reflected in the highly variable stability of patient T cell frequency. Many factors influence T cell percentage in the PBMC, including disease progression, co-morbidities and infections, as well as aging (257,302,328). Analysis of this cohort however showed very little correlation between T cell frequency and patient age – instead it appears that CLL is the key factor in determining T cell percentage. A potential drawback of the longitudinal analysis presented here is the infrequency with which many patients with indolent disease attend clinics, thanks to the ‘watch and wait’ strategy often employed by clinicians (329). Due to the “snapshot” nature of individual samples, the preference for longitudinal follow-up would be regular samples at short intervals, so that fluctuations caused, for example, by infections could be clearly distinguished as outliers. However, since many patients attend clinics only once or twice per year, it can often be difficult to determine whether any large changes in T cell frequency are reflective of their CLL or other factors.

The CD4:CD8 ratio has been implicated in CLL progression risk (19,22,239,255) and changes in this ratio have been observed in elderly people (330). The results in this study suggest that there is heterogeneity in CLL patients' ratio stability. It seems unlikely that the observed changes in ratio are caused simply by advancing age, both because our data show only a minor correlation between age and ratio and because a large number of the patients would not normally be considered as elderly (>65 years old). Conversely to expectations, it appeared that an inverted ratio phenotype was more stable than a normal ratio – the data suggest that an inversion of the ratio is established early in disease and that very few patients revert to a normal ratio over time. Results from patients who have received therapy with Ibrutinib also seem to support the stability of the inverted ratio phenotype – interestingly, patients with an inverted ratio before treatment maintained this inversion once their treatment had commenced. The impact of Ibrutinib on T cells in CLL is not particularly well characterised, as reviewed by Man and Henley (304). Therefore, the maintenance of this inverted ratio phenotype post-therapy is of potentially great interest, since the treatment does not appear to reset the T cell population to normal – it follows that the associated immune dysfunction characteristic of CLL may also be maintained after treatment and could be biomarker for risk of relapse.

CD4⁺HLA-DR⁺PD-1⁺ T cells have not been studied longitudinally before, so nothing is known about changes in their frequency over time. The data in this study showed CD4⁺HLA-DR⁺PD-1⁺ cells to be a dynamic population, with large differences observed in some patients in periods of only a few months. This may reflect changing

CLL tumour burden, perhaps shifting the balance between suppression and activation of T cells (321). Interestingly, higher frequencies of CD4⁺HLA-DR⁺PD-1⁺ T cells tended to be more stable than lower frequencies, although some patients showed temporary spikes in the frequency of these cells perhaps associated with infections. Treatment with Ibrutinib did not cause a definitive pattern of change in the frequency of CD4⁺HLA-DR⁺PD-1⁺ cells. This is perhaps surprising, since previous reports have found PD-1 expression on T cells to be downregulated following Ibrutinib therapy (331–333), although this effect was not seen in CD4⁺ T cells until much later than their CD8⁺ counterparts. Other studies have observed increases in fungal infection susceptibility in CLL patients taking Ibrutinib long-term (334,335), perhaps reflecting changes to their T cells. Therefore, continued follow-up of treated patients over a longer timespan will be necessary to assess definitively the impact of Ibrutinib therapy on the T cell compartment.

This chapter has sought to elucidate the biology of CD4⁺HLA-DR⁺PD-1⁺ T cells in CLL. The availability of long-term patient data on a large scale provides an important resource for further investigation into patient prognosis. There is remarkable heterogeneity in the CD4⁺HLA-DR⁺PD-1⁺ population, which appears to be composed of at least 32 subsets bearing different combinations of markers. It remains unclear whether the phenotypically defined subsets perform different functional roles, or whether CD4⁺HLA-DR⁺PD-1⁺ cells as a whole contribute to a single function. Despite its power to explore single cell phenotypes, standard flow cytometry is limited by the number of targets of interest that can be investigated at

one time. Therefore, in order to increase the number of potential defining markers of CD4⁺HLA-DR⁺PD-1⁺ T cells, and to potentially identify indicators of their functional role, a gene expression study using DNA microarray technology has been conducted, the results of which are presented in the following chapter.

4 Gene Expression Analysis of CD4⁺ T Cells in CLL

Modern techniques and equipment have driven a huge growth in the complexity of analysis that can be conducted in immunology research, particularly using flow cytometry. This capability has led to the definition of many distinct immune cell populations, with a wide array of phenotypic and functional markers used to characterise these populations. In light of this, investigation of an unknown cell population can be challenging given the sheer number of potential markers of interest. Therefore, a more global approach to analysis may offer a better option. Such approaches can provide a 'big picture' overview of the population and help inform downstream analysis by identifying common pathways and processes that may be important in disease.

DNA microarray technology is one example of a global analysis approach. As used in this chapter, DNA microarrays permit the investigation of the level of expression of over 20,000 human genes, offering a potential wealth of information about the cell populations analysed. Such a large volume of data is difficult to interpret, so the use of specialised software packages is essential. Methodologies including pathway analysis and gene set enrichment analysis allow exploration of gene expression data for discrete cell populations and can identify key molecules and signalling pathways that may be common to other diseases or completely novel.

In this chapter, the gene expression profiles of T cells from both CLL patients and healthy donors were investigated. As observed in *Chapter 3*, the frequency of

CD4⁺HLA-DR⁺PD-1⁺ T cells is significantly greater in CLL compared to healthy controls and this subset showed a large degree of phenotypic complexity. However, whether CD4⁺HLA-DR⁺PD-1⁺ T cells contribute to disease progression, and the manner in which they might do this, was unclear. Previous studies have demonstrated the ability of gene expression analyses to define disease-specific signatures in heterogeneous T cell populations (336), and in this study a similar approach was used to investigate CD4⁺HLA-DR⁺PD-1⁺ T cells.

4.1 Experimental Scheme for DNA Microarray Experiments

In order to explore the gene expression profile of CD4⁺HLA-DR⁺PD-1⁺ T cells from CLL patients and investigate their potential role in disease, identifying distinct and characteristic genes and molecules was of vital importance. Therefore, an experimental scheme that allowed the relative comparison of CD4⁺HLA-DR⁺PD-1⁺ T cells with other T cell subsets, both from CLL patients and healthy donors, was required.

To this end, fresh blood samples from 4 age-matched healthy donors were obtained along with samples from 5 untreated CLL patients. Since the analysis was conducted on specific T cell subsets rather than the global T cell population, the number of individuals analysed could be lower than in other, globally focused, microarray experiments. PBMC were isolated and subjected to FACS (Fluorescence-Assisted Cell Sorting) to obtain purified CD4⁺ T cell subsets, from which RNA was extracted for use in DNA microarrays. The cell yield from the FACS process, and therefore the RNA yield, was variable, so the amount of RNA used for each microarray was normalised. The characteristics of the CLL patients and healthy donors and the FACS cell yields are shown in *Table 13*. The CLL patients used were specifically chosen due to their high frequencies of CD4⁺HLA-DR⁺PD-1⁺ T cells, in order to facilitate the collection of this minority subset.

As well as CD4⁺HLA-DR⁺PD-1⁺ T cells, two control subsets of T cells were purified by FACS and included in the microarray experiments:

1. CD4⁺HLA-DR⁻PD-1⁻ T cells, which comprise a majority of the CD4⁺ T cells, were used as a proxy for the general CD4⁺ T cell population.

2. CD4⁺HLA-DR⁺PD-1⁺ cells to allow assessment of the impact of PD-1 signalling.

Figure 4.1 shows a schematic diagram of the T cell populations used for DNA microarray analysis and the comparisons analysed.

Due to the large number of comparisons analysed across samples from 9 individuals for each gene, it was important to be mindful of the potential for a high false discovery rate, wherein the statistical analysis suggests a significant difference where in reality the difference is not significant. In the analysis of the DNA microarray data in this study, the Benjamini-Hochberg method was used to adjust the generated p-values to control the false discovery rate. While other methods, such as familywise error rate control, can be used to reduce false positives more stringently, these come at the cost of reducing the power to detect true differences compared to the false discovery rate control method used here.

Sample	CD4 ⁺ :CD8 ⁺ Ratio	Age	Gender	Cell Population	Cell Yield
CLL 1	Inverted	89	M	CD4 ⁺ HLA-DR ⁻ PD-1 ⁻	316245
				CD4 ⁺ HLA-DR ⁻ PD-1 ⁺	505769
				CD4 ⁺ HLA-DR ⁺ PD-1 ⁺	182104
CLL 2	Normal	73	M	CD4 ⁺ HLA-DR ⁻ PD-1 ⁻	258049
				CD4 ⁺ HLA-DR ⁻ PD-1 ⁺	332330
				CD4 ⁺ HLA-DR ⁺ PD-1 ⁺	101324
CLL 3	Normal	78	M	CD4 ⁺ HLA-DR ⁻ PD-1 ⁻	647470
				CD4 ⁺ HLA-DR ⁻ PD-1 ⁺	335287
				CD4 ⁺ HLA-DR ⁺ PD-1 ⁺	47481
CLL 4	Inverted	58	M	CD4 ⁺ HLA-DR ⁻ PD-1 ⁻	500994
				CD4 ⁺ HLA-DR ⁻ PD-1 ⁺	350057
				CD4 ⁺ HLA-DR ⁺ PD-1 ⁺	87650
CLL 5	Inverted	81	M	CD4 ⁺ HLA-DR ⁻ PD-1 ⁻	362507
				CD4 ⁺ HLA-DR ⁻ PD-1 ⁺	127784
				CD4 ⁺ HLA-DR ⁺ PD-1 ⁺	103165
HD 1	Inverted	76	M	CD4 ⁺ HLA-DR ⁻ PD-1 ⁻	796383
				CD4 ⁺ HLA-DR ⁻ PD-1 ⁺	436260
				CD4 ⁺ HLA-DR ⁺ PD-1 ⁺	54212
HD 2	Normal	73	M	CD4 ⁺ HLA-DR ⁻ PD-1 ⁻	758679
				CD4 ⁺ HLA-DR ⁻ PD-1 ⁺	392326
				CD4 ⁺ HLA-DR ⁺ PD-1 ⁺	45332
HD 3	Normal	69	F	CD4 ⁺ HLA-DR ⁻ PD-1 ⁻	710117
				CD4 ⁺ HLA-DR ⁻ PD-1 ⁺	573608
				CD4 ⁺ HLA-DR ⁺ PD-1 ⁺	40248
HD 4	Normal	83	F	CD4 ⁺ HLA-DR ⁻ PD-1 ⁻	799169
				CD4 ⁺ HLA-DR ⁻ PD-1 ⁺	595383
				CD4 ⁺ HLA-DR ⁺ PD-1 ⁺	64626

Table 13: Characteristics of CLL Patients and Healthy Donors Used in DNA Microarray Experiments.

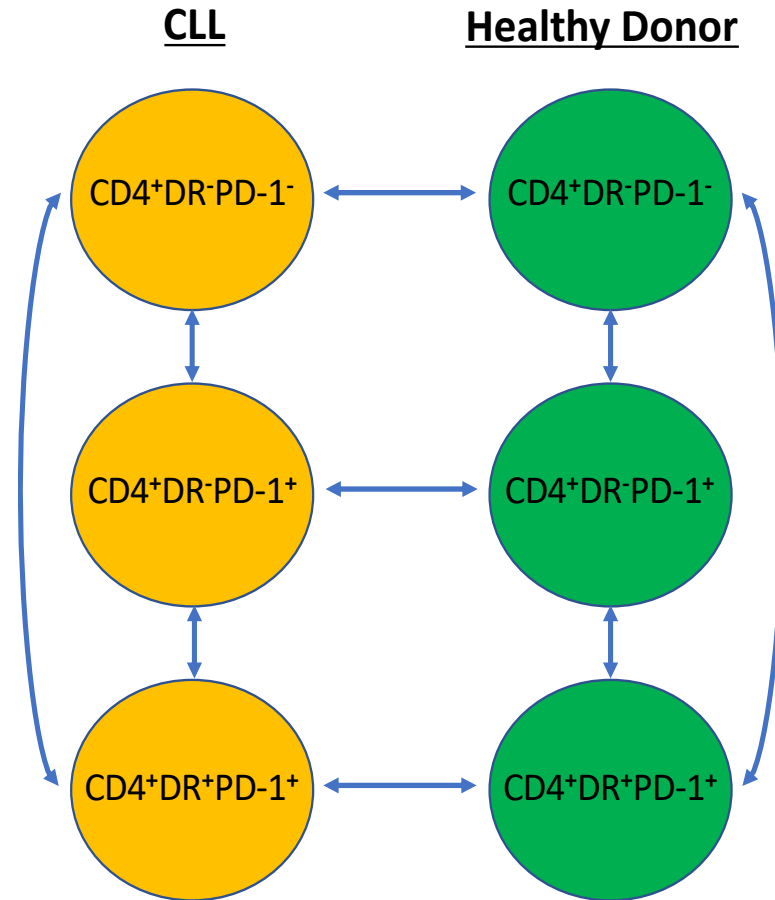


Figure 4.1: Schematic Diagram of the Analysed Comparisons Between Microarray Samples

4.2 Gene Expression Analysis

DNA microarray technology allows for the exploration of the level of expression of thousands of human genes and the patterns of expression of genes in different cell populations. Such data offer an insight into the key commonalities and differences between populations and permit identification of targets of interest for further study.

In the present study, three CD4⁺ T cell subsets were purified from blood samples from both CLL patients and healthy donors. *Figure 4.2* shows a Principal Component Analysis (PCA) of the entire dataset obtained from these microarrays. PCA is a statistical tool which reduces the dimensionality of data i.e. transforms the data into a more interpretable form while retaining as much of the information as possible. In this instance, this involves transforming the gene expression data for each sample analysed into a single point on a biaxial graph, such that those datasets that are more similar will be closer together.

As can be clearly observed in *Figure 4.2*, for each T cell population analysed there is a marked difference in clustering, with the subsets from CLL patients and healthy donors being very distinct. The same is also true within each group – in both CLL and healthy control groups, each T cell subset formed a distinct cluster, with a particularly clearly defined separation in the healthy donor group. Taken together, this provides evidence that gene expression patterns varied significantly between CLL patients and healthy controls and also that the three T cell subsets defined by HLA-DR and PD-1 expression were distinct.

Further evidence of the distinctness of these T cell populations, as well as the validity of the gene expression data, can be observed from the expression of key individual genes including HLA-DR, with particular interest in those that were assessed phenotypically in *Chapter 3*. As shown in *Figure 3.6*, the expression of both granzyme B and Ki-67 were significantly increased in CD4⁺HLA-DR⁺PD-1⁺ T cells compared to total CD4⁺ T cells and the same pattern was also observed in the gene expression data. This was also true for the gene expression patterns of TIGIT and CD38, which closely resembled the protein expression patterns of these markers shown in *Figure 3.7*. Gene expression data for these genes of interest can be seen in *Appendix Figure 8.1*.

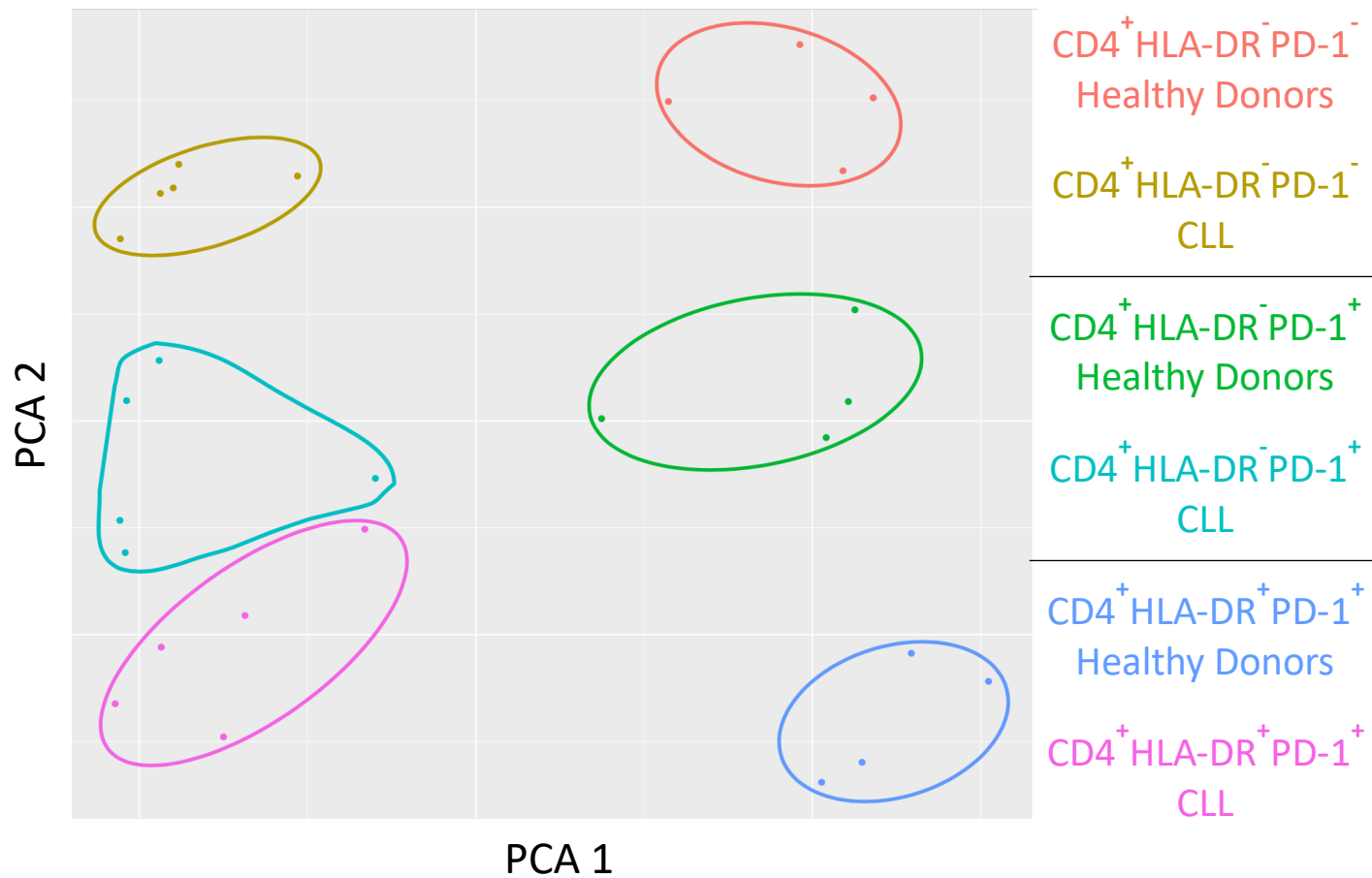


Figure 4.2: PCA Plot Showing Distinct Clustering of Microarray Samples

Principal Component Analysis was conducted on gene expression data collected from DNA microarrays of CD4⁺ T cells from 5 CLL patients and 4 healthy donors. There was clear differential clustering of samples from each T cell subset both in CLL patients and healthy donors, as well as between these two groups.

While PCA provides an overarching view of the gene expression datasets, allowing the similarities and differences in overall gene expression between samples to be clearly observed, it does not enable deeper exploration of the data. Instead, visualising gene expression data at the level of individual genes offers the ability to observe the patterns and numbers of differentially expressed genes across samples.

In order to obtain such a perspective, heatmaps are commonly used. A heatmap showing the expression data from this study is shown in *Figure 4.3*. This represents the expression of 22743 genes, all of the coding regions of the human genome. The mean expression of each gene was calculated from the expression values of the gene from each patient or healthy donor. The mean expression values from each T cell subset were used to generate the heatmap using a scale relative to the other T cell subsets, to ensure that differences between lowly expressed genes could be easily distinguished.

The heatmap in *Figure 4.3* shows some differences in gene expression patterns between CLL patients and healthy donors. There were also differences in gene expression patterns between each T cell subset, both in CLL and healthy donors, although the sets of genes showing differential expression differed between the two groups. Overall, the patterns of gene expression in *Figure 4.3* do not show major differences, as would be expected when comparing global gene expression between cells of the same type.

The concept of a gene expression signature for CLL T cells is explored in *Figure 4.4*. For this heatmap, the genes that were most significantly differentially expressed

between CD4⁺HLA-DR⁺PD-1⁺ T cells from CLL patients and healthy donors were determined, using cut-off values of $p < 0.05$ for statistical significance and a log fold change value of greater than 1. The mean expression of the 1312 genes which fell within the cut-offs was calculated for all the T cell subsets from both CLL and healthy donors and used to generate the heatmap.

Figure 4.4 shows that the vast majority of the 550 genes that were relatively highly expressed in CD4⁺HLA-DR⁺PD-1⁺ cells from CLL patients were also relatively highly expressed in both of the other CLL T cell subsets analysed. Most of these genes were relatively poorly expressed in healthy control T cells from all subsets, providing further evidence for a CLL CD4⁺ T cell gene signature. The reverse pattern was also observed, with a set of genes showing relatively high expression in all the T cell subsets from healthy donors with low expression in CLL.

Interestingly, a large number of genes were most highly expressed in CD4⁺HLA-DR⁺PD-1⁺ cells from healthy donors when compared to the other healthy donor T cell subsets, perhaps a reflection of the distinct nature of these cells in healthy people. In particular, a group of 74 genes were observed to be highly expressed solely in the healthy donor CD4⁺HLA-DR⁺PD-1⁺ subset, with little expression in other healthy donor T cell subsets or CLL T cells.

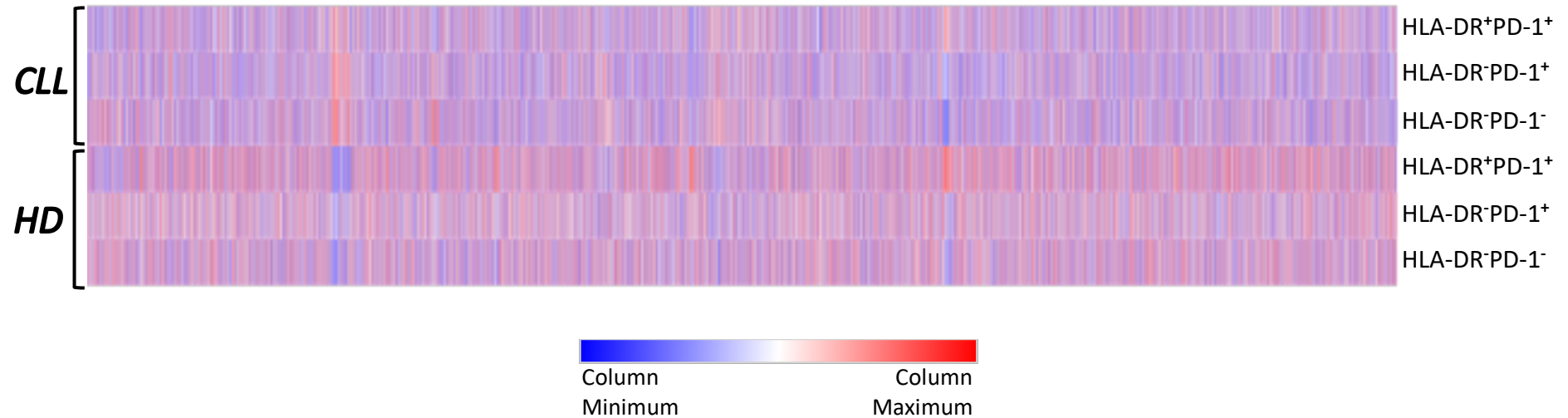


Figure 4.3: Gene Expression Patterns are Different Between T Cell Subsets and Between CLL Patients and Healthy Donors

A heatmap illustrating the relative expression of 22743 genes was generated from pooled data from 5 CLL patients and 4 healthy donors, separated into CD4⁺HLA-DR⁻PD-1⁻, CD4⁺HLA-DR⁻PD-1⁺ and CD4⁺HLA-DR⁺PD-1⁺ subsets. Each column represents a gene and the mean expression level of each gene in the samples in each group (e.g. CD4⁺HLA-DR⁺PD-1⁺ cells from CLL patients) was plotted. Heatmap was created using Morpheus software (Broad Institute).

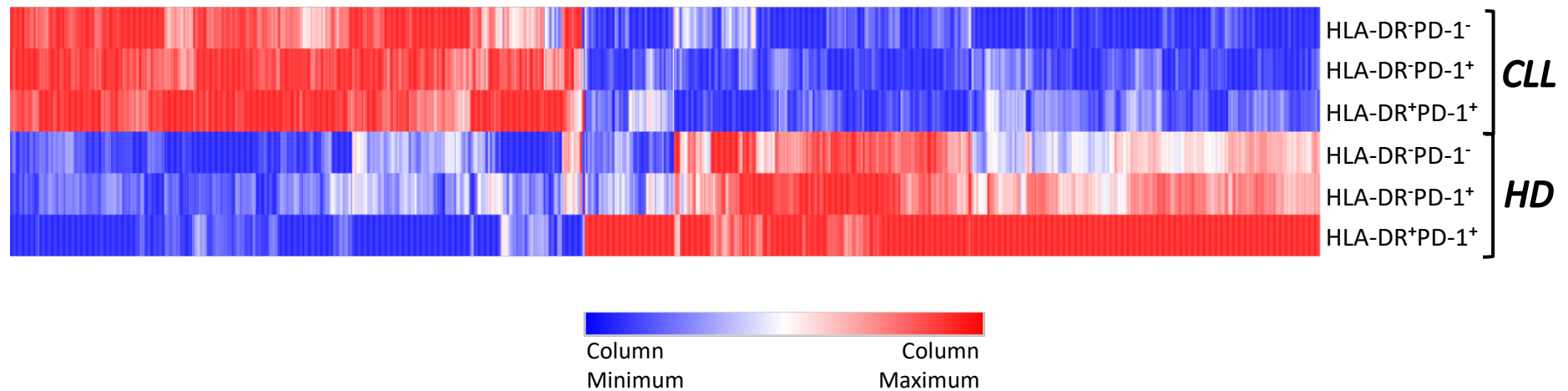


Figure 4.4: T Cells from CLL Patients Have a Distinctive Gene Expression Signature

The expression of the most highly differentially expressed genes from CD4⁺HLA-DR⁺PD-1⁺ T cells is conserved across other subsets in CLL, giving a distinct signature of 550 relatively highly expressed genes.

Using cut-offs of $p < 0.05$ and log fold change > 1 , the genes most differentially expressed between CD4⁺HLA-DR⁺PD-1⁺ T cells from CLL and healthy donors were determined. The mean expression level of these 1312 genes, represented by each column, was calculated for each T cell subset and used to plot a heatmap. *Heatmap was created using Morpheus software (Broad Institute).*

4.3 Ingenuity Pathway Analysis

Section 4.2 provides a “big picture” overview of the patterns of gene expression observed in T cells from CLL patients and their healthy counterparts. However, it is important to explore the biological relevance of these patterns and the cellular functions and processes that are underpinned by the genes in question.

There are a number of software packages and online tools available which allow the user to investigate gene expression data, of which Ingenuity Pathway Analysis (IPA) is one of the most widely used. This software package provides a suite of analysis options that can compare gene expression data against the Ingenuity Knowledge Base, a vast repository of curated publications on cellular signalling pathways, molecular interactions, functional outputs and more. In this manner, users can build detailed pictures of the networks of interactions and pathways that are present or enriched in their dataset, as well as the potential biological implications of their gene expression patterns.

In order to perform the investigative analysis of the gene expression data in this study, formatted datasets including the log fold change in gene expression between different populations were input to IPA. Using user-defined cut-off values of $p < 0.05$ and log fold change > 1 , the software determined which genes showed significant differential expression and should therefore be included in the downstream analysis. *Figure 4.5* displays the number of distinct and overlapping differentially expressed genes, as determined by IPA, for this study.

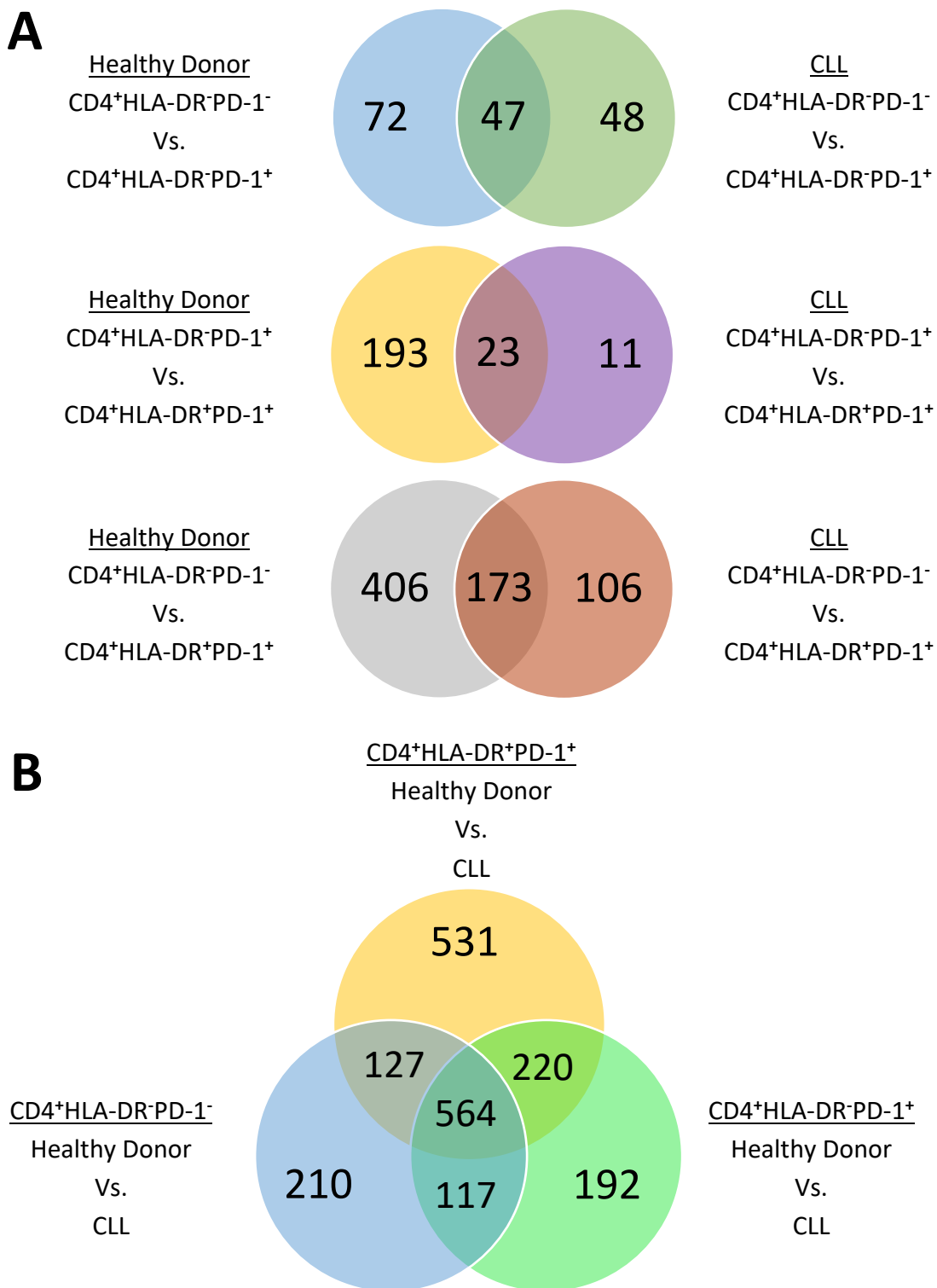


Figure 4.5: Numbers of Significantly Differentially Expressed Genes between Different Comparison Groups

Gene expression data from DNA microarrays conducted on T cells from 5 CLL patients and 4 healthy donors was input to Ingenuity Pathway Analysis software. Using cut-offs of $p < 0.05$ and log fold change > 1 , genes that were significantly differentially expressed between the two groups or between T cell subsets were determined by the software. The numbers of differentially expressed genes that were distinct to each comparison or overlapping between comparisons is shown.

Figure 4.5A shows the numbers of significantly differentially expressed genes when comparing the three CD4⁺ T cell subsets analysed in this study. For each comparison, the number of these differentially expressed genes that are observed in healthy donors, CLL patients or both groups is displayed. The number of differentially expressed genes was much greater for the CD4⁺HLA-DR⁻PD-1⁻ vs. CD4⁺HLA-DR⁺PD-1⁺ comparison (685) than the CD4⁺HLA-DR⁻PD-1⁻ vs. CD4⁺HLA-DR⁻PD-1⁺ comparison (167) or the CD4⁺HLA-DR⁻PD-1⁺ vs. CD4⁺HLA-DR⁺PD-1⁺ comparison (227). Within the 167 differentially expressed genes for CD4⁺HLA-DR⁻PD-1⁻ vs. CD4⁺HLA-DR⁻PD-1⁺ T cells, 48 were seen only in CLL patients, with a similar number present in both CLL patient and healthy donor T cells. When comparing CD4⁺HLA-DR⁻PD-1⁺ and CD4⁺HLA-DR⁺PD-1⁺ T cells, the vast majority of differentially expressed genes were observed in healthy donors only, with just 34 genes found to be different in CLL patients. Similarly, the majority of differentially expressed genes between CD4⁺HLA-DR⁻PD-1⁻ and CD4⁺HLA-DR⁺PD-1⁺ T cells were found in healthy donors, but a significant proportion of these genes were also expressed in CLL patients. Taken together, *Figure 4.5A* demonstrates that the T cell subsets in healthy donors have larger differences in gene expression between them than the same subsets in CLL, reinforcing the results seen in *Figure 4.4*.

The comparison of differentially expressed genes between CLL patients and healthy donors for each T cell subset is displayed in *Figure 4.5B*. The numbers of genes differentially expressed only in CD4⁺HLA-DR⁻PD-1⁻ (210) or CD4⁺HLA-DR⁻PD-1⁺ (192) T cells when comparing CLL to healthy donors was much lower than in CD4⁺HLA-DR⁺PD-1⁺ cells (531). This large difference in gene expression supports the

concept that the CD4⁺HLA-DR⁺PD-1⁺ subset is distinct between the two groups. Interestingly, 564 genes common to all three T cell subsets were observed to be differentially expressed between CLL patients and healthy donors – this observation suggests a pattern of gene expression that defines the difference between these two groups and as such reinforces the concept of a CLL gene expression signature, as seen in *Figure 4.4*.

Taken together, the comparisons in *Figure 4.5* show the same patterns as those observed in the Principal Component Analysis in *Figure 4.2*, with each population having distinct expression of genes but with a greater difference between CLL patients and healthy donors than between the three T cell subsets in either group.

Having input the gene expression data and defined the significantly differentially expressed genes, several analysis options are available within the IPA software. For this study core analysis was performed, with both upregulated and downregulated genes taken into account. This analysis attempts to match the significant genes to known biological processes and signalling pathways and allows the user to visualise the interactions of these pathways in wider signalling networks. As well as this, the analysis can suggest potential upstream signalling pathways or molecules that may be responsible for the gene expression differences observed.

In order to assess how strongly the gene expression data relates to a given pathway, IPA generates a statistical value called the activation z-score. Using the information in the Ingenuity Knowledge Base, the activation z-score is calculated

taking into account the number of genes from the dataset that appear in the pathway and whether their direction of change (i.e. upregulated or downregulated) match what would be expected for that pathway, as well as the statistical significance and size of the difference in expression of those genes. In this manner, the activation z-score is used to predict whether a pathway is likely to be activated or inhibited and gives a statistical measure of the strength of that prediction (337).

The following *Figures (4.6 to 4.10)* present the results of the IPA core analysis. This includes the most highly activated canonical pathways, signatures of diseases and cellular functions and potential upstream signalling molecules as predicted by the software from the input gene expression data.

4.3.1 Diseases and Functions

The Diseases and Functions section of the IPA core analysis provides a “big picture” overview of the user’s data. This analysis attempts to match the significant genes in the input gene expression data to a database of cellular functions and diseases for which the gene expression profile is known. As well as the significance and direction (upregulated or downregulated) of the input genes, the proportion of user input genes that overlap with the known genes in the functional signature is taken into account when calculating the activation z-score for each function/disease.

4.3.1.1 CD4⁺HLA-DR⁻PD-1⁻ vs. CD4⁺HLA-DR⁺PD-1⁺ T Cells

Figure 4.6 displays the top results of the Diseases and Functions analysis of the comparison between CD4⁺HLA-DR⁻PD-1⁻ and CD4⁺HLA-DR⁺PD-1⁺ T cells. The output of this analysis sorted by highest activation z-score is shown in *Figure 4.6A*. All of the top 10 diseases and functions were present in both CLL and healthy donor T cells, with 9 of them being observed in CD4⁺HLA-DR⁻PD-1⁻ cells, the exception being ‘Transmembrane potential of mitochondria’. Key functions highlighted by this analysis were cytotoxicity and DNA processing, alongside more general lymphocyte-related processes such as chemotaxis.

The top 10 diseases and functions in CD4⁺HLA-DR⁺PD-1⁺ T cells in CLL are shown in *Figures 4.6B*. For CD4⁺HLA-DR⁺PD-1⁺ cells, interestingly only 3 of the top functions were also observed in this subset in healthy donors, suggesting this subset is functionally distinct in each group. Interestingly, ‘Response of helper T lymphocytes’ was actually more associated with CD4⁺HLA-DR⁻PD-1⁻ cells in healthy

donors. Processes related to inflammation and allergy feature heavily for CD4⁺HLA-DR⁺PD-1⁺ cells, as well as 'Activation-induced cell death'.

Figure 4.6C displays the top 10 diseases and functions for CD4⁺HLA-DR⁻PD-1⁻ T cells in CLL. The CD4⁺HLA-DR⁻PD-1⁻ subset represents the majority of CD4⁺ T cells in both CLL and healthy donors, so it was interesting to note that there was a clear difference between the cells from each group, with only 6 of these top functions appearing in both. All of the functions observed for CLL only related to the interactions of lymphocytes, perhaps reflecting the impact of disease state. There is a large expansion in the number of T cells in CLL and this is reflected in the presence of processes related to proliferation and viability, supporting the phenotypic data observed in *Section 3.2.1*.

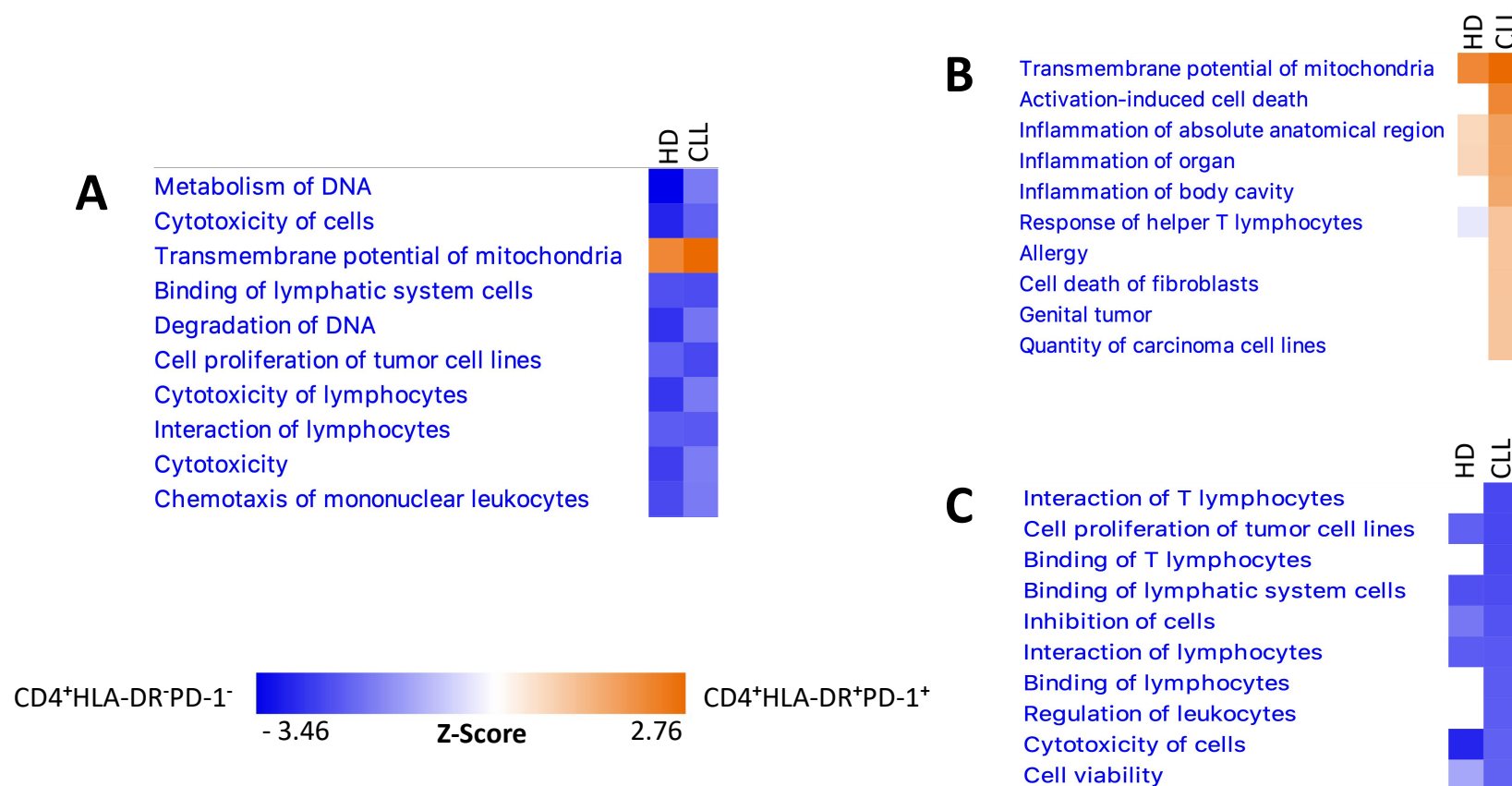


Figure 4.6: Top Diseases and Functions in CD4⁺HLA-DR⁻PD-1⁻ and CD4⁺HLA-DR⁺PD-1⁺ T Cells

Ingenuity Pathway Analysis software was used to uncover disease and functional signatures suggested by the gene expression data for the comparison CD4⁺HLA-DR⁻PD-1⁻ Vs. CD4⁺HLA-DR⁺PD-1⁺ T cells, both in CLL patients and healthy donors.

A) The top 10 disease/function signatures for this comparison sorted by largest activation z-score.

B) The top 10 disease/function signatures in CD4⁺HLA-DR⁺PD-1⁺ cells *cf.* CD4⁺HLA-DR⁻PD-1⁻ cells in CLL.

C) The top 10 disease/function signatures in CD4⁺HLA-DR⁻PD-1⁻ cells *cf.* CD4⁺HLA-DR⁺PD-1⁺ cells in CLL.

4.3.1.2 CLL vs. Healthy Donor T Cells

The top results from the Diseases and Functions analysis of CLL vs. healthy donor T cells is shown in *Figure 4.7*. This uses the gene expression data comparing each individual T cell subset from CLL patients and healthy donors. The top 10 diseases and functions by activation z-score are displayed in *Figure 4.7A*, with 6 functions from CLL T cells and 4 from healthy donor T cells. The healthy donor-associated processes mainly related to viral replication, while the CLL-associated ones were more varied, including cellular activation, death and DNA binding. All of the top 10 functions were present in all three T cell subsets (with the exception of 'Activation of leukocytes' in CD4⁺HLA-DR⁻PD-1⁺ cells), which reinforces the concept of a distinct genetic pattern in CLL T cells.

Figure 4.7B shows the top 10 diseases and functions for CD4⁺HLA-DR⁺PD-1⁺ T cells in CLL compared to CD4⁺HLA-DR⁺PD-1⁺ cells in healthy donors. Interestingly, only 2 of these functions were also present for the comparisons of both CD4⁺HLA-DR⁻PD-1⁻ and CD4⁺HLA-DR⁻PD-1⁺ cells in CLL vs. healthy donors, with 4 being unique to the CD4⁺HLA-DR⁺PD-1⁺ comparison. Processes related to cytotoxicity and activation feature strongly, reflecting previous phenotyping results (see *Section 3.2.1*), but the presence of three kidney/urinary tract cancer signatures was unexpected.

The top 10 diseases and functions for CD4⁺HLA-DR⁺PD-1⁺ T cells in healthy donors compared to those in CLL are displayed in *Figure 4.7C*. Almost all of the top functions also featured for the other T cell subset comparisons between healthy donors and CLL, although 'Cell viability' and 'Cell survival' were more associated with

CLL-derived CD4⁺HLA-DR⁺PD-1⁺ cells. 5 of the top processes for CD4⁺HLA-DR⁺PD-1⁺ T cells in healthy donors were related to viral replication and life cycle, with the rest mostly connected to cellular viability.

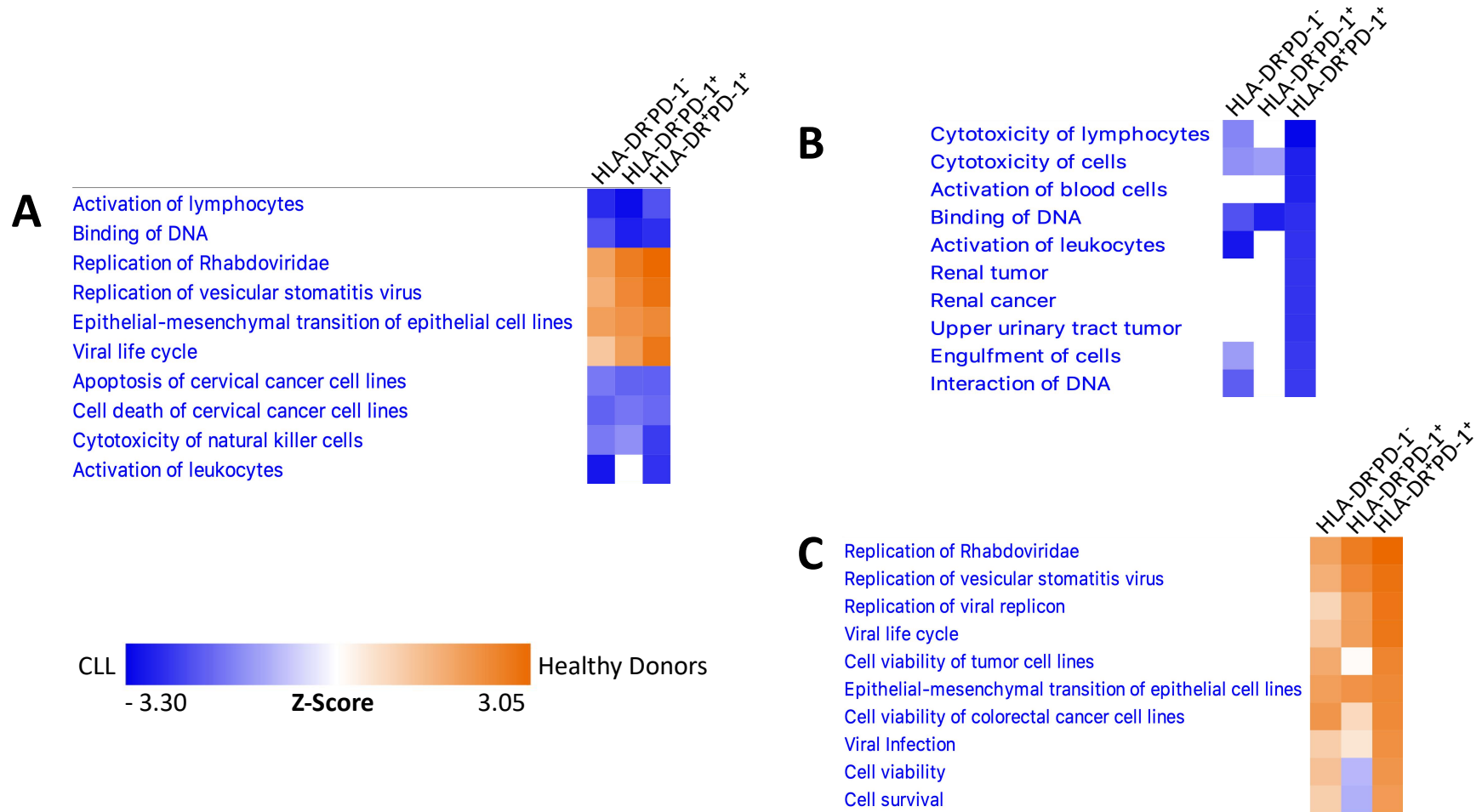


Figure 4.7: Top Diseases and Functions in CLL and Healthy Donor T Cells

Ingenuity Pathway Analysis software was used to uncover disease and functional signatures suggested by the gene expression data for the comparison of each T cell subset from CLL patients and healthy donors.

- A) The top 10 disease/function signatures for this comparison sorted by largest activation z-score.
- B) The top 10 disease/function signatures in CD4⁺HLA-DR⁺PD-1⁺ cells in CLL *cf.* healthy donors.
- C) The top 10 disease/function signatures in CD4⁺HLA-DR⁺PD-1⁺ cells in healthy donors *cf.* CLL.

4.3.2 Canonical Pathways

The Canonical Pathways element of the IPA core analysis provides detailed information about the signalling and cellular pathways that are activated or repressed in the user's gene expression data. This allows for the mechanisms that underlie the Diseases and Functions seen in *Section 4.3.1* to be investigated. The Canonical Pathways analysis takes into account the overlap of genes in the user's data with those in each pathway, as well as their significance and direction of change, when computing the activation z-score.

4.3.2.1 CD4⁺HLA-DR⁻PD-1⁻ vs. CD4⁺HLA-DR⁺PD-1⁺ T Cells

The top Canonical Pathways for the comparison of CD4⁺HLA-DR⁻PD-1⁻ vs. CD4⁺HLA-DR⁺PD-1⁺ T cells, both in CLL patients and in healthy donors, are displayed in *Figure 4.8*. The top 10 results sorted by greatest activation z-score are shown in *Figure 4.8A*, with 8 of these pathways being associated with CD4⁺HLA-DR⁻PD-1⁻ cells and all of them present for both CLL and healthy donor T cells. Both of the CD4⁺HLA-DR⁺PD-1⁺ cell-associated pathways were related to responses to signalling from soluble factors, whereas those pathways activated in CD4⁺HLA-DR⁻PD-1⁻ cells were mainly linked to T cell regulation in several disease contexts.

Figure 4.8B shows the top pathways in CD4⁺HLA-DR⁺PD-1⁺ compared to CD4⁺HLA-DR⁻PD-1⁻ T cells in CLL, of which there were only 8. As would be expected, the PD-1/PD-L1 signalling pathway was activated in CD4⁺HLA-DR⁺PD-1⁺ cells for both CLL and healthy donors, however not all the pathways were observed in both groups. In particular, 'Th2 Pathway' was associated with CD4⁺HLA-DR⁺PD-1⁺ cells in CLL but

with CD4⁺HLA-DR⁻PD-1⁻ cells in healthy donors. The majority of the other pathways in CD4⁺HLA-DR⁺PD-1⁺ cells related to intracellular transduction of signals from external factors, such as Wnt.

The top 10 Canonical Pathways activated in CD4⁺HLA-DR⁻PD-1⁻ T cells vs. CD4⁺HLA-DR⁺PD-1⁺ cells in CLL are displayed in *Figure 4.8C*. All of these pathways were active in CD4⁺HLA-DR⁻PD-1⁻ cells from both CLL patients and healthy donors, except for 'Cardiac Hypertrophy Signalling'. In contrast to CD4⁺HLA-DR⁺PD-1⁺ cells in CLL, the 'Th1 Pathway' was activated in CD4⁺HLA-DR⁻PD-1⁻ cells. Many of the other top pathways related to inflammatory/immune responses, often in disease settings, although surprisingly these included the 'Dendritic Cell Maturation' pathway.

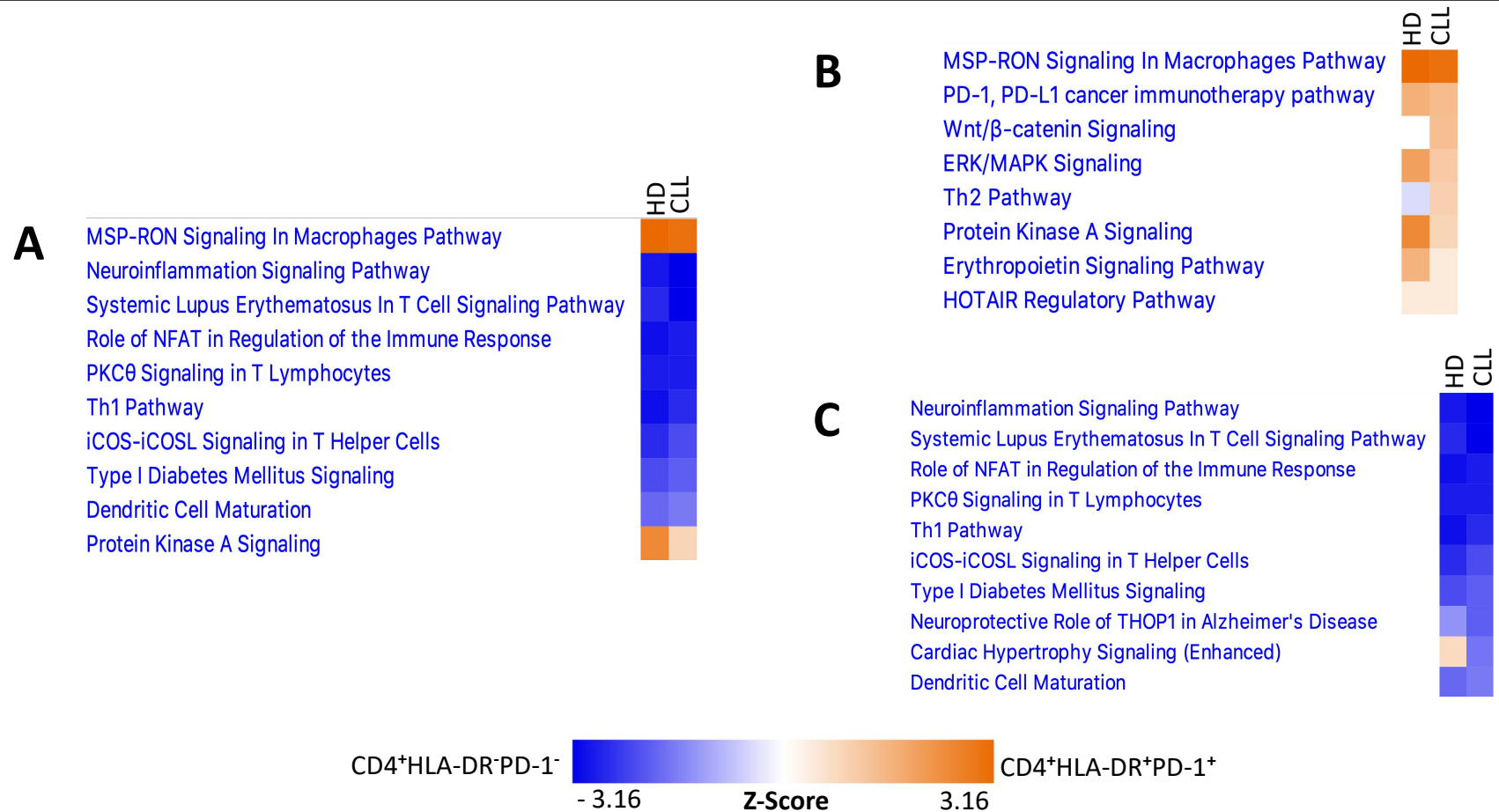


Figure 4.8: Top Canonical Pathways Activated in CD4⁺HLA-DR⁻PD-1⁻ and CD4⁺HLA-DR⁺PD-1⁺ T Cells

Ingenuity Pathway Analysis software was used to uncover activated pathways in the gene expression data for the comparison CD4⁺HLA-DR⁻PD-1⁻ Vs. CD4⁺HLA-DR⁺PD-1⁺ T cells, both in CLL patients and healthy donors. **A)** The top 10 pathways for this comparison sorted by largest activation z-score. **B)** The top 8 pathways in CD4⁺HLA-DR⁺PD-1⁺ cells *cf.* CD4⁺HLA-DR⁻PD-1⁻ cells in CLL. **C)** The top 10 pathways in CD4⁺HLA-DR⁻PD-1⁻ cells *cf.* CD4⁺HLA-DR⁺PD-1⁺ cells in CLL.

4.3.2.2 CLL vs. Healthy Donor T Cells

Figure 4.9 shows the top Canonical Pathways when comparing CLL vs. healthy donor T cells, across all three T cell subsets. The top 10 pathways differentially activated are shown in *Figure 4.9A*, sorted by activation z-score. 3 of these were activated in CLL T cells while the other 7 were associated with healthy donor T cells – all of the top pathways featured in all three T cell subsets. T cell exhaustion and β -oxidation of fatty acids were highly activated in CLL and had the greatest activation z-scores seen across all of the Canonical Pathways analysis. The pathways in healthy donor T cells were varied, but included several pathways associated with cell types other than T cells, such as macrophages.

In *Figure 4.9B* are shown the top 10 pathways in CD4⁺HLA-DR⁺PD-1⁺ T cells from CLL patients vs. those in healthy donors. Only 6 of these were present in all three T cell subsets in CLL, with fairly low activation z-scores also observed in some cases. Both ‘Oxidative Phosphorylation’ and β -oxidation of fatty acids were highly activated in CD4⁺HLA-DR⁺PD-1⁺ cells, suggesting high metabolic activity, perhaps in response to inflammatory signalling activated through interferon and TNF receptor pathways. The ‘T Cell Exhaustion Signalling Pathway’ was the most highly activated pathway in all three T cell subsets, reflective of the widespread dysfunction reported in T cells in CLL.

The top 10 pathways activated in healthy donor CD4⁺HLA-DR⁺PD-1⁺ T cells vs. those from CLL patients are displayed in *Figure 4.9C*. All of these pathways were present in all three T cell subsets in healthy donors, although almost all of them were most highly activated in CD4⁺HLA-DR⁺PD-1⁺ cells. Many of the top pathways related

to signalling from soluble mediators or their cell surface receptors, including hepatocyte growth factor and vascular endothelial growth factor. Surprisingly, pathways associated with Acute Myeloid Leukaemia and the B cell receptor were also observed.

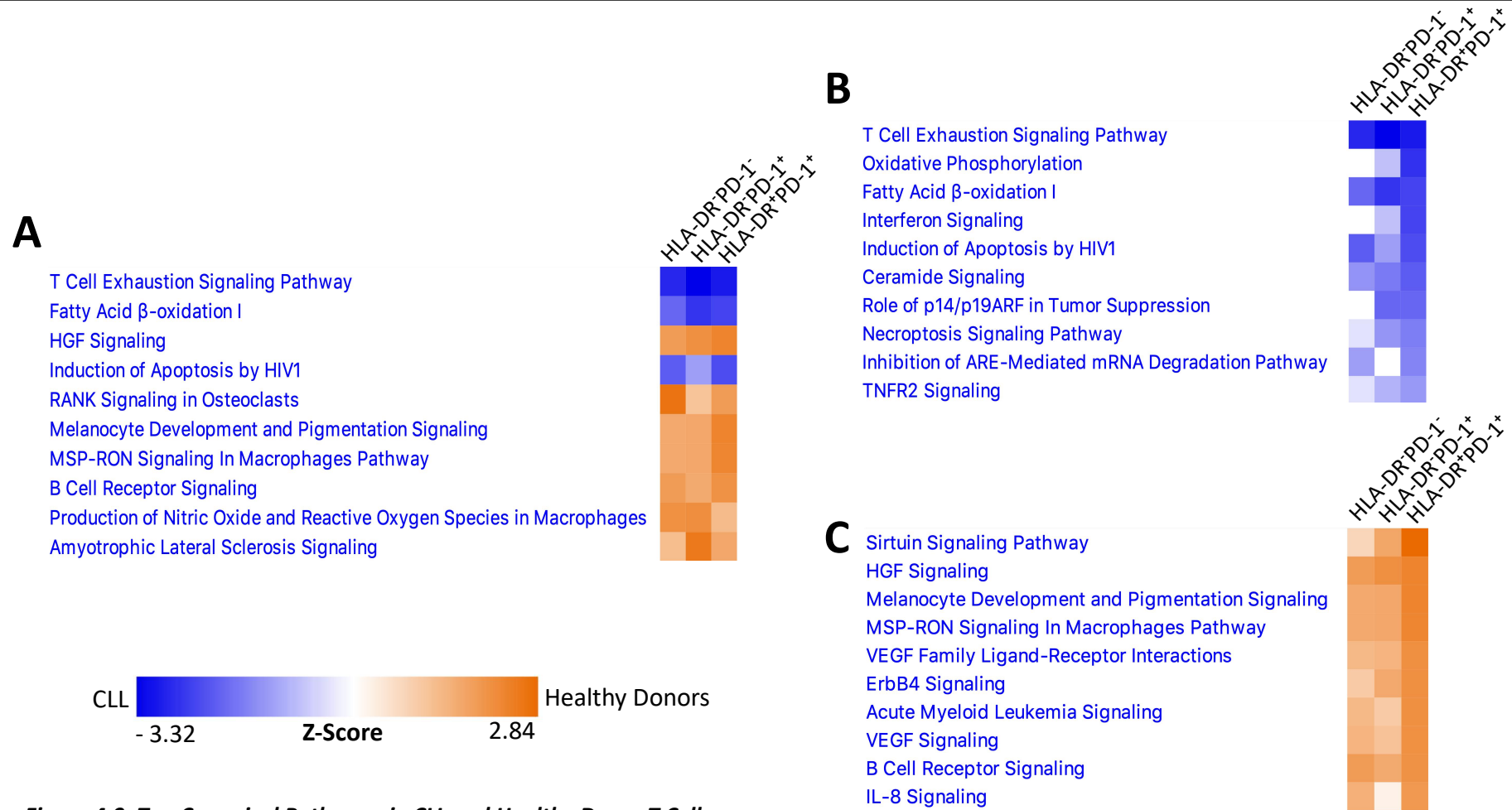


Figure 4.9: Top Canonical Pathways in CLL and Healthy Donor T Cells

Ingenuity Pathway Analysis software was used to uncover activated pathways suggested by the gene expression data for the comparison of each T cell subset from CLL patients and healthy donors. **A)** The top 10 pathways for this comparison sorted by largest activation z-score.

B) The top 10 pathways most highly activated in CD4⁺HLA-DR⁺PD-1⁺ cells in CLL *cf.* healthy donors. **C)** The top 10 pathways most highly activated in CD4⁺HLA-DR⁺PD-1⁺ cells in healthy donors *cf.* CLL.

4.3.3 Upstream Regulators

The Upstream Regulators element of IPA core analysis attempts to predict the signals whose activity cause the patterns in the user's data. The gene expression differences in the input data are compared to a database of the downstream actions of cytokines, receptors and intracellular signalling proteins to determine those which are most likely to be responsible for the patterns observed. For each molecule, the overlap of input genes with its downstream effects is considered, along with the statistical significance and magnitude of the difference, to calculate an activation z-score. The results of the Upstream Regulators analysis in this study are displayed in *Figure 4.10*.

4.3.3.1 CD4⁺HLA-DR⁻PD-1⁻ vs. CD4⁺HLA-DR⁺PD-1⁺ T Cells

The top 10 upstream molecules for the comparison of CD4⁺HLA-DR⁻PD-1⁻ vs. CD4⁺HLA-DR⁺PD-1⁺ T cells, ordered by activation z-score, are shown in *Figure 4.10A*. All of these molecules featured for both CLL and healthy donor T cells, with 7 associated with CD4⁺HLA-DR⁻PD-1⁻ cells and 3 associated with CD4⁺HLA-DR⁺PD-1⁺ cells. The predicted regulators of CD4⁺HLA-DR⁺PD-1⁺ T cells included PD-1 (PDCD1), as would be expected, while for CD4⁺HLA-DR⁻PD-1⁻ cells molecules were varied, including transcription factors, cytokines and intracellular proteins.

Figure 4.10B shows the top 10 Upstream Regulators of CD4⁺HLA-DR⁺PD-1⁺ compared to CD4⁺HLA-DR⁻PD-1⁻ T cells in CLL. 9 of the predicted regulators were also strongly associated with CD4⁺HLA-DR⁺PD-1⁺ cells in healthy donors, with PD-1 reassuringly having the highest activation z-score in both. The only suggested

upstream molecule associated solely with CLL was TGF β , a multi-functional cytokine with a context-dependent pro- or anti-inflammatory action. Most of the predicted regulators were proteins related to regulation of the cell cycle and proliferation, including the known tumour suppressors p53 and PTEN and the microRNA 'let-7', which has also been linked to cell proliferation regulation.

The top 10 predicted regulators of CD4⁺HLA-DR⁻PD-1⁻ T cells in CLL are displayed in *Figure 4.10C*. All of these featured for CD4⁺HLA-DR⁻PD-1⁻ cells in healthy donors as well, except for IL-4 which was associated with CD4⁺HLA-DR⁺PD-1⁺ cells in healthy donors. Many of the upstream molecules suggested had an immune function, including several cytokines related to the development of a T_H1 phenotype, such as IL-27 and IFN γ , and proteins involved with T cell receptor signalling including CD3.

4.3.3.2 CLL vs. Healthy Donor T Cells

In *Figure 4.10D* the top 10 Upstream Regulators, sorted by activation z-score, are shown for the comparison of CLL vs. healthy donor T cells, across all three subsets. All of the molecules featured in every T cell subset, with 3 associated with CLL and 7 with healthy donors. Several proteins related to responses to cellular stress and inflammatory signals were suggested, while the highest activation z-score was seen for oncostatin M, a pleiotropic cytokine with links to inflammation (338).

Figure 4.10E displays the top 10 predicted upstream regulators of CD4⁺HLA-DR⁺PD-1⁺ T cells from CLL patients vs. those in healthy donors. Only half of these molecules were associated with all the T cell subsets, while both 'IFNL1' and

'IRF7' were associated with healthy donor derived CD4⁺HLA-DR⁻PD-1⁻ cells rather than CLL. For CD4⁺HLA-DR⁺PD-1⁺ T cells in CLL patients, there were a number of interferon-related upstream molecules, with IFN γ having the highest activation z-score. Also featured were IL-27 and 'STAT1' which, together with IFN γ , control T_H1 cell differentiation. These results point towards CD4⁺HLA-DR⁺PD-1⁺ T cells being the product of an inflammatory environment in CLL.

The top 10 upstream molecules for healthy donor CD4⁺HLA-DR⁺PD-1⁺ T cells vs. those from CLL patients are shown in *Figure 4.10F*. 6 of these molecules featured as predicted regulators of all of the T cell subsets in healthy donors, while 4 did not, with 'TRAP1' only associated with CD4⁺HLA-DR⁺PD-1⁺ cells. In the top 10 upstream regulators there were 4 microRNAs, as well as several intracellular signalling transducer proteins, while the most strongly predicted molecule was the transcription factor 'NUPR1' which controls a programme of resistance in situations of cellular stress (339).

In both CLL and healthy donors, the different patterns of predicted upstream regulators in the CD4⁺HLA-DR⁺PD-1⁺ population compared to the other subsets further reinforce the concept that these cells are a distinct functional subset.

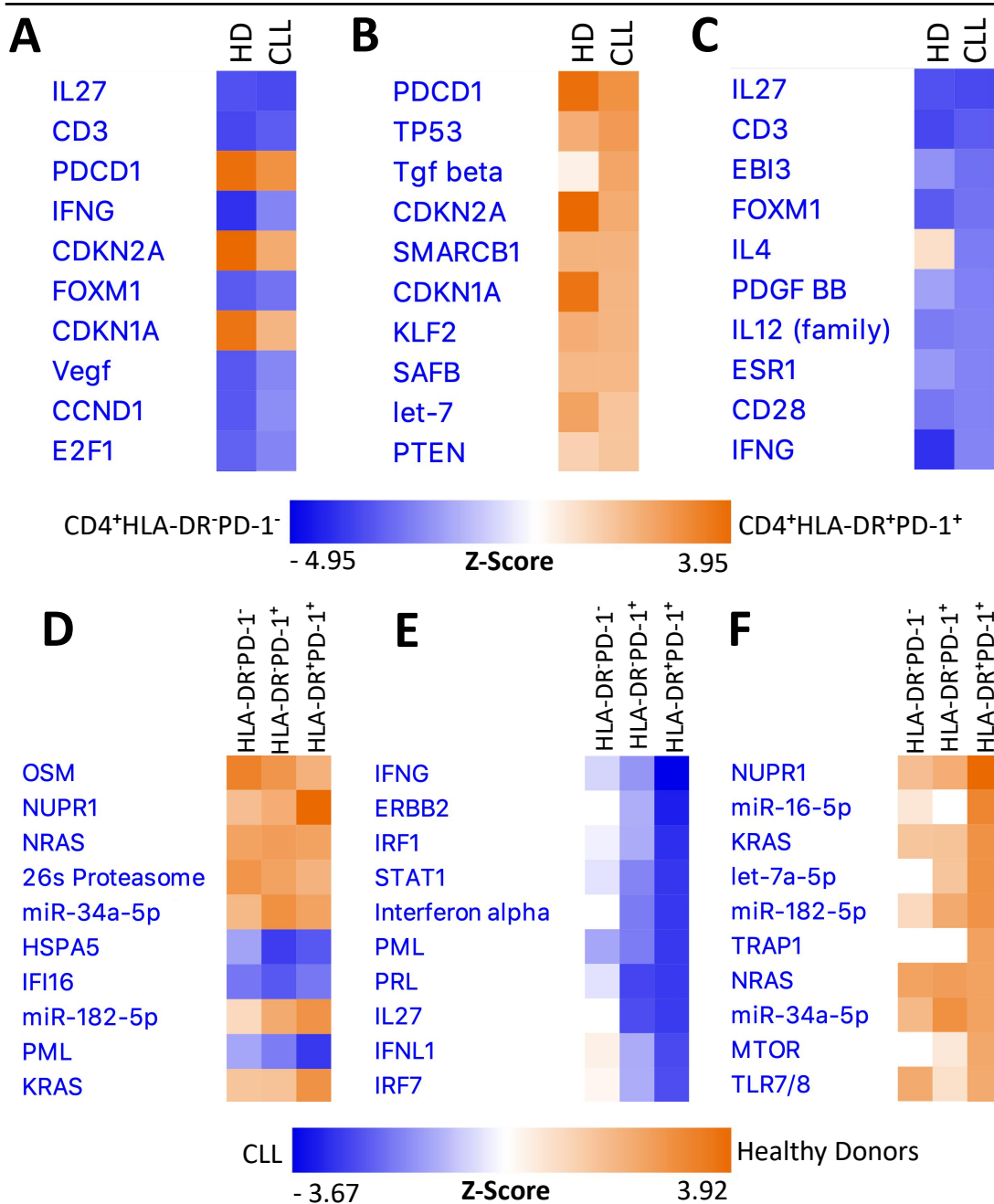


Figure 4.10: Top Upstream Regulators

Ingenuity Pathway Analysis software was used to predict upstream molecules responsible for the patterns of gene expression observed, comparing both CD4⁺HLA-DR⁻PD-1⁻ Vs. CD4⁺HLA-DR⁺PD-1⁺ T cells and CLL Vs. healthy donor T cells.

A) The top 10 upstream regulators for CD4⁺HLA-DR⁻PD-1⁻ Vs. CD4⁺HLA-DR⁺PD-1⁺ cells sorted by largest activation z-score.

B) The top 10 upstream regulators for CD4⁺HLA-DR⁺PD-1⁺ cells *cf.* CD4⁺HLA-DR⁻PD-1⁻ cells in CLL.

C) The top 10 upstream regulators for CD4⁺HLA-DR⁻PD-1⁻ cells *cf.* CD4⁺HLA-DR⁺PD-1⁺ cells in CLL.

D) The top 10 upstream regulators for CLL Vs. healthy donor T cells sorted by largest activation z-score.

E) The top 10 upstream regulators for CD4⁺HLA-DR⁺PD-1⁺ cells in CLL *cf.* healthy donors.

F) The top 10 upstream regulators for CD4⁺HLA-DR⁺PD-1⁺ cells in healthy donors *cf.* CLL.

4.4 Gene Expression Validation

The investigation of gene expression by DNA microarrays and subsequent analyses provides deep insight into the key genes and pathways that generate a specific phenotype. The data and information produced by such experiments must however be verified experimentally, to ensure its accuracy and validity. This is particularly important in light of the fact that RNA expression, and the level thereof, does not always correlate to equivalent protein expression.

In this study, validation of gene expression data obtained from DNA microarrays was conducted using two techniques: quantitative Polymerase Chain Reaction (qPCR) and flow cytometry.

4.4.1 qPCR Validation of Gene Expression

In order to validate the levels of gene expression observed from the DNA microarrays data, a shortlist of potential genes was determined for use in qPCR analysis. The criteria for this selection were statistically significant differences in expression between CLL patients and healthy donors, along with consistently high expression across all three T cell subsets analysed. Finally two genes, *SLAMF6* (*Signalling Lymphocyte Activation Molecule Family member 6*) and *PELI1* (*Pellino E3 Ubiquitin Protein Ligase 1*), were chosen for validation, with the housekeeping gene *GAPDH* (*Glyceraldehyde 3-Phosphate Dehydrogenase*) included as a reference. qPCR experiments were conducted using pooled RNA samples from 11 CLL patients and 6 age-matched healthy donors.

The SLAMF6 gene encodes a homotypic immunoglobulin superfamily receptor, also called SLAMF6, which is expressed constitutively on T cells and other haematopoietic cells including B and NK cells. The function of this receptor has long been unclear, but recent work has shown it to act as an immune checkpoint in T cells in mouse models, wherein knockout or blocking of SLAMF6 improved anti-tumour responses (340,341).

In the DNA microarrays in this study, SLAMF6 expression was observed to be higher in CLL T cells than those from healthy donors across all three T cell subsets, with a mean log fold change of 2.33. As can be observed in *Figure 4.11*, qPCR analysis of SLAMF6 expression in the pooled CLL samples was also notably higher than in the healthy donor samples, with CLL showing a 1.72 times greater expression.

E3 ubiquitin ligase enzymes catalyse the addition of ubiquitin molecules to specific intracellular protein targets, which can alter their function or mark these proteins for degradation by the proteasome. The PELI1 gene encodes an E3 ubiquitin ligase which targets ubiquitylation to IRAK1 (*Interleukin-1 receptor-associated kinase 1*), a key signalling molecule downstream of both the IL-1 receptor and Toll-like receptors. The action of PELI1 on IRAK1 leads to the assembly of signalling complexes that in turn induce the activation of NF- κ B, a key regulator of inflammation and immune responses (342,343).

The DNA microarrays in this study showed PELI1 expression to be greater in T cells from healthy donors than those from CLL patients, with log fold changes of 2.40, 2.46 and 2.58 across the three subsets. qPCR analysis of PELI1 expression

revealed the same pattern of higher expression in healthy donor T cells, however the magnitude of the difference was smaller with T cells from healthy donors showing 1.07 times higher expression (*Figure 4.11*).

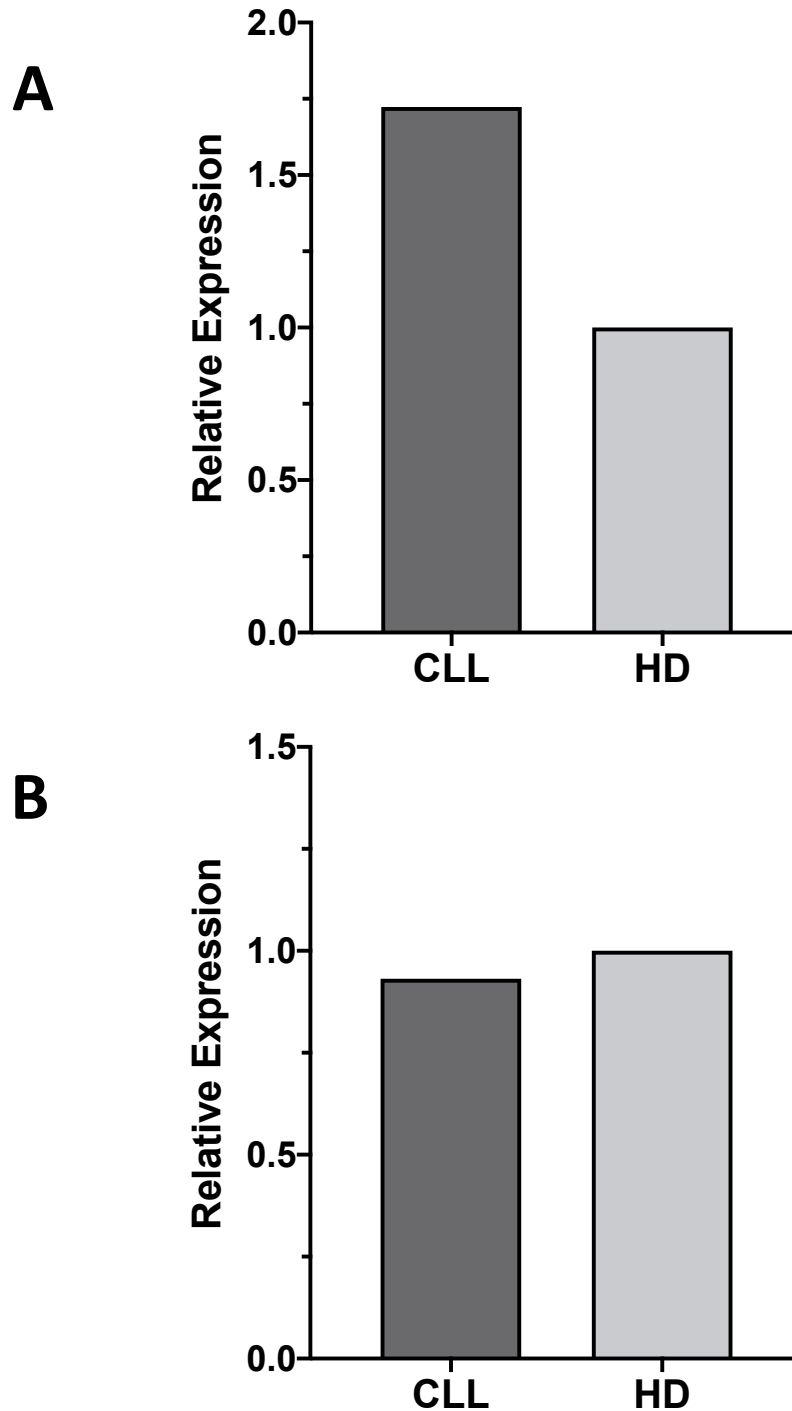


Figure 4.11: qPCR Validation of SLAMF6 and PELI1 Expression

Total RNA from CD4⁺HLA-DR⁻PD-1⁻, CD4⁺HLA-DR⁻PD-1⁺ and CD4⁺HLA-DR⁺PD-1⁺ T cells from 11 CLL patients and 6 age-matched healthy donors were pooled and expression of the genes SLAMF6 (A) and PELI1 (B) was measured in triplicate by qPCR. The qPCR data was analysed using the Applied Biosystems qPCR analysis web app, utilising the relative quantification method. The level of expression of each gene is shown relative to its expression in the healthy donor sample pool.

Graphs generated using GraphPad Prism software.

4.4.2 Flow Cytometry Validation of Gene Expression

The validation of gene expression by qPCR in *Section 4.4.1* used gene targets that showed large differences between CD4⁺ T cells from CLL patients and healthy donors. However, comparisons of gene expression patterns between the three T cell subsets also formed a vital part of the microarray experiments, so these were validated using flow cytometry. The selection criteria for genes for these experiments were high levels of expression and significant differences in expression between CD4⁺HLA-DR⁺PD-1⁺ and CD4⁺HLA-DR⁻PD-1⁻ T cells, with this difference observed both in CLL and healthy donor samples. The availability of flow cytometry antibodies against the encoded proteins was also taken into account. Two targets were eventually selected, Granzyme A and TOX (*Thymocyte selection-associated HMG Box*).

Granzyme A is a member of the granzyme family of cytotoxic molecules and is highly expressed in the granules of cytotoxic T lymphocytes and NK cells. Unlike the also abundantly expressed Granzyme B, Granzyme A causes cell death in a caspase-independent manner by cleaving mitochondrial proteins and inducing reactive oxygen species release. This alternative mechanism of action to Granzyme B helps to ensure cytotoxic cells can kill their targets, even if they have resistance to caspase-mediated apoptosis (167).

In the DNA microarray analysis in this study, Granzyme A expression was found to be significantly upregulated in CD4⁺HLA-DR⁺PD-1⁺ T cells, with a mean log fold change of 4.20 compared to CD4⁺HLA-DR⁻PD-1⁻ cells. For flow cytometry

validation, blood samples from 24 CLL patients were analysed for expression of Granzyme A, with the results shown in *Figure 4.12A*. A significantly greater proportion of CD4⁺HLA-DR⁺PD-1⁺ T cells expressed Granzyme A compared to their CD4⁺HLA-DR⁻PD-1⁻ counterparts (32.9% vs. 9.8%). There was also a significant difference in the average level of Granzyme A protein expression per cell, as measured using Median Fluorescence Intensity (MFI), with 2.78 times higher expression in CD4⁺HLA-DR⁺PD-1⁺ cells.

TOX is a transcription factor that plays a vital role in the development of T cells, regulating positive selection of thymocytes in the thymus. It also has important functions in the development of innate lymphoid cells and NK cell progenitors, as well as in neurogenesis. Recent evidence has also suggested that TOX is a master regulator of CD8⁺ T cell exhaustion, although there is conflicting evidence as to whether this is the case in humans (344–346).

In this study's DNA microarray results, expression of TOX was the most statistically significant gene expression difference between CD4⁺HLA-DR⁺PD-1⁺ and CD4⁺HLA-DR⁻PD-1⁻ T cells, both in CLL patients and healthy donors, with a mean log fold change of 2.64. For validation, TOX protein expression was measured by flow cytometry in samples from 20 CLL patients, shown in *Figure 4.12B*. TOX protein was expressed by a significantly greater proportion of CD4⁺HLA-DR⁺PD-1⁺ T cells (89.6%) compared to CD4⁺HLA-DR⁻PD-1⁻ cells (68.1%). Using MFI to assess the expression per cell also found a significant difference, with TOX protein found to be expressed at a 1.81 times greater level in CD4⁺HLA-DR⁺PD-1⁺ T cells.

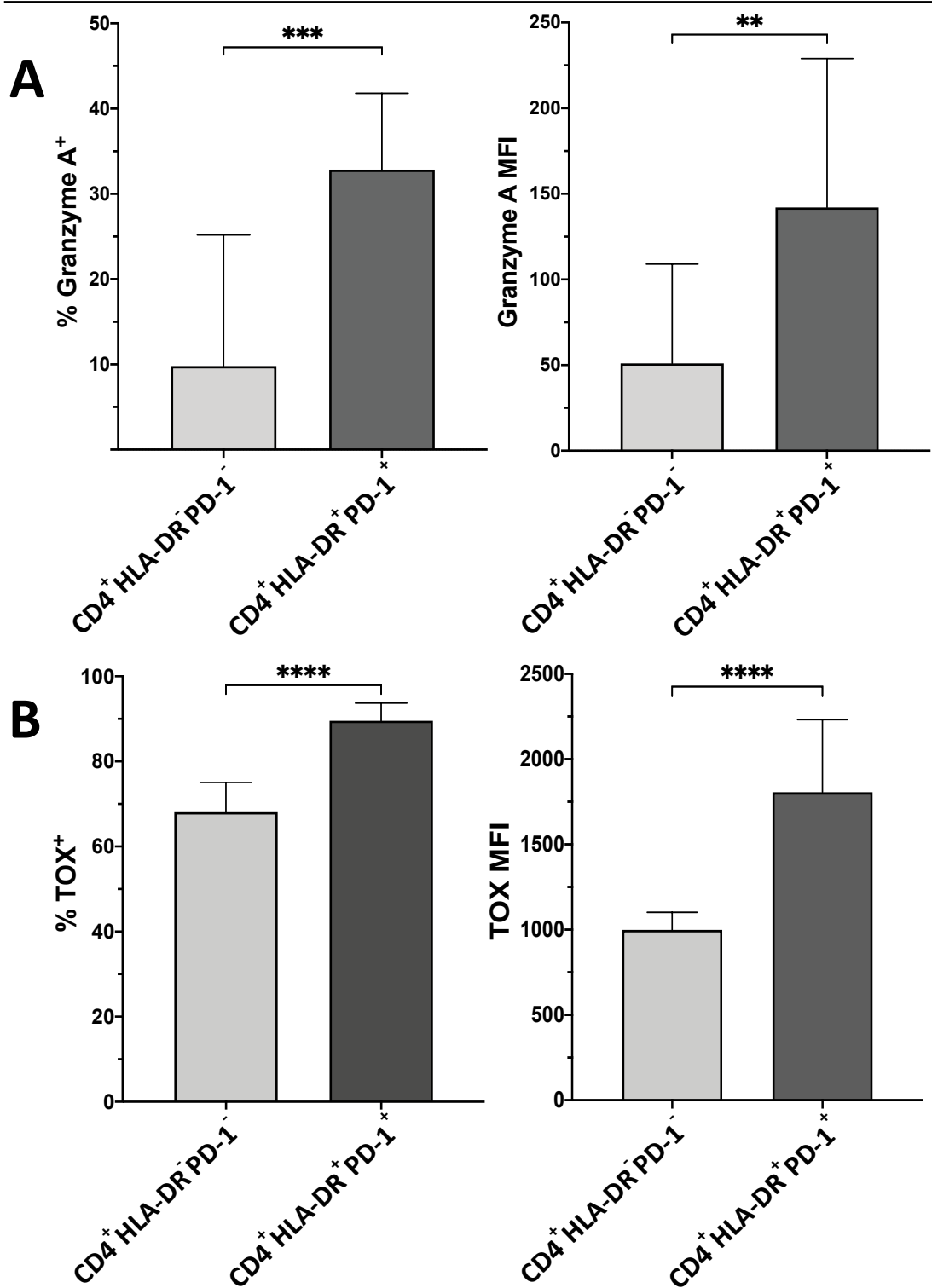


Figure 4.12: CD4⁺HLA-DR⁺PD-1⁺ T Cells Express Higher Levels Granzyme A and TOX

A) Granzyme A expression was analysed by flow cytometry on blood samples from 24 CLL patients. CD4⁺HLA-DR⁺PD-1⁺ T cells more frequently expressed Granzyme A and at a higher level per cell.

B) Expression of TOX protein was measured using flow cytometry on blood samples from 20 CLL patients. A greater proportion of CD4⁺HLA-DR⁺PD-1⁺ T cells expressed TOX protein, and the expression per cell was also higher.

Bars represent median \pm 95% confidence interval. Significance was assessed by Mann Whitney Test. **** = $p < 0.0001$ *** = $p < 0.001$ ** = $p < 0.01$

4.5 Discussion

This chapter has sought to define a gene expression signature for CD4⁺HLA-DR⁺PD-1⁺ T cells in CLL and to elucidate the potential mechanisms by which this subset may influence disease progression. As has been shown in *Chapter 3* and previously (256), the CD4⁺HLA-DR⁺PD-1⁺ subset is more frequently observed in CLL patients and has a clear association with poorer prognosis, however whether these cells are directly affecting the disease course or are bystanders is unclear. Phenotypic data in this study revealed CD4⁺HLA-DR⁺PD-1⁺ T cells to be highly heterogeneous, with many discrete subpopulations able to be defined (*Section 3.2.2*). The results also suggested that CD4⁺HLA-DR⁺PD-1⁺ T cells in CLL might be functionally different from those in healthy donors. To address this, a broader survey was required to investigate in greater detail the nature of CD4⁺HLA-DR⁺PD-1⁺ cells in CLL. By using FACS to purify T cell subsets followed by DNA microarrays, a method which has been used successfully previously (347), the gene expression profile of CD4⁺HLA-DR⁺PD-1⁺ T cells was revealed, allowing a global perspective on the potential biological pathways and functions of these cells in CLL patients.

Investigations of gene expression profiles of immune cells have been carried out in both autoimmune disease and cancer settings, and there have been a number of attempts to define specific gene expression signatures associated with a particular disease (336,348,349). In this study, a potential gene signature defining CLL T cells was discovered. This signature was found by comparing the most significantly differentially expressed genes between CD4⁺HLA-DR⁺PD-1⁺ T cells from CLL patients

and those from healthy donors, upon which it was clear that most of these genes were also highly expressed in other T cell subsets in CLL. These 550 genes included many proteins related to cell division, such as cyclins and cyclin-dependent kinases, and several components of the PI3 Kinase/AKT signalling pathway. Further investigation of this gene signature, in particular to uncover the most important genes within it controlling the CLL T cell phenotype, may yield new markers that could diagnose patients susceptible to CLL development before their disease manifests.

The gene expression analysis in this study not only found a CLL T cell signature, but also revealed a distinct set of 74 genes highly expressed only in CD4⁺HLA-DR⁺PD-1⁺ T cells from healthy donors. As shown in *Chapter 3*, the CD4⁺HLA-DR⁺PD-1⁺ subset is highly heterogeneous in healthy donors as well as in CLL patients, but this 74 gene expression profile helps to delineate the differences between them. Of particular interest is the expression of FOXP3 and CCR8, shown to be markers of key T_{Reg} cells (350). Previous work has demonstrated that CD4⁺HLA-DR⁺PD-1⁺ cells in CLL are not T_{Reg} (256), but the findings here suggest that T_{Reg} may form a significant element of this subset in healthy people. Also, CD4⁺HLA-DR⁺PD-1⁺ T cells in healthy donors expressed Ki67 at levels above even those seen in CLL T cells (*Figure 3.6*), marking these cells as very highly proliferative. Considering the association between CD4⁺HLA-DR⁺PD-1⁺ cells and poorer outcomes in CLL, and the contribution of T_{Reg} to immunosuppression and worse prognosis in solid cancers (351), further study of this subset in healthy older people, with a view to assessment of clinical outcomes, could provide novel insight.

The use of Ingenuity Pathway Analysis software provides a powerful unbiased tool for investigating gene expression differences in their biological context, rather than as single discrete genes. The ability to analyse networks of genes, and the functional endpoints of those networks, allow for a deeper understanding of input dataset, while the suggestion of potential upstream molecules offers the possibility of new therapeutic targets.

The analysis in this study showed PD-1/PD-L1 signalling as the second most upregulated pathway in CD4⁺HLA-DR⁺PD-1⁺ T cells compared to CD4⁺HLA-DR⁻PD-1⁻ cells in CLL, with PD-1 being the most likely upstream regulator of the CD4⁺HLA-DR⁺PD-1⁺ phenotype. This provides reassurance that the differences observed are real and that the FACS was efficient at purifying the desired populations. A key distinction between the observed pathways in CD4⁺HLA-DR⁺PD-1⁺ vs. CD4⁺HLA-DR⁻PD-1⁻ T cells in CLL was in differentiation, with the T_H2 pathway being associated with CD4⁺HLA-DR⁺PD-1⁺ T cells and the T_H1 pathway linked to CD4⁺HLA-DR⁻PD-1⁻ cells. Since the canonical T_H2 cytokine IL-4 has been shown to increase B cell receptor signalling in CLL (352), this suggests a possible role for CD4⁺HLA-DR⁺PD-1⁺ T cells in supporting CLL cells. Further evidence for a T_H1 phenotype in the CD4⁺HLA-DR⁻PD-1⁻ subset is found in the upstream regulators analysis, where the T_H1-polarising cytokines IL-27, IL-12 and IFN γ were all associated with these cells (353,354). Counterintuitively, the canonical T_H2 cytokine IL-4 was also a suggested upstream molecule for CD4⁺HLA-DR⁻PD-1⁻ cells in CLL, perhaps reflecting that this subset represents the majority of CD4⁺ T cells and will almost certainly contain some T_H2 cells.

As opposed to the T_H2 lineage, the upregulation of certain genes in the CD4⁺HLA-DR⁺PD-1⁺ T cell subset in CLL suggest these cells could be T regulatory type 1-like (Tr1-like) cells. This rare subset of T cells has the capacity to suppress immune responses and recent work has shown that the transcription factor EOMES is a master regulator of these cells and that they express both granzyme K and granzyme A (355). All of these Tr1-like cell-associated genes were significantly upregulated in CD4⁺HLA-DR⁺PD-1⁺ T cells in CLL, with granzyme A in particular having the largest log fold change of all the genes studied. Interestingly, Tr1-like cells expressing both EOMES and PD-1 have very recently been observed in CLL patients (356), although the key cytokine produced by these cells is IL-10, which was not significantly differentially expressed in CD4⁺HLA-DR⁺PD-1⁺ T cells in CLL. However, new evidence has emerged that the presence of Tr1-like cells is associated with worse clinical outcomes in several solid cancers (357), so further investigation of this interesting subset is certainly warranted in CLL.

As well as the T_H2 pathway, several other pathways and functions were unique to the CD4⁺HLA-DR⁺PD-1⁺ subset in CLL. The Wnt/ β -catenin pathway was the third most strongly associated pathway in CD4⁺HLA-DR⁺PD-1⁺ T cells in CLL, but was not associated with these cells in healthy donors. The Wnt/ β -catenin pathway is important in controlling cell proliferation and differentiation and has been shown to play a role in a number of cancers (358). There have been several studies of Wnt signalling in a leukaemia context and it has been demonstrated that at least a subset of CLL cells have overactivity of this pathway (359–361). Interestingly, there also is evidence that the Wnt/ β -catenin pathway promotes differentiation of CD4⁺ T cells

into a T_H2 phenotype by upregulating the transcription factor GATA3 (362). Therefore, the association of Wnt signalling with CD4⁺HLA-DR⁺PD-1⁺ T cells in CLL may contribute to both their highly proliferative phenotype and their strong T_H2 gene expression profile.

In the Diseases and Functions analysis, the oxidative phosphorylation (OXPHOS) pathway was strongly associated with CD4⁺HLA-DR⁺PD-1⁺ T cells in CLL, but only to a much lesser extent with CD4⁺HLA-DR⁻PD-1⁺ cells and not at all with CD4⁺HLA-DR⁻PD-1⁻ cells. The role of OXPHOS in T cells is complex – traditionally naïve T cells were considered to use OXPHOS while effector T cells switched to glycolysis, with a reversion to OXPHOS in memory T cells (363–365). Recent evidence has also suggested a requirement for OXPHOS for T cell proliferation and the avoidance of exhaustion in tumour-infiltrating T cells (366), which makes the association of CD4⁺HLA-DR⁺PD-1⁺ T cells with an exhaustion profile as well as OXPHOS an intriguing finding. In the CLL T cell signature described above and in *Section 4.4*, several members of the PI3K/AKT pathway were observed, while another protein in this pathway, PTEN, was suggested to be an upstream molecule associated with CD4⁺HLA-DR⁺PD-1⁺ T cells in CLL (*Figure 4.10B*). This adds further complexity to the findings, since the PI3K/AKT pathway has been shown to regulate T cell switching away from OXPHOS to glycolysis during differentiation (365,367,368). With another metabolic pathway, fatty acid β -oxidation, also being strongly associated with CLL T cells, it is apparent that the metabolic processes and their relation to differentiation and function in CD4⁺HLA-DR⁺PD-1⁺ T cells will require further investigation.

In the Diseases and Functions analysis, processes related to “activation of blood cells” were strongly related to just CD4⁺HLA-DR⁺PD-1⁺ T cells in CLL, while processes related to “activation of leukocytes” were associated with the CD4⁺HLA-DR⁺PD-1⁺ and CD4⁺HLA-DR⁻PD-1⁻ subsets. It is notable that both of these cellular activation functions were not associated with CD4⁺HLA-DR⁻PD-1⁻ T cells, suggesting an inactivated state in this subset. PD-1 has traditionally been known as an immunoinhibitory molecule and marker of T cell exhaustion (261,369), but other studies have demonstrated that PD-1 can in fact be a marker of functional, activated cells (271,273,370). The results here reinforce that dichotomy, with the presence of another activation marker in HLA-DR appearing to delineate the activated and non-activated PD-1⁺ cells.

Activation-induced cell death (AICD) was strongly associated with CD4⁺HLA-DR⁺PD-1⁺ T cells in CLL but not in those from healthy donors. AICD is an important regulatory mechanism during immune responses, acting to delete highly activated T cells to prevent damage to the host (371). The presence of the gene expression profile for AICD in CLL-derived CD4⁺HLA-DR⁺PD-1⁺ T cells has relevance for the experimental study of this subset, since many T cell functional assays involve activation of the cells and as such may cause considerable cell death in this subset.

In T cells from age-matched healthy donors, and in particular in the CD4⁺HLA-DR⁺PD-1⁺ subset, the replication and life cycle processes of viruses were strongly associated with their gene expression profile, comprising all of the top four outputs from the Diseases and Functions analysis. It is known that in the older population there is a high prevalence of infection with chronic viruses such as CMV

(372), and that such infections lead to increased mortality owing to the burden placed on the immune system (254,330). However, in this study the processes were related to acute viruses, mainly of the *Rhabdoviridae* family. An exploration of the genes considered by the IPA software to be involved in these viral processes reveals that many of them are related to cellular survival and apoptosis signalling (for example: TP53, BAX and Caspase 2). Most of the other top Diseases and Functions in healthy donor T cells were associated with cell viability, with similar sets of genes involved. Therefore, it seems likely that the gene expression profiles for T cells in healthy donors are reflective of changes in cell viability and survival, rather than mass viral infection. This example illustrates a drawback of IPA, wherein function outputs that comprise several elements can achieve a high activation z-scores with only some of those elements being upregulated., leading to potentially misleading conclusions.

IPA software provides a useful tool for the exploration of gene expression data and how the results acquired translate into biological processes and pathways. An alternative method for investigating gene expression data involves the comparison of the user's data with gene expression profiles from published studies, to search for common signatures. With an ever-growing number of gene expression datasets, from a wide variety of cell types and disease states, publicly available, this method allows the user to quickly determine whether the patterns of gene expression in their data match those for known phenotypes or diseases. Gene Set Enrichment Analysis (GSEA) software is the foremost exponent of this methodology (373). For this study, GSEA was conducted using the C7 Immunologic Signatures

dataset on the significantly differentially expressed genes ($p < 0.05$ and $\log_{2}FC > 1$) for the comparison of CLL-derived CD4⁺HLA-DR⁺PD-1⁺ cells vs. healthy donor CD4⁺HLA-DR⁺PD-1⁺ cells (top results shown in *Appendix Tables 15 and 16*).

For CLL-derived CD4⁺HLA-DR⁺PD-1⁺ cells, there were no T cell-associated gene sets significantly enriched. Among the top gene sets that did not reach significance were genes related to HIV-specific T cells and genes upregulated in IL-4/TGF β treated T cells. As a chronic disease with T cell dysfunction (374), HIV has similarities to CLL and thus some overlap of the gene expression profiles would be expected. The combination of IL-4 and TGF β has been shown to promote a T_H9 polarisation of naïve T cells (375,376), with this subset of T cells having roles in allergy and antitumour responses (377). Whether in CLL the CD4⁺HLA-DR⁺PD-1⁺ subset, or a subpopulation within it, are T_H9 cells would be of interest to explore.

In healthy donor CD4⁺HLA-DR⁺PD-1⁺ cells the only significantly enriched T cell gene set was genes upregulated in late-stage chronic viral infection compared to the early stages. As mentioned above, there is a high prevalence of chronic viruses in the older population, from which these samples were drawn, so this result may well indicate the presence of an infection such as CMV in the healthy donors. Also enriched but not reaching significance in healthy donor CD4⁺HLA-DR⁺PD-1⁺ cells were genes upregulated in T_{Reg} cells compared to T_H2 cells. This supports the concept described earlier that T_{Reg} cells may comprise a significant proportion of the CD4⁺HLA-DR⁺PD-1⁺ subset in healthy people.

The GSEA results for this study showed no evidence in CLL-derived CD4⁺HLA-DR⁺PD-1⁺ cells of significant enrichment of genes associated with a specific

T cell subtype or with previously published T cell phenotypes, for example T_{Reg} or T_{H2}. This leads to two possible conclusions: that this is a novel subset of CD4⁺ T cells that has not been previously studied or that the CD4⁺HLA-DR⁺PD-1⁺ population is so heterogeneous that individual phenotypes are difficult to distinguish. In either case, further investigation is justified to determine whether these cells affect CLL disease course and the methods by which they might exert their influence.

The immunoglobulin superfamily member SLAMF6 was chosen as a qPCR validation target for the gene expression data (see *Figure 4.11*) and was found to be expressed in CLL-derived T cells at almost twice the level of T cells from healthy donors. This finding is of particular interest in light of recent studies that have suggested that SLAMF6 is a checkpoint in T cells, functioning to attenuate anti-tumour immune responses (341). This concept has also been observed in mouse models of CLL, wherein SLAMF6 expression caused an increase in CD8⁺ T cells with defective cytotoxic function and anti-SLAMF6 antibodies were able to reduce the leukaemic burden (340). This opens a potential new therapeutic target in CLL and a combination study using anti-SLAMF6 antibodies with ibrutinib has already shown promising results, again in a mouse model (378). It appears that SLAMF6 may be an interesting candidate for CLL therapy in future, although significant work using human CLL samples will be required to prove that the auspicious results in mice can be translated to a patient setting.

In all three T cell subsets studied here, the T cell exhaustion pathway was the most significantly upregulated pathway in CLL compared to healthy donors. The gene TOX has been recently described as the master regulator of exhaustion in CD8⁺ T cells, both in mice (379,380) and in humans (381). However, other evidence points towards a more complicated role for TOX, with its expression observed in non-exhausted functional CD8⁺ T cells in humans (346). Little is known, however, about the role of TOX in CD4⁺ T cells in humans and whether its putative control of CD8⁺ T cell exhaustion extends to their CD4⁺ counterparts. Due to its novelty and unclear role, TOX is not considered as part of the T cell exhaustion signalling pathway in IPA, however it was the most significantly differentially expressed gene between CD4⁺HLA-DR⁻PD-1⁻ and CD4⁺HLA-DR⁺PD-1⁺ T cells in both CLL and healthy donors. The question of whether TOX causes exhaustion in CD4⁺ T cells and if so, why T cell exhaustion signalling is so highly associated with CD4⁺HLA-DR⁻PD-1⁻ T cells despite their relatively low TOX expression, warrants further investigation and will be explored in *Chapter 5*.

In summary, analysis of the gene expression profiles of CD4⁺ T cell subsets from both CLL and healthy donors has revealed additional insights not apparent from the phenotyping data in *Chapter 3*. In particular, it was demonstrated that CLL has a global impact on CD4⁺ T cell gene expression, leading to a characteristic signature. Furthermore, CD4⁺HLA-DR⁺PD-1⁺ T cells were observed to be a distinct population from other CD4⁺ T cells, but this subset also differed between CLL patients and healthy donors.

5 Investigating Exhaustion and the Role of TOX in CD4⁺ T Cells in CLL

In order to carry out their functions within the immune system, CD4⁺ T cells rely on their abilities to produce cytokines and proliferate. However, in situations of chronic activation T cells can become exhausted, a state which is associated with a progressive loss of their key functionalities (260). After initial discovery in the context of chronic viral infections, the importance of T cell exhaustion in cancer has become clear in recent years, with exhausted T cells losing their ability to keep tumour growth in check (369). Therefore, a chronic cancer such as CLL would appear to be a likely setting for widespread T cell exhaustion to be observed – however evidence to date has been inconclusive, particularly around the role of PD-1 (see *Section 1.3.3*). In the previous chapter, T cell exhaustion signalling was found to be the most significantly upregulated pathway in CLL T cells compared to those from healthy donors, particularly in CD4⁺HLA-DR⁺PD-1⁺ cells. Given the complex and heterogeneous phenotype of this subset observed in *Chapter 3*, such a strong association with one pathway was unexpected.

As described in *Section 4.4.2*, TOX is a transcription factor with important roles in thymic T cell development that has more recently been implicated in regulating T cell exhaustion in mouse models (379,380). Despite the fact that exhaustion signalling was observed in all three T cell subsets investigated in CLL, TOX was the most significantly differentially expressed gene between CD4⁺HLA-DR⁺PD-1⁺

and CD4⁺HLA-DR⁺PD-1⁻ T cells in CLL, as well as in healthy donors. There is conflicting evidence of the role of TOX in T cell exhaustion in humans (346) and a lack of clarity regarding T cell exhaustion in CLL, providing a strong rationale to explore these topics.

This chapter aims to investigate both T cell exhaustion and the role of TOX in CD4⁺ T cells in CLL patients using multiparameter flow cytometry. The functional capabilities of T cells from CLL patients and healthy donors were assessed by analysis of key cytokine production and proliferation under different stimulation conditions.

5.1 Cytokine Production

The main function of CD4⁺ T cells is to support and orchestrate immune responses and this is conducted via the production and secretion of cytokines, whose signalling activity can modulate the behaviour of target cells. In this study, T cells were assessed for their production of three of the most important cytokines in immune responses: interferon- γ (IFN γ), tumour necrosis factor α (TNF α) and interleukin-2 (IL-2).

IFN γ is a type II interferon with potent immunomodulatory capabilities, as well as causing increased cellular antiviral responses. Signalling from IFN γ activates macrophages and promotes NK cell activity, along with causing upregulation of antigen processing and presentation genes to further stimulate immune responses. Furthermore, in T cells IFN γ promotes adhesion and extravasation to allow T cells to reach the area of infection. IFN γ is the characteristic cytokine produced by T_H1 cells and is also the key cytokine in the differentiation of naïve T cells into T_H1 cells.

TNF α is a small cytokine produced by a variety of immune cells that plays a vital role in causing inflammation and fever during infections. In non-immune cells, TNF α signalling through TNF receptor 1 can initiate apoptotic cell death or inflammatory reactions in a context-dependent manner. In immune responses, TNF α enhances macrophage phagocytosis and attracts neutrophils to sites of infection, as well as causing differentiation and proliferation in T cells.

IL-2 is a key cytokine for T cell activity, particularly in immune responses, with T cells themselves being the major source of IL-2 production. During T cell development in the thymus, IL-2 signalling helps to promote the generation of

regulatory T cells to combat autoimmunity. Post-infection, IL-2 functions to enhance proliferation and survival of T cells, as well as working in tandem with other cytokines to induce differentiation of naïve T cells into either T_H1 or T_H2 cells. Depletion of IL-2 via the expression of the high affinity IL-2 receptor (CD25) is an important mechanism for T_{Reg} cells to control immune responses.

Apart from cytokines, CD4⁺ T cells are able to secrete cytotoxic molecules, such as perforin and granzymes, in some circumstances, although this is not a common feature (289). Such molecules are stored in intracellular vesicles (or granules) in readiness for release via exocytosis. During this process, transmembrane proteins on the vesicles become displayed on the cell surface following fusion of the vesicles with the cell membrane. Therefore, measurement of surface levels of these proteins can be used to indicate degranulation. CD107a is one such protein, the usual function of which is to maintain the integrity of the intracellular vesicles, but which has become a commonly used marker of cellular degranulation.

In order to induce production of cytokines, T cells require activation. *In vitro*, this can be achieved by stimulation of T cells with various agents and in this study two of the most common stimulation methods were used: CD3/CD28 beads and PMA/Ionomycin.

CD3/CD28 beads consist of anti-CD3 and anti-CD28 antibodies bound to polymer beads which are added to cell cultures. Binding of these antibodies to their respective targets replicates the two signals needed to activate T cells, namely activation of the T cell receptor and co-stimulation, in order to induce activation in a

physiological manner. The use of anti-CD3 bypasses the need for peptide:MHC recognition by the T cell receptor and anti-CD28 removes the requirement of antigen-presenting cells to provide co-stimulatory signals via CD80/86 engagement.

PMA/Ionomycin stimulation uses the small molecule Phorbol 12-myristate 13-acetate (PMA) and the calcium ionophore Ionomycin to mimic the downstream signalling of the T cell receptor. PMA activates the signalling enzyme Protein Kinase C (PKC) via its similarity to the usual PKC activator diacylglycerol. Ionomycin increases the intracellular calcium ion level leading to activation of the calcineurin signalling pathway and subsequent transcription factor activity. By bypassing upstream signalling pathways, PMA/Ionomycin provide a potent stimulation greater than the normal physiological signals and so acts as a positive control for T cell stimulation.

5.1.1 Cytokine Production in Total CD4⁺ T Cells

Figure 5.1 displays the results of cytokine production and degranulation analysis of the total CD4⁺ T cell population, from 20 CLL patients and 4 healthy donors. For all of the cytokines measured, the pattern of response to the different stimulation conditions was very similar between CLL and healthy donor T cells.

IFN γ (*Figure 5.1A*) was not expressed by any T cells that were not stimulated from either CLL patients or healthy donors, with only a small number of individuals showing a minor increase in IFN γ expression following CD3/CD28 stimulation. On the other hand, PMA/Ionomycin stimulation caused a significant increase in the proportion of IFN γ ⁺ cells in samples from both CLL and healthy donors, with over 50% of cells showing IFN γ expression in some cases. However, in both groups there was wide variation, particularly in CLL where around a quarter of patients showed no increase in IFN γ expression after stimulation.

As seen in *Figure 5.1B*, TNF α was not expressed by unstimulated T cells from either CLL or healthy donors. Unlike for IFN γ however, CD3/CD28 stimulation led to increased proportions of cells expressing TNF α , with a median of around 13% TNF α ⁺ cells in both groups (although statistical significance was not reached in healthy donors). PMA/Ionomycin stimulation induced further increases in TNF α expression, particularly in healthy donors (median 58%). There was again a large degree of variation, especially in CLL where T cells from three individuals failed to respond to either CD3/CD28 or PMA/Ionomycin stimulation.

Expression of IL-2 (*Figure 5.1C*) was not seen under unstimulated conditions in either CLL or healthy donors. Stimulation with CD3/CD28 beads induced

expression of IL-2 in T cells in around one third of CLL patients, but did not have any effect on healthy donor T cells. PMA/Ionomycin stimulation led to significantly increased proportions of IL-2⁺ cells in both CLL and healthy donor T cells (medians around 20%), although there was again a wide range of responses.

Degranulation, as measured by CD107a expression (*Figure 5.1D*), was seen in T cells from only one individual without stimulation in both CLL and healthy donors. Both groups had an increased proportion of CD107a⁺ cells following CD3/CD28 stimulation, although in CLL one quarter of patients did not show an increase. PMA/Ionomycin stimulation led to a further increase in the percentage of CD107a-expressing cells in healthy donors (median 27.6%), but a decreased proportion compared to CD3/CD28 stimulation in CLL (median 5.7% vs. 15.5%) although this was still greater than in unstimulated cells.

These results show that the cytokine production and degranulation capabilities of CD4⁺ T cells are very similar between CLL patients and healthy donors, which suggests that the overall CD4⁺ T cell population in CLL is not functionally exhausted.

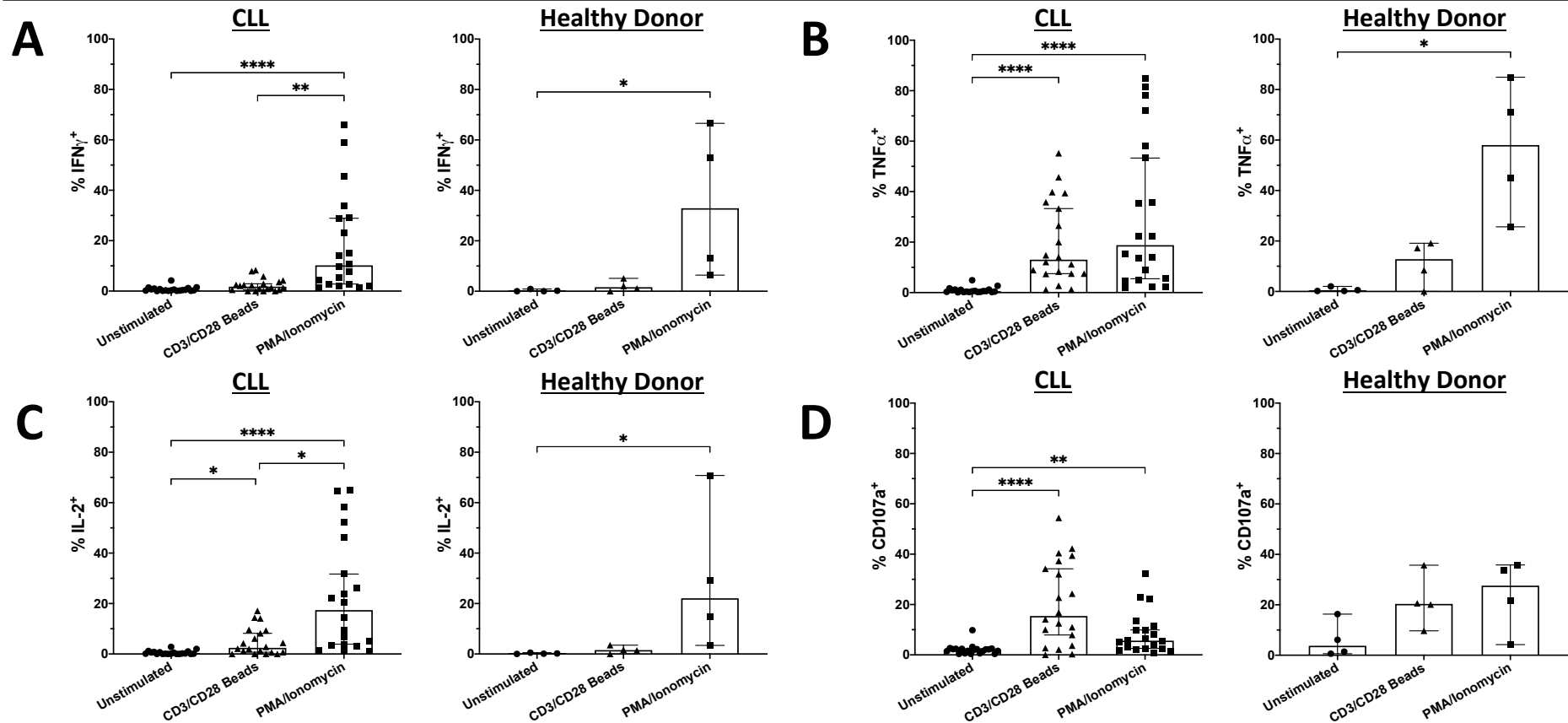


Figure 5.1: CD4⁺ T Cells Have Similar Cytokine Production Capabilities in CLL and Healthy Donors

Cytokine production and cellular degranulation were measured by flow cytometry in CD4⁺ T cells from 20 CLL patients and 4 healthy donors following either no stimulation or stimulation with CD3/CD28 beads or PMA/Ionomycin for 6 hours. **A)** Production of IFN γ was only upregulated by PMA/Ionomycin stimulation in both CLL and healthy donors. **B)** TNF α production was upregulated by CD3/CD28 stimulation in CLL and by PMA/Ionomycin stimulation in both CLL and healthy donors. **C)** Production of IL-2 was upregulated by CD3/CD28 stimulation and PMA/Ionomycin stimulation in CLL and but only PMA/Ionomycin stimulation healthy donors. **D)** CD107a expression was upregulated by both CD3/CD28 and PMA/Ionomycin stimulations in CLL and healthy donors. Bars represent median \pm 95% confidence interval. Significance was determined by Kruskal-Wallis test with Dunn's multiple comparisons ****= $p < 0.0001$ **= $p < 0.01$ *= $p < 0.05$

5.1.2 Cytokine Production in CD4⁺ T Cell Subsets

Figure 5.2 displays the results of cytokine production and degranulation analysis for the three CD4⁺ T cell subsets assessed in *Chapter 4* (CD4⁺HLA-DR⁻PD-1⁻, CD4⁺HLA-DR⁻PD-1⁺ and CD4⁺HLA-DR⁺PD-1⁺). Total T cells taken from 20 CLL patients and 4 healthy donors were used and were subdivided into the three subsets during the analysis. The results of the previous gene expression analysis showed considerable differences between these populations, despite exhaustion signalling being associated with all three subsets, so analysis of their functional characteristics was warranted. This is particularly pertinent for CD4⁺HLA-DR⁺PD-1⁺ cells, which comprise less than 5% of the total CD4⁺ population and as such would be masked in the analysis in *Section 5.1.1*.

In *Figure 5.2A* the levels of IFN γ expression are shown. In both CLL and healthy donors, there were very few cells expressing any IFN γ under unstimulated conditions in any of the T cell subsets, with the exception of low expression in CD4⁺HLA-DR⁺PD-1⁺ cells from a small number of CLL patients. Following CD3/CD28 stimulation, there was no difference in healthy donor T cells, while in CLL there was an increase in the proportion of IFN γ ⁺ cells in the CD4⁺HLA-DR⁺PD-1⁺ and CD4⁺HLA-DR⁻PD-1⁺ subsets in around one third of patients. Stimulation with PMA/Ionomycin led to significant increases in the percentage of IFN γ -expressing cells in CLL, with CD4⁺HLA-DR⁺PD-1⁺ cells having the greatest median (34.2%) and CD4⁺HLA-DR⁻PD-1⁺ cells the lowest (6.3%). The same pattern was observed in healthy donors, although there was a very wide range of responses.

In both CLL and healthy donor T cells, TNF α (*Figure 5.2B*) was not expressed by CD4⁺HLA-DR⁻PD-1⁻ cells when unstimulated. However, TNF α expression was observed at low levels in CD4⁺HLA-DR⁻PD-1⁺ and CD4⁺HLA-DR⁺PD-1⁺ cells from several individuals. Following CD3/CD28 stimulation, there was a slight increase in the median percentage of TNF α ⁺ cells in healthy donors, with one individual showing almost 100% TNF α ⁺ cells in the CD4⁺HLA-DR⁻PD-1⁺ subset. In CLL, CD3/CD28 stimulation also caused small increases in the proportion of TNF α -expressing cells for the CD4⁺HLA-DR⁻PD-1⁻ and CD4⁺HLA-DR⁻PD-1⁺ subsets, but there was a large increase for CD4⁺HLA-DR⁺PD-1⁺ cells (median 33.3% *cf.* 3.7% in unstimulated CD4⁺HLA-DR⁺PD-1⁺ cells). PMA/Ionomycin stimulation induced significant increases in the proportion of cells expressing TNF α in all three subsets in CLL, although to a lesser extent than CD3/CD28 stimulation for CD4⁺HLA-DR⁺PD-1⁺ cells. For healthy donors PMA/Ionomycin stimulation increased TNF α expression in all subsets, although the inverse pattern to that seen for IFN γ was observed – the CD4⁺HLA-DR⁺PD-1⁺ subset having the lowest proportion of TNF α ⁺ cells (median 34.5%) and the CD4⁺HLA-DR⁻PD-1⁻ subset the highest (median 68.9%).

Figure 5.2C shows the expression of IL-2. In unstimulated conditions, there was little, if any, expression of IL-2 in either CLL or healthy donor T cells and this was not impacted by CD3/CD28 stimulation in healthy donors. In CLL, CD3/CD28 stimulation led to no increase in the median percentage of IL-2⁺ cells, although cells from around a third of individuals showed a modest response. PMA/Ionomycin stimulation caused a significant increase in the proportion of IL-2 expressing cells in all three T cell subsets in CLL, with CD4⁺HLA-DR⁻PD-1⁺ cells showing the highest

expression level (median 34%). In contrast for healthy donors, although PMA/Ionomycin stimulation also increased the proportion of IL-2⁺ cells in all three subsets, CD4⁺HLA-DR⁻PD-1⁺ cells had the lowest percentage (median 7.6%).

CD107a expression for each T cell subset is shown in *Figure 5.2D*. Without stimulation, a proportion of CD107a⁺ cells was seen in the CD4⁺HLA-DR⁺PD-1⁺ subset from over half of healthy donors and CLL patients. Following CD3/CD28 stimulation, both CLL and healthy donors showed small increases in the proportion of CD107a⁺ cells in the CD4⁺HLA-DR⁻PD-1⁻ subset and large increases in the CD4⁺HLA-DR⁺PD-1⁺ subset (CLL median 37.1% vs. 3.9% when unstimulated). PMA/Ionomycin stimulation caused further increases in the percentage of CD107a-expressing cells in all three subsets in healthy donors, while in CLL there were small increases in the CD4⁺HLA-DR⁺PD-1⁺ and CD4⁺HLA-DR⁻PD-1⁺ subsets compared to unstimulated conditions. Similar to the results for TNF α expression (*Fig. 5.2B*), the median proportion of CD107a⁺ cells in the CD4⁺HLA-DR⁺PD-1⁺ subset was lower following PMA/Ionomycin than after CD3/CD28 stimulation.

These results suggest that the CD4⁺HLA-DR⁺PD-1⁺ subset in CLL is not functionally exhausted, being able to produce IL-2 and degranulate at physiological levels of stimulation. However, while all the subsets showed increased cytokine production following strong PMA/Ionomycin stimulation, both CD4⁺HLA-DR⁻PD-1⁺ and CD4⁺HLA-DR⁻PD-1⁻ cells showed only very minor, if any, responses to CD3/CD28 stimulation. In comparison, healthy donor T cells across all three subsets were observed to have minimal, if any, response to CD3/CD28 stimulation in regard to

cytokine production, but showed modest increases in degranulation. However, all three subsets were able to upregulate expression of these cytokines and degranulation when stimulated with PMA/Ionomycin.

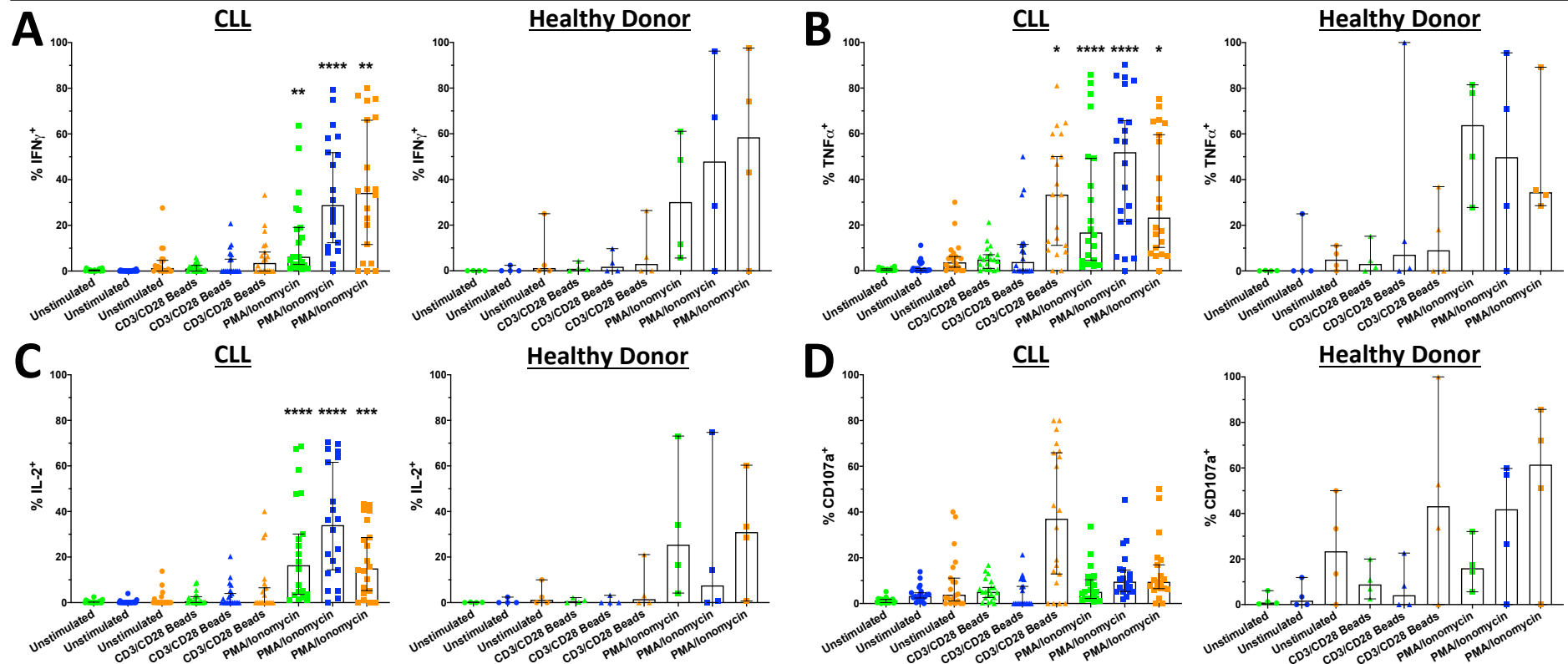


Figure 5.2: CD4⁺HLA-DR⁺PD-1⁺ T Cells Are Not More Exhausted Than Other T Cell Subsets

Cytokine production and cellular degranulation were measured by flow cytometry in CD4⁺ T cells from 20 CLL patients and 4 healthy donors following either no stimulation or stimulation with CD3/CD28 beads or PMA/Ionomycin for 6 hours. **A)** Production of IFN γ was only upregulated by PMA/Ionomycin stimulation for all three T cell subsets in both CLL and healthy donors. **B)** TNF α production was upregulated by PMA/Ionomycin stimulation in all T cell subsets in CLL and healthy donors and by CD3/CD28 stimulation in CD4⁺HLA-DR⁺PD-1⁺ cells in CLL. **C)** Production of IL-2 was upregulated only by PMA/Ionomycin stimulation for all T cell subsets in CLL and CD4⁺HLA-DR⁺PD-1⁺ and CD4⁺HLA-DR⁻PD-1⁻ cells in healthy donors. **D)** CD107a expression was upregulated in CD4⁺HLA-DR⁺PD-1⁺ cells in CLL and healthy donors by CD3/CD28 stimulation and by PMA/Ionomycin stimulation in all three subsets in healthy donors. Bars represent median \pm 95% confidence interval. Significance was assessed compared to unstimulated conditions and was determined by Kruskal-Wallis test with Dunn's multiple comparisons ****= $p < 0.0001$ ***= $p < 0.001$ **= $p < 0.01$ *= $p < 0.05$

Key
■ CD4⁺ HLA-DR⁻ PD-1⁻
■ CD4⁺ HLA-DR⁻ PD-1⁺
■ CD4⁺ HLA-DR⁺ PD-1⁺

5.1.3 Effect of TOX Expression on Cytokine Production in CD4⁺ T Cells

To investigate whether expression of the transcription factor TOX, a potential regulator of T cell exhaustion, impacted CD4⁺ T cell function in CLL, cytokine production and degranulation were assessed in TOX⁺ and TOX⁻ CD4⁺ T cells. These populations were determined by flow cytometry, conducted on samples from 20 CLL patients and 4 healthy controls. The proportions of TOX-expressing cells from these two groups are shown in *Figure 5.3* and the results of the cytokine production and degranulation analysis are displayed in *Figure 5.4*.

In unstimulated CD4⁺ T cells in CLL (*Figure 5.3A*), a majority of cells expressed TOX (median 70.3%). Following stimulation with CD3/CD28 beads, there was a slight increase in proportion of TOX⁺ cells, with a further small increase observed after PMA/Ionomycin stimulation (median 77.9%). However, these differences were not statistically significant, such that the percentage of TOX-expressing cells can be considered to remain consistent across the stimulation conditions.

In healthy donors, the proportions of TOX⁺ cells under each of the stimulation conditions were lower than for their CLL counterparts, with a similar range of variation. When unstimulated, a majority of cells expressed TOX (median 55.9%) but the percentage of cells expressing TOX decreased following CD3/CD28 stimulation (median 48.5%). PMA/Ionomycin stimulation led to an increase in the proportion of TOX⁺ cells above unstimulated levels, but still lower than in CLL. As with the CLL results, there were no statistically significant differences observed and the percentage of TOX-expressing cells can be considered consistent for healthy donors.

Expression of IFN γ (*Figure 5.4A*) was not observed under unstimulated conditions in either CLL or healthy donor T cells, regardless of TOX expression. After CD3/CD28 stimulation this was unchanged for healthy donors, but in CLL there was a slight increase in the percentage of IFN γ ⁺ cells in some individuals, particularly in the TOX⁺ group. PMA/Ionomycin stimulation led to a further increased proportion of cells expressing IFN γ in CLL although there was no significant difference between TOX⁺ (median 10.4%) and TOX⁻ (median 9%) cells. In healthy donors, PMA/Ionomycin stimulation also caused an increase in the proportion of IFN γ ⁺ cells, with a slightly higher median, albeit along with a greater range, in TOX⁺ cells.

Figure 5.4B shows the percentages of TNF α -expressing cells, of which there were few, if any, observed without stimulation for both CLL patients and healthy donors. In both groups, there was an increase in the proportion of TNF α ⁺ cells following CD3/CD28 stimulation, particularly in TOX⁺ cells, with the median percentage of TNF α -expressing cells more than double that of TOX⁻ cells in CLL (15.2% vs. 7.3%). This difference was not maintained after PMA/Ionomycin stimulation however, with both TOX⁺ and TOX⁻ cells having similar proportions of TNF α ⁺ cells, although these proportions were considerably greater in healthy donors than CLL patients (medians ~57% vs. ~19%).

IL-2 (*Figure 5.4C*) was not found to be expressed by any T cells from either CLL patients or healthy donors under unstimulated conditions. After CD3/CD28 stimulation, the proportion of IL-2⁺ cells increased slightly in CLL T cells, both TOX⁺ and TOX⁻, while healthy donor T cells continued to show no IL-2 expression. PMA/Ionomycin stimulation caused a large increase in the percentage of cells

expressing IL-2 in CLL, with TOX⁺ and TOX⁻ cells having almost identical medians (16.5% vs. 16.9%). The proportion of IL-2⁺ cells was also increased in healthy donors by PMA/Ionomycin to a slightly greater extent than in CLL, with TOX⁻ cells observed to have the greater percentage (median 26%).

CD107a expression (*Figure 5.4D*), measuring degranulation, was seen at very low levels in T cells without stimulation from both CLL patients and healthy donors. CD3/CD28 stimulation led to an increase in the proportion of CD107a⁺ cells in both CLL and healthy donor T cells, with TOX⁺ cells having around twice the percentage of TOX⁻ cells in both groups. Following PMA/Ionomycin stimulation, the percentage of cells expressing CD107a in CLL decreased compared to CD3/CD28 stimulation, particularly in the TOX⁺ population, although remained greater than in unstimulated cells. In comparison, healthy donor T cells had very similar proportions of CD107a⁺ cells for both the CD3/CD28 and PMA/Ionomycin stimulation conditions, with the greater expression in TOX⁺ cells maintained after the stronger stimulus.

Across all four cytokines in these experiments only trends were observed, with no statistically significant differences. These trends suggested⁴ minimal impact of TOX expression on the cytokine production capabilities of CD4⁺ T cells in CLL and do not support the concept that TOX is a marker of T cell exhaustion. In fact, TOX⁺ cells were observed to have greater degranulation than their TOX⁻ counterparts following physiological levels of stimulation, both in CLL and healthy donor T cells, while cytokine production in both groups was broadly similar regardless of TOX expression.

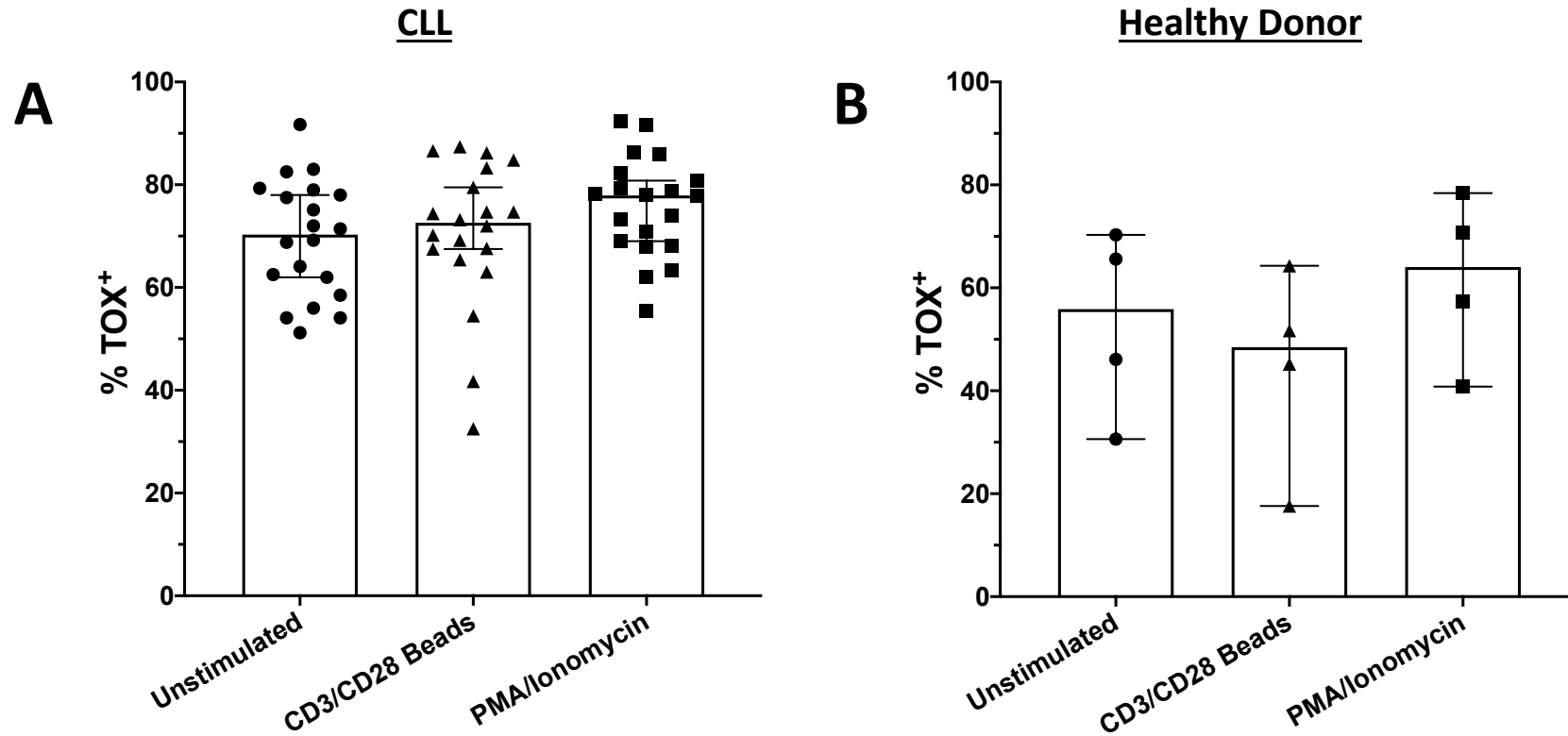


Figure 5.3: TOX Expression is More Common in CLL T Cells But is Not Affected by Stimulation

TOX expression was measured by flow cytometry in CD4⁺ T cells from 20 CLL patients and 4 healthy donors following either no stimulation or stimulation with CD3/CD28 beads or PMA/Ionomycin for 6 hours.

A) Expression of TOX in CLL was consistent, with around 75% of T cells being TOX⁺ regardless of stimulation.

B) TOX was expressed by a lower proportion of T cells in healthy donors than CLL patients under all stimulation conditions, with no significant change observed between unstimulated and stimulated cells.

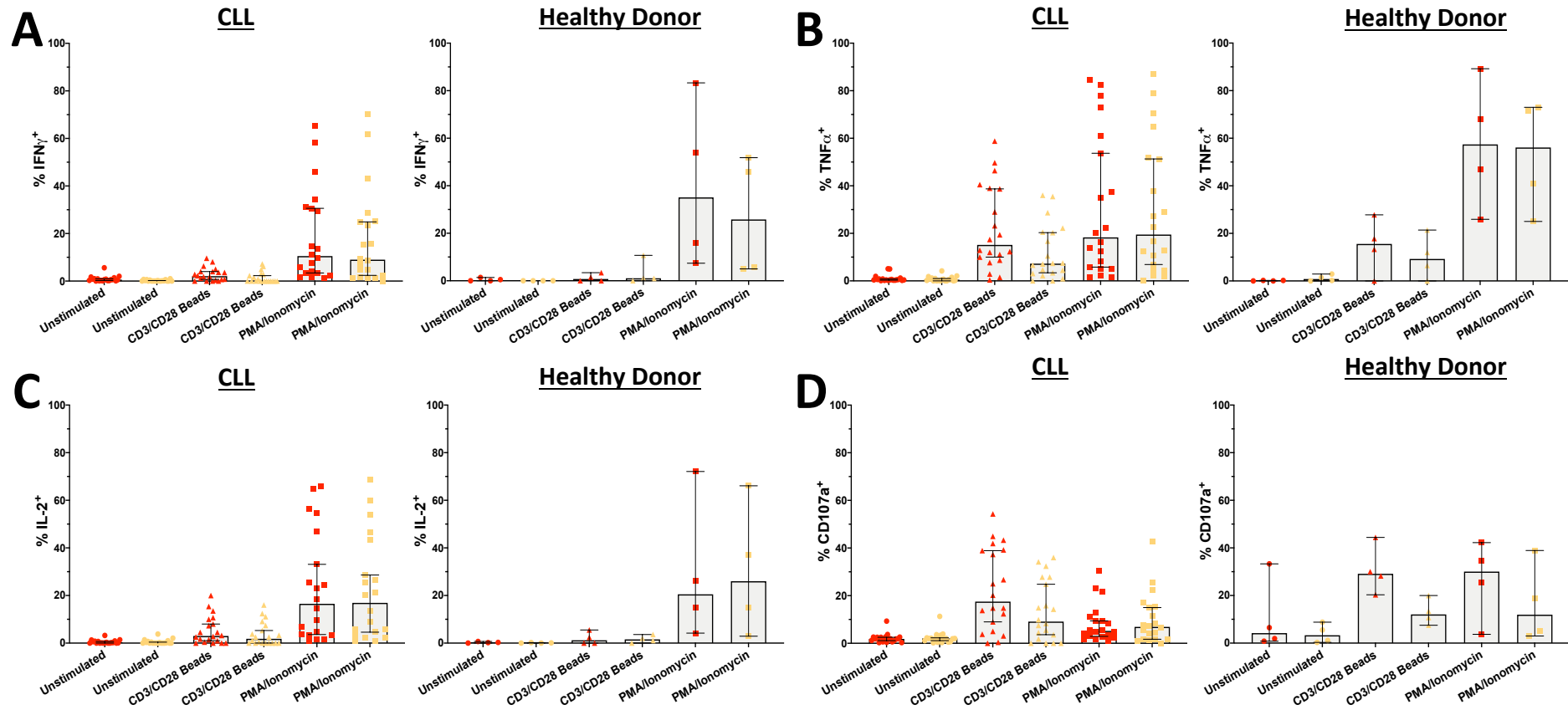


Figure 5.4: TOX Expression Does Not Affect Cytokine Production in CLL

Cytokine production and cellular degranulation were measured by flow cytometry in CD4⁺ T cells from 20 CLL patients and 4 healthy donors following either no stimulation or stimulation with CD3/CD28 beads or PMA/Ionomycin for 6 hours. **A)** Production of IFN γ was only upregulated by PMA/Ionomycin stimulation for both TOX⁺ and TOX⁻ cells in both CLL and healthy donors. **B)** TNF α production was upregulated by both CD3/CD28 and PMA/Ionomycin stimulations, for TOX⁺ and TOX⁻ cells, in both CLL and healthy donors. **C)** Production of IL-2 was only upregulated by PMA/Ionomycin stimulation for both TOX⁺ and TOX⁻ cells in both CLL and healthy donors. **D)** CD107a expression was upregulated via both CD3/CD28 and PMA/Ionomycin stimulations in CLL and healthy donors, for both TOX⁺ and TOX⁻ cells. Bars represent median \pm 95% confidence interval. Significance was assessed by Kruskal-Wallis test with Dunn's multiple comparisons.

Key
■ TOX⁺
■ TOX⁻

5.2 T Cell Proliferation

As well as cytokine production, a key component of T cell responses to infections or cancer is the ability to expand specific T cell numbers through proliferation. Due to the nature of T cell receptor selection and recombination, there are very few circulating T cells able to recognise any given peptide antigen, so expansion following recognition of an antigen is vital to generate a large population of specific T cells that are able to respond.

In this study, T cell proliferation was assessed using the same stimulation conditions as in *Section 5.1*, but over a longer time period (4 days) to allow for several rounds of proliferation to take place. T cells were stained with CFSE (Carboxyfluorescein succinimidyl ester), a commonly used tool for the measurement of proliferation. CFSE is a fluorescent, cell-permeable dye that irreversibly binds to intracellular proteins and whose presence can subsequently be detected by flow cytometry. During cell division, approximately half of the CFSE labelled proteins will be distributed to each daughter cell and as such the level of CFSE fluorescence will halve.

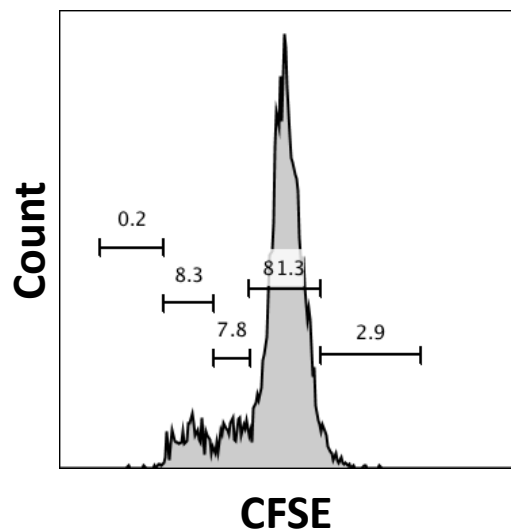


Figure 5.5: Representative CFSE Dilution Plot

CD4⁺ T cells were stained with CFSE and allowed to proliferate for 4 days. CFSE dilution was analysed by flow cytometry. Moving from right to left each peak represents one cell division, starting with 0 divisions. The proportion of cells in each gate is shown.

Depending on the labelling protocol used, around 7 or 8 cell divisions can theoretically be detected by the CFSE dilution method, after which the CFSE signal is indistinguishable from background. In this study, low cell numbers caused identification of individual peaks of 4 or more divisions to be difficult and so the classification “4+ Divisions” was used. A representative plot of CFSE staining in CD4⁺ T cells after CD3/CD28 stimulation is shown in *Figure 5.5*.

No statistical analysis was conducted comparing the different proliferation plots in *Section 5.2* – this was due to the nature of the plotted data, for which a valid statistical test could not be found. Considering this, along with the preliminary nature of the experiments which only assessed one timepoint, the results here should not lead to firm conclusions but should instead be used to inform future work.

5.2.1 Proliferation of Total CD4⁺ T Cells

The results of the proliferation analysis for the total CD4⁺ T cell populations from 14 CLL patients and 5 healthy donors are shown in *Figure 5.6*.

Under unstimulated conditions, T cells from CLL patients had a slightly higher proportion of undivided cells than healthy donor cells, but a much smaller percentage of cells that had undergone a single division (mean 60.8% vs. 83.5%). In contrast, the proportion of cells that had divided twice was much higher in CLL, forming almost a quarter of the total population. The combined percentage of cells in the 3 and 4+ divisions categories together was similar in the two groups.

Following CD3/CD28 stimulation, both CLL and healthy donors had a decreased proportion of undivided cells. For CLL T cells, there was minimal change in the percentage of cells that had undergone 1 division, but this category saw a large decrease in healthy donors. Similarly, there was little change in the proportion of twice divided cells in CLL, while there was a small increase in the healthy donor T cells. The percentage of cells in the 3 divisions after CD3/CD28 stimulation category saw a large increase in healthy donors (mean 1.1% vs. 22.2%), with a smaller increase also seen in CLL. The proportion of cells with 4+ divisions showed a small increase in CLL but was slightly reduced in healthy donors.

PMA/Ionomycin stimulation caused a large increase in the proportion of undivided cells compared to both unstimulated and CD3/CD28 stimulated cells, such that they comprised almost a quarter of the total. In contrast, there was a decreased proportion of undivided cells following PMA/Ionomycin stimulation in healthy donors, as well as increases in the percentages of the 2 and 3 divisions categories

compared to unstimulated conditions. In CLL the proportion of cells that had undergone 2 divisions was reduced, and the 3 and 4 divisions categories unchanged, compared to unstimulated cells. In both groups, overall proliferation appeared to be decreased after PMA/Ionomycin stimulation when compared to CD3/CD28 stimulated cells, however this may reflect the impact of Activation-Induced Cell Death (see *Section 5.3*).

These results demonstrate that CD4⁺ T cells in CLL are able to proliferate in response to physiological levels of stimulation and therefore do not appear to be exhausted. The significantly higher level of T cell proliferation in CLL compared to healthy donors in the absence of stimulation may reflect the activation of T cells in the leukaemia setting, and perhaps goes some way to explain the muted response to further stimulations.

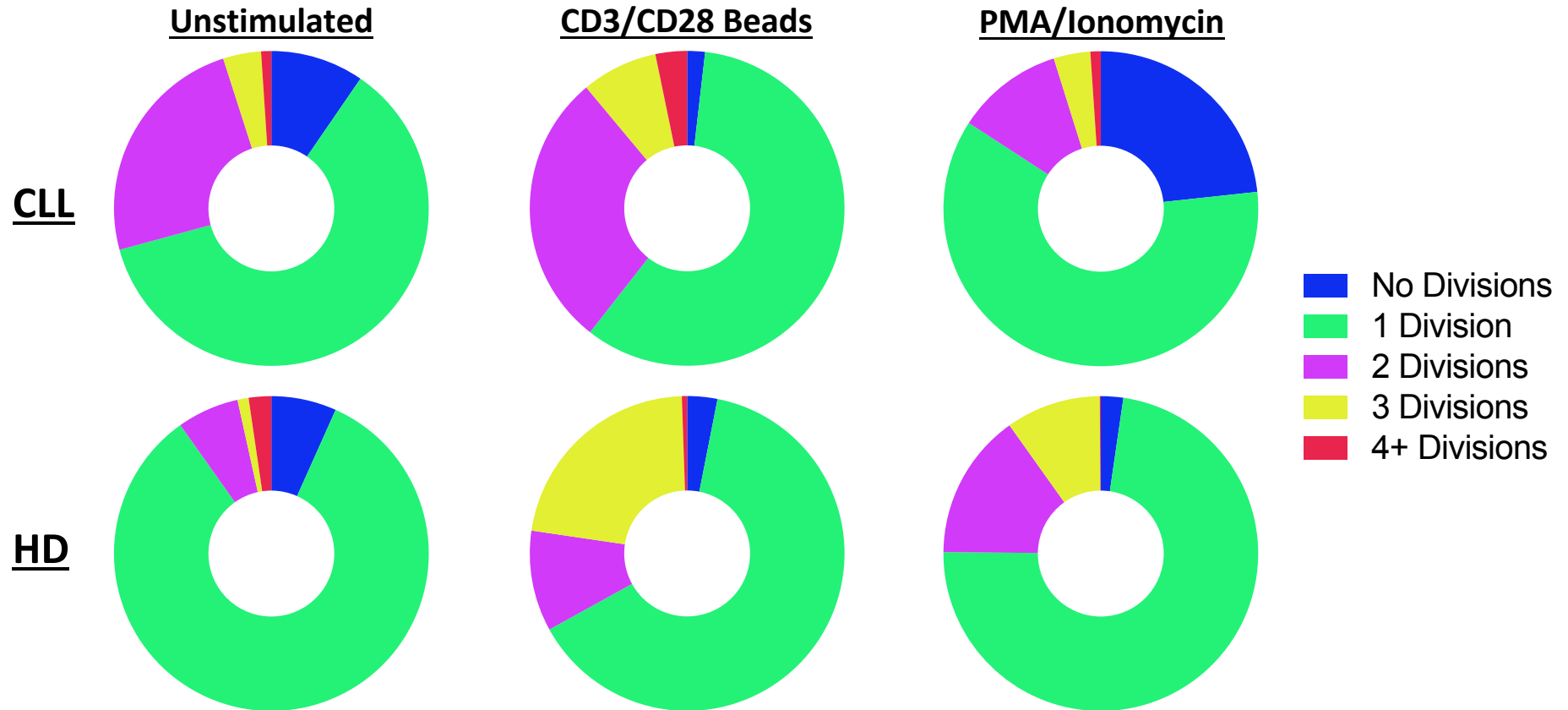


Figure 5.6: CD4⁺ T Cells from Healthy Donors Respond Better to Stimulation Than Those from CLL Patients

T cells from 14 CLL patients and 5 healthy donors were labelled with CFSE then treated with either vehicle control or stimulation with CD3/CD28 beads or PMA/Ionomycin for 4 days. Subsequently, T cell proliferation was assessed by CFSE dilution using flow cytometry.

T cells from CLL patients were more proliferative than those from healthy donors under unstimulated conditions, but were less able to respond to stimulation. *Plots represent mean percentages.*

5.2.2 Proliferation of CD4⁺ T Cell Subsets

Previous work in this study demonstrated that CD4⁺HLA-DR⁺PD-1⁺ T cells had significantly greater expression of the proliferation marker Ki-67 than the total CD4⁺ population (*Figure 3.6B*). To therefore verify this, proliferation was analysed by CFSE dilution in the three T cell subsets used in *Section 5.1*. The results of the proliferation analysis for these CD4⁺HLA-DR⁺PD-1⁺, CD4⁺HLA-DR⁻PD-1⁺ and CD4⁺HLA-DR⁻PD-1⁻ T cells, taken from 14 CLL patients and 5 healthy donors, are shown in *Figure 5.7*.

Under unstimulated conditions, the CD4⁺HLA-DR⁻PD-1⁻ subset had the highest proportion of undivided cells, but the lowest proportion of cells with 1 division. The CD4⁺HLA-DR⁻PD-1⁺ population was the least proliferative, with almost three quarters of these cells undergoing 0 or 1 divisions. The CD4⁺HLA-DR⁻PD-1⁻ subset also had the highest percentage of cells that had divided twice (32.5%), with CD4⁺HLA-DR⁻PD-1⁺ and CD4⁺HLA-DR⁺PD-1⁺ cells showing a very similar proportion of cells (~19%) in this category. The CD4⁺HLA-DR⁺PD-1⁺ subset had the largest percentage of highly proliferative cells, with almost a quarter in the combined 3 and 4+ divisions categories.

CD3/CD28 stimulation had a small impact on the proliferation of CD4⁺HLA-DR⁻PD-1⁻ T cells, with small decreases in the proportions of undivided cells and cells that had divided twice, and a concomitant increase in the 1 division category. In the CD4⁺HLA-DR⁻PD-1⁺ population, CD3/CD28 stimulation caused an almost total reduction in undivided cells, with the proportions of the 2,3 and 4+ divisions categories all increasing, in particular 3 divisions which more than doubled compared to unstimulated cells (13.2% vs. 5.3%). The largest impact of CD3/CD28

stimulation was observed in the CD4⁺HLA-DR⁺PD-1⁺ subset, which also had an almost total loss of undivided cells, along with increases in the proportions of cells in the 2 and 3 divisions categories and a large increase in the 4+ divisions category. Together, cells in the highly proliferative 3 and 4+ divisions categories formed more than one third of the total population.

PMA/Ionomycin stimulation of the CD4⁺HLA-DR⁻PD-1⁻ subset had minimal effect on the proportion of undivided cells, but led to a large increase in cells with 1 division such that these cells comprised nearly two thirds of the total. However, compared to both unstimulated and CD3/CD28 stimulated conditions, there were large reductions in the percentages of cells in the 2, 3 and 4+ divisions categories. For the CD4⁺HLA-DR⁻PD-1⁺ population, PMA/Ionomycin stimulated cells had the highest proportion of undivided cells, with a concomitant decrease in the 1 division category. The percentages in the 2,3 and 4+ divisions categories remained very similar to those following CD3/CD28 stimulation. In the CD4⁺HLA-DR⁺PD-1⁺ subset, PMA/Ionomycin stimulation led to a large increase in the 2 divisions category, but a decrease in the 4+ divisions category, compared to unstimulated conditions. The 2, 3 and 4+ divisions categories were all decreased compared to CD3/CD28 stimulation, suggesting that PMA/Ionomycin induced a weaker proliferative response in this subset.

The results in *Figure 5.7* demonstrate that CD4⁺HLA-DR⁺PD-1⁺ T cells in CLL are more proliferative than the other subsets in their natural state, but are also able to respond better to physiological levels of stimulation. By comparison, the CD4⁺HLA-DR⁻PD-1⁻ subset, a proxy for the general CD4⁺ T cell population, consistently

had the greatest proportion of undivided cells across all conditions. In all three subsets, the proliferative response to PMA/Ionomycin appeared to be worse than for CD3/CD28 stimulation, while in CD4⁺HLA-DR⁻PD-1⁻ cells PMA/Ionomycin appeared to have a negative impact of proliferation, however this may reflect the impact of Activation-Induced Cell Death (see *Section 5.3*)

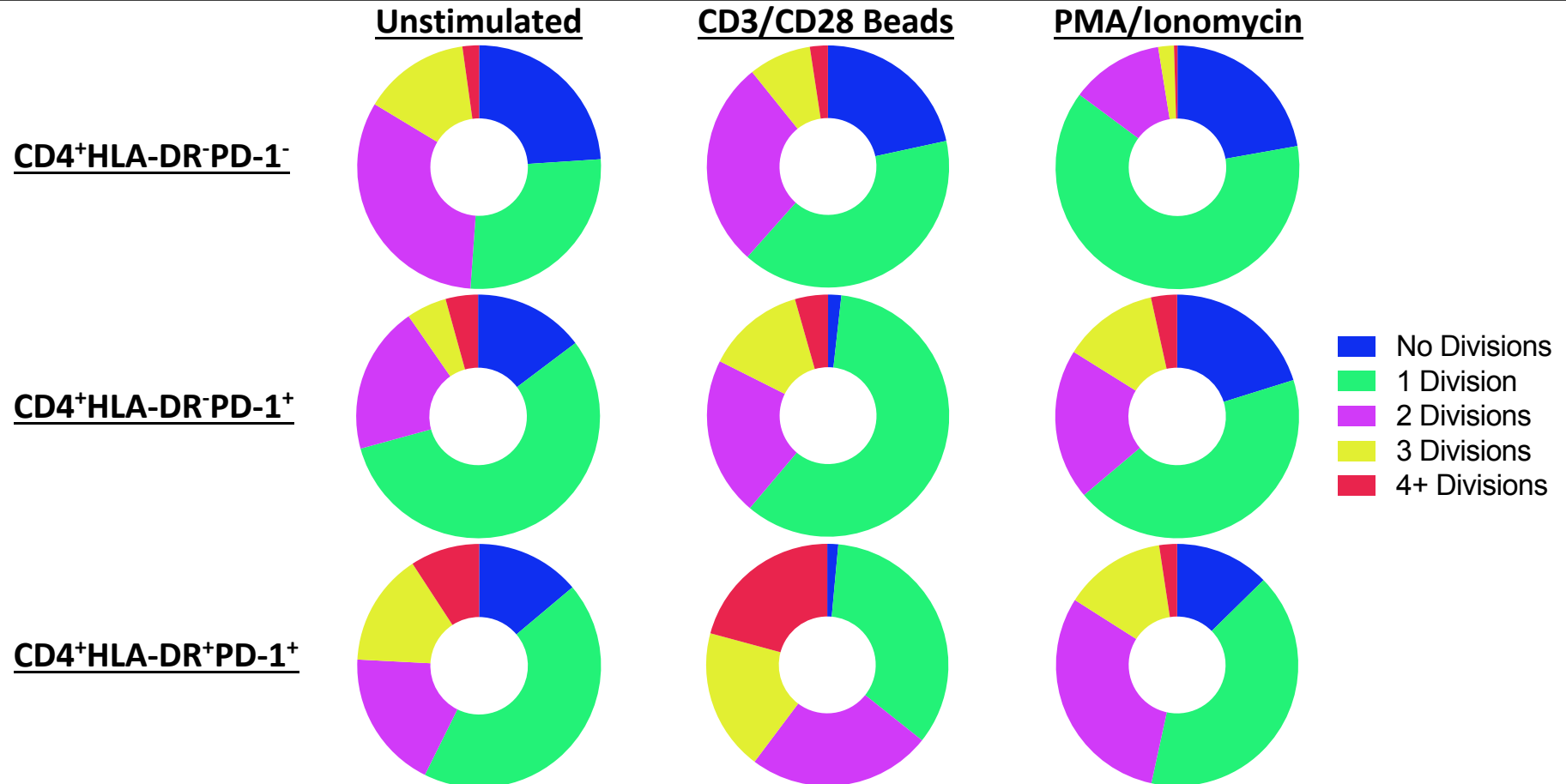


Figure 5.7: CD4⁺HLA-DR⁺PD-1⁺ T Cells Are the Most Proliferative and Respond Best to Physiological Stimulation

T cells from 14 CLL patients were labelled with CFSE then treated with either vehicle control or stimulation with CD3/CD28 beads or PMA/Ionomycin for 4 days. Subsequently, T cell proliferation was assessed by CFSE dilution using flow cytometry.

CD4⁺HLA-DR⁺PD-1⁺ T cells were the most proliferative subset under unstimulated conditions and also had the best responses to physiological levels of stimulation. *Plots represent mean percentages.*

5.2.3 Effect of TOX Expression on Proliferation of CD4⁺ T Cells

The transcription factor TOX has been posited as a regulator of T cell exhaustion, a hallmark of which is reduced proliferation. Therefore, the impact of TOX expression on proliferation was analysed in CD4⁺ T cells from 14 CLL patients and 5 healthy donors, the results of which are displayed in *Figure 5.8* and *Figure 5.9* respectively.

In CLL, under unstimulated conditions TOX⁺ T cells had a slightly greater proportion of undivided cells and cells with 1 division compared to TOX⁻ T cells, whereas there was a higher percentage of cells that had undergone 2, 3 and 4+ divisions in the TOX⁻ population. Overall, both groups had broadly similar proliferation profiles.

For unstimulated T cells from healthy donors, both TOX⁺ and TOX⁻ cells had similar profiles, with a large majority of cells in the 1 division category, although there was a slightly higher proportion of cells in the 2,3 and 4+ divisions categories in the TOX⁻ group as in CLL. However, overall healthy donor T cells were considerably less proliferative than their CLL counterparts in the absence of stimulation.

Following CD3/CD28 stimulation of CLL T cells, there was an increase in proliferating cells in both the TOX⁺ and TOX⁻ groups, with almost total loss of undivided cells and concomitant increase in the 2,3 and 4+ divisions categories. Although TOX⁻ cells had more than double the percentage of cells in the 4+ divisions category (2% vs. 5.1%), both groups ended with overall similar profiles post-

stimulation, suggesting that the TOX⁺ cells had responded better to the CD3/CD28 stimulation.

In healthy donors, there were also decreases in the proportions of undivided cells following CD3/CD28 stimulation in both TOX⁺ and TOX⁻ cells. However, although TOX⁻ cells had no change in the percentage of cells with 1 division like in CLL, healthy donor TOX⁺ cells were observed to have a large decrease in this category. While there was a modest increase in the proportion of twice divided cells, the 3 divisions category saw a large increase to comprise around a quarter of the TOX⁺ population. TOX⁻ cells showed small increases in the percentages of cells with 2 and 3 divisions alongside a small reduction in the 4+ divisions category that was mirrored by the TOX⁺ group.

In healthy donor T cells, there was minimal change to the proliferation profile of TOX⁻ T cells following CD3/CD28 stimulation. In contrast, the TOX⁺ population saw a large increase in proliferation after stimulation, with the proportion of undivided cells decreasing by more than half (mean 3.1% vs. 8.4%). This was accompanied by a large increase in the percentage of cells that had undergone 3 divisions, which comprised a quarter of the TOX⁺ population post-stimulation.

For both TOX⁺ and TOX⁻ cells in CLL, PMA/Ionomycin stimulation appeared to cause large increases in the proportion of undivided cells, alongside reductions in the percentages of the combined 2,3 and 4+ divisions categories, with this impact more marked in TOX⁻ cells. Overall, both groups ended with similar proliferation profiles following PMA/Ionomycin stimulation.

In healthy donors, PMA/Ionomycin stimulation had different effects on the TOX⁺ and TOX⁻ T cell populations. For TOX⁺ cells, there was increased proliferation post-stimulation compared to unstimulated conditions, with a reduction in undivided cells and increased proportions of cells that had undergone 2 and 3 divisions – however, this increased proliferation was not as great as that seen following CD3/CD28 stimulation of TOX⁺ cells. In contrast, PMA/Ionomycin stimulation of TOX⁻ T cells had a mixed impact. Compared to unstimulated TOX⁻ cells, there was a large increase in the percentage of cells that had undergone 3 divisions (1.5% vs. 17.4%), but there was also a marked increase in the proportion of undivided cells (4.7% vs. 15.6%).

These results provide evidence that TOX-expressing CD4⁺ T cells are not exhausted in either CLL patients or healthy donors. In both groups, TOX⁺ cells proliferated to a similar extent compared to their TOX⁻ counterparts in the absence of stimulation. The effect of TOX expression on proliferative responses to stimulation was markedly greater in healthy donors, wherein TOX⁺ cells were able to respond better to both CD3/CD28 and PMA/Ionomycin stimulations, whereas in CLL there was a much smaller difference between TOX⁺ and TOX⁻ cells. This supports the concept that CLL changes the behaviour of T cells but it is likely that a number of genes will play a role in determining the functions of CLL T cells.

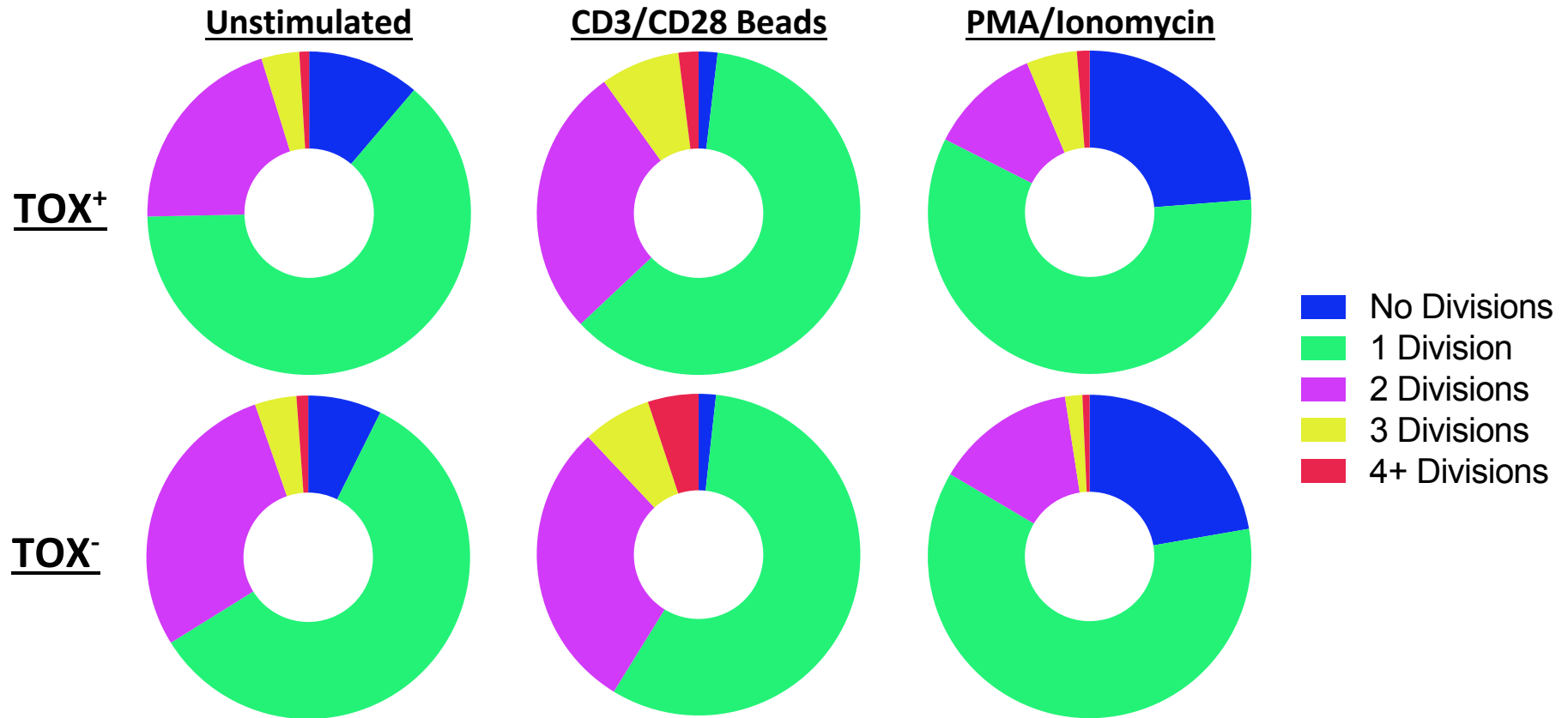


Figure 5.8: TOX⁺ T Cells Have a Better Proliferation Response to Physiological Stimulation Than TOX⁻ T Cells in CLL

T cells from 14 CLL patients were labelled with CFSE then treated with either vehicle control or stimulation with CD3/CD28 beads or PMA/Ionomycin for 4 days. Subsequently, T cell proliferation was assessed by CFSE dilution using flow cytometry.

Without stimulation, TOX⁻ cells were more proliferative than TOX⁺ cells. Following CD3/CD28 stimulation TOX⁺ cells showed an increase in proliferation, but there was a much smaller effect on TOX⁻ cells. PMA/Ionomycin stimulation caused decreased proliferation in both TOX⁺ and TOX⁻ cells, with a greater impact on the TOX⁻ population. *Plots represent mean percentages.*

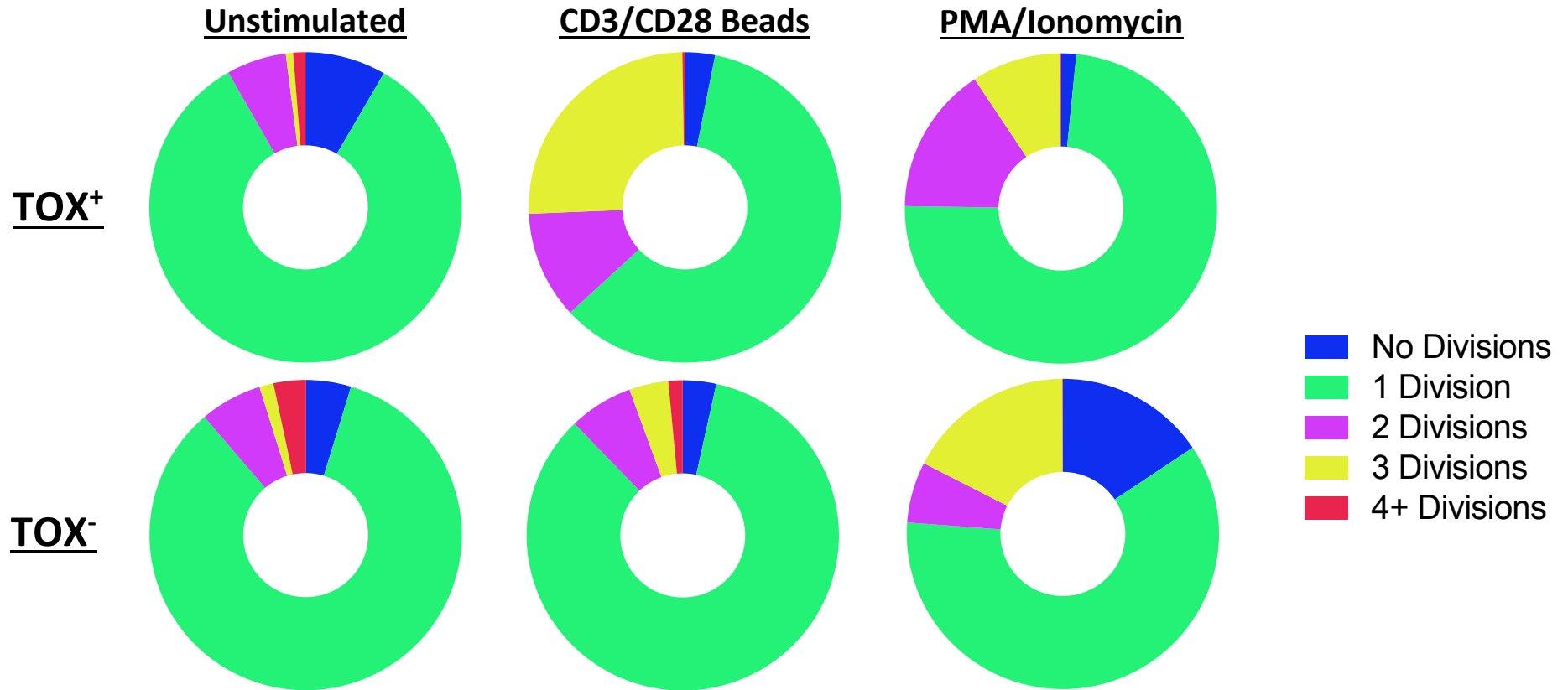


Figure 5.9: TOX⁺ T Cells Respond Better to Physiological Stimulation Than TOX⁻ T Cells in Healthy Donors

T cells from 5 healthy donors were labelled with CFSE then treated with either vehicle control or stimulation with CD3/CD28 beads or PMA/Ionomycin for 4 days. Subsequently, T cell proliferation was assessed by CFSE dilution using flow cytometry.

Without stimulation, TOX⁻ cells were slightly more proliferative than TOX⁺ cells. Following CD3/CD28 stimulation TOX⁺ cells showed a large increase in proliferation, but there was minimal effect on TOX⁻ cells. PMA/Ionomycin stimulation caused increased proliferation in TOX⁺ cells but to a lesser extent than CD3/CD28 stimulation, while TOX⁻ cells showed an overall decrease in proliferation. *Plots represent mean percentages.*

5.3 Discussion

This chapter has sought to investigate T cell exhaustion and elucidate the potential role of the transcription factor TOX in controlling this process. The topic of T cell exhaustion, and more recently the function of TOX within it, has generated great interest, particularly with regard to its role in cancer and the potential for therapeutic intervention (369,382). CLL, as a chronic cancer with various T cell dysfunctions, represents an intriguing model for studying T cell exhaustion in a human setting, and the results in *Chapter 4* in this study appeared to confirm that exhaustion signalling was prominent in CLL T cells. Allied to the gene expression data showing TOX as the most significantly differentially expressed gene in CD4⁺HLA-DR⁺PD-1⁺ compared to CD4⁺HLA-DR⁺PD-1⁻ T cells, this study provided an opportunity to simultaneously explore both exhaustion and the effect of TOX expression in human T cells.

As with the previous work in this study, the experiments in this chapter relied upon the use of fresh blood samples from CLL patients and healthy control individuals. Although a sufficient number of CLL patient samples were able to be obtained once haematology clinics resumed operating, the restrictions caused by the COVID-19 pandemic rendered acquisition of healthy donor samples very difficult. As a result, the number of samples analysed was low and those used were not age-matched in the manner previously possible in *Chapters 2 and 3*. This reduced the statistical power of experiments, and given the considerable variation seen in the healthy donor results it is likely that a large number of age-matched samples would be needed to validate the findings.

Across both CLL patients and healthy donors, a consistent theme was differential T cell responses to CD3/CD28 stimulation depending on the cytokine analysed. Both IFN γ and IL-2 were expressed by only a very small proportion of cells, if any, after stimulation with CD3/CD28, whereas there were significant increases in the percentage of cells expressing TNF α compared to unstimulated cells. The reason for this is likely to be the kinetics of the production of these cytokines under physiological conditions. Both IFN γ and IL-2 have been observed to have maximal expression 18-24 hours after stimulation (383,384), but in contrast TNF α is produced more rapidly, peaking at 4 hours post-stimulation (385). Since the experiments here were conducted with a 6-hour stimulation period before analysis, only TNF α would be expected to have high expression and this is borne out in the results. A longer experimental period, for example overnight, would be required to fully assess the change in expression of IFN γ and IL-2 following CD3/CD28 stimulation.

Differential responses to CD3/CD28 stimulation were also observed between the three CD4⁺ T cell subsets in CLL. In the case of TNF α expression, although there were only minimal responses to CD3/CD28 stimulation for the CD4⁺HLA-DR⁻PD-1⁻ and CD4⁺HLA-DR⁻PD-1⁺ subsets, there was a large response in CD4⁺HLA-DR⁺PD-1⁺ T cells. A very similar pattern was observed for CD107a expression, while CD4⁺HLA-DR⁺PD-1⁺ T cells also had the strongest proliferation response to CD3/CD28 stimulation. As observed in *Figure 3.9*, all three CD4⁺ T cell subsets had very high proportions of CD28-expressing cells, so it is likely that the high level of baseline activation in the CD4⁺HLA-DR⁺PD-1⁺ subset primes these cells to respond more effectively to physiological levels of stimulation.

Another consistent finding in these experiments was a lack of evidence for T cell exhaustion in CLL. CD4⁺ T cells from CLL patients were able to produce cytokines and degranulate to a similar extent as their healthy donor-derived counterparts, while CLL T cells were in fact more proliferative than those from healthy donors. This stands in stark contrast to the pathway analysis results in *Chapter 4*, wherein T cell exhaustion signalling was the pathway most significantly associated with CLL CD4⁺ T cells. The exhaustion of CD8⁺ T cells has been shown to be hierarchical, with a progressive loss of functions over time, beginning with a failure of IL-2 production and cell killing (386). This hierarchical model could explain the discrepancy between the gene expression data and the functional data in this study, if the CD4⁺ T cells in CLL were at an early stage of exhaustion and so had yet to lose most of their functions. Although IL-2 production was lost early in the exhaustion pathway in CD8⁺ T cells, since CD4⁺ T cells are the main source of IL-2 they may be more resistant to this element of the exhaustion pathway (107). Experimental work analysing CD4⁺ T cells stimulated over longer periods of time, simulating a chronic disease setting, would be needed to explore this possibility further.

In both CLL patients and healthy donors, PMA/Ionomycin stimulation led to the highest median proportion of cytokine-expressing cells, with the exception of CD107a in CLL. Despite this, among the CLL patients around one third had few, if any, cells expressing the cytokines post-stimulation with PMA/Ionomycin. Furthermore, it was observed that PMA/Ionomycin stimulation led to decreased proliferation in T cells from CLL patients, which was not the case for healthy donor T cells.

A possible explanation for these observations is activation-induced cell death (AICD). During normal immune responses, AICD functions to delete autoreactive T cells and prevent damage to the host from highly activated T cells (371), often through the mechanism of Fas/FasL interaction (387). T cells in CLL are known to be highly activated (268), and previous work has suggested that inhibition of AICD, through reduced expression of Fas, is a potential mechanism of improved T cell numbers following ibrutinib treatment of CLL patients (332). From the gene expression data in this study, as observed in *Figure 4.6*, AICD signalling was highly enriched in CD4⁺HLA-DR⁺PD-1⁺ T cells in CLL, while processes related to cell viability and survival were associated with healthy donor T cells compared to CLL T cells (*Figure 4.7*). These results suggest that, following *ex vivo* stimulation with either CD3/CD28 or, in particular, PMA/Ionomycin, there would be increased AICD in T cells from CLL patients, especially those with progressive disease. AICD of the most highly activated, and therefore most proliferative, T cells from CLL patients provides a potential explanation for the reduced proliferation observed post-stimulation with PMA/Ionomycin.

To address this question, future experiments could make use of earlier and more frequent timepoints in order to capture proliferative events before AICD, with experiments here only assessing proliferation after four days. Further information on AICD in this experimental system could be obtained through measurement of the levels of apoptosis, using a method such as Annexin V staining (388).

The role of the transcription factor TOX in T cell exhaustion has only recently begun to be explored and has focused almost exclusively on CD8⁺ T cells. Initial studies revealed TOX as the master regulator of the exhaustion phenotype in CD8⁺ T cells, although this work was conducted using murine models (379,380,389). However, whether a similar role would be carried out by TOX in human T cells was unclear, given the well-known discrepancies between the human and murine immune systems (390). Subsequent work studying the effect of TOX in human CD8⁺ T cells has shown a similar outcome to that in mice, with TOX expression observed to be correlated with exhaustion and the expression of inhibitory receptors (391). However, the picture in human T cells appears to be more complex – *Scott et al.* (392) reported that TOX deletion, although it reduced inhibitory receptor expression, did not rescue T cell dysfunction. Other work has suggested that TOX can be expressed by both exhausted and functional human CD8⁺ T cells (346,393), and that TOX expression in the context of chronic viral infections has differential impacts depending on the virus in question (381). The contrasting results of studies in this area mean there is still significant scope for research into the role and mechanisms of action of TOX in T cells, not least in hitherto unstudied CD4⁺ T cells.

In this study, there was no suggestion that TOX-expressing CD4⁺ T cells were more exhausted than their TOX⁻ counterparts, with similar, and in some cases better, responses to stimulation both in terms of cytokine production and proliferation. This was a somewhat unexpected result, given the strong association between T cell exhaustion signalling and CLL T cells observed in the gene expression analysis in *Chapter 4*. The proportion of PD-1-expressing cells in the TOX⁺ CD4⁺ T cell population

was slightly higher than in the TOX⁻ population, which supports the TOX-dependent expression of inhibitory receptors posited by *Scott et al.* (392), but their observation of continued T cell dysfunction was not replicated here. Taken together, the results in this study suggest that TOX is not a regulator of exhaustion in CD4⁺ T cells in humans and that the characteristic exhaustion signalling in CLL T cells must be controlled by an alternative regulator gene or genes.

In summary, this chapter has sought to address the questions, raised by the results of the gene expression data in *Chapter 4*, around exhaustion and the role of TOX in human CD4⁺ T cells. It was found that CD4⁺ T cells from CLL patients did not appear to be exhausted and were capable of cytokine production and proliferation to an extent at least equal to those T cells from healthy donors. Furthermore, the results suggested that TOX is not the master regulator of exhaustion in CD4⁺ T cells and that expression of TOX in fact caused no functional impairment.

6 General Discussion

The purpose of this thesis has been to explore the nature, functions and biological role of CD4⁺HLA-DR⁺PD-1⁺ T cells in CLL, with a view to establishing whether this subset could be used as a prognostic indicator for CLL patients. Having been first reported by our laboratory (256), this study used a larger cohort of patients to successfully confirm that a higher proportion of CD4⁺HLA-DR⁺PD-1⁺ T cells is associated with poorer prognosis in CLL. Furthermore, having also been previously reported by our laboratory (19), this study used the same larger patient cohort to confirm that an inverted CD4⁺:CD8⁺ T cell ratio is a prognostic marker in CLL.

There is a clear need for new and better prognostic markers in CLL due to the chronic nature of the disease and the fact that around two thirds of patients are asymptomatic with indolent disease at diagnosis. From a patient perspective, the reassurance and peace of mind provided by tests suggesting a good prognosis are extremely valuable, particularly with regards to anxiety and other mental health problems. On the other hand, the presence of markers of poor prognosis allows clinicians to prioritise those patients who need closer monitoring or more immediate treatment.

Unlike in acute myeloid leukaemia (394) or acute lymphoblastic leukaemia (395), the number of prognostic and predictive markers in CLL is low. The results of this study show that assessment of T cell parameters compares favourably with currently utilised clinical prognostic markers. An analysis of CLL prognostic factors by

Li *et al.* (396) found Rai stage III/IV to be the strongest predictor of time to first treatment (hazard ratio 4.2), followed by deletion of 17p (hazard ratio 2.5) then unmutated IGHV (hazard ratio 2.4). By comparison, this study found hazard ratios of 2.64 for inverted CD4⁺:CD8⁺ T cell ratio and 2.36 for a CD4⁺HLA-DR⁺PD-1⁺ T cell percentage above the median. Considering that CLL is a disease of B cells, it is perhaps surprising how favourably T cell parameters compare with other the prognostic factors. Although larger-scale analysis would be required for confirmation, it appears that CD4⁺:CD8⁺ T cell ratio represents an excellent candidate for inclusion in routine monitoring of CLL patients, particularly given the ease with which it can be measured by flow cytometry.

The exact part played by T cells in CLL has been, and continues to be, difficult to elucidate – are dysfunctional T cells drivers of the CLL disease course or does the development of CLL lead to the induction of T cell dysfunction? What is clear is that the presence of T cells is vital to CLL cell survival and proliferation (397,398).

Within this context, key to understanding the role of CD4⁺HLA-DR⁺PD-1⁺ T cells in CLL is the interaction between these T cells and the CLL cells themselves. It is currently unknown whether CLL cells can induce the CD4⁺HLA-DR⁺PD-1⁺ T cell phenotype, or whether CD4⁺HLA-DR⁺PD-1⁺ T cells are driving the survival and expansion of CLL cells – the mechanisms underpinning such interactions also remain to be elucidated. These questions could potentially be explored via the use of *in vitro* co-culture systems, monitoring the phenotype and functions of T cells from both CLL patients and healthy donors in the presence of CLL cells. Similar experiments could

also be conducted using transwells to assess the requirements for cell-cell contact vs. soluble signalling factors in these interactions. Understanding the nature of the interactions between CLL cells and CD4⁺HLA-DR⁺PD-1⁺ T cells could provide important insight into CLL disease course and potential new therapeutic targets.

The presence in CLL of major stereotypes, groups of unrelated patients with identical or near-identical B cell receptors, has been known about for a number of years (399). However, evidence has begun to accumulate that a similar phenomenon may exist within the T cell repertoire of CLL patients – the observed TCR sequences from T cell clones do not appear to match those from other diseases or from healthy individuals, suggesting antigens that are conserved across CLL (400). Identification of such antigens would represent a major advance in the understanding of T cells in CLL and would provide evidence for a model in which CLL develops first and then T cell dysfunction is induced during the immune response against the CLL cells.

Interestingly, whereas traditional chemoimmunotherapy leads to reconstitution of the T cell repertoire of CLL patients, treatment with BCR signalling inhibitors such as ibrutinib maintained these conserved T cell clones, which suggests that an anti-leukaemic immune response could be retained throughout treatment (401). It would be of interest to this study to investigate whether CD4⁺HLA-DR⁺PD-1⁺ T cells represent one of the identified conserved clones, particularly in light of the results in *Figure 3.11* which showed no pattern of change in the frequency of CD4⁺HLA-DR⁺PD-1⁺ T cells after ibrutinib therapy. Since in a large cohort of CLL patients those with higher frequencies of CD4⁺HLA-DR⁺PD-1⁺ T cells displayed worse prognosis, this could suggest that this subset is likely to recognise conserved antigens

and play the same CLL-supportive role in all patients. Furthermore, it would be of interest to investigate whether CD4⁺HLA-DR⁺PD-1⁺ T cells in healthy individuals also recognise the same antigens, as this would suggest that this subset recognised a common somatic antigen rather than a tumour neoantigen. Evidence from the gene expression study here suggested that CD4⁺HLA-DR⁺PD-1⁺ T cells may be enriched for T_{Reg} cells in healthy individuals, so it is possible that they are responsible for immune tolerance towards a common protein.

Vaccination has long been a gold standard in the prevention of infections and millions of vaccine doses are given in the UK each year. However, CLL patients are well known to have very poor vaccine responses (6). A portion of blame for these poor responses may lie in the fact that CLL patients are often elderly, with immune responses to new antigens greatly decreasing with advancing age (402). It is likely though that the immunodeficiency caused by CLL is also a major factor.

The use and efficacy of vaccines has become prominent in the public consciousness thanks to the Covid-19 pandemic. With the procurement of sufficient doses of several effective vaccines representing the only part of the pandemic response successfully handled by the UK Government, interest has turned to the best protocols to use to maximise the benefits of vaccination for the most vulnerable, including cancer patients. It has been reported that solid cancer patients have a response rate of only 38% following one vaccine dose, compared to 94% for healthy controls, however this improves significantly to 95% following a second dose after 21 days (compared to 100% in healthy controls) (403). The picture is less positive for

patients with haematological cancers, with response rates of just 18% and 60% after one or two doses respectively. This represents a potentially serious issue for CLL patients, who are likely to have even worse vaccination response rates (6).

The causes of these poor responses to Covid-19 vaccination in haematological patients are not clear, but clues may be gleaned from the immune responses of cancer patients to infection with Covid-19 itself. Abdul-Jawad *et al.* studied the immune responses of cancer and non-cancer patients with Covid-19 and following their recovery (404). It is reported that both solid cancer and non-cancer patients had similar immune responses to Covid-19 infection and returned to similar immune signatures post-recovery. In contrast, haematological cancer patients displayed less effective immune responses and retained disrupted T cell phenotypes after recovering. Of particular note, haematological cancer patients were observed to have high frequencies of exhausted T cells, especially CD8⁺ T cells, which concurs with previous reports of T cell exhaustion in Covid-19 patients (405).

CLL patients are at particularly high risk of severe Covid-19 infections, even among cancer patients (406). As observed in several reports, patients with haematological malignancies have poorer immune responses to Covid-19, likely in part due to T cell exhaustion (405). The gene expression data in this study revealed a strong association between T cell exhaustion signalling and T cells from CLL patients, meaning the anti-Covid-19 T cell response may be disrupted in CLL patients, although the functional data in *Chapter 5* suggest the picture could be more complicated. Any dysfunction in the anti-Covid-19 T cell response, when taken together with the hypogammaglobulinaemia that is characteristic of CLL (6), would mean that both

arms of the adaptive immune response were diminished in CLL, rendering CLL patients extremely vulnerable to severe infection.

For a number of years the standard therapy for CLL has been chemoimmunotherapy, usually consisting of the combination fludarabine/cyclophosphamide/rituximab (FCR), while chemotherapy alone was used prior to the addition of the anti-CD20 monoclonal antibody rituximab (407). However, despite the overall impressive results for FCR, this treatment is much less effective in high risk patients such as those with unmutated IGHV genes (35). In response to this problem, recent years have seen the advent of new, targeted therapies which aim to achieve specific targeting of CLL cells to give high risk patients new treatment options while also reducing side effects compared to chemoimmunotherapy.

Due to the highly abnormal nature of T cells in CLL, it is of interest to assess the impact of new therapies on the T cell compartment as well as CLL cells themselves. Unlike traditional chemotherapy, which causes a significant decrease in the numbers of both CD4⁺ and CD8⁺ T cells in CLL (408), these new therapies may in fact have a beneficial effect on the composition of the T cell compartment, although the evidence is often conflicting.

One such targeted therapy for CLL is ibrutinib, an inhibitor of the B cell receptor signalling pathway member Bruton's Tyrosine Kinase (BTK). As well as inhibiting BTK, ibrutinib also inhibits IL-2-inducible kinase (ITK), which is found in T cells, and as such can have a large impact on the T cell pool. Several studies have

published discordant results on the effect of ibrutinib on T cell numbers, with both increases (332) and decreases (331) observed. However, both of those studies found reduced expression of PD-1 on T cells following ibrutinib treatment. In this study though, no clear pattern of change was seen in the proportion of CD4⁺HLA-DR⁺PD-1⁺ T cells after ibrutinib, however the time period was relatively short and longer-term follow up may have revealed a more distinct effect. Furthermore, this study also showed no overall change in CD4⁺:CD8⁺ T cell ratio following ibrutinib treatment, supporting the recently published findings of Abrisqueta *et al.* (409). This suggests that the inverted CD4⁺:CD8⁺ T cell ratio, having been established early in disease (19), remains stable even after treatment has reduced the disease burden.

Recent work has shown ibrutinib treatment leads to a reduction in the proportion of T_H2 cells, with a concomitant increase in the proportion of T_H1 cells, and that this change in the T_H2/T_H1 ratio is associated with achievement of complete remission (410). In this study, the T_H2 pathway was associated with CD4⁺HLA-DR⁺PD-1⁺ T cells in CLL patients, while the T_H1 pathway was more associated with CD4⁺HLA-DR⁻PD-1⁻ T cells. Whether the ratios of these subsets change following ibrutinib treatment, and any subsequent impact on patient outcomes, would be valuable to explore in future studies.

The advent of low toxicity targeted therapies for CLL, such as ibrutinib and venetoclax, brings with it the possibility of increased lifespans for even high risk CLL patients, potentially running into decades. Results from the ongoing CAPTIVATE study indicate that in combination, ibrutinib and venetoclax can produce progression-free

survival of 95% after 2 years (411), representing an improvement on classical FCR treatment (35). As combinations are optimised and new agents brought to market, there is strong likelihood that these figures will improve even further. However, the impact that these therapies and combinations have on the immune system, in particular T cells, will require considerable exploration. CLL patients are already susceptible to infections (412) and this will be worsened if treatment causes impairment of T cell responses, such as by depleting T cell numbers as has been reported for ibrutinib (331).

The studying and monitoring of T cell populations is likely to remain of key importance, both to provide important information to oncologists treating CLL and to ensure that the benefits of new treatment regimens are fully realised. However, a significant challenge remains in defining the exact parameters that are the most clinically relevant and practical for routine monitoring.

As well as their utility in treatment monitoring, T cells can also be cancer treatments themselves. This can either be achieved directly, through the infusion of expanded tumour specific T cells in adoptive cell therapy (413), or indirectly through the use of checkpoint inhibitors that release the host T cells to destroy the tumour (264) or so called cancer vaccines (414). This third method, however, is particularly unlikely to be successful in CLL due to patients' characteristic poor vaccine responses. This is a multifactorial problem, but is caused at least in part by the skewing away from naïve towards highly differentiated T cells and the presence of significant T cell exhaustion (6,415).

In recent years a fourth option T cell therapeutic strategy has emerged, namely Chimeric Antigen Receptor (CAR) T-cells. These CAR T-cells are host T cells engineered to express a combination of an antibody-derived variable chain fragment with the CD3 ζ chain, along with co-stimulatory domains from proteins such as 4-1BB (416). Together, these complexes allow the CAR T-cell to recognise and respond to target antigens in an MHC-independent manner.

The majority of CAR T-cell usage in patients to date has been in those with haematological cancers. Anti-CD19 CAR T-cells have been used successfully in Acute Lymphoblastic Leukaemia (417), Diffuse Large B Cell Lymphoma (418) and Multiple Myeloma (419), while CAR T-cells directed against other targets have also been trialled (420). Results in CLL have however been mixed, with excellent responses sometimes observed but often only in a small proportion of patients (421,422).

The reasons for the comparatively poor responses of CLL patients to CAR T-cell therapy have not been fully elucidated, but it is likely that the abnormal and dysfunctional nature of the T cell compartment in CLL is a key factor. Since CAR T-cells are generated from apheresed cells from the patient, the composition of the individual's T cell pool will impact on the infused CAR T-cell product. Fraietta *et al.* attempted to explore this by profiling CAR T-cells derived from both responder and non-responder CLL patients (423). They observed that increased frequencies of naïve-like T cells pre-apheresis correlated with response and that CAR T-cells from responder patients showed expression of genes related to memory. Perhaps unsurprisingly, genes related to exhaustion and apoptosis were seen in CAR T-cells from non-responder patients, similar to the signatures observed for CD4⁺ T cells from

CLL patients in this study. Understanding the nature of T cells in CLL, and the mechanisms behind their failure to control the disease, could prove extremely valuable in the design of future generations of CAR T-cell therapies.

The above results suggested that CLL-derived T cells are unlikely to represent good candidates for CAR engineering. This is exacerbated by the presence of increased frequencies of T_{Reg} cells in CLL patients (240), a key issue for the CAR T-cell field. The process of engineering CAR T-cells is non-specific and as such all the T cells apheresed from the patient's blood have the possibility of obtaining CAR expression. This includes T_{Reg} cells, which have been shown to retain their immunosuppressive activity after CAR engineering (424). The activation caused by the recognition of its target by the CAR in T_{Reg} cells will lead to increased production of inhibitory cytokines and potentially negate the positive influence that other CAR T-cells may exert. It may be necessary to introduce a T_{Reg} depletion step to the CAR T-cell engineering process in order to maximise the potential beneficial effect of the treatment.

Currently, CAR-T cells are not approved for the treatment of CLL. However, the onset of new generations of CARs and slowly improving knowledge of the factors that determine the efficacy of CAR T-cells suggest that there is at least hope for future CLL patients that this powerful therapeutic option may become available to them.

The results in this study and others (256,425) clearly demonstrate that there is a significant increase in the frequency of CD4⁺HLA-DR⁺PD-1⁺ T cells in CLL compared to healthy donors (maximum 31.9% vs 5.9%). However, it is not known what factors may have caused this expansion. A potential method of exploring this is single cell T

cell receptor (TCR) sequencing. This technique would allow the determination of whether CD4⁺HLA-DR⁺PD-1⁺ T cells are clonal, i.e. share common TCRs, and as such represent a response to a specific antigen or antigens. Although unlikely, there is a possibility that the discovered TCR sequences match previously identified sequences and therefore reveal the antigen in question. Even uncovering a clonal expansion of CD4⁺HLA-DR⁺PD-1⁺ T cells would represent an important step into understanding the nature of this key T cell subset in CLL.

It is also unclear whether CD4⁺HLA-DR⁺PD-1⁺ T cells represent a long-lived population that has proliferated repeatedly throughout the CLL disease course or whether new CD4⁺HLA-DR⁺PD-1⁺ T cells are being continuously generated through activation. This question could be addressed through the use of telomere length analysis. Telomeres are structures that protect the ends of chromosomes, which are known to gradually erode with successive cell divisions (426). Therefore, analysis of telomere lengths allows an estimate of the degree of cell division undertaken by a cell. Short telomeres in the CD4⁺HLA-DR⁺PD-1⁺ T cell population, in comparison to the whole T cell compartment, would suggest that these cells have undergone many divisions and as such have been expanding since early in the CLL disease course.

In conclusion, this study has provided strong evidence that both the frequency of CD4⁺HLA-DR⁺PD-1⁺ T cells and the CD4⁺:CD8⁺ T cell ratio are prognostic markers in CLL. For the latter, given the ease of measurement and strong prognostic power, a large-scale UK-wide analysis of this parameter could provide haematologists with an

important new tool with which to inform both themselves and CLL patients going forward.

In depth phenotypic analysis revealed CD4⁺HLA-DR⁺PD-1⁺ T cells to be a heterogeneous population, with an enrichment of cytotoxic and actively proliferating cells. Gene expression analysis confirmed that this subset is a mixed population and demonstrated strong associations with T cell exhaustion pathways and the transcription factor TOX in CLL-derived T cells. However, cytokine production and proliferation assays showed CD4⁺HLA-DR⁺PD-1⁺ T cells retained their functionality and did not provide evidence of this exhausted phenotype *in vitro*.

Further investigation of CD4⁺HLA-DR⁺PD-1⁺ T cells and the mechanisms that drive their expansion is warranted given their potential prognostic importance and the complex and heterogeneous nature of this subset revealed here. Defining the specificity and functional role of this and other CD4⁺ T cell subsets in CLL will not only enhance knowledge of this disease, but may allow for the development of strategies to improve immunotherapies and therefore offer new hope to those patients with poor prognosis.

7 Bibliography

1. Oscier D, Fegan C, Hillmen P, Illidge T, Johnson S, Maguire P, et al. Guidelines on the diagnosis and management of chronic lymphocytic leukaemia. *Br J Haematol.* 2004;125(3):294–317.
2. Oscier D, Dearden C, Eren E, Fegan C, Follows G, Hillmen P, et al. Guidelines on the diagnosis, investigation and management of chronic lymphocytic leukaemia. *Br J Haematol.* 2012;159(5):541–64.
3. Haematological Malignancy Research Network. Incidence [Internet]. 2016. Available from: <https://www.hmrn.org/statistics/incidence>
4. Damle RN. B-cell chronic lymphocytic leukemia cells express a surface membrane phenotype of activated, antigen-experienced B lymphocytes. *Blood.* 2002 May 13;99(11):4087–93.
5. Hamblin TJ. Chronic lymphocytic leukaemia. *Baillières Clin Haematol.* 1987 Jun;1(2):449–91.
6. Hamblin AD, Hamblin TJ. The immunodeficiency of chronic lymphocytic leukaemia. *Br Med Bull.* 2008;87:49–62.
7. Itala M, Helenius H, Nikoskelainen J, Remes K. Infections and serum IgG levels in patients with chronic lymphocytic leukemia. *Eur J Haematol.* 1992;48(5):266–70.
8. Parry HM, Birtwistle J, Whitelegg A, Hudson C, McSkeane T, Hazlewood P, et al. Poor functional antibody responses are present in nearly all patients with chronic lymphocytic leukaemia, irrespective of total IgG concentration, and are associated with increased risk of infection. *Br J Haematol.* 2015;171(5):887–90.
9. Ravandi F, O'Brien S. Immune defects in patients with chronic lymphocytic leukemia. *Cancer Immunol Immunother.* 2006 Feb;55(2):197–209.
10. Pourgheysari B, Bruton R, Parry H, Billingham L, Fegan C, Murray J, et al. The number of cytomegalovirus-specific CD4+ T cells is markedly expanded in patients with B-cell chronic lymphocytic leukemia and determines the total CD4+ T-cell repertoire. *Blood.* 2010 Oct 21;116(16):2968–74.
11. Scarfò L, Ferreri AJM, Ghia P. Chronic lymphocytic leukaemia. *Crit Rev Oncol Hematol.* 2016 Aug;104:169–82.
12. Slager SL, Caporaso NE, de Sanjose S, Goldin LR. Genetic Susceptibility to Chronic Lymphocytic Leukemia. *Semin Hematol.* 2013 Oct;50(4):296–302.

13. Slager SL, Benavente Y, Blair A, Vermeulen R, Cerhan JR, Costantini AS, et al. Medical History, Lifestyle, Family History, and Occupational Risk Factors for Chronic Lymphocytic Leukemia/Small Lymphocytic Lymphoma: The InterLymph Non-Hodgkin Lymphoma Subtypes Project. *JNCI Monogr.* 2014 Aug 1;2014(48):41–51.
14. Brown JR. Inherited susceptibility to chronic lymphocytic leukemia: evidence and prospects for the future. *Ther Adv Hematol.* 2013 Aug;4(4):298–308.
15. Mackus WJM. Expansion of CMV-specific CD8+CD45RA+CD27- T cells in B-cell chronic lymphocytic leukemia. *Blood.* 2003 Apr 3;102(3):1057–63.
16. Walton JA, Lydyard PM, Nathwani A, Emery V, Akbar A, Glennie MJ, et al. Patients with B cell chronic lymphocytic leukaemia have an expanded population of CD4+ perforin expressing T cells enriched for human cytomegalovirus specificity and an effector-memory phenotype. *Br J Haematol.* 2010 Jan;148(2):274–84.
17. Steininger C, Rassenti LZ, Vanura K, Eigenberger K, Jäger U, Kipps TJ, et al. Relative seroprevalence of human herpes viruses in patients with chronic lymphocytic leukaemia. *Eur J Clin Invest.* 2009 Jun;39(6):497–506.
18. Parry HM, Damery S, Hudson C, Maurer MJ, Cerhan JR, Pachnio A, et al. Cytomegalovirus infection does not impact on survival or time to first treatment in patients with chronic lymphocytic leukemia: Cytomegalovirus does not impact on CLL Prognosis. *Am J Hematol.* 2016 Aug;91(8):776–81.
19. Nunes C, Wong R, Mason M, Fegan C, Man S, Pepper C. Expansion of a CD8+PD-1+ Replicative Senescence Phenotype in Early Stage CLL Patients Is Associated with Inverted CD4:CD8 Ratios and Disease Progression. *Clin Cancer Res.* 2012 Feb 1;18(3):678–87.
20. Tsai HT, Cross AJ, Graubard BI, Oken M, Schatzkin A, Caporaso NE. Dietary factors and risk of chronic lymphocytic leukemia and small lymphocytic lymphoma: a pooled analysis of two prospective studies. *Cancer Epidemiol Biomark Prev Publ Am Assoc Cancer Res Cosponsored Am Soc Prev Oncol.* 2010 Oct;19(10):2680–4.
21. Vrijheid M, Cardis E, Ashmore P, Auvinen A, Gilbert E, Habib RR, et al. Ionizing Radiation and Risk of Chronic Lymphocytic Leukemia in the 15-Country Study of Nuclear Industry Workers. *Radiat Res.* 2008 Nov;170(5):661–5.
22. Guarini A. Chronic lymphocytic leukemia patients with highly stable and indolent disease show distinctive phenotypic and genotypic features. *Blood.* 2003 Apr 3;102(3):1035–41.
23. Rodrigues CA, Gonçalves MV, Ikoma MRV, Lorand-Metze I, Pereira AD, Farias DLC de, et al. Diagnosis and treatment of chronic lymphocytic leukemia:

- recommendations from the Brazilian Group of Chronic Lymphocytic Leukemia. *Rev Bras Hematol E Hemoter*. 2016;38(4):346–57.
24. Eichhorst B, Robak T, Montserrat E, Ghia P, Hillmen P, Hallek M, et al. Chronic lymphocytic leukaemia: ESMO Clinical Practice Guidelines for diagnosis, treatment and follow-up. *Ann Oncol*. 2015 Sep;26:v78–84.
 25. Hallek M, Cheson BD, Catovsky D, Caligaris-Cappio F, Dighiero G, Döhner H, et al. iwCLL guidelines for diagnosis, indications for treatment, response assessment, and supportive management of CLL. *Blood*. 2018 Jun 21;131(25):2745–60.
 26. Rai KR, Sawitsky A, Cronkite EP, Chanana AD, Levy RN, Pasternack BS. Clinical staging of chronic lymphocytic leukemia. *Blood*. 1975 Aug;46(2):219–34.
 27. Binet JL, Auquier A, Dighiero G, Chastang C, Piguët H, Goasguen J, et al. A new prognostic classification of chronic lymphocytic leukemia derived from a multivariate survival analysis. *Cancer*. 1981 Jul 1;48(1):198–206.
 28. Hamblin TJ, Davis Z, Gardiner A, Oscier DG, Stevenson FK. Unmutated Ig V(H) genes are associated with a more aggressive form of chronic lymphocytic leukemia. *Blood*. 1999 Sep 15;94(6):1848–54.
 29. Damle RN, Wasil T, Fais F, Ghiotto F, Valetto A, Allen SL, et al. Ig V gene mutation status and CD38 expression as novel prognostic indicators in chronic lymphocytic leukemia. *Blood*. 1999 Sep 15;94(6):1840–7.
 30. Di Noia JM, Neuberger MS. Molecular Mechanisms of Antibody Somatic Hypermutation. *Annu Rev Biochem*. 2007;76(1):1–22.
 31. Hamblin TJ, Orchard JA, Ibbotson RE, Davis Z, Thomas PW, Stevenson FK, et al. CD38 expression and immunoglobulin variable region mutations are independent prognostic variables in chronic lymphocytic leukemia, but CD38 expression may vary during the course of the disease. *Blood*. 2002 Feb 1;99(3):1023–9.
 32. Güssow D, Rein R, Ginjaar I, Hochstenbach F, Seemann G, Kottman A, et al. The human beta 2-microglobulin gene. Primary structure and definition of the transcriptional unit. *J Immunol Baltim Md 1950*. 1987 Nov 1;139(9):3132–8.
 33. Li L, Dong M, Wang XG. The Implication and Significance of Beta 2 Microglobulin: A Conservative Multifunctional Regulator. *Chin Med J (Engl)*. 2016 Feb 20;129(4):448–55.
 34. Wierda W, O’Brien S, Wen S, Faderl S, Garcia-Manero G, Thomas D, et al. Chemoimmunotherapy With Fludarabine, Cyclophosphamide, and Rituximab for Relapsed and Refractory Chronic Lymphocytic Leukemia. *J Clin Oncol*

- [Internet]. 2016 Sep 21 [cited 2020 Apr 3]; Available from: <https://ascopubs.org/doi/pdf/10.1200/JCO.2005.12.516>
35. Thompson PA, Tam CS, OBrien SM, Wierda WG, Stingo F, Plunkett W, et al. Fludarabine, cyclophosphamide, and rituximab treatment achieves long-term disease-free survival in IGHV-mutated chronic lymphocytic leukemia. *Blood*. 2016 Jan 21;127(3):303–9.
 36. Lane DP. p53, guardian of the genome. *Nature*. 1992 Jul;358(6381):15–6.
 37. Levine AJ, Oren M. The first 30 years of p53: growing ever more complex. *Nat Rev Cancer*. 2009 Oct;9(10):749–58.
 38. Catherwood MA, Gonzalez D, Donaldson D, Clifford R, Mills K, Thornton P. Relevance of TP53 for CLL diagnostics. *J Clin Pathol*. 2019 May;72(5):343–6.
 39. Clarke AR, Purdie CA, Harrison DJ, Morris RG, Bird CC, Hooper ML, et al. Thymocyte apoptosis induced by p53-dependent and independent pathways. *Nature*. 1993;362.
 40. Puiggros A, Blanco G, Espinet B. Genetic Abnormalities in Chronic Lymphocytic Leukemia: Where We Are and Where We Go. *BioMed Res Int* [Internet]. 2014 [cited 2020 Apr 3];2014. Available from: <https://www.ncbi.nlm.nih.gov/pmc/articles/PMC4054680/>
 41. Döhner H, Stilgenbauer S, Benner A, Leupolt E, Kröber A, Bullinger L, et al. Genomic Aberrations and Survival in Chronic Lymphocytic Leukemia. *N Engl J Med*. 2000 Dec 28;343(26):1910–6.
 42. Döhner H, Fischer K, Bentz M, Hansen K, Benner A, Cabot G, et al. p53 gene deletion predicts for poor survival and non-response to therapy with purine analogs in chronic B-cell leukemias. *Blood*. 1995 Mar 15;85(6):1580–9.
 43. Gonzalez D, Martinez P, Wade R, Hockley S, Oscier D, Matutes E, et al. Mutational Status of the TP53 Gene As a Predictor of Response and Survival in Patients With Chronic Lymphocytic Leukemia: Results From the LRF CLL4 Trial. *J Clin Oncol* [Internet]. 2011 Apr 11 [cited 2020 Apr 3]; Available from: <https://ascopubs.org/doi/pdf/10.1200/JCO.2010.32.0838>
 44. Zenz T, Eichhorst B, Busch R, Denzel T, Häbe S, Winkler D, et al. TP53 mutation and survival in chronic lymphocytic leukemia. *J Clin Oncol Off J Am Soc Clin Oncol*. 2010 Oct 10;28(29):4473–9.
 45. Dighiero G, Maloum K, Desablens B, Cazin B, Navarro M, Leblay R, et al. Chlorambucil in Indolent Chronic Lymphocytic Leukemia. *N Engl J Med*. 1998 May 21;338(21):1506–14.

46. Shustik C, Mick R, Silver R, Sawitsky A, Rai K, Shapiro L. Treatment of early chronic lymphocytic leukemia: intermittent chlorambucil versus observation. *Hematol Oncol.* 1988 Mar;6(1):7–12.
47. CLL Trialists' Collaborative Group. Chemotherapeutic options in chronic lymphocytic leukemia: a meta-analysis of the randomized trials. *J Natl Cancer Inst.* 1999 May 19;91(10):861–8.
48. Hallek M, Fischer K, Fingerle-Rowson G, Fink AM, Busch R, Mayer J, et al. Addition of rituximab to fludarabine and cyclophosphamide in patients with chronic lymphocytic leukaemia: a randomised, open-label, phase 3 trial. *Lancet Lond Engl.* 2010 Oct 2;376(9747):1164–74.
49. Fischer K, Bahlo J, Fink AM, Goede V, Herling CD, Cramer P, et al. Long-term remissions after FCR chemoimmunotherapy in previously untreated patients with CLL: updated results of the CLL8 trial. *Blood.* 2016 Jan 14;127(2):208–15.
50. Eichhorst B, Fink AM, Bahlo J, Busch R, Kovacs G, Maurer C, et al. First-line chemoimmunotherapy with bendamustine and rituximab versus fludarabine, cyclophosphamide, and rituximab in patients with advanced chronic lymphocytic leukaemia (CLL10): an international, open-label, randomised, phase 3, non-inferiority trial. *Lancet Oncol.* 2016 Jul;17(7):928–42.
51. Hillmen P, Robak T, Janssens A, Babu KG, Kloczko J, Grosicki S, et al. Chlorambucil plus ofatumumab versus chlorambucil alone in previously untreated patients with chronic lymphocytic leukaemia (COMPLEMENT 1): a randomised, multicentre, open-label phase 3 trial. *Lancet Lond Engl.* 2015 May 9;385(9980):1873–83.
52. Goede V, Fischer K, Busch R, Engelke A, Eichhorst B, Wendtner CM, et al. Obinutuzumab plus Chlorambucil in Patients with CLL and Coexisting Conditions. *N Engl J Med.* 2014 Mar 20;370(12):1101–10.
53. Hoellenriegel J, Meadows SA, Sivina M, Wierda WG, Kantarjian H, Keating MJ, et al. The phosphoinositide 3'-kinase delta inhibitor, CAL-101, inhibits B-cell receptor signaling and chemokine networks in chronic lymphocytic leukemia. *Blood.* 2011 Sep 29;118(13):3603–12.
54. Jou ST, Carpino N, Takahashi Y, Piekorz R, Chao JR, Carpino N, et al. Essential, nonredundant role for the phosphoinositide 3-kinase p110delta in signaling by the B-cell receptor complex. *Mol Cell Biol.* 2002 Dec;22(24):8580–91.
55. Okkenhaug K, Vanhaesebroeck B. PI3K in lymphocyte development, differentiation and activation. *Nat Rev Immunol.* 2003 Apr;3(4):317–30.
56. Burger JA, Wiestner A. Targeting B cell receptor signalling in cancer: preclinical and clinical advances. *Nat Rev Cancer.* 2018 Jan 19;18(3):148–67.

57. Pentimalli F. BCL2: a 30-year tale of life, death and much more to come. *Cell Death Differ.* 2018 Jan;25(1):7–9.
58. Robertson LE, Plunkett W, McConnell K, Keating MJ, McDonnell TJ. Bcl-2 expression in chronic lymphocytic leukemia and its correlation with the induction of apoptosis and clinical outcome. *Leukemia.* 1996 Mar;10(3):456–9.
59. Del Gaizo Moore V, Brown JR, Certo M, Love TM, Novina CD, Letai A. Chronic lymphocytic leukemia requires BCL2 to sequester prodeath BIM, explaining sensitivity to BCL2 antagonist ABT-737. *J Clin Invest.* 2007 Jan 2;117(1):112–21.
60. Roberts AW, Davids MS, Pagel JM, Kahl BS, Puvvada SD, Gerecitano JF, et al. Targeting BCL2 with Venetoclax in Relapsed Chronic Lymphocytic Leukemia. *N Engl J Med.* 2016 Jan 28;374(4):311–22.
61. Eyre TA, Kirkwood AA, Gohill S, Follows G, Walewska R, Walter H, et al. Efficacy of venetoclax monotherapy in patients with relapsed chronic lymphocytic leukaemia in the post-BCR inhibitor setting: a UK wide analysis. *Br J Haematol.* 2019;185(4):656–69.
62. Stilgenbauer S, Eichhorst B, Schetelig J, Hillmen P, Seymour JF, Coutre S, et al. Venetoclax for Patients With Chronic Lymphocytic Leukemia With 17p Deletion: Results From the Full Population of a Phase II Pivotal Trial. *J Clin Oncol* [Internet]. 2018 May 1 [cited 2020 Apr 8]; Available from: <https://ascopubs.org/doi/pdf/10.1200/JCO.2017.76.6840>
63. Tausch E, Close W, Dolnik A, Bloehdorn J, Chyla B, Bullinger L, et al. Venetoclax resistance and acquired BCL2 mutations in chronic lymphocytic leukemia. *Haematologica.* 2019 Sep;104(9):e434–7.
64. Blombery P, Anderson MA, Gong J nan, Thijssen R, Birkinshaw RW, Thompson ER, et al. Acquisition of the Recurrent Gly101Val Mutation in BCL2 Confers Resistance to Venetoclax in Patients with Progressive Chronic Lymphocytic Leukemia. *Cancer Discov.* 2019 Mar;9(3):342–53.
65. Schneider C, Steinbrecher D, Stilgenbauer S. Targeted therapy in CLL: changing the treatment paradigm. *Oncotarget.* 2019 Jun 18;10(40):4002–3.
66. Kater AP, Seymour JF, Hillmen P, Eichhorst B, Langerak AW, Owen C, et al. Fixed Duration of Venetoclax-Rituximab in Relapsed/Refractory Chronic Lymphocytic Leukemia Eradicates Minimal Residual Disease and Prolongs Survival: Post-Treatment Follow-Up of the MURANO Phase III Study. *J Clin Oncol* [Internet]. 2018 Dec 3 [cited 2020 Apr 8]; Available from: <https://ascopubs.org/doi/pdf/10.1200/JCO.18.01580>
67. Flinn IW, Gribben JG, Dyer MJS, Wierda W, Maris MB, Furman RR, et al. Phase 1b study of venetoclax-obinutuzumab in previously untreated and

- relapsed/refractory chronic lymphocytic leukemia. *Blood*. 2019 27;133(26):2765–75.
68. Wierda WG, Siddiqi T, Flinn I, Badoux XC, Kipps TJ, Allan JN, et al. Phase 2 CAPTIVATE results of ibrutinib (ibr) plus venetoclax (ven) in first-line chronic lymphocytic leukemia (CLL). *J Clin Oncol*. 2018 May 20;36(15_suppl):7502–7502.
69. Jain N, Keating M, Thompson P, Ferrajoli A, Burger J, Borthakur G, et al. Ibrutinib and Venetoclax for First-Line Treatment of CLL. *N Engl J Med*. 2019 30;380(22):2095–103.
70. Jeyakumar D, O’Brien S. B cell receptor inhibition as a target for CLL therapy. *Best Pract Res Clin Haematol*. 2016 Mar;29(1):2–14.
71. Maddocks K, Jones JA. Bruton tyrosine kinase inhibition in chronic lymphocytic leukemia. *Semin Oncol*. 2016 Apr;43(2):251–9.
72. Advani RH, Buggy JJ, Sharman JP, Smith SM, Boyd TE, Grant B, et al. Bruton tyrosine kinase inhibitor ibrutinib (PCI-32765) has significant activity in patients with relapsed/refractory B-cell malignancies. *J Clin Oncol Off J Am Soc Clin Oncol*. 2013 Jan 1;31(1):88–94.
73. Byrd JC, Furman RR, Coutre SE, Flinn IW, Burger JA, Blum KA, et al. Targeting BTK with ibrutinib in relapsed chronic lymphocytic leukemia. *N Engl J Med*. 2013 Jul 4;369(1):32–42.
74. Burger JA, Tedeschi A, Barr PM, Robak T, Owen C, Ghia P, et al. Ibrutinib as Initial Therapy for Patients with Chronic Lymphocytic Leukemia. *N Engl J Med*. 2015 Dec 17;373(25):2425–37.
75. Farooqui MZH, Valdez J, Martyr S, Aue G, Saba N, Niemann CU, et al. Ibrutinib for previously untreated and relapsed or refractory chronic lymphocytic leukaemia with TP53 aberrations: a phase 2, single-arm trial. *Lancet Oncol*. 2015 Feb;16(2):169–76.
76. Woyach JA, Ruppert AS, Heerema NA, Zhao W, Booth AM, Ding W, et al. Ibrutinib Regimens versus Chemoimmunotherapy in Older Patients with Untreated CLL. *N Engl J Med*. 2018 27;379(26):2517–28.
77. Furman RR, Cheng S, Lu P, Setty M, Perez AR, Perez AR, et al. Ibrutinib resistance in chronic lymphocytic leukemia. *N Engl J Med*. 2014 Jun 12;370(24):2352–4.
78. Woyach JA, Furman RR, Liu TM, Ozer HG, Zapatka M, Ruppert AS, et al. Resistance mechanisms for the Bruton’s tyrosine kinase inhibitor ibrutinib. *N Engl J Med*. 2014 Jun 12;370(24):2286–94.

79. Maddocks KJ, Ruppert AS, Lozanski G, Heerema NA, Zhao W, Abruzzo L, et al. Etiology of Ibrutinib Therapy Discontinuation and Outcomes in Patients With Chronic Lymphocytic Leukemia. *JAMA Oncol.* 2015 Apr;1(1):80–7.
80. Kaur V, Swami A. Ibrutinib in CLL: a focus on adverse events, resistance, and novel approaches beyond ibrutinib. *Ann Hematol.* 2017 Jul;96(7):1175–84.
81. Byrd JC, Harrington B, O’Brien S, Jones JA, Schuh A, Devereux S, et al. Acalabrutinib (ACP-196) in Relapsed Chronic Lymphocytic Leukemia. *N Engl J Med.* 2016 Jan 28;374(4):323–32.
82. Patel V, Balakrishnan K, Bibikova E, Ayres M, Keating MJ, Wierda WG, et al. Comparison of Acalabrutinib, A Selective Bruton Tyrosine Kinase Inhibitor, with Ibrutinib in Chronic Lymphocytic Leukemia Cells. *Clin Cancer Res Off J Am Assoc Cancer Res.* 2017 Jul 15;23(14):3734–43.
83. Blunt MD, Koehrer S, Dobson RC, Larrayoz M, Wilmore S, Hayman A, et al. The Dual Syk/JAK Inhibitor Cerdulatinib Antagonizes B-cell Receptor and Microenvironmental Signaling in Chronic Lymphocytic Leukemia. *Clin Cancer Res Off J Am Assoc Cancer Res.* 2017 May 1;23(9):2313–24.
84. Hing ZA, Mantel R, Beckwith KA, Guinn D, Williams E, Smith LL, et al. Selinexor is effective in acquired resistance to ibrutinib and synergizes with ibrutinib in chronic lymphocytic leukemia. *Blood.* 2015 May 14;125(20):3128–32.
85. Hing ZA, Fung HYJ, Ranganathan P, Mitchell S, El-Gamal D, Woyach JA, et al. Next-generation XPO1 inhibitor shows improved efficacy and in vivo tolerability in hematological malignancies. *Leukemia.* 2016;30(12):2364–72.
86. Murphy K. *Janeway’s Immunobiology* [Internet]. 9th ed. 9th edition. | New York, NY : Garland Science/Taylor & Francis: Garland Science; 2016 [cited 2020 Apr 9]. Available from: <https://www.taylorfrancis.com/books/9781315533247>
87. Wood P. *Understanding immunology.* 3rd ed. Harlow, England ; New York: Prentice Hall; 2011. 363 p.
88. Boehm T. Thymus development and function. *Curr Opin Immunol.* 2008 Apr;20(2):178–84.
89. Gameiro J, Nagib P, Verinaud L. The thymus microenvironment in regulating thymocyte differentiation. *Cell Adhes Migr.* 2010 Sep;4(3):382–90.
90. Anderson G, Takahama Y. Thymic epithelial cells: working class heroes for T cell development and repertoire selection. *Trends Immunol.* 2012 Jun;33(6):256–63.

91. Alves NL, Huntington ND, Rodewald HR, Di Santo JP. Thymic epithelial cells: the multi-tasking framework of the T cell 'cradle'. *Trends Immunol.* 2009 Oct;30(10):468–74.
92. Lucas B, White AJ, Parnell SM, Henley PM, Jenkinson WE, Anderson G. Progressive Changes in CXCR4 Expression That Define Thymocyte Positive Selection Are Dispensable For Both Innate and Conventional $\alpha\beta$ T-cell Development. *Sci Rep [Internet].* 2017 Dec [cited 2018 Aug 16];7(1). Available from: <http://www.nature.com/articles/s41598-017-05182-7>
93. Dzhagalov I, Phee H. How to find your way through the thymus: a practical guide for aspiring T cells. *Cell Mol Life Sci CMLS.* 2012 Mar;69(5):663–82.
94. Ladi E, Yin X, Chtanova T, Robey EA. Thymic microenvironments for T cell differentiation and selection. *Nat Immunol.* 2006 Apr;7(4):338–43.
95. Krangel MS. Mechanics of T cell receptor gene rearrangement. *Curr Opin Immunol.* 2009 Apr;21(2):133–9.
96. Starr TK, Jameson SC, Hogquist KA. Positive and negative selection of T cells. *Annu Rev Immunol.* 2003;21:139–76.
97. Ioannidis V, Beermann F, Clevers H, Held W. The β -catenin–TCF-1 pathway ensures CD4+CD8+ thymocyte survival. *Nat Immunol.* 2001 Aug;2(8):691–7.
98. Klein L, Kyewski B, Allen PM, Hogquist KA. Positive and negative selection of the T cell repertoire: what thymocytes see (and don't see). *Nat Rev Immunol.* 2014 Jun;14(6):377–91.
99. Derbinski J, Schulte A, Kyewski B, Klein L. Promiscuous gene expression in medullary thymic epithelial cells mirrors the peripheral self. *Nat Immunol.* 2001 Nov;2(11):1032–9.
100. Anderson MS, Venanzi ES, Klein L, Chen Z, Berzins SP, Turley SJ, et al. Projection of an immunological self shadow within the thymus by the aire protein. *Science.* 2002 Nov 15;298(5597):1395–401.
101. Perniola R. Expression of the Autoimmune Regulator Gene and Its Relevance to the Mechanisms of Central and Peripheral Tolerance. *Clin Dev Immunol.* 2012;2012:1–12.
102. PETERSON P, PITKÄNEN J, SILLANPÄÄ N, KROHN K. Autoimmune polyendocrinopathy candidiasis ectodermal dystrophy (APECED): a model disease to study molecular aspects of endocrine autoimmunity. *Clin Exp Immunol.* 2004 Mar;135(3):348–57.
103. Millet V, Naquet P, Guinamard RR. Intercellular MHC transfer between thymic epithelial and dendritic cells. *Eur J Immunol.* 2008 May;38(5):1257–63.

104. Allende ML, Dreier JL, Mandala S, Proia RL. Expression of the Sphingosine 1-Phosphate Receptor, S1P1, on T-cells Controls Thymic Emigration. *J Biol Chem*. 2004 Apr 9;279(15):15396–401.
105. Hsieh CS, Lee HM, Lio CWJ. Selection of regulatory T cells in the thymus. *Nat Rev Immunol*. 2012 Feb 10;12(3):157–67.
106. Jeffery LE, Henley P, Marium N, Filer A, Sansom DM, Hewison M, et al. Decreased sensitivity to 1,25-dihydroxyvitamin D3 in T cells from the rheumatoid joint. *J Autoimmun*. 2018 Mar;88:50–60.
107. Zhu J, Paul WE. CD4 T cells: fates, functions, and faults. *Blood*. 2008 Sep 1;112(5):1557–69.
108. Zhu J, Yamane H, Paul WE. Differentiation of Effector CD4 T Cell Populations. *Annu Rev Immunol*. 2010;28:445–89.
109. Szabo SJ, Kim ST, Costa GL, Zhang X, Fathman CG, Glimcher LH. A novel transcription factor, T-bet, directs Th1 lineage commitment. *Cell*. 2000 Mar 17;100(6):655–69.
110. Morandi B, Bougras G, Muller WA, Ferlazzo G, Münz C. NK cells of human secondary lymphoid tissues enhance T cell polarization via IFN-gamma secretion. *Eur J Immunol*. 2006 Sep;36(9):2394–400.
111. Brummelman J, Pilipow K, Lugli E. The Single-Cell Phenotypic Identity of Human CD8+ and CD4+ T Cells. *Int Rev Cell Mol Biol*. 2018;341:63–124.
112. Schoenborn JR, Wilson CB. Regulation of interferon-gamma during innate and adaptive immune responses. *Adv Immunol*. 2007;96:41–101.
113. Williams MA, Tyznik AJ, Bevan MJ. Interleukin-2 signals during priming are required for secondary expansion of CD8+ memory T cells. *Nature*. 2006 Jun 15;441(7095):890–3.
114. Lord GM, Rao RM, Choe H, Sullivan BM, Lichtman AH, Luscinskas FW, et al. T-bet is required for optimal proinflammatory CD4+ T-cell trafficking. *Blood*. 2005 Nov 15;106(10):3432–9.
115. Stetson DB, Voehringer D, Grogan JL, Xu M, Reinhardt RL, Scheu S, et al. Th2 cells: orchestrating barrier immunity. *Adv Immunol*. 2004;83:163–89.
116. Zheng W, Flavell RA. The transcription factor GATA-3 is necessary and sufficient for Th2 cytokine gene expression in CD4 T cells. *Cell*. 1997 May 16;89(4):587–96.

117. Lee HJ, Takemoto N, Kurata H, Kamogawa Y, Miyatake S, O'Garra A, et al. GATA-3 induces T helper cell type 2 (Th2) cytokine expression and chromatin remodeling in committed Th1 cells. *J Exp Med*. 2000 Jul 3;192(1):105–15.
118. Swain SL, Weinberg AD, English M, Huston G. IL-4 directs the development of Th2-like helper effectors. *J Immunol Baltim Md 1950*. 1990 Dec 1;145(11):3796–806.
119. Le Gros G, Ben-Sasson SZ, Seder R, Finkelman FD, Paul WE. Generation of interleukin 4 (IL-4)-producing cells in vivo and in vitro: IL-2 and IL-4 are required for in vitro generation of IL-4-producing cells. *J Exp Med*. 1990 Sep 1;172(3):921–9.
120. Cote-Sierra J, Foucras G, Guo L, Chiodetti L, Young HA, Hu-Li J, et al. Interleukin 2 plays a central role in Th2 differentiation. *Proc Natl Acad Sci U S A*. 2004 Mar 16;101(11):3880–5.
121. Cosmi L, Annunziato F, Galli MIG null, Maggi RME null, Nagata K, Romagnani S. CRTH2 is the most reliable marker for the detection of circulating human type 2 Th and type 2 T cytotoxic cells in health and disease. *Eur J Immunol*. 2000 Oct;30(10):2972–9.
122. Imai T, Nagira M, Takagi S, Kakizaki M, Nishimura M, Wang J, et al. Selective recruitment of CCR4-bearing Th2 cells toward antigen-presenting cells by the CC chemokines thymus and activation-regulated chemokine and macrophage-derived chemokine. *Int Immunol*. 1999 Jan;11(1):81–8.
123. Tanaka K, Ogawa K, Sugamura K, Nakamura M, Takano S, Nagata K. Cutting edge: differential production of prostaglandin D2 by human helper T cell subsets. *J Immunol Baltim Md 1950*. 2000 Mar 1;164(5):2277–80.
124. Xue L, Barrow A, Pettipher R. Novel Function of CRTH2 in Preventing Apoptosis of Human Th2 Cells through Activation of the Phosphatidylinositol 3-Kinase Pathway. *J Immunol*. 2009 Jun 15;182(12):7580–6.
125. Gould HJ, Beavil RL, Vercelli D. IgE isotype determination: epsilon-germline gene transcription, DNA recombination and B-cell differentiation. *Br Med Bull*. 2000;56(4):908–24.
126. Coffman RL, Seymour BW, Hudak S, Jackson J, Rennick D. Antibody to interleukin-5 inhibits helminth-induced eosinophilia in mice. *Science*. 1989 Jul 21;245(4915):308–10.
127. Wynn TA. IL-13 effector functions. *Annu Rev Immunol*. 2003;21:425–56.
128. Korn T, Oukka M, Kuchroo V, Bettelli E. Th17 cells: effector T cells with inflammatory properties. *Semin Immunol*. 2007 Dec;19(6):362–71.

129. Ivanov II, McKenzie BS, Zhou L, Tadokoro CE, Lepelley A, Lafaille JJ, et al. The orphan nuclear receptor ROR γ directs the differentiation program of proinflammatory IL-17+ T helper cells. *Cell*. 2006 Sep 22;126(6):1121–33.
130. Mangan PR, Harrington LE, O’Quinn DB, Helms WS, Bullard DC, Elson CO, et al. Transforming growth factor- β induces development of the T(H)17 lineage. *Nature*. 2006 May 11;441(7090):231–4.
131. Korn T, Bettelli E, Gao W, Awasthi A, Jäger A, Strom TB, et al. IL-21 initiates an alternative pathway to induce proinflammatory T(H)17 cells. *Nature*. 2007 Jul 26;448(7152):484–7.
132. Bettelli E, Carrier Y, Gao W, Korn T, Strom TB, Oukka M, et al. Reciprocal developmental pathways for the generation of pathogenic effector TH17 and regulatory T cells. *Nature*. 2006 May 11;441(7090):235–8.
133. Ishigame H, Kakuta S, Nagai T, Kadoki M, Nambu A, Komiyama Y, et al. Differential roles of interleukin-17A and -17F in host defense against mucoc epithelial bacterial infection and allergic responses. *Immunity*. 2009 Jan 16;30(1):108–19.
134. Leonard WJ, Spolski R. Interleukin-21: a modulator of lymphoid proliferation, apoptosis and differentiation. *Nat Rev Immunol*. 2005 Sep;5(9):688–98.
135. Acosta-Rodriguez EV, Rivino L, Geginat J, Jarrossay D, Gattorno M, Lanzavecchia A, et al. Surface phenotype and antigenic specificity of human interleukin 17-producing T helper memory cells. *Nat Immunol*. 2007 Jun;8(6):639–46.
136. Wilson NJ, Boniface K, Chan JR, McKenzie BS, Blumenschein WM, Mattson JD, et al. Development, cytokine profile and function of human interleukin 17-producing helper T cells. *Nat Immunol*. 2007 Sep;8(9):950–7.
137. Crotty S. Follicular helper CD4 T cells (TFH). *Annu Rev Immunol*. 2011;29:621–63.
138. Victora GD, Schwickert TA, Fooksman DR, Kamphorst AO, Meyer-Hermann M, Dustin ML, et al. Germinal center dynamics revealed by multiphoton microscopy with a photoactivatable fluorescent reporter. *Cell*. 2010 Nov 12;143(4):592–605.
139. Fazilleau N, Mark L, McHeyzer-Williams LJ, McHeyzer-Williams MG. Follicular Helper T Cells: Lineage and Location. *Immunity*. 2009 Mar 20;30(3):324–35.
140. Nurieva RI, Chung Y, Martinez GJ, Yang XO, Tanaka S, Matskevitch TD, et al. Bcl6 mediates the development of T follicular helper cells. *Science*. 2009 Aug 21;325(5943):1001–5.

141. Glatman Zaretsky A, Taylor JJ, King IL, Marshall FA, Mohrs M, Pearce EJ. T follicular helper cells differentiate from Th2 cells in response to helminth antigens. *J Exp Med*. 2009 May 11;206(5):991–9.
142. Nurieva RI, Chung Y, Hwang D, Yang XO, Kang HS, Ma L, et al. Generation of T follicular helper cells is mediated by interleukin-21 but independent of T helper 1, 2, or 17 cell lineages. *Immunity*. 2008 Jul 18;29(1):138–49.
143. Schaerli P, Willimann K, Lang AB, Lipp M, Loetscher P, Moser B. CXC chemokine receptor 5 expression defines follicular homing T cells with B cell helper function. *J Exp Med*. 2000 Dec 4;192(11):1553–62.
144. Rasheed AU, Rahn HP, Sallusto F, Lipp M, Müller G. Follicular B helper T cell activity is confined to CXCR5(hi)ICOS(hi) CD4 T cells and is independent of CD57 expression. *Eur J Immunol*. 2006 Jul;36(7):1892–903.
145. Hams E, McCarron MJ, Amu S, Yagita H, Azuma M, Chen L, et al. Blockade of B7-H1 (programmed death ligand 1) enhances humoral immunity by positively regulating the generation of T follicular helper cells. *J Immunol Baltim Md 1950*. 2011 May 15;186(10):5648–55.
146. Allen CDC, Okada T, Cyster JG. Germinal-center organization and cellular dynamics. *Immunity*. 2007 Aug;27(2):190–202.
147. Basso K, Saito M, Sumazin P, Margolin AA, Wang K, Lim WK, et al. Integrated biochemical and computational approach identifies BCL6 direct target genes controlling multiple pathways in normal germinal center B cells. *Blood*. 2010 Feb 4;115(5):975–84.
148. Guzman-Rojas L, Sims-Mourtada JC, Rangel R, Martinez-Valdez H. Life and death within germinal centres: a double-edged sword. *Immunology*. 2002 Oct;107(2):167–75.
149. Sakaguchi S, Miyara M, Costantino CM, Hafler DA. FOXP3+ regulatory T cells in the human immune system. *Nat Rev Immunol*. 2010 Jul;10(7):490–500.
150. Roncador G, Brown PJ, Maestre L, Hue S, Martínez-Torrecedrada JL, Ling KL, et al. Analysis of FOXP3 protein expression in human CD4+CD25+ regulatory T cells at the single-cell level. *Eur J Immunol*. 2005 Jun;35(6):1681–91.
151. Chen W, Jin W, Hardegen N, Lei KJ, Li L, Marinos N, et al. Conversion of peripheral CD4+CD25- naive T cells to CD4+CD25+ regulatory T cells by TGF-beta induction of transcription factor Foxp3. *J Exp Med*. 2003 Dec 15;198(12):1875–86.
152. Zheng SG, Wang JH, Gray JD, Soucier H, Horwitz DA. Natural and induced CD4+CD25+ cells educate CD4+CD25- cells to develop suppressive activity: the

- role of IL-2, TGF-beta, and IL-10. *J Immunol Baltim Md* 1950. 2004 May 1;172(9):5213–21.
153. Kretschmer K, Apostolou I, Hawiger D, Khazaie K, Nussenzweig MC, von Boehmer H. Inducing and expanding regulatory T cell populations by foreign antigen. *Nat Immunol*. 2005 Dec;6(12):1219–27.
154. Seddiki N, Santner-Nanan B, Martinson J, Zaunders J, Sasson S, Landay A, et al. Expression of interleukin (IL)-2 and IL-7 receptors discriminates between human regulatory and activated T cells. *J Exp Med*. 2006 Jul 10;203(7):1693–700.
155. Shevach EM. Mechanisms of foxp3+ T regulatory cell-mediated suppression. *Immunity*. 2009 May;30(5):636–45.
156. Collison LW, Workman CJ, Kuo TT, Boyd K, Wang Y, Vignali KM, et al. The inhibitory cytokine IL-35 contributes to regulatory T-cell function. *Nature*. 2007 Nov 22;450(7169):566–9.
157. O’Garra A, Vieira PL, Vieira P, Goldfeld AE. IL-10-producing and naturally occurring CD4+ Tregs: limiting collateral damage. *J Clin Invest*. 2004 Nov;114(10):1372–8.
158. Pandiyan P, Zheng L, Ishihara S, Reed J, Lenardo MJ. CD4+CD25+Foxp3+ regulatory T cells induce cytokine deprivation-mediated apoptosis of effector CD4+ T cells. *Nat Immunol*. 2007 Dec;8(12):1353–62.
159. Grossman WJ, Verbsky JW, Barchet W, Colonna M, Atkinson JP, Ley TJ. Human T regulatory cells can use the perforin pathway to cause autologous target cell death. *Immunity*. 2004 Oct;21(4):589–601.
160. Zhang N, Bevan MJ. CD8+ T Cells: Foot Soldiers of the Immune System. *Immunity*. 2011 Aug;35(2):161–8.
161. Bennett SR, Carbone FR, Karamalis F, Flavell RA, Miller JF, Heath WR. Help for cytotoxic-T-cell responses is mediated by CD40 signalling. *Nature*. 1998 Jun 4;393(6684):478–80.
162. Rutishauser RL, Martins GA, Kalachikov S, Chandele A, Parish IA, Meffre E, et al. Transcriptional repressor Blimp-1 promotes CD8(+) T cell terminal differentiation and represses the acquisition of central memory T cell properties. *Immunity*. 2009 Aug 21;31(2):296–308.
163. Kallies A, Xin A, Belz GT, Nutt SL. Blimp-1 transcription factor is required for the differentiation of effector CD8(+) T cells and memory responses. *Immunity*. 2009 Aug 21;31(2):283–95.
164. Lopez JA, Susanto O, Jenkins MR, Lukoyanova N, Sutton VR, Law RHP, et al. Perforin forms transient pores on the target cell plasma membrane to facilitate

- rapid access of granzymes during killer cell attack. *Blood*. 2013 Apr 4;121(14):2659–68.
165. Voskoboinik I, Whisstock JC, Trapani JA. Perforin and granzymes: function, dysfunction and human pathology. *Nat Rev Immunol*. 2015 Jun;15(6):388–400.
166. Sutton VR, Davis JE, Cancilla M, Johnstone RW, Ruefli AA, Sedelies K, et al. Initiation of Apoptosis by Granzyme B Requires Direct Cleavage of Bid, but Not Direct Granzyme B–Mediated Caspase Activation. *J Exp Med*. 2000 Nov 20;192(10):1403–14.
167. Lieberman J. Granzyme A activates another way to die. *Immunol Rev*. 2010 May;235(1):93–104.
168. Hukelmann JL, Anderson KE, Sinclair LV, Grzes KM, Murillo AB, Hawkins PT, et al. The cytotoxic T cell proteome and its shaping by the kinase mTOR. *Nat Immunol*. 2016 Jan;17(1):104–12.
169. Sanin DE, Pearce EJ. The cell identity of cytotoxic T lymphocytes. *Nat Immunol*. 2016 Jan;17(1):45–6.
170. Stinchcombe JC, Majorovits E, Bossi G, Fuller S, Griffiths GM. Centrosome polarization delivers secretory granules to the immunological synapse. *Nature*. 2006 Sep 28;443(7110):462–5.
171. Isaaz S, Baetz K, Olsen K, Podack E, Griffiths GM. Serial killing by cytotoxic T lymphocytes: T cell receptor triggers degranulation, re-filling of the lytic granules and secretion of lytic proteins via a non-granule pathway. *Eur J Immunol*. 1995 Apr;25(4):1071–9.
172. Bossi G, Griffiths GM. Degranulation plays an essential part in regulating cell surface expression of Fas ligand in T cells and natural killer cells. *Nat Med*. 1999 Jan;5(1):90–6.
173. Brunner T, Wasem C, Torgler R, Cima I, Jakob S, Corazza N. Fas (CD95/Apo-1) ligand regulation in T cell homeostasis, cell-mediated cytotoxicity and immune pathology. *Semin Immunol*. 2003 Jun;15(3):167–76.
174. Rouvier E, Luciani MF, Golstein P. Fas involvement in Ca²⁺-independent T cell-mediated cytotoxicity. *J Exp Med*. 1993 Jan 1;177(1):195–200.
175. Yamada A, Arakaki R, Saito M, Kudo Y, Ishimaru N. Dual Role of Fas/FasL-Mediated Signal in Peripheral Immune Tolerance. *Front Immunol* [Internet]. 2017 Apr 5 [cited 2020 May 7];8. Available from: <https://www.ncbi.nlm.nih.gov/pmc/articles/PMC5380675/>

176. el-Khatib M, Stanger BZ, Dogan H, Cui H, Ju ST. The molecular mechanism of FasL-mediated cytotoxicity by CD4+ Th1 clones. *Cell Immunol.* 1995 Jul;163(2):237–44.
177. Malek TR, Castro I. Interleukin-2 Receptor Signaling: At the Interface between Tolerance and Immunity. *Immunity.* 2010 Aug 27;33(2):153–65.
178. Teixeira LK, Fonseca BPF, Vieira-de-Abreu A, Barboza BA, Robbs BK, Bozza PT, et al. IFN-gamma production by CD8+ T cells depends on NFAT1 transcription factor and regulates Th differentiation. *J Immunol Baltim Md 1950.* 2005 Nov 1;175(9):5931–9.
179. Ratner A, Clark WR. Role of TNF-alpha in CD8+ cytotoxic T lymphocyte-mediated lysis. *J Immunol Baltim Md 1950.* 1993 May 15;150(10):4303–14.
180. Palmer EM, Holbrook BC, Arimilli S, Parks GD, Alexander-Miller MA. IFN-gamma-producing, virus-specific CD8+ effector cells acquire the ability to produce IL-10 as a result of entry into the infected lung environment. *Virology.* 2010 Sep 1;404(2):225–30.
181. Sun J, Madan R, Karp CL, Braciale TJ. Effector T cells control lung inflammation during acute influenza virus infection by producing IL-10. *Nat Med.* 2009 Mar;15(3):277–84.
182. Godfrey DI, Uldrich AP, McCluskey J, Rossjohn J, Moody DB. The burgeoning family of unconventional T cells. *Nat Immunol.* 2015 Nov;16(11):1114–23.
183. Brennan PJ, Brigl M, Brenner MB. Invariant natural killer T cells: an innate activation scheme linked to diverse effector functions. *Nat Rev Immunol.* 2013 Feb;13(2):101–17.
184. Godfrey DI, Berzins SP. Control points in NKT-cell development. *Nat Rev Immunol.* 2007 Jul;7(7):505–18.
185. Bendelac A, Savage PB, Teyton L. The Biology of NKT Cells. *Annu Rev Immunol.* 2007;25(1):297–336.
186. Gapin L. Development of invariant natural killer T cells. *Curr Opin Immunol.* 2016 Apr;39:68–74.
187. Seach N, Guerri L, Le Bourhis L, Mburu Y, Cui Y, Bessoles S, et al. Double Positive Thymocytes Select Mucosal-Associated Invariant T Cells. *J Immunol.* 2013 Dec 15;191(12):6002–9.
188. Kjer-Nielsen L, Patel O, Corbett AJ, Le Nours J, Meehan B, Liu L, et al. MR1 presents microbial vitamin B metabolites to MAIT cells. *Nature.* 2012 Nov;491(7426):717–23.

189. Godfrey DI, Koay HF, McCluskey J, Gherardin NA. The biology and functional importance of MAIT cells. *Nat Immunol*. 2019 Sep;20(9):1110–28.
190. Vantourout P, Hayday A. Six-of-the-best: unique contributions of $\gamma\delta$ T cells to immunology. *Nat Rev Immunol*. 2013 Feb;13(2):88–100.
191. Chien Y hsiu, Meyer C, Bonneville M. $\gamma\delta$ T Cells: First Line of Defense and Beyond. *Annu Rev Immunol*. 2014;32(1):121–55.
192. Kotsias F, Cebrian I, Alloatti A. Antigen processing and presentation. *Int Rev Cell Mol Biol*. 2019;348:69–121.
193. Steinman RM, Hemmi H. Dendritic cells: translating innate to adaptive immunity. *Curr Top Microbiol Immunol*. 2006;311:17–58.
194. Chen X, Jensen PE. The role of B lymphocytes as antigen-presenting cells. *Arch Immunol Ther Exp (Warsz)*. 2008 Apr;56(2):77–83.
195. Murray PJ, Wynn TA. Protective and pathogenic functions of macrophage subsets. *Nat Rev Immunol*. 2011 Oct 14;11(11):723–37.
196. Jakubzick CV, Randolph GJ, Henson PM. Monocyte differentiation and antigen-presenting functions. *Nat Rev Immunol*. 2017 Jun;17(6):349–62.
197. Villadangos JA, Schnorrer P. Intrinsic and cooperative antigen-presenting functions of dendritic-cell subsets in vivo. *Nat Rev Immunol*. 2007 Jul;7(7):543–55.
198. Rock KL, Goldberg AL. Degradation of cell proteins and the generation of MHC class I-presented peptides. *Annu Rev Immunol*. 1999;17:739–79.
199. Murata S, Takahama Y, Kasahara M, Tanaka K. The immunoproteasome and thymoproteasome: functions, evolution and human disease. *Nat Immunol*. 2018;19(9):923–31.
200. Ritter C, Quirin K, Kowarik M, Helenius A. Minor folding defects trigger local modification of glycoproteins by the ER folding sensor GT. *EMBO J*. 2005 May 4;24(9):1730–8.
201. Wosen JE, Mukhopadhyay D, Macaubas C, Mellins ED. Epithelial MHC Class II Expression and Its Role in Antigen Presentation in the Gastrointestinal and Respiratory Tracts. *Front Immunol*. 2018 Sep 25;9:2144.
202. Mukherjee P, Dani A, Bhatia S, Singh N, Rudensky AY, George A, et al. Efficient presentation of both cytosolic and endogenous transmembrane protein antigens on MHC class II is dependent on cytoplasmic proteolysis. *J Immunol Baltim Md 1950*. 2001 Sep 1;167(5):2632–41.

203. McCormick PJ, Martina JA, Bonifacino JS. Involvement of clathrin and AP-2 in the trafficking of MHC class II molecules to antigen-processing compartments. *Proc Natl Acad Sci U S A*. 2005 May 31;102(22):7910–5.
204. Jurewicz MM, Stern LJ. Class II MHC antigen processing in immune tolerance and inflammation. *Immunogenetics*. 2019;71(3):171–87.
205. Sarkar S, Kalia V, Haining WN, Konieczny BT, Subramaniam S, Ahmed R. Functional and genomic profiling of effector CD8 T cell subsets with distinct memory fates. *J Exp Med*. 2008 Mar 17;205(3):625–40.
206. Omilusik KD, Goldrath AW. The origins of memory T cells. *Nature*. 2017 21;552(7685):337–9.
207. Kaech SM, Cui W. Transcriptional control of effector and memory CD8+ T cell differentiation. *Nat Rev Immunol*. 2012 Nov;12(11):749–61.
208. Akondy RS, Fitch M, Edupuganti S, Yang S, Kissick HT, Li KW, et al. Origin and differentiation of human memory CD8 T cells after vaccination. *Nature*. 2017 21;552(7685):362–7.
209. Pepper M, Jenkins MK. Origins of CD4(+) effector and central memory T cells. *Nat Immunol*. 2011 Jun;12(6):467–71.
210. Yuzefpolskiy Y, Baumann FM, Kalia V, Sarkar S. Early CD8 T-cell memory precursors and terminal effectors exhibit equipotent in vivo degranulation. *Cell Mol Immunol*. 2015 Jul;12(4):400–8.
211. Sallusto F, Lenig D, Förster R, Lipp M, Lanzavecchia A. Two subsets of memory T lymphocytes with distinct homing potentials and effector functions. *Nature*. 1999 Oct 14;401(6754):708–12.
212. Masopust D, Vezys V, Marzo AL, Lefrançois L. Preferential localization of effector memory cells in nonlymphoid tissue. *Science*. 2001 Mar 23;291(5512):2413–7.
213. Seder RA, Ahmed R. Similarities and differences in CD4+ and CD8+ effector and memory T cell generation. *Nat Immunol*. 2003 Sep;4(9):835–42.
214. Sallusto F, Geginat J, Lanzavecchia A. Central memory and effector memory T cell subsets: function, generation, and maintenance. *Annu Rev Immunol*. 2004;22:745–63.
215. Klebanoff CA, Gattinoni L, Restifo NP. CD8+ T-cell memory in tumor immunology and immunotherapy. *Immunol Rev*. 2006 Jun;211:214–24.
216. Mueller SN, Gebhardt T, Carbone FR, Heath WR. Memory T cell subsets, migration patterns, and tissue residence. *Annu Rev Immunol*. 2013;31:137–61.

217. Henson SM, Riddell NE, Akbar AN. Properties of end-stage human T cells defined by CD45RA re-expression. *Curr Opin Immunol*. 2012 Aug;24(4):476–81.
218. Geginat J, Lanzavecchia A, Sallusto F. Proliferation and differentiation potential of human CD8+ memory T-cell subsets in response to antigen or homeostatic cytokines. *Blood*. 2003 Jun 1;101(11):4260–6.
219. Dunne PJ, Belaramani L, Fletcher JM, Fernandez de Mattos S, Lawrenz M, Soares MVD, et al. Quiescence and functional reprogramming of Epstein-Barr virus (EBV)-specific CD8+ T cells during persistent infection. *Blood*. 2005 Jul 15;106(2):558–65.
220. Callender LA, Carroll EC, Beal RWJ, Chambers ES, Nourshargh S, Akbar AN, et al. Human CD8+ EMRA T cells display a senescence-associated secretory phenotype regulated by p38 MAPK. *Aging Cell*. 2018;17(1).
221. Henson SM, Macaulay R, Riddell NE, Nunn CJ, Akbar AN. Blockade of PD-1 or p38 MAP kinase signaling enhances senescent human CD8(+) T-cell proliferation by distinct pathways. *Eur J Immunol*. 2015 May;45(5):1441–51.
222. Di Mitri D, Azevedo RI, Henson SM, Libri V, Riddell NE, Macaulay R, et al. Reversible senescence in human CD4+CD45RA+CD27- memory T cells. *J Immunol Baltim Md 1950*. 2011 Sep 1;187(5):2093–100.
223. Waller ECP, McKinney N, Hicks R, Carmichael AJ, Sissons JGP, Wills MR. Differential costimulation through CD137 (4-1BB) restores proliferation of human virus-specific ‘effector memory’ (CD28(-) CD45RA(HI)) CD8(+) T cells. *Blood*. 2007 Dec 15;110(13):4360–6.
224. Gattinoni L, Lugli E, Ji Y, Pos Z, Paulos CM, Quigley MF, et al. A human memory T cell subset with stem cell-like properties. *Nat Med*. 2011 Sep 18;17(10):1290–7.
225. Gattinoni L, Speiser DE, Lichterfeld M, Bonini C. T memory stem cells in health and disease. *Nat Med*. 2017 06;23(1):18–27.
226. Gattinoni L, Zhong XS, Palmer DC, Ji Y, Hinrichs CS, Yu Z, et al. Wnt signaling arrests effector T cell differentiation and generates CD8+ memory stem cells. *Nat Med*. 2009 Jul;15(7):808–13.
227. Li G, Yang Q, Zhu Y, Wang HR, Chen X, Zhang X, et al. T-Bet and Eomes Regulate the Balance between the Effector/Central Memory T Cells versus Memory Stem Like T Cells. *PLoS One*. 2013;8(6):e67401.
228. Chang JT, Ciocca ML, Kinjyo I, Palanivel VR, McClurkin CE, Dejong CS, et al. Asymmetric proteasome segregation as a mechanism for unequal partitioning of the transcription factor T-bet during T lymphocyte division. *Immunity*. 2011 Apr 22;34(4):492–504.

229. Mueller SN, Mackay LK. Tissue-resident memory T cells: local specialists in immune defence. *Nat Rev Immunol*. 2016 Feb;16(2):79–89.
230. Mackay LK, Rahimpour A, Ma JZ, Collins N, Stock AT, Hafon ML, et al. The developmental pathway for CD103(+)CD8+ tissue-resident memory T cells of skin. *Nat Immunol*. 2013 Dec;14(12):1294–301.
231. Gaide O, Emerson RO, Jiang X, Gulati N, Nizza S, Desmarais C, et al. Common clonal origin of central and resident memory T cells following skin immunization. *Nat Med*. 2015 Jun;21(6):647–53.
232. Schreiner D, King CG. CD4+ Memory T Cells at Home in the Tissue: Mechanisms for Health and Disease. *Front Immunol*. 2018;9:2394.
233. Catovsky D, Miliiani E, Okos A, Galton DA. Clinical significance of T-cells in chronic lymphocytic leukaemia. *Lancet Lond Engl*. 1974 Sep 28;2(7883):751–2.
234. Platsoucas CD, Galinski M, Kempin S, Reich L, Clarkson B, Good RA. Abnormal T lymphocyte subpopulations in patients with B cell chronic lymphocytic leukemia: an analysis by monoclonal antibodies. *J Immunol Baltim Md* 1950. 1982 Nov;129(5):2305–12.
235. Catovsky D, Lauria F, Matutes E, Foa R, Mantovani V, Tura S, et al. Increase in T_H Lymphocytes in B-Cell Chronic Lymphocytic Leukaemia.: II. CORRELATION WITH CLINICAL STAGE AND FINDINGS IN B-PROLYMPHOCYTIC LEUKAEMIA. *Br J Haematol*. 1981 Apr;47(4):539–44.
236. Herrmann F, Lochner A, Philippen H, Jauer B, Rühl H. Imbalance of T cell subpopulations in patients with chronic lymphocytic leukaemia of the B cell type. *Clin Exp Immunol*. 1982 Jul;49(1):157–62.
237. Matutes E, Wechsler A, Gomez R, Cherchi M, Catovsky D. Unusual T-Cell Phenotype in Advanced B-Chronic Lymphocytic Leukaemia. *Br J Haematol*. 1981 Dec;49(4):635–42.
238. McBride JA, Striker R. Imbalance in the game of T cells: What can the CD4/CD8 T-cell ratio tell us about HIV and health? Coyne CB, editor. *PLOS Pathog*. 2017 Nov 2;13(11):e1006624.
239. Wu J, Xu X, Lee EJ, Shull AY, Pei L, Awan F, et al. Phenotypic alteration of CD8+ T cells in chronic lymphocytic leukemia is associated with epigenetic reprogramming. *Oncotarget*. 2016 Jun 10;7(26):40558–70.
240. Piper KP, Karanth M, McLarnon A, Kalk E, Khan N, Murray J, et al. Chronic lymphocytic leukaemia cells drive the global CD4+ T cell repertoire towards a regulatory phenotype and leads to the accumulation of CD4+ forkhead box P3+ T cells: CLL drives T cells towards regulation. *Clin Exp Immunol*. 2011 Nov;166(2):154–63.

241. Biancotto A, Dagur PK, Fuchs JC, Wiestner A, Bagwell CB, McCoy JP. Phenotypic complexity of T regulatory subsets in patients with B-chronic lymphocytic leukemia. *Mod Pathol*. 2012 Feb;25(2):246–59.
242. De Matteis S, Molinari C, Abbati G, Rossi T, Napolitano R, Ghetti M, et al. Immunosuppressive Treg cells acquire the phenotype of effector-T cells in chronic lymphocytic leukemia patients. *J Transl Med [Internet]*. 2018 Dec [cited 2018 Aug 21];16(172). Available from: <https://translational-medicine.biomedcentral.com/articles/10.1186/s12967-018-1545-0>
243. Beyer M, Kochanek M, Darabi K, Popov A, Jensen M, Endl E, et al. Reduced frequencies and suppressive function of CD4+CD25hi regulatory T cells in patients with chronic lymphocytic leukemia after therapy with fludarabine. *Blood*. 2005 Sep 15;106(6):2018–25.
244. de Weerd I, Hofland T, de Boer R, Dobber JA, Dubois J, van Nieuwenhuize D, et al. Distinct immune composition in lymph node and peripheral blood of CLL patients is reshaped during venetoclax treatment. *Blood Adv*. 2019 Sep 10;3(17):2642–52.
245. Hus I, Bojarska-Junak A, Chocholska S, Tomczak W, Woś J, Dmoszyńska A, et al. Th17/IL-17A might play a protective role in chronic lymphocytic leukemia immunity. *PloS One*. 2013;8(11):e78091.
246. Ahearne MJ, Willimott S, Piñon L, Kennedy DB, Miall F, Dyer MJS, et al. Enhancement of CD154/IL4 proliferation by the T follicular helper (Tfh) cytokine, IL21 and increased numbers of circulating cells resembling Tfh cells in chronic lymphocytic leukaemia. *Br J Haematol*. 2013 Aug;162(3):360–70.
247. Qiu L, Zhou Y, Yu Q, Zheng S, Wang Z, Huang Q. Elevated levels of follicular T helper cells and their association with therapeutic effects in patients with chronic lymphocytic leukaemia. *Immunol Lett*. 2018;197:15–28.
248. Porakishvili N, Roschupkina T, Kalber T, Jewell AP, Patterson K, Yong K, et al. Expansion of CD4+ T cells with a cytotoxic phenotype in patients with B-chronic lymphocytic leukaemia (B-CLL). *Clin Exp Immunol*. 2001 Oct;126(1):29–36.
249. Monserrat J, Sánchez MÁ, de Paz R, Díaz D, Mur S, Reyes E, et al. Distinctive patterns of naïve/memory subset distribution and cytokine expression in CD4 T lymphocytes in ZAP-70 B-chronic lymphocytic patients: Cytokine Production by CD4 T Cells from B-CLL. *Cytometry B Clin Cytom*. 2014 Jan;86(1):32–43.
250. Peller S, Kaufman S. Decreased CD45RA T cells in B-cell chronic lymphatic leukemia patients: correlation with disease stage. *Blood*. 1991 Sep 15;78(6):1569–73.

251. Serrano D, Monteiro J, Allen SL, Kolitz J, Schulman P, Lichtman SM, et al. Clonal expansion within the CD4+CD57+ and CD8+CD57+ T cell subsets in chronic lymphocytic leukemia. *J Immunol Baltim Md* 1950. 1997 Feb 1;158(3):1482–9.
252. Tinhofer I, Weiss L, Gassner F, Rubenzer G, Holler C, Greil R. Difference in the Relative Distribution of CD4+ T-cell Subsets in B-CLL With Mutated and Unmutated Immunoglobulin (Ig) VH Genes: Implication for the Course of Disease. *J Immunother*. 2009 Apr;32(3):302–9.
253. Koch S, Larbi A, Derhovanessian E, Ozcelik D, Naumova E, Pawelec G. Multiparameter flow cytometric analysis of CD4 and CD8 T cell subsets in young and old people. *Immun Ageing A*. 2008 Jul 25;5:6.
254. Wikby A, Månsson IA, Johansson B, Strindhall J, Nilsson SE. The immune risk profile is associated with age and gender: findings from three Swedish population studies of individuals 20–100 years of age. *Biogerontology*. 2008 Oct;9(5):299–308.
255. Gonzalez-Rodriguez AP, Contesti J, Huergo-Zapico L, Lopez-Soto A, Fernández-Guizán A, Acebes-Huerta A, et al. Prognostic significance of CD8 and CD4 T cells in chronic lymphocytic leukemia. *Leuk Lymphoma*. 2010 Oct;51(10):1829–36.
256. Elston L, Fegan C, Hills R, Hashimdeen SS, Walsby E, Henley P, et al. Increased frequency of CD4+PD-1+HLA-DR+ T cells is associated with disease progression in CLL. *Br J Haematol*. 2020;188(6):872–80.
257. Wikby A, Johansson B, Olsson J, Löfgren S, Nilsson BO, Ferguson F. Expansions of peripheral blood CD8 T-lymphocyte subpopulations and an association with cytomegalovirus seropositivity in the elderly: the Swedish NONA immune study. *Exp Gerontol*. 2002 Mar;37(2–3):445–53.
258. Riches JC, Davies JK, McClanahan F, Fatah R, Iqbal S, Agrawal S, et al. T cells from CLL patients exhibit features of T-cell exhaustion but retain capacity for cytokine production. *Blood*. 2013 Feb 28;121(9):1612–21.
259. Hanna BS, Roessner PM, Yazdanparast H, Colomer D, Campo E, Kugler S, et al. Control of chronic lymphocytic leukemia development by clonally-expanded CD8+ T-cells that undergo functional exhaustion in secondary lymphoid tissues. *Leukemia*. 2019 Mar;33(3):625–37.
260. Wherry EJ. T cell exhaustion. *Nat Immunol*. 2011 Jun;12(6):492–9.
261. Day CL, Kaufmann DE, Kiepiela P, Brown JA, Moodley ES, Reddy S, et al. PD-1 expression on HIV-specific T cells is associated with T-cell exhaustion and disease progression. *Nature*. 2006 Sep 21;443(7109):350–4.
262. Ahmadzadeh M, Johnson LA, Heemskerk B, Wunderlich JR, Dudley ME, White DE, et al. Tumor antigen-specific CD8 T cells infiltrating the tumor express high

- levels of PD-1 and are functionally impaired. *Blood*. 2009 Aug 20;114(8):1537–44.
263. Giannopoulos K. Targeting Immune Signaling Checkpoints in Acute Myeloid Leukemia. *J Clin Med*. 2019 Feb 12;8(2).
264. Pardoll DM. The blockade of immune checkpoints in cancer immunotherapy. *Nat Rev Cancer*. 2012 Mar 22;12(4):252–64.
265. Seidel JA, Otsuka A, Kabashima K. Anti-PD-1 and Anti-CTLA-4 Therapies in Cancer: Mechanisms of Action, Efficacy, and Limitations. *Front Oncol*. 2018;8:86.
266. European Medicines Agency. Keytruda. 2015 Jul. Report No.: EMEA/H/C/003820.
267. Brusa D, Serra S, Coscia M, Rossi D, D’Arena G, Laurenti L, et al. The PD-1/PD-L1 axis contributes to T-cell dysfunction in chronic lymphocytic leukemia. *Haematologica*. 2013 Jun;98(6):953–63.
268. Palma M, Gentilcore G, Heimersson K, Mozaffari F, Näsman-Glaser B, Young E, et al. T cells in chronic lymphocytic leukemia display dysregulated expression of immune checkpoints and activation markers. *Haematologica*. 2017 Mar;102(3):562–72.
269. te Raa GD, Pascutti MF, García-Vallejo JJ, Reinen E, Remmerswaal EBM, ten Berge IJM, et al. CMV-specific CD8+ T-cell function is not impaired in chronic lymphocytic leukemia. *Blood*. 2014 Jan 30;123(5):717–24.
270. Ding W, LaPlant BR, Call TG, Parikh SA, Leis JF, He R, et al. Pembrolizumab in patients with CLL and Richter transformation or with relapsed CLL. *Blood*. 2017 Jun 29;129(26):3419–27.
271. Duraiswamy J, Ibegbu CC, Masopust D, Miller JD, Araki K, Doho GH, et al. Phenotype, Function, and Gene Expression Profiles of Programmed Death-1hi CD8 T Cells in Healthy Human Adults. *J Immunol Baltim Md 1950*. 2011 Apr 1;186(7):4200–12.
272. Tötterman TH, Carlsson M, Simonsson B, Bengtsson M, Nilsson K. T-cell activation and subset patterns are altered in B-CLL and correlate with the stage of the disease. *Blood*. 1989 Aug 1;74(2):786–92.
273. Legat A, Speiser DE, Pircher H, Zehn D, Fuertes Marraco SA. Inhibitory Receptor Expression Depends More Dominantly on Differentiation and Activation than ‘Exhaustion’ of Human CD8 T Cells. *Front Immunol*. 2013;4:455.

-
274. Roederer M, Nozzi J, Nason M. SPICE: Exploration and Analysis of Post-Cytometric Complex Multivariate Datasets. *Cytom Part J Int Soc Anal Cytol*. 2011 Feb;79(2):167–74.
275. R Core Team. R: A language and environment for statistical computing. [Internet]. R Foundation for Statistical Computing, Vienna, Austria; 2013. Available from: <http://www.R-project.org/>
276. Carvalho BS, Irizarry RA. A framework for oligonucleotide microarray preprocessing. *Bioinformatics*. 2010 Oct 1;26(19):2363–7.
277. Irizarry RA. Exploration, normalization, and summaries of high density oligonucleotide array probe level data. *Biostatistics*. 2003 Apr 1;4(2):249–64.
278. Ritchie ME, Phipson B, Wu D, Hu Y, Law CW, Shi W, et al. limma powers differential expression analyses for RNA-sequencing and microarray studies. *Nucleic Acids Res*. 2015 Apr 20;43(7):e47–e47.
279. Smyth GK. Linear Models and Empirical Bayes Methods for Assessing Differential Expression in Microarray Experiments. *Stat Appl Genet Mol Biol*. 2004 Jan 12;3(1):1–25.
280. Benjamini Y, Hochberg Y. Controlling the False Discovery Rate: A Practical and Powerful Approach to Multiple Testing. *J R Stat Soc Ser B Methodol*. 1995 Jan;57(1):289–300.
281. MacDonald, James W. *hugene20sttranscriptcluster.db: Affymetrix hugene20 annotation data (chip hugene20sttranscriptcluster)*. 2017.
282. Ye J, Coulouris G, Zaretskaya I, Cutcutache I, Rozen S, Madden TL. Primer-BLAST: A tool to design target-specific primers for polymerase chain reaction. *BMC Bioinformatics*. 2012 Jun 18;13:134.
283. Altschul SF, Gish W, Miller W, Myers EW, Lipman DJ. Basic local alignment search tool. *J Mol Biol*. 1990 Oct;215(3):403–10.
284. Gallagher KME, Man S. Identification of HLA-DR1- and HLA-DR15-restricted human papillomavirus type 16 (HPV16) and HPV18 E6 epitopes recognized by CD4+ T cells from healthy young women. *J Gen Virol*. 2007 May 1;88(5):1470–8.
285. Elston L. Exploring the role of CD8+ T-cells in Chronic Lymphocytic Leukaemia [Doctor of Philosophy]. Cardiff University; 2016.
286. Agata Y, Kawasaki A, Nishimura H, Ishida Y, Tsubat T, Yagita H, et al. Expression of the PD-1 antigen on the surface of stimulated mouse T and B lymphocytes. *Int Immunol*. 1996;8(5):765–72.

287. Gerdes J, Lemke H, Baisch H, Wacker HH, Schwab U, Stein H. Cell cycle analysis of a cell proliferation-associated human nuclear antigen defined by the monoclonal antibody Ki-67. *J Immunol Baltim Md* 1950. 1984 Oct;133(4):1710–5.
288. Halle S, Halle O, Förster R. Mechanisms and Dynamics of T Cell-Mediated Cytotoxicity In Vivo. *Trends Immunol*. 2017 Jun;38(6):432–43.
289. Takeuchi A, Saito T. CD4 CTL, a Cytotoxic Subset of CD4+ T Cells, Their Differentiation and Function. *Front Immunol* [Internet]. 2017 Feb 23 [cited 2019 Jun 26];8. Available from: <http://journal.frontiersin.org/article/10.3389/fimmu.2017.00194/full>
290. Takeuchi A, Badr MESG, Miyauchi K, Ishihara C, Onishi R, Guo Z, et al. CRTAM determines the CD4+ cytotoxic T lymphocyte lineage. *J Exp Med*. 2016 Jan 11;213(1):123–38.
291. Man S, Lechler RI, Batchelor JR, Sharrock CE. Individual variation in the frequency of HLA class II-specific cytotoxic T lymphocyte precursors. *Eur J Immunol*. 1990 Apr;20(4):847–54.
292. Wang Z, Zhu L, Nguyen THO, Wan Y, Sant S, Quiñones-Parra SM, et al. Clonally diverse CD38+HLA-DR+CD8+ T cells persist during fatal H7N9 disease. *Nat Commun* [Internet]. 2018 Dec [cited 2020 Apr 28];9(1). Available from: <http://www.nature.com/articles/s41467-018-03243-7>
293. Kared H, Martelli S, Ng TP, Pender SLF, Larbi A. CD57 in human natural killer cells and T-lymphocytes. *Cancer Immunol Immunother*. 2016 Apr;65(4):441–52.
294. Anderson AC, Joller N, Kuchroo VK. Lag-3, Tim-3, and TIGIT: Co-inhibitory Receptors with Specialized Functions in Immune Regulation. *Immunity*. 2016 May;44(5):989–1004.
295. Wajant H. Therapeutic targeting of CD70 and CD27. *Expert Opin Ther Targets*. 2016 Aug;20(8):959–73.
296. Nagai S, Azuma M. The CD28-B7 Family of Co-signaling Molecules. *Adv Exp Med Biol*. 2019;1189:25–51.
297. Larbi A, Fulop T. From ‘truly naïve’ to ‘exhausted senescent’ T cells: when markers predict functionality. *Cytom Part J Int Soc Anal Cytol*. 2014 Jan;85(1):25–35.
298. Appay V, van Lier RAW, Sallusto F, Roederer M. Phenotype and function of human T lymphocyte subsets: consensus and issues. *Cytom Part J Int Soc Anal Cytol*. 2008 Nov;73(11):975–83.

-
299. Xu W, Larbi A. Markers of T Cell Senescence in Humans. *Int J Mol Sci*. 2017 Aug 10;18(8).
 300. Crespo M, Bosch F, Villamor N, Bellosillo B, Colomer D, Rozman M, et al. ZAP-70 Expression as a Surrogate for Immunoglobulin-Variable-Region Mutations in Chronic Lymphocytic Leukemia. *N Engl J Med*. 2003 May;348(18):1764–75.
 301. Zhang S, Kipps TJ. The Pathogenesis of Chronic Lymphocytic Leukemia. *Annu Rev Pathol*. 2014;9:103–18.
 302. Kaech SM, Wherry EJ, Ahmed R. Effector and memory T-cell differentiation: implications for vaccine development. *Nat Rev Immunol*. 2002 Apr;2(4):251–62.
 303. Vela CM, McBride A, Jaglowski SM, Andritsos LA. Ibrutinib for treatment of chronic lymphocytic leukemia. *Am J Health Syst Pharm*. 2016 Mar 15;73(6):367–75.
 304. Man S, Henley P. Chronic lymphocytic leukaemia: the role of T cells in a B cell disease. *Br J Haematol* [Internet]. [cited 2019 Jun 18];0(0). Available from: <https://onlinelibrary.wiley.com/doi/abs/10.1111/bjh.15918>
 305. Haanen JB, Toebes M, Cordaro TA, Wolkers MC, Kruisbeek AM, Schumacher TN. Systemic T cell expansion during localized viral infection. *Eur J Immunol*. 1999;29(4):1168–74.
 306. Lindqvist CA, Christiansson LH, Thörn I, Mangsbo S, Paul-Wetterberg G, Sundström C, et al. Both CD4+ FoxP3+ and CD4+ FoxP3– T cells from patients with B-cell malignancy express cytolytic markers and kill autologous leukaemic B cells in vitro. *Immunology*. 2011 Jul;133(3):296–306.
 307. Ramsay AG, Clear AJ, Fatah R, Gribben JG. Multiple inhibitory ligands induce impaired T-cell immunologic synapse function in chronic lymphocytic leukemia that can be blocked with lenalidomide: establishing a reversible immune evasion mechanism in human cancer. *Blood*. 2012 Aug 16;120(7):1412–21.
 308. Ramsay AG, Johnson AJ, Lee AM, Gorgün G, Le Dieu R, Blum W, et al. Chronic lymphocytic leukemia T cells show impaired immunological synapse formation that can be reversed with an immunomodulating drug. *J Clin Invest* [Internet]. 2008 Jun 1 [cited 2018 Aug 23]; Available from: <http://www.jci.org/articles/view/35017>
 309. Ramsay AG, Gribben JG. Immune dysfunction in chronic lymphocytic leukemia T cells and lenalidomide as an immunomodulatory drug. *Haematologica*. 2009 Sep;94(9):1198–202.
 310. Dustin ML. The immunological synapse. *Cancer Immunol Res*. 2014 Nov;2(11):1023–33.

311. Dieckmann NMG, Frazer GL, Asano Y, Stinchcombe JC, Griffiths GM. The cytotoxic T lymphocyte immune synapse at a glance. *J Cell Sci.* 2016 Aug 1;129(15):2881–6.
312. Fuertes Marraco SA, Neubert NJ, Verdeil G, Speiser DE. Inhibitory Receptors Beyond T Cell Exhaustion. *Front Immunol* [Internet]. 2015 Jun 26 [cited 2018 Aug 22];6. Available from: <http://journal.frontiersin.org/Article/10.3389/fimmu.2015.00310/abstract>
313. Chew GM, Fujita T, Webb GM, Burwitz BJ, Wu HL, Reed JS, et al. TIGIT Marks Exhausted T Cells, Correlates with Disease Progression, and Serves as a Target for Immune Restoration in HIV and SIV Infection. Silvestri G, editor. *PLOS Pathog.* 2016 Jan 7;12(1):e1005349.
314. Josefsson SE, Huse K, Kolstad A, Beiske K, Pende D, Steen CB, et al. T Cells Expressing Checkpoint Receptor TIGIT Are Enriched in Follicular Lymphoma Tumors and Characterized by Reversible Suppression of T-cell Receptor Signaling. *Clin Cancer Res.* 2018 Feb 15;24(4):870–81.
315. Guillerey C, Harjunpää H, Carrié N, Kassem S, Teo T, Miles K, et al. TIGIT immune checkpoint blockade restores CD8+ T cell immunity against multiple myeloma. *Blood.* 2018 Jul 9;blood-2018-01-825265.
316. Kong Y, Zhu L, Schell TD, Zhang J, Claxton DF, Ehmann WC, et al. T-Cell Immunoglobulin and ITIM Domain (TIGIT) Associates with CD8+ T-Cell Exhaustion and Poor Clinical Outcome in AML Patients. *Clin Cancer Res.* 2016 Jun 15;22(12):3057–66.
317. Catakovic K, Gassner FJ, Ratswohl C, Zaborsky N, Rebhandl S, Schubert M, et al. TIGIT expressing CD4+T cells represent a tumor-supportive T cell subset in chronic lymphocytic leukemia. *Oncolimmunology.* 2018 Jan 2;7(1):e1371399.
318. Os A, Bürgler S, Ribes AP, Funderud A, Wang D, Thompson KM, et al. Chronic Lymphocytic Leukemia Cells Are Activated and Proliferate in Response to Specific T Helper Cells. *Cell Rep.* 2013 Aug;4(3):566–77.
319. Bagnara D, Kaufman MS, Calissano C, Marsilio S, Patten PEM, Simone R, et al. A novel adoptive transfer model of chronic lymphocytic leukemia suggests a key role for T lymphocytes in the disease. *Blood.* 2011 May 19;117(20):5463–72.
320. Tinhofer I, Rubenzer G, Holler C, Hofstaetter E, Stoecher M, Egle A, et al. Expression levels of CD38 in T cells predict course of disease in male patients with B-chronic lymphocytic leukemia. *Blood.* 2006 Nov 1;108(9):2950–6.
321. Parry RV, Chemnitz JM, Frauwirth KA, Lanfranco AR, Braunstein I, Kobayashi SV, et al. CTLA-4 and PD-1 Receptors Inhibit T-Cell Activation by Distinct Mechanisms. *Mol Cell Biol.* 2005 Nov 1;25(21):9543–53.

322. Eller MA, Blom KG, Gonzalez VD, Eller LA, Naluyima P, Laeyendecker O, et al. Innate and Adaptive Immune Responses Both Contribute to Pathological CD4 T Cell Activation in HIV-1 Infected Ugandans. Ndhlovu LC, editor. PLoS ONE. 2011 Apr 19;6(4):e18779.
323. Göthert JR, Eisele L, Klein-Hitpass L, Weber S, Zesewitz ML, Sellmann L, et al. Expanded CD8+ T cells of murine and human CLL are driven into a senescent KLRG1+ effector memory phenotype. Cancer Immunol Immunother. 2013 Nov;62(11):1697–709.
324. Pawelec G. Immune parameters associated with mortality in the elderly are context-dependent: lessons from Sweden, Holland and Belgium. Biogerontology [Internet]. 2017 Nov 28 [cited 2018 Aug 24]; Available from: <http://link.springer.com/10.1007/s10522-017-9739-z>
325. Pawelec G. Immune signatures associated with mortality differ in elderly populations from different birth cohorts and countries even within northern Europe. Mech Ageing Dev [Internet]. 2018 Apr 11 [cited 2018 Aug 24]; Available from: <https://linkinghub.elsevier.com/retrieve/pii/S004763741830054X>
326. Pawelec G. Does patient age influence anti-cancer immunity? Semin Immunopathol [Internet]. 2018 Jul 13 [cited 2018 Aug 24]; Available from: <http://link.springer.com/10.1007/s00281-018-0697-6>
327. Rusak M, Eljaszewicz A, Bołkun Ł, Łuksza E, Łapuć I, Piszcz J, et al. Prognostic significance of PD-1 expression on peripheral blood CD4+ T cells in patients with newly diagnosed chronic lymphocytic leukemia. Pol Arch Intern Med. 2015 Jul 3;125(7–8):553–9.
328. Alés-Martínez JoséE, Alvarez-Mon M, Merino F, Bonilla F, Martínez-A C, Durántez A, et al. Decreased TcR-CD3+ T cell numbers in healthy aged humans. Evidence that T cell defects are masked by a reciprocal increase of TcR-CD3–CD2+ natural killer cells. Eur J Immunol. 1988 Nov;18(11):1827–30.
329. Gribben JG. How I treat CLL up front. Blood. 2010 Jan 14;115(2):187–97.
330. Strindhall J, Löfgren S, Främsth C, Matussek A, Bengner M, Ernerudh J, et al. CD4/CD8 ratio < 1 is associated with lymphocyte subsets, CMV and gender in 71-year old individuals: 5-Year follow-up of the Swedish HEXA Immune Longitudinal Study. Exp Gerontol. 2017 Sep;95:82–7.
331. Niemann CU, Herman SEM, Maric I, Gomez-Rodriguez J, Biancotto A, Chang BY, et al. Disruption of in vivo chronic lymphocytic leukemia tumor-microenvironment interactions by ibrutinib – findings from an investigator initiated phase 2 study. Clin Cancer Res Off J Am Assoc Cancer Res. 2016 Apr 1;22(7):1572–82.

332. Long M, Beckwith K, Do P, Mundy BL, Gordon A, Lehman AM, et al. Ibrutinib treatment improves T cell number and function in CLL patients. *J Clin Invest*. 2017 Jul 17;127(8):3052–64.
333. Parry HM, Mirajkar N, Cutmore N, Zuo J, Long H, Kwok M, et al. Long-Term Ibrutinib Therapy Reverses CD8+ T Cell Exhaustion in B Cell Chronic Lymphocytic Leukaemia. *Front Immunol* [Internet]. 2019 Dec 12 [cited 2019 Dec 17];10. Available from: <https://www.frontiersin.org/article/10.3389/fimmu.2019.02832/full>
334. Ahn IE, Jerussi T, Farooqui M, Tian X, Wiestner A, Gea-Banacloche J. Atypical *Pneumocystis jirovecii* pneumonia in previously untreated patients with CLL on single-agent ibrutinib. *Blood*. 2016 Oct 13;128(15):1940–3.
335. Chamilos G, Lionakis MS, Kontoyiannis DP. Call for Action: Invasive Fungal Infections Associated With Ibrutinib and Other Small Molecule Kinase Inhibitors Targeting Immune Signaling Pathways. *Clin Infect Dis Off Publ Infect Dis Soc Am*. 2018 Jan 1;66(1):140–8.
336. McKinney EF, Lyons PA, Carr EJ, Hollis JL, Jayne DRW, Willcocks LC, et al. A CD8+ T cell transcription signature predicts prognosis in autoimmune disease. *Nat Med*. 2010 May;16(5):586–91.
337. Krämer A, Green J, Pollard J, Tugendreich S. Causal analysis approaches in Ingenuity Pathway Analysis. *Bioinforma Oxf Engl*. 2014 Feb 15;30(4):523–30.
338. Brown TJ, Rowe JM, Liu JW, Shoyab M. Regulation of IL-6 expression by oncostatin M. *J Immunol Baltim Md 1950*. 1991 Oct 1;147(7):2175–80.
339. Santofimia-Castaño P, Lan W, Bintz J, Gayet O, Carrier A, Lomber G, et al. Inactivation of NUPR1 promotes cell death by coupling ER-stress responses with necrosis. *Sci Rep*. 2018 Dec;8(1):16999.
340. Yigit B, Wang N, ten Hacken E, Chen SS, Bhan AK, Suarez-Fueyo A, et al. SLAMF6 as a Regulator of Exhausted CD8+ T Cells in Cancer. *Cancer Immunol Res*. 2019 Sep;7(9):1485–96.
341. Hajaj E, Eisenberg G, Klein S, Frankenburg S, Merims S, Ben David I, et al. SLAMF6 deficiency augments tumor killing and skews toward an effector phenotype revealing it as a novel T cell checkpoint. *eLife* [Internet]. 2020 Mar 3 [cited 2021 Feb 4];9. Available from: <https://elifesciences.org/articles/52539>
342. Jiang Z, Johnson HJ, Nie H, Qin J, Bird TA, Li X. Pellino 1 Is Required for Interleukin-1 (IL-1)-mediated Signaling through Its Interaction with the IL-1 Receptor-associated Kinase 4 (IRAK4)-IRAK-Tumor Necrosis Factor Receptor-associated Factor 6 (TRAF6) Complex. *J Biol Chem*. 2003 Mar;278(13):10952–6.

343. Butler MP, Hanly JA, Moynagh PN. Kinase-active Interleukin-1 Receptor-associated Kinases Promote Polyubiquitination and Degradation of the Pellino Family. *J Biol Chem*. 2007 Oct;282(41):29729–37.
344. Yun S, Lee SH, Yoon SR, Kim MS, Piao ZH, Myung PK, et al. TOX regulates the differentiation of human natural killer cells from hematopoietic stem cells in vitro. *Immunol Lett*. 2011 Apr;136(1):29–36.
345. Bordon Y. TOX for tired T cells. *Nat Rev Immunol*. 2019 Aug;19(8):476–476.
346. Sekine T, Perez-Potti A, Nguyen S, Gorin JB, Wu VH, Gostick E, et al. TOX is expressed by exhausted and polyfunctional human effector memory CD8+ T cells. *Sci Immunol*. 2020 Jul 3;5(49):eaba7918.
347. Ono C, Yu Z, Kasahara Y, Kikuchi Y, Ishii N, Tomita H. Fluorescently Activated Cell Sorting Followed by Microarray Profiling of Helper T Cell Subtypes from Human Peripheral Blood. Shiku H, editor. *PLoS ONE*. 2014 Nov 7;9(11):e111405.
348. Ghatalia P, Gordetsky J, Kuo F, Dulaimi E, Cai KQ, Devarajan K, et al. Prognostic impact of immune gene expression signature and tumor infiltrating immune cells in localized clear cell renal cell carcinoma. *J Immunother Cancer*. 2019 Dec;7(1):139.
349. Greenough TC, Straubhaar JR, Kamga L, Weiss ER, Brody RM, McManus MM, et al. A Gene Expression Signature That Correlates with CD8+ T Cell Expansion in Acute EBV Infection. *J Immunol*. 2015 Nov 1;195(9):4185–97.
350. Barsheshet Y, Wildbaum G, Levy E, Vitenshtein A, Akinseye C, Griggs J, et al. CCR8+ FOXP3+ Treg cells as master drivers of immune regulation. *Proc Natl Acad Sci*. 2017 Jun 6;114(23):6086–91.
351. Takeuchi Y, Nishikawa H. Roles of regulatory T cells in cancer immunity. *Int Immunol*. 2016 Aug;28(8):401–9.
352. Guo B, Zhang L, Chiorazzi N, Rothstein TL. IL-4 rescues surface IgM expression in chronic lymphocytic leukemia. *Blood*. 2016 Jul 28;128(4):553–62.
353. Lucas S, Ghilardi N, Li J, de Sauvage FJ. IL-27 regulates IL-12 responsiveness of naive CD4+ T cells through Stat1-dependent and -independent mechanisms. *Proc Natl Acad Sci*. 2003 Dec 9;100(25):15047–52.
354. Kaiko GE, Horvat JC, Beagley KW, Hansbro PM. Immunological decision-making: how does the immune system decide to mount a helper T-cell response? *Immunology*. 2008 Mar;123(3):326–38.
355. Gruarin P, Maglie S, Simone M, Häringer B, Vasco C, Ranzani V, et al. Eomesodermin controls a unique differentiation program in human IL-10 and IFN- γ coproducing regulatory T cells. *Eur J Immunol*. 2019 Jan;49(1):96–111.

356. Roessner PM, Llaó Cid L, Lupar E, Roeder T, Bordas M, Schifflers C, et al. EOMES and IL-10 regulate antitumor activity of T regulatory type 1 CD4+ T cells in chronic lymphocytic leukemia. *Leukemia* [Internet]. 2021 Feb 1 [cited 2021 May 20]; Available from: <http://www.nature.com/articles/s41375-021-01136-1>
357. Bonnal RJP, Rossetti G, Lugli E, De Simone M, Gruarin P, Brummelman J, et al. Clonally expanded EOMES+ Tr1-like cells in primary and metastatic tumors are associated with disease progression. *Nat Immunol*. 2021 Jun;22(6):735–45.
358. Zhan T, Rindtorff N, Boutros M. Wnt signaling in cancer. *Oncogene*. 2017 Mar;36(11):1461–73.
359. Lu D, Zhao Y, Tawatao R, Cottam HB, Sen M, Leoni LM, et al. Activation of the Wnt signaling pathway in chronic lymphocytic leukemia. *Proc Natl Acad Sci*. 2004 Mar 2;101(9):3118–23.
360. Luis TC, Ichii M, Brugman MH, Kincade P, Staal FJT. Wnt signaling strength regulates normal hematopoiesis and its deregulation is involved in leukemia development. *Leukemia*. 2012 Mar;26(3):414–21.
361. Wang L, Shalek AK, Lawrence M, Ding R, Gaublomme JT, Pochet N, et al. Somatic mutation as a mechanism of Wnt/ β -catenin pathway activation in CLL. *Blood*. 2014 Aug 14;124(7):1089–98.
362. Notani D, Gottimukkala KP, Jayani RS, Limaye AS, Damle MV, Mehta S, et al. Global Regulator SATB1 Recruits β -Catenin and Regulates TH2 Differentiation in Wnt-Dependent Manner. Nusse R, editor. *PLoS Biol*. 2010 Jan 26;8(1):e1000296.
363. Windt GJW, Pearce EL. Metabolic switching and fuel choice during T-cell differentiation and memory development. *Immunol Rev*. 2012 Sep;249(1):27–42.
364. Wang R, Dillon CP, Shi LZ, Milasta S, Carter R, Finkelstein D, et al. The Transcription Factor Myc Controls Metabolic Reprogramming upon T Lymphocyte Activation. *Immunity*. 2011 Dec;35(6):871–82.
365. Almeida L, Lochner M, Berod L, Sparwasser T. Metabolic pathways in T cell activation and lineage differentiation. *Semin Immunol*. 2016 Oct;28(5):514–24.
366. Vardhana SA, Hwee MA, Berisa M, Wells DK, Yost KE, King B, et al. Impaired mitochondrial oxidative phosphorylation limits the self-renewal of T cells exposed to persistent antigen. *Nat Immunol*. 2020 Sep;21(9):1022–33.
367. Fox CJ, Hammerman PS, Thompson CB. Fuel feeds function: energy metabolism and the T-cell response. *Nat Rev Immunol*. 2005 Nov;5(11):844–52.

368. Delgoffe GM, Kole TP, Zheng Y, Zarek PE, Matthews KL, Xiao B, et al. The mTOR Kinase Differentially Regulates Effector and Regulatory T Cell Lineage Commitment. *Immunity*. 2009 Jun;30(6):832–44.
369. Catakovic K, Klieser E, Neureiter D, Geisberger R. T cell exhaustion: from pathophysiological basics to tumor immunotherapy. *Cell Commun Signal* [Internet]. 2017 Dec [cited 2018 Aug 22];15(1). Available from: <http://biosignaling.biomedcentral.com/articles/10.1186/s12964-016-0160-z>
370. Inozume T, Hanada K ichi, Wang QJ, Ahmadzadeh M, Wunderlich JR, Rosenberg SA, et al. Selection of CD8+PD-1+ Lymphocytes in Fresh Human Melanomas Enriches for Tumor-reactive T Cells. *J Immunother*. 2010 Nov;33(9):956–64.
371. Arakaki R, Yamada A, Kudo Y, Hayashi Y, Ishimaru N. Mechanism of Activation-Induced Cell Death of T Cells and Regulation of FasL Expression. *Crit Rev Immunol*. 2014;34(4):301–14.
372. Parry HM, Zuo J, Frumento G, Mirajkar N, Inman C, Edwards E, et al. Cytomegalovirus viral load within blood increases markedly in healthy people over the age of 70 years. *Immun Ageing*. 2016 Dec;13(1):1.
373. Subramanian A, Tamayo P, Mootha VK, Mukherjee S, Ebert BL, Gillette MA, et al. Gene set enrichment analysis: A knowledge-based approach for interpreting genome-wide expression profiles. *Proc Natl Acad Sci*. 2005 Oct 25;102(43):15545–50.
374. Palmer BE, Blyveis N, Fontenot AP, Wilson CC. Functional and phenotypic characterization of CD57+CD4+ T cells and their association with HIV-1-induced T cell dysfunction. *J Immunol Baltim Md 1950*. 2005 Dec 15;175(12):8415–23.
375. Dardalhon V, Awasthi A, Kwon H, Galileos G, Gao W, Sobel RA, et al. IL-4 inhibits TGF- β -induced Foxp3+ T cells and, together with TGF- β , generates IL-9+ IL-10+ Foxp3– effector T cells. *Nat Immunol*. 2008 Dec;9(12):1347–55.
376. Veldhoen M, Uyttenhove C, van Snick J, Helmby H, Westendorf A, Buer J, et al. Transforming growth factor- β ‘reprograms’ the differentiation of T helper 2 cells and promotes an interleukin 9–producing subset. *Nat Immunol*. 2008 Dec;9(12):1341–6.
377. Lu Y, Wang Q, Xue G, Bi E, Ma X, Wang A, et al. Th9 Cells Represent a Unique Subset of CD4+ T Cells Endowed with the Ability to Eradicate Advanced Tumors. *Cancer Cell*. 2018 Jun;33(6):1048-1060.e7.
378. Yigit B, Halibocek PJ, Chen SS, O’Keeffe MS, Arnason J, Avigan D, et al. A combination of an anti-SLAMF6 antibody and ibrutinib efficiently abrogates expansion of chronic lymphocytic leukemia cells. *Oncotarget*. 2016 May 3;7(18):26346–60.

379. Alfei F, Kanev K, Hofmann M, Wu M, Ghoneim HE, Roelli P, et al. TOX reinforces the phenotype and longevity of exhausted T cells in chronic viral infection. *Nature*. 2019 Jul;571(7764):265–9.
380. Khan O, Giles JR, McDonald S, Manne S, Ngiow SF, Patel KP, et al. TOX transcriptionally and epigenetically programs CD8+ T cell exhaustion. *Nature*. 2019 Jul;571(7764):211–8.
381. Heim K, Binder B, Sagar, Wieland D, Hensel N, Llewellyn-Lacey S, et al. TOX defines the degree of CD8+ T cell dysfunction in distinct phases of chronic HBV infection. *Gut*. 2020 Oct 23;gutjnl-2020-322404.
382. Yi JS, Cox MA, Zajac AJ. T-cell exhaustion: characteristics, causes and conversion. *Immunology*. 2010 Apr;129(4):474–81.
383. Sandvig S, Laskay T, Andersson J, Ley M, Andersson U. Gamma-Interferon is Produced by CD3+ and CD3- Lymphocytes. *Immunol Rev*. 1987 Jun;97(1):51–65.
384. Carlsson R, Sjögren HO. Kinetics of IL-2 and interferon- γ production, expression of IL-2 receptors, and cell proliferation in human mononuclear cells exposed to staphylococcal enterotoxin A. *Cell Immunol*. 1985 Nov;96(1):175–83.
385. DeForge LE, Remick DG. Kinetics of TNF, IL-6, and IL-8 gene expression in LPS-stimulated human whole blood. *Biochem Biophys Res Commun*. 1991 Jan;174(1):18–24.
386. Wherry EJ, Blattman JN, Murali-Krishna K, van der Most R, Ahmed R. Viral Persistence Alters CD8 T-Cell Immunodominance and Tissue Distribution and Results in Distinct Stages of Functional Impairment. *J Virol*. 2003 Apr 15;77(8):4911–27.
387. Green DR, Droin N, Pinkoski M. Activation-induced cell death in T cells. *Immunol Rev*. 2003 Jun;193(1):70–81.
388. van Engeland M, Nieland LJW, Ramaekers FCS, Schutte B, Reutelingsperger CPM. Annexin V-Affinity assay: A review on an apoptosis detection system based on phosphatidylserine exposure. *Cytometry*. 1998 Jan 1;31(1):1–9.
389. Seo H, Chen J, González-Avalos E, Samaniego-Castruita D, Das A, Wang YH, et al. TOX and TOX2 transcription factors cooperate with NR4A transcription factors to impose CD8+ T cell exhaustion. *Proc Natl Acad Sci*. 2019 Jun 18;116(25):12410–5.
390. Mestas J, Hughes CCW. Of Mice and Not Men: Differences between Mouse and Human Immunology. *J Immunol*. 2004 Mar 1;172(5):2731–8.

391. Kim K, Park S, Park SY, Kim G, Park SM, Cho JW, et al. Single-cell transcriptome analysis reveals TOX as a promoting factor for T cell exhaustion and a predictor for anti-PD-1 responses in human cancer. *Genome Med.* 2020 Dec;12(1):22.
392. Scott AC, Dündar F, Zumbo P, Chandran SS, Klebanoff CA, Shakiba M, et al. TOX is a critical regulator of tumour-specific T cell differentiation. *Nature.* 2019 Jul;571(7764):270–4.
393. Utzschneider DT, Kallies A. Human effector T cells express TOX—Not so “TOX”ic after all. *Sci Immunol.* 2020 Jul 3;5(49):eabc8272.
394. Kayser S, Levis MJ. Clinical implications of molecular markers in acute myeloid leukemia. *Eur J Haematol.* 2019 Jan;102(1):20–35.
395. Moorman AV. New and emerging prognostic and predictive genetic biomarkers in B-cell precursor acute lymphoblastic leukemia. *Haematologica.* 2016 Apr;101(4):407–16.
396. Li H, Yi SH, Xiong WJ, Liu HM, Lyu R, Wang TY, et al. Chronic Lymphocytic Leukemia Prognostic Index: A New Integrated Scoring System to Predict the Time to First Treatment in Chinese Patients with Chronic Lymphocytic Leukemia. *Chin Med J (Engl).* 2017 Jan 20;130(2):135–42.
397. Grioni M, Brevi A, Cattaneo E, Rovida A, Bordini J, Bertilaccio MTS, et al. CD4+ T cells sustain aggressive chronic lymphocytic leukemia in E μ -TCL1 mice through a CD40L-independent mechanism. *Blood Adv.* 2021 Jul 27;5(14):2817–28.
398. Patten PE, Chen SS, Bagnara D, Simone R, Marsilio S, Tong T, et al. Engraftment of CLL-Derived T Cells in NSG Mice Is Feasible, Can Support CLL Cell Proliferation, and Eliminates the Need for Third Party Antigen Presenting Cells. *Blood.* 2011 Nov 18;118(21):975–975.
399. Stamatopoulos K, Agathangelidis A, Rosenquist R, Ghia P. Antigen receptor stereotypy in chronic lymphocytic leukemia. *Leukemia.* 2017 Feb;31(2):282–91.
400. Vardi A, Vlachonikola E, Karypidou M, Stalika E, Bikos V, Gemenetzi K, et al. Restrictions in the T-cell repertoire of chronic lymphocytic leukemia: high-throughput immunoprofiling supports selection by shared antigenic elements. *Leukemia.* 2017 Jul;31(7):1555–61.
401. Vardi A, Vlachonikola E, Papazoglou D, Psomopoulos F, Kotta K, Ioannou N, et al. T-Cell Dynamics in Chronic Lymphocytic Leukemia under Different Treatment Modalities. *Clin Cancer Res.* 2020 Sep 15;26(18):4958–69.
402. Lord JM. The effect of aging of the immune system on vaccination responses. *Hum Vaccines Immunother.* 2013 Jun 12;9(6):1364–7.

403. Monin L, Laing AG, Muñoz-Ruiz M, McKenzie DR, del Molino del Barrio I, Alaguthurai T, et al. Safety and immunogenicity of one versus two doses of the COVID-19 vaccine BNT162b2 for patients with cancer: interim analysis of a prospective observational study. *Lancet Oncol*. 2021 Jun;22(6):765–78.
404. Abdul-Jawad S, Baù L, Alaguthurai T, del Molino del Barrio I, Laing AG, Hayday TS, et al. Acute Immune Signatures and Their Legacies in Severe Acute Respiratory Syndrome Coronavirus-2 Infected Cancer Patients. *Cancer Cell*. 2021 Feb;39(2):257-275.e6.
405. Diao B, Wang C, Tan Y, Chen X, Liu Y, Ning L, et al. Reduction and Functional Exhaustion of T Cells in Patients With Coronavirus Disease 2019 (COVID-19). *Front Immunol*. 2020 May 1;11:827.
406. Mato AR, Roeker LE, Lamanna N, Allan JN, Leslie L, Pagel JM, et al. Outcomes of COVID-19 in patients with CLL: a multicenter international experience. *Blood*. 2020 Sep 3;136(10):1134–43.
407. Tam CS, O’Brien S, Wierda W, Kantarjian H, Wen S, Do KA, et al. Long-term results of the fludarabine, cyclophosphamide, and rituximab regimen as initial therapy of chronic lymphocytic leukemia. *Blood*. 2008 Aug 15;112(4):975–80.
408. Gassner FJ, Weiss L, Geisberger R, Hofbauer JP, Egle A, Hartmann TN, et al. Fludarabine modulates composition and function of the T cell pool in patients with chronic lymphocytic leukaemia. *Cancer Immunol Immunother*. 2011 Jan;60(1):75–85.
409. Abrisqueta P, Loscertales J, Terol MJ, Payer ÁR, Ortiz M, Pérez I, et al. Real-world characteristics and outcome of patients treated with single-agent ibrutinib for chronic lymphocytic leukemia in Spain (IBRORS-LLC Study). *Clin Lymphoma Myeloma Leuk*. 2021 Aug;S2152265021003037.
410. Puzzolo MC, Del Giudice I, Peragine N, Mariglia P, De Propriis MS, Cappelli LV, et al. TH2/TH1 Shift Under Ibrutinib Treatment in Chronic Lymphocytic Leukemia. *Front Oncol*. 2021 Apr 15;11:637186.
411. Ghia P, Allan JN, Siddiqi T, Kipps TJ, Jacobs R, Opat S, et al. Fixed-duration (FD) first-line treatment (tx) with ibrutinib (I) plus venetoclax (V) for chronic lymphocytic leukemia (CLL)/small lymphocytic lymphoma (SLL): Primary analysis of the FD cohort of the phase 2 captivate study. *J Clin Oncol*. 2021 May 20;39(15_suppl):7501–7501.
412. Nosari A. Infectious Complications In Chronic Lymphocytic Leukaemia. *Mediterr J Hematol Infect Dis*. 2012 Nov 5;4(1):e2012070.
413. Perica K, Varela JC, Oelke M, Schneck J. Adoptive T Cell Immunotherapy For Cancer. *Rambam Maimonides Med J*. 2015 Jan 29;6(1):e0004.

414. Vermaelen K. Vaccine Strategies to Improve Anti-cancer Cellular Immune Responses. *Front Immunol*. 2019 Jan 22;10:8.
415. Arruga F, Gyau BB, Iannello A, Vitale N, Vaisitti T, Deaglio S. Immune Response Dysfunction in Chronic Lymphocytic Leukemia: Dissecting Molecular Mechanisms and Microenvironmental Conditions. *Int J Mol Sci* [Internet]. 2020 Mar 6 [cited 2020 Apr 1];21(5). Available from: <https://www.ncbi.nlm.nih.gov/pmc/articles/PMC7084946/>
416. June CH, O'Connor RS, Kawalekar OU, Ghassemi S, Milone MC. CAR T cell immunotherapy for human cancer. *Science*. 2018 Mar 23;359(6382):1361–5.
417. Lee DW, Kochenderfer JN, Stetler-Stevenson M, Cui YK, Delbrook C, Feldman SA, et al. T cells expressing CD19 chimeric antigen receptors for acute lymphoblastic leukaemia in children and young adults: a phase 1 dose-escalation trial. *The Lancet*. 2015 Feb;385(9967):517–28.
418. Locke FL, Neelapu SS, Bartlett NL, Siddiqi T, Chavez JC, Hosing CM, et al. Phase 1 Results of ZUMA-1: A Multicenter Study of KTE-C19 Anti-CD19 CAR T Cell Therapy in Refractory Aggressive Lymphoma. *Mol Ther*. 2017 Jan;25(1):285–95.
419. Garfall AL, Maus MV, Hwang WT, Lacey SF, Mahnke YD, Melenhorst JJ, et al. Chimeric Antigen Receptor T Cells against CD19 for Multiple Myeloma. *N Engl J Med*. 2015 Sep 10;373(11):1040–7.
420. Guo B, Chen M, Han Q, Hui F, Dai H, Zhang W, et al. CD138-directed adoptive immunotherapy of chimeric antigen receptor (CAR)-modified T cells for multiple myeloma. *J Cell Immunother*. 2016 Mar;2(1):28–35.
421. Porter DL, Hwang WT, Frey NV, Lacey SF, Shaw PA, Loren AW, et al. Chimeric antigen receptor T cells persist and induce sustained remissions in relapsed refractory chronic lymphocytic leukemia. *Sci Transl Med*. 2015 Sep 2;7(303):303ra139.
422. Turtle CJ, Hay KA, Hanafi LA, Li D, Cherian S, Chen X, et al. Durable Molecular Remissions in Chronic Lymphocytic Leukemia Treated With CD19-Specific Chimeric Antigen Receptor-Modified T Cells After Failure of Ibrutinib. *J Clin Oncol Off J Am Soc Clin Oncol*. 2017 Sep 10;35(26):3010–20.
423. Fraietta JA, Lacey SF, Orlando EJ, Pruteanu-Malinici I, Gohil M, Lundh S, et al. Determinants of response and resistance to CD19 chimeric antigen receptor (CAR) T cell therapy of chronic lymphocytic leukemia. *Nat Med*. 2018 May;24(5):563–71.
424. Imura Y, Ando M, Kondo T, Ito M, Yoshimura A. CD19-targeted CAR regulatory T cells suppress B cell pathology without GvHD. *JCI Insight*. 2020 Jul 23;5(14):e136185.

425. Pedersen CB, Dam SH, Barnkob MB, Leipold MD, Purroy N, Rassenti LZ, et al. Robust integration of single-cell cytometry datasets [Internet]. *Bioinformatics*; 2021 Jun [cited 2021 Aug 2]. Available from: <http://biorxiv.org/lookup/doi/10.1101/2021.06.28.450128>
426. Turner K, Vasu V, Griffin D. Telomere Biology and Human Phenotype. *Cells*. 2019 Jan 19;8(1):73.

8 Appendices

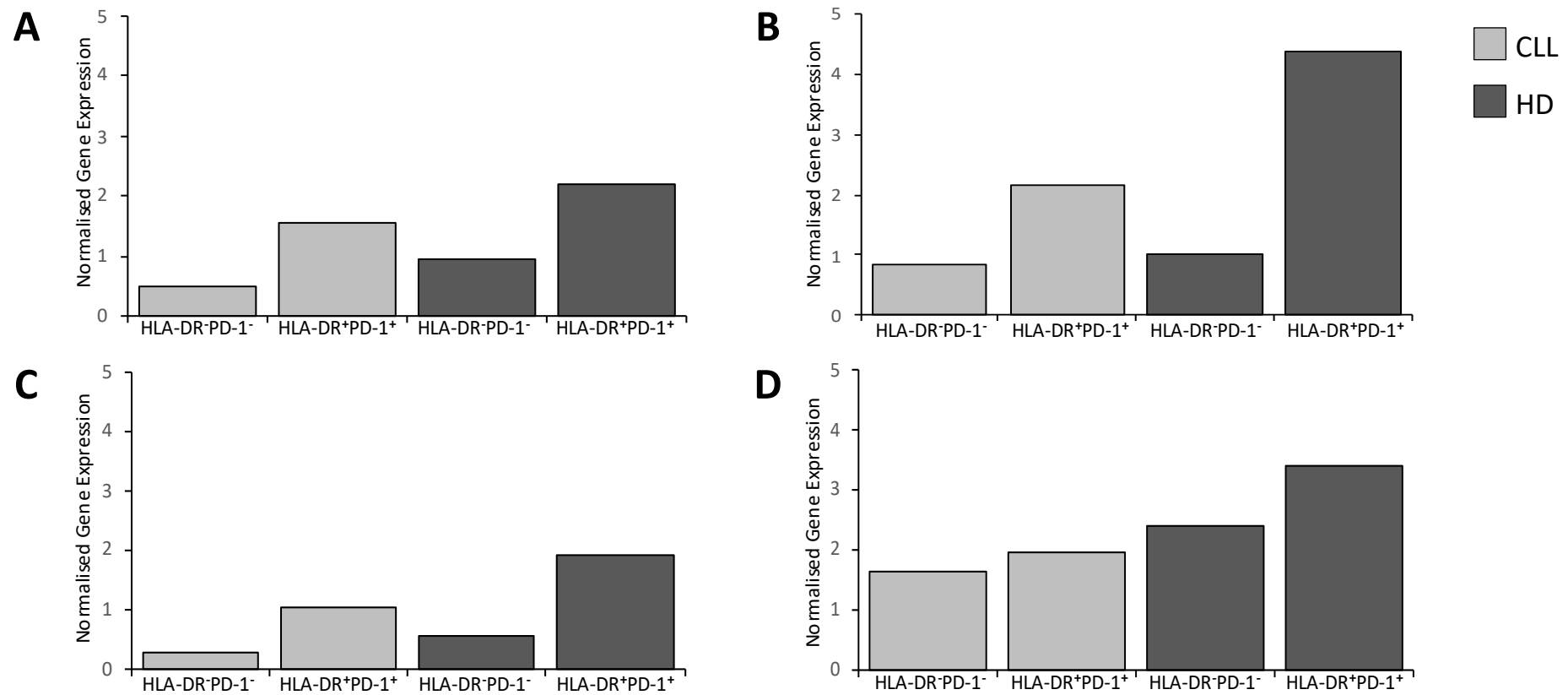


Figure 8.1: Gene Expression Patterns of Key Genes of Interest Match Phenotypic Observations

Gene expression data was obtained for T cells from 5 CLL patients and 4 healthy donors using DNA microarray technology. Plots depict the normalised level of gene expression for four genes of interest analysed phenotypically in *Chapter 3* as follows: **A**) Granzyme **B**) Ki-67 **C**) TIGIT **D**) CD38. The patterns of expression in the gene expression data closely matched those from the phenotypic data.

Gene Name	Gene Symbol
A-kinase interacting protein 1	AKIP1
ALG14, UDP-N-acetylglucosaminyltransferase subunit	ALG14
anti-silencing function 1B histone chaperone	ASF1B
aurora kinase B	AURKB
breast carcinoma amplified sequence 1	BCAS1
coiled-coil domain containing 28B	CCDC28B
cyclin A2	CCNA2
cyclin B1	CCNB1
cyclin B2	CCNB2
C-C motif chemokine receptor 10	CCR10
C-C motif chemokine receptor 4	CCR4
C-C motif chemokine receptor 8	CCR8
CD70 molecule	CD70
cell division cycle 6	CDC6
cyclin dependent kinase 5	CDK5
cyclin dependent kinase inhibitor 3	CDKN3
centromere protein W	CENPW
centromere protein X	CENPX
centrosomal protein 55	CEP55
coiled-coil-helix-coiled-coil-helix domain containing 1	CHCHD1
class II major histocompatibility complex transactivator	CIITA
CDC28 protein kinase regulatory subunit 2	CKS2
coronin 1C	CORO1C
dehydrogenase E1 and transketolase domain containing 1	DHTKD1
E2F transcription factor 2	E2F2
coagulation factor V	F5
forkhead box P3	FOXP3
GINS complex subunit 2	GINS2
glioblastoma down-regulated RNA	GLIDR
gametocyte specific factor 1 like	GTSF1L
H2A histone family member J	H2AFJ
3-hydroxyacyl-CoA dehydratase 1	HACD1
histone cluster 1 H2B family member h	HIST1H2BH
histone cluster 1 H2B family member m	HIST1H2BM
histone cluster 1 H3 family member i	HIST1H3I
histone cluster 1 H4 family member c	HIST1H4C
major histocompatibility complex, class II, DM beta	HLA-DMB
major histocompatibility complex, class II, DR beta 3	HLA-DRB3
major histocompatibility complex, class II, DR beta 4	HLA-DRB4
heat shock factor binding protein 1	HSBP1
interleukin 7	IL7

ISG15 ubiquitin-like modifier	ISG15
KDM7A divergent transcript	KDM7A-DT
long intergenic non-protein coding RNA 1727	LINC01727
long intergenic non-protein coding RNA 2195	LINC02195
lymphocyte antigen 96	LY96
methyltransferase like 7A	METTL7A
MIR4435-2 host gene	MIR4435-2HG
marker of proliferation Ki-67	MKI67
meiotic nuclear divisions 1	MND1
mitochondrial ribosomal protein L54	MRPL54
mitochondrial ribosomal protein L58	MRPL58
neutrophil cytosolic factor 4	NCF4
NADH:ubiquinone oxidoreductase subunit A2	NDUFA2
NADH:ubiquinone oxidoreductase subunit B3	NDUFB3
NADH:ubiquinone oxidoreductase subunit B6	NDUFB6
nth like DNA glycosylase 1	NTHL1
phosphatidylinositol glycan anchor biosynthesis class F	PIGF
polo like kinase 1	PLK1
PR/SET domain 8	PRDM8
peroxiredoxin 3	PRDX3
RAB33A, member RAS oncogene family	RAB33A
rhopilin associated tail protein 1 like	ROPN1L
ribosomal protein L39 like	RPL39L
receptor transporter protein 4	RTP4
RWD domain containing 2B	RWDD2B
solute carrier family 35 member D2	SLC35D2
SLIT-ROBO Rho GTPase activating protein 2	SRGAP2
thymidine kinase 1	TK1
TNFRSF14 antisense RNA 1	TNFRSF14-AS1
thioredoxin domain containing 17	TXNDC17
thymidylate synthetase	TYMS
zinc finger C2HC-type containing 1A	ZC2HC1A
zymogen granule protein 16B	ZG16B

Table 14: Genes Upregulated Solely in Healthy Donor CD4⁺HLA-DR⁺PD-1⁺ T Cells

Gene Set	p-Value
GSE11864_UNTREATED_VS_CSF1_IFNG_PAM3CYS_IN_MAC_DN	0.031
GSE25088_IL4_VS_IL4_AND_ROSIGLITAZONE_STIM_MACROPHAGE_DAY10_UP	0.068
GSE16450_IMMATURE_VS_MATURE_NEURON_CELL_LINE_UP	0.079
GSE17721_CPG_VS_GARDIQUIMOD_24H_BMDC_UP	0.099
GSE9988_LPS_VS_LPS_AND_ANTI_TREM1_MONOCYTE_DN	0.111
GSE22886_NAIVE_BCELL_VS_BLOOD_PLASMA_CELL_UP	0.114
GSE24081_CONTROLLER_VS_PROGRESSOR_HIV_SPECIFIC_CD8_TCELL_UP	0.114
GSE20727_H2O2_VS_ROS_INHIBITOR_TREATED_DC_UP	0.135
GSE7852_LN_VS_FAT_TCONV_UP	0.151

Table 15: Most Highly Enriched Gene Sets in CLL-Derived CD4⁺HLA-DR⁺PD-1⁺ T Cells

Gene Set	p-Value
GSE2706_UNSTIM_VS_2H_LPS_AND_R848_DC_UP	0
GSE339_CD8POS_VS_CD4CD8DN_DC_IN_CULTURE_UP	0.032
GSE2197_IMMUNOSUPPRESSIVE_DNA_VS_UNTREATED_IN_DC_UP	0.039
GSE41867_DAY6_VS_DAY15_LCMV_ARMSTRONG_EFFECTOR_CD8_TCELL_DN	0.041
GSE27786_BCELL_VS_CD4_TCELL_UP	0.044
GSE17721_CTRL_VS_PAM3CSK4_6H_BMDC_UP	0.048
GSE11961_PLASMA_CELL_DAY7_VS_MEMORY_BCELL_DAY40_UP	0.051
GSE15330_LYMPHOID_MULTIPOTENT_VS_MEGAKARYOCYTE_ERYTHROID_PRO GENITOR_DN	0.051
GSE5099_UNSTIM_VS_MCSF_TREATED_MONOCYTE_DAY3_UP	0.088

Table 16: Most Highly Enriched Gene Sets in Healthy Donor-Derived CD4⁺HLA-DR⁺PD-1⁺ T Cells

